IMPROVED SYNTHESIS OF ACETYL-COA AND MALONYL-COA ANALOGS AND THEIR USE TO STUDY STRUCTURE-FUNCTION RELATIONSHIPS OF ACYLTRANSFERASES

by

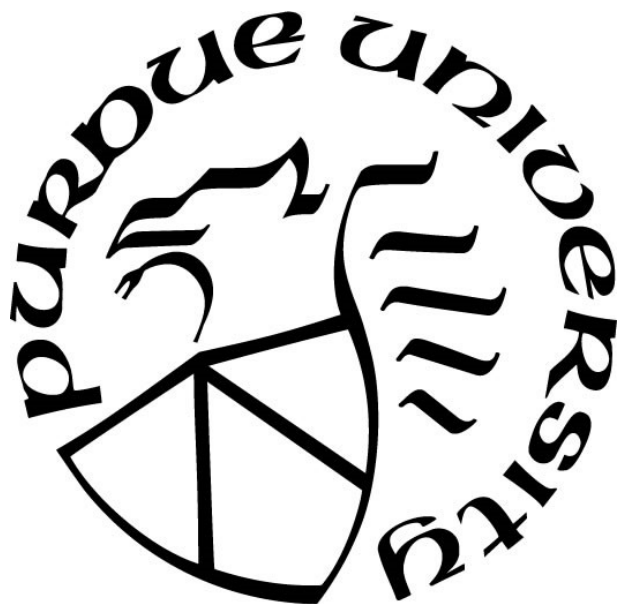**Aaron Benjamin**

A Dissertation

Submitted to the Faculty of Purdue University
In Partial Fulfillment of the Requirements for the degree of

Doctor of Philosophy

Department of Biochemistry

West Lafayette, Indiana

August 2020

THE PURDUE UNIVERSITY GRADUATE SCHOOL
STATEMENT OF COMMITTEE APPROVAL

Dr. Jeremy R. Lohman, Chair

School of Biochemistry

Dr. Barbara L. Golden

School of Biochemistry

Dr. Brian Dilkes

School of Biochemistry

Dr. Nicholas Noinaj

School of Biological Sciences

Approved by:

Dr. Andrew D. Mesecar

I dedicate this thesis to my loving parents, sister and brother-in-law, and all of my friends who have helped me throughout my life.

ACKNOWLEDGMENTS

TABLE OF CONTENTS

LIST OF TABLES

LIST OF FIGURES

LIST OF SCHEMES

LIST OF ABBREVIATIONS

AAC – aminoglycoside acyltransferase

ACC – acetyl-CoA carboxylase

Ac-CoA – acetyl-CoA

ACN – acetonitrile

ACP – acyl carrier protein

ACS – acetyl-CoA synthetase

AT(s) – acyltransferase(s), specifically in polyketide and fatty acid synthase pathways

ATP – adenosine triphosphate

CATIII – Chloramphenicol acetyltransferase Type III

CF – chloroform

CoA – Coenzyme A

DCM – dichloromethane

DH – β-hydroxyacyl dehydratase

DMF – dimethylformamide

DMP – 2,2-dimethoxypropane

ECF – ethylchloroformate

EtOAc – ethyl acetate

EtOH – ethanol

ER – enoyl-reductase

FA – Formic acid

MAT – Malonyl CoA-acyl carrier protein transacylase

KasIII – 3-oxoacyl-[acyl-carrier-protein] synthase 3

FAS – fatty acid synthase

GNAT – GCN5-related N-acetyltransferase

ITC – Isothermal Calorimetry

KR – β-ketoacyl reductase

KS – ketosynthase

Mal-CoA – malonyl-CoA

N.I. – not isolated

pant – pantetheine

Ppant – phosphopantetheine

PDB – protein databank

PKS – polyketide synthase

PTM – posttranslational modification

pTsOH – p-toluenesulfonic acid

RMSD – root-mean-square deviations

TE – thioesterase

TEA – trimethylamine

TFA – trifluoroacetic acid

ABSTRACT

Thioesters are highly reactive centers for acyl-CoAs which allows them to be utilized in a variety of differing enzyme chemistries. As a result of this reactivity, structure-function studies of enzymes using acyl-CoA substrates is difficult. When acyl-CoAs are used in structure-function studies, they often result in a hydrolyzed CoA substrate fragment bound in the active site or require only one of multiple substrates in order to be bound. This results in a lack of information regarding enzyme interactions with the key thioester and acyl chain. To overcome this challenging problem, I have synthesized acetyl- and malonyl-CoA analogs where the thioester has been replaced by an ester (oxygen), amide (nitrogen), or carbonyl (carbon) in a way that is easier, cheaper, and more efficient than performed previously. In addition, we used our synthetic analogs to study a enzymes which span different acyltransferase mechanisms in a combination of kinetics and structure. With this work, it was determined that the amide analogs were stable in all enzymes it was utilized for, while the ester analogs were mostly stable, except the acetyl analog in KasIII, where it acted as a pseudo substrate. As such, these synthetic analogs may have future potential in either type of enzyme for structure-function studies, albeit limited for the acetyl ester analog.

CHAPTER 1.   ACYLTRANSFERASE ENZYME FAMILY: THE SWISS ARMY KNIFE OF LIFE

1.1   Challenges in acyltransferase structure-function studies.

Acyltransferase enzyme family (**E.C. 2.3.X.X**) are a class of enzyme seen throughout the tree of life. They are involved in many biological processes such as: biosynthesis of fatty acids for membranes [1], biosynthesis of natural products that we use as drugs [2, 3], modification of antibiotics as a mechanism of resistance in bacteria [4, 5], a wide variety of metabolic pathways and gene regulation [6-8], Figure 1.1. My focus has been on the vast majority of acyltransferases (**E.C. 2.3.1.X**) that use an acyl-thioester substrate, such as acetyl-CoA the major cellular acyl-CoA. Despite their importance throughout the tree of life, our ability to obtain pictures of acyltransferases bound to the substrates is challenging due to the high reactivity of acyl-thioesters. Nevertheless, it is the high reactivity of the acyl-thioester that powers catalysis by acyltransferases. Stable analogs of acyl-CoAs have been reported for the study of acyltransferases and other enzymes. However, application of these analogs has been limited due to difficulties in their synthesis, which I have worked on overcoming. These analogs are needed to determine pictures of acyltransferases in catalytically relevant states. Such pictures will provide fundamental insight into the catalytic enzyme:substrate interactions that are needed for rational drug design, and rational enzyme engineering to accept alternative substrates for the production of novel natural products as drugs, agrochemicals and biofuels. The following sections outline what we know about some of the acyltransferases I have worked with or are of great significance and how the acyl-CoA analogs I have synthesized can be used for their study.

1.2   Acyltransferase active sites have some conserved features, although small differences between the different families allow for variability in substrate preferences

The residues involved in catalysis throughout the acyltransferase family can be generalized into three major categories, Figure 1.1. Each of these categories has significance towards the understanding of drug development and cellular functions. As such, understanding how these enzymes are able to catalyze their reactions and utilize specific substrates to do so is vital. This section will go over the common features within each of these clusters in detail and will be applied to future sections for reference. Understanding the similarities and differences within these groups
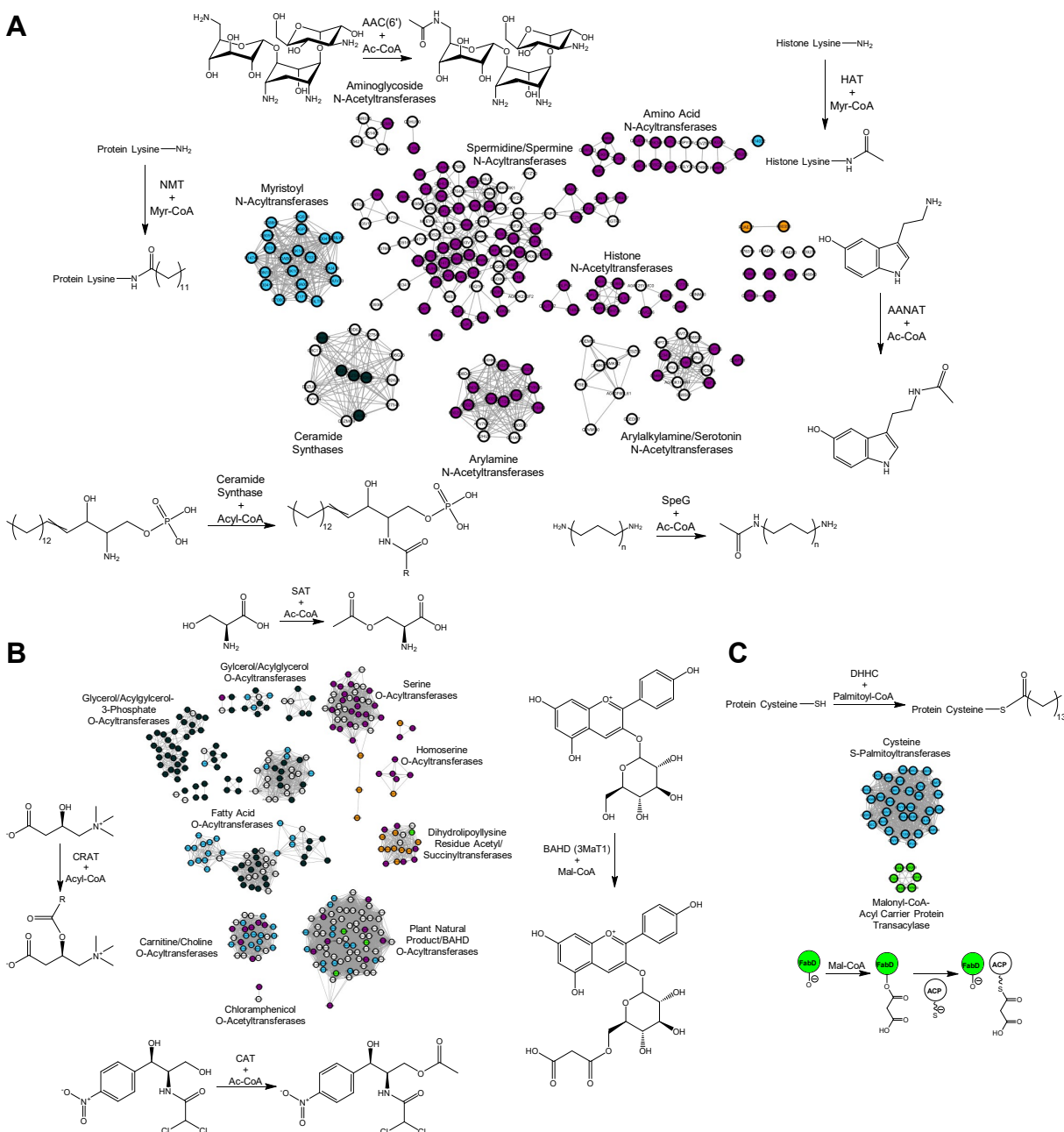
Figure 1.1 Clustering of acyltransferases found in the BRENDA database that have been either biochemically or genetically characterized. Enzyme functions are generalized either above or below select clusters. Colors represent the following: purple use acetyl-CoA, green use (methyl)malonyl-CoA, orange use succinyl-CoA, light blue use long-chain acyl-CoAs, dark green use acyl-CoAs, and white are unknown. Clustering of **A)** GNATs and other N-acyltransferases such as aminoglycoside acetyltransferases (Top Middle), histone acetyltransferases (Top Right), Arylamine/Arylalkylamine Acyltransferases (Right), Ceramide synthases (Bottom), and Myristoyl-CoA N-acyltransferases, **B)** O-acyltransferases undergoing direct acyl transfer including serine acetyltransferase (Top), anthocyanin acyltransferases (Right), chloramphenicol acetyltransferases (Bottom), and Carnitine acyltransferases (Left), and **C)** ping-pong mechanism S-acyltransferases such as such as malonyl-CoA:ACP transacylase and cysteine S-palmitoyltransferases.

ES   Tetrahedral   P
                  Intermediate (TI)

Oxyanion Hole

BH_2 BH_2 BH_2

CoA/ACP—X

O   ⊖O   O

? for N/Q

CoA/ACP—**X**   R   CoA/ACP—**X**   R   Nuc   R
        H—Nuc   **?**   Nuc

A   AH   A

HS—R'

A, BH$_2$ =   Amino acid backbone,   **X** = S, O, NH   **Nuc** = H_2N—R'
                   side chain,
                   water   HO—R'
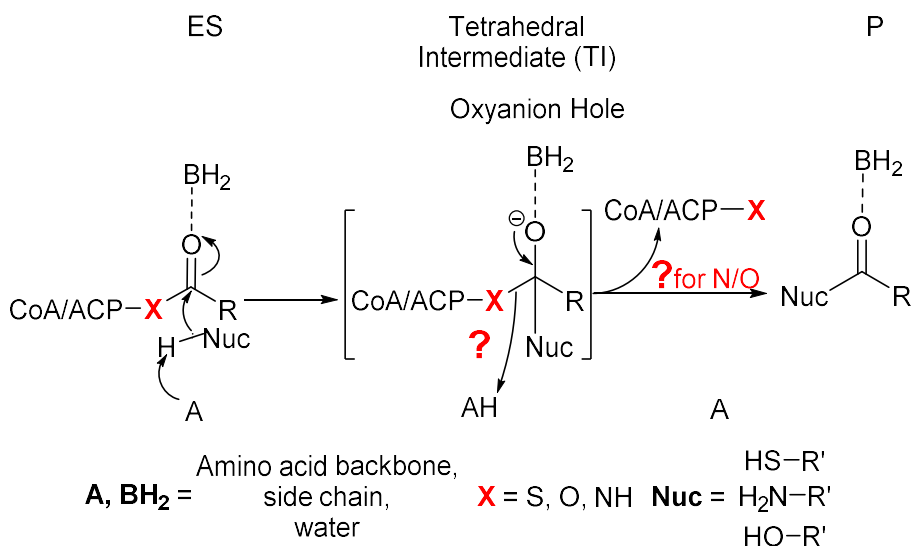
Figure 1.2 Basic reaction scheme of acyltransferase active sites. Some Acyl-CoA/ACP is attacked by a nucleophile, which is mostly sulfur, nitrogen, or oxygen, and becomes acylated after transitioning through a tetrahedral intermediate. Acyl-CoA/ACP analogs where the sulfur is replaced with an ester (oxygen) or amide (nitrogen), may not be able to perform the reaction with specific enzymes. The central question pertaining to these analogs is if they are stable enough to be used in a crystallographic setting.

of acyltransferases are vital for the development of tools, something which is lacking severely. For example, the enzyme:substrate complex active site for acyltransferases generally consists of the following features: 1) a nucleophile from either the protein or external substrate which attacks the thioester carbonyl of the acyl-CoA, 2) an oxyanion hole to stabilize the tetrahedral intermediate that forms during attack, and often 3) a residue or water molecule which deprotonates the nucleophile so it can attack the thioester carbonyl, Figure 1.2. Each of these features varies slightly, ranging from smaller ones such as the nucleophile that attacks, to larger ones such as the specific residues needed for stabilization of the oxyanion hole and residues involved in substrate selectivity within the acyltransferase. The effect that the nucleophile has on acyl transfer is difficult to know, as even enzymes with the same nucleophile do not use the same mechanism all the time. While the nucleophile can vary in terms of the specific substrate being acylated, the three major nucleophiles that act as acceptors are nitrogen (amines), oxygen (alcohols), and sulfur (thiols) [2, 8-11]. These nucleophiles are usually seen in the form of lysine or primary amines on aminoglycosides and xenobiotics for nitrogen, sugars, serine, threonine, or tyrosine for oxygen, and mostly cysteines for sulfur. The acyltransferases can be split into families based off of the residues involved in catalysis and stabilization, seen in the sequence similarity network in Figure 1.1. The nucleophile

used in acyl transfer is important too and plays a small role into the residues involved in catalysis. The residues involved in catalysis are often similar to a serine protease across all acyltransferases, as these will help deprotonate the nucleophiles for attack. The residues involved in substrate specificity are often trickier to pinpoint as structural information is limited for this class of enzymes, often due to the high reactivity of the thioester bond in acyl-CoAs an acyl-ACPs. This information will be used in the next sections to look at the key features to consider when attempting to study the acyltransferase enzyme class through a diversity of different experimentation, especially biophysical and structural work.

1.2.1 N-acyltransferases contain the GNAT superfamily which is one of the largest superfamilies and which primarily utilizes a sequential mechanism to acylate secondary substrates

This section will discuss the differences and similarities with acyltransferases that utilize nitrogen as the nucleophile for attack. Nitrogen from an aminoglycoside, lysine, histidine, amongst others act as nucleophiles in a vast quantity of acyltransferases. In fact, one of the largest and most well-known superfamilies is the GCN5-Related N-acetyltransferases (GNATs). This superfamily encompasses enzymes that have a variety of functions, including aminoglycoside inactivation, gene regulation, and polyketide formation [12-16]. While each of these subclasses have different substrates, they all acylate an amine and have a similar fold in their structures. For all N-acyltransferases, it is important to make sure that they are uncharged when bound in the active site. With the charge, the nitrogen will be unable to attack the thioester carbonyl. As such, most N-acyltransferases use histidine or aspartic/glutamic acid to remove the proton from the primary amine in the active site [9, 13, 16]. Catalytically, the GNAT family is believed to mostly use direct acetyl transfer rather than a ping-pong mechanism. One exception to this is the arylalkylamine N-acetyltransferase family (NAT), which will be discussed later. For other GNATs, this is supported by a variety of biochemical data. Kinetic experiments such as the ones performed with a serotonin N-acetyltransferase and a histone acetyltransferase (HAT) suggested that both enzymes utilized the ternary complex as was seen in their double reciprocal plots [17, 18]. Thiol blocking agents were also used in an effort to inactivate yGCN5, however these agents were unable to so [17]. To further support the notion that these enzymes utilized ternary complexes, structures of GNATs were unable to find cysteines close enough to perform nucleophilic attack on acetyl-CoA [19, 20]. This was

reinforced with structures with ternary complexes bound [19, 20]. Structurally, the GNAT family is generally made up of 10 to 11 strands, 6 to 7 of which are β-sheets and 4 of which are α-helices [13]. The order of these strands is as follows: β0-β1-α1-α2-β2-β3-β4-α3-β5-α4-β6 [13]. These strands make 4 motifs, A-D, which are ordered C (β1-α1), D (β2-β3), A (β4-α3), and B (β5-α4) [13]. The A motif consists of a P-loop where the acetyl-CoA binds. Despite the structural similarities within the GNAT superfamily, the pairwise sequence identity only ranges from 3-23% [16]. This sequence identity is weak to moderate at best but increases as each subfamily is looked at on an individual basis. Some of the subfamilies include the aminoglycoside N-acetyltransferases (AAC), histone acetyltransferases, arylalkylamine N-acetyltransferases, N-myristoyltransferases, and spermidine/spermine N1-acetyltransferases, Figure 1.1 A.

Aminoglycoside N-Acetyltransferases (AAC)

There are a wide variety of aminoglycosides which are acetylated by the aminoglycoside N-acetyltransferases. Common aminoglycosides that are used in the lab setting include kanamycin, apramycin, and ribostamycin which are used along with their resistance genes as selectivity markers during cloning and transformation procedures. The AACs involved in resistance do not inhibit each other and are able to modify multiple

Figure 1.3 An aminoglycoside (ribostamycin), showing the enzyme subfamilies and where they modify the aminoglycoside.

different aminoglycosides, albeit at differing rates for each [4, 12, 21]. Despite their ability to acetylate at a variety of positions, AACs have a simple nomenclature which describes their preferred acetylation site. There are four main classes of AAC: AAC(1), AAC(2'), AAC(3), and AAC(6'), Figure 1.3 [12, 13]. Each one of these classes prefers to acetylate their substrates at the carbon position of the aminoglycoside seen in the name. An example of this would be AAC(3)-IV, which acetylates aminoglycosides at C-3, such as apramycin [22]. The roman numeral states the resistance profile, which describes the antibiotic resistance pattern seen within all isolates of the subclass [4].

Figure 1.4 Structures of AAC(6')-Ib in complex with **A)** Kanamcyin C and Ac-CoA (PDB: 1V0C), **B)** Parmomycin and Ac-CoA (PDB: 2VQY), and **C)** Ribostamycin and CoA (PDB: 2BUE). For all, gray dotted lines represent hydrogen bonds. Gln116 and Asp115 are involved with the oxyanion hole and deprotonation of the amine by AAC(6')-Ib.

Interestingly, while rare, some of these AACs such as AAC(2')-Ic from *M. tuberculosis* have been shown to acetylate both amines and alcohols [23]. This raises the question of how this enzyme is able to acetylate both nucleophiles compared to the many others that have been tested and are unable to do the same. While several of these aminoglycoside subfamilies have some structural information about them described in the literature, most of the structural information is pertaining to members of the AAC(6') subfamily with 4 members having solved structures [24-27]. One successful study looked at *E. coli* AAC(6')-Ib, where it found kanamycin C or paromomycin bound with acetyl-CoA in the active site, Figure 1.4 [25]. Both of these antibiotics have a 6' hydroxyl and cannot react with acetyl-CoA in this enzyme. Interestingly, when co-crystals of ribostamycin, which has a 6' amine, and acetyl-CoA were attempted, hydrolyzed CoA was found in place of where acetyl-CoA had been found for the previous structures [25]. Other variants of the AAC(6') subfamily such as AAC(6')-Ii from *Enterococcus faecium* have also been successfully crystalized.

In one study, acetyl-CoA was found in the active site, near a tyrosine residue believed to be important in proper orientation of acetyl-CoA in the active site [28]. In conjunction with kinetic studies, it was determined that the reaction followed an ordered sequential mechanism where acetyl-CoA bound first, followed by the aminoglycoside [28, 29]. In addition, there was also studies done on bisubstrates of CoA and an aminoglycoside which showed promise as they inhibited at nanomolar concentrations [30].

While information about the AAC(6') subfamily is plenty, there is minimal structural information about the other subfamilies, 1 member of each of the AAC(3) [31] and AAC(2') [23] subfamilies to be specific. Similarly to some of the AAC(6') structures, structures of AAC(3) from *S. marcescens* and AAC(2')-Ic from *M. tuberculosis* have hydrolyzed versions of acetyl-CoA bound in their active site, a common result when attempting crystallography with acyl-CoAs [23, 31]. Interestingly, the structures of AAC(2')-Ic in complex with CoA and kanamycin A or ribostamycin both have plenty of space in the active site for an acetyl-moiety to be placed, however there are several potential residues, including backbone amides of Val84 and Gly83 or Ser117 and Ser118, Figure 1.5. Unfortunately, because of the fact that it is the backbone which may be involved in the tetrahedral intermediate, it is difficult to pinpoint exactly which residues are involved in stabilization of the tetrahedral intermediate. In order to be able to get a clearer picture, it is necessary to have analogs which act similarly to acyl-CoAs, while also not hydrolyzing on the crystallographic scale. The analogs similar to acyl-CoAs will be discussed later on, however suffice it to say that due to the lack of use of these analogs, much of the information necessary for developing drugs to overcome these antibiotic resistance genes is unknown.

Arylalkylamine and Arylamine N-Acetyltransferases (AANAT and NAT)

Another two families within the superfamily of GNATs that are similar in function are the arylalkylamine N-acetyltransferases (AANATs) and arylamine N-acetyltransferases (NATs). AANATs shares many of the same features that the AAC family, such as the general fold or that bisubstrates analogs are highly potent inhibitors [32-34]. Interestingly, there are no family members found in insects, nematodes, and some plants; members are found in vertebrates, gram-positive bacteria, algae, and fungi [35]. Functionally, this makes some sense, as AANAT acts as a timekeeper in vertebrates as it is known to be involved in melatonin production in the pineal gland [36, 37]. Similar

to the AACs, AANATs have a some variety of substrates they can acetylate, including serotonin [18], dopamine [38], and phenylethylamine [39]. The AANAT from *Ovis aries* (sheep) was shown to have major rearrangements induced upon acetyl-CoA binding which helped form the binding pocket for serotonin [13, 18, 40]. As a result of this and some kinetics studies, it was determined that OaAANAT underwent an ordered sequential mechanism and diffusion of product from the active site was the rate-limiting step [16, 40]. The *Drosophila melanogaster* homologs of OaAANAT also underwent an ordered sequential mechanism, suggesting that most of the family members of the AANAT family likely also undergo this same mechanism [36, 41]. Structures in the AANAT family mostly have bisubstrate analogs bound. The use of non-hydrolyzable analogs has not been used and may provide additional details for future drug design for behavioral and sleep-based illnesses and disorders.

The second family, the arylamine N-acetyltransferases, are similar to AANAT, except that they can acetylate both arylamines and arylalkylamines [42]. Unlike AANATs, NATs are expressed throughout the body, especially in the liver, where they are involved with pharmaceutical modifications [43, 44]. Interestingly, NATs are found in organisms including bacteria, birds, and mammals. Catalytically, NATs differ from other GNATs. Pigeon liver NAT was shown to undergo a ping-pong mechanism using both aniline and p-nitroacetanilide [45]. Interestingly, there was initial controversy as to whether the NAT family was responsible for acylation of arylhydroxylamines as well as arylamines. A study in 1992 was able to confirm that this was in fact the case [46]. From here, the structure of *Salmonella typhimurium* NAT was able to identify the catalytic cysteine, as well as the rest of the catalytic triad, a histidine and an aspartate [47]. While many of these studies were initially done to look at the role of NAT on the anti-mycobacterial, isoniazid, when the *nat* gene was deleted from strains such as *Mycobacterium bovis*, the cells were unable to survive in the host macrophages [48, 49]. The antibacterial function of NAT will be discussed in a later section pertaining to antibiotic resistance. NATs from humans and other mammals are interesting, as they have been shown to have multiple polymorphisms. These NAT polymorphisms have altered enzymatic activity, one of which is "slow" and the other "fast" [43]. The NAT that is slow or fast can change from species to species. For example, in rodents NAT1 is the equivalent to human NAT2 and vice versa [50]. Structures of these NATs from humans show some of the differences between the prokaryote homologs [51]. Most of the differences found were predicted to cause stricter substrate specificity in mammals over the prokaryotic NATs [51]. In these structures and others,
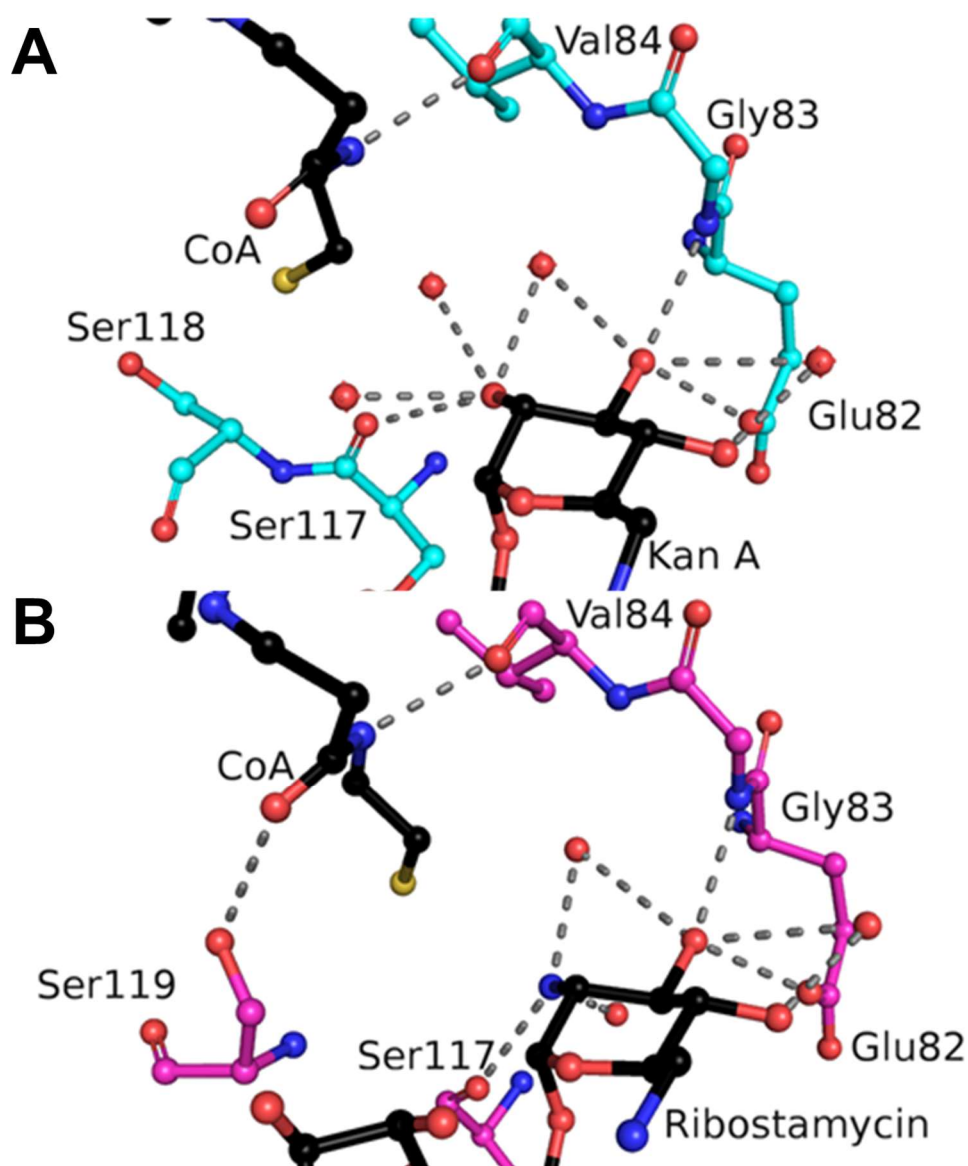
Figure 1.6 Structures of Aac(II')-Ic in complex with **A)** CoA and Kanamycin A, and **B)** CoA and Ribostamycin. Dotted gray lines represent hydrogen bonds. Both structures show Ac-CoA hydrolyzed during the crystallographic time course.

however, the only molecule bound in the active site is CoA [51]. While this provided details pertaining to CoA binding, it has left questions as to which residues are specifically involved in the binding of the acetyl moiety of acetyl-CoA. Due to the implications of NATs and bladder cancer, fully understanding how the mutations that are present are able to cause the disease is crucial [52]. There are some studies which have shown mutagenesis of residues such as an aspartate near the active site are necessary for catalysis [53], however structures with analogs of acetyl-CoA

may be able to give a clearer picture of the specific residues that could be targeted for drug design. They may also be able to give a clear picture as to all of the potential substrates that these enzymes are able acetylate.

Spermidine and Spermine N-Acetyltransferases (SSAT)

Polyamines are important in the cell as they play a role in response to chemical and physical stress. Spermidine and spermine are polyamines shown to have some amount of antioxidant properties, are essential in the stabilization of DNA and RNA, and are involved in the regulation of the ribosome [54-57]. There is evidence that accumulation of these polyamines can be toxic to the cell, and subsequent acetylation helps prevent this toxicity [55]. This acetylation is performed by spermidine/spermine N-acetyltransferases (SSAT) family. While this family is distinct from the others in the GNAT family, it should be noted that histone acetyltransferases (HATs), which will be discussed in the next section, were shown to have limited ability to acetylate polyamines too [58]. Despite this, SSATs are vital for the breakdown and excretion of polyamines within the cell. Structurally, SSATs have structures from a few organisms, including *Bacillus subtilis*, humans, *Vibrio cholerae*, and *E. coli*. Structures from *B. subtilis* SSAT (BsPaiA), a monomer in solution, were solved as a dimer where one subunit contained a single CoA bound while the other contained the dimerized CoA [59]. This study also showed that there were key differences in the structure of BsPaiA compared to other GNATs in the loop where β3 and β4 come in close proximity to the β6 and β7 strands [59]. In this same study, the K_m was calculated to be 76 μM, the k_{cat} 19.1 min^{-1}, and the V_{max} to be 480 nmol/min/mg enzyme [59]. Unfortunately, due to the lack of both substrates being bound and not hydrolyzed, the best prediction the authors could make was that there was a tyrosine that was likely acting as a general acid in catalysis. Structures of SSAT homologs showed dimerization in their structures as well, except for *V. cholerae* (SpeG), which was a dodecamer both in solution and in the crystal form [60]. SpeG is interesting as it is different to human or mouse homologs, but is similar to GNATs such as EfAAC(6')-Ii [61]. Another interesting feature of SpeG is the fact that it has an allosteric site where a polyamine will bind, inducting changes in the structure that allow for acetyl-CoA and another polyamine to bind and react [62]. This study did not reflect on the kinetics of SpeG; however, homologs from rat liver were shown to have an ordered sequential mechanism [63] while homologs from human and *B. subtilis* were determined to have random-ordered mechanisms [59]. One problem left from most of this work is the lack of structures
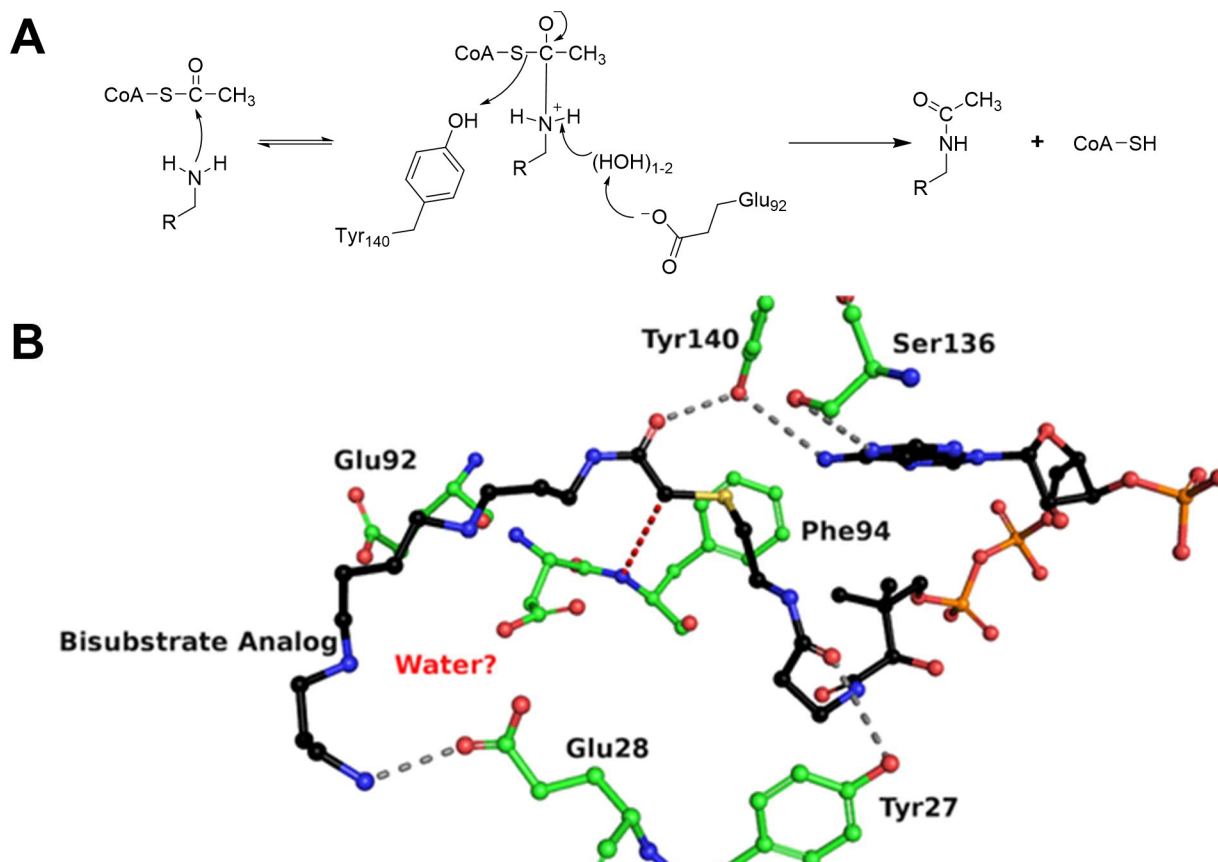
Figure 1.7 **A)** Predicted mechanism of SpeG according to *Hegde et al (2007)*. Tyr140 is involved in protonation of CoA as collapse of the tetrahedral intermediate occurs. Glu92 is predicted to deprotonate water which is predicted to deprotonate the acetyl-spermidine-CoA intermediate, helping push the reaction forward. **B)** Structure of human spermidine acetyltransferase (SpeG) with bisubstrate inhibitor bound, PDB: 2JEV. Residues from SpeG are in green and the bisubstrate is seen in black. Hydrogen bonds are marked with dashed gray lines. The dotted red line is my prediction to a backbone amide which may be involved in hydrogen bonding for the tetrahedral intermediate. Tyr140 is predicted to be involved with stabilization of the tetrahedral intermediate, however no other residues are seen within hydrogen bonding distance.

with both substrates bound in the active site. Since there are predicted conformational changes that occur in this family, predictions with only one substrate bound may not provide the best information towards substrate specificity and the residues involved in catalysis for SSATs. This can be seen in structures of SpeG, such as the one from human, Figure 1.6. This structure has a bisubstrate inhibitor where the acyl-CoA has had the carbonyl moved to the β position and has been fused with spermidine [64]. In this structure, the oxyanion hole is only made up of a tyrosine residue [64]. While this tyrosine may be important, it is highly unlikely that it is the only residue involved in stabilization of the tetrahedral intermediate that forms during catalysis. There are

backbone amides near this area, which may be involved in stabilization including Phe94, Figure 1.6. The authors predicted that Glu92 was involved deprotonation of a set of orders waters, which in turn deprotonated the amide in the tetrahedral intermediate, Figure 1.6 [64]. Unfortunately, the structure they solved did not have waters in the active site. The lack of structures with both substrates or structures with near-natural, non-hydrolyzable analogs of acetyl-CoA leaves the question of the residues involved for tetrahedral intermediate stabilization clouded at best.

Histone Acetyltransferases (HATs)

One of the most famous GNAT family members is the histone acetyltransferase (HAT) family. HATs are activators of transcription, doing so by acetylating the lysine residues of histone tail at the N-terminal. Interestingly, there are two types of HATs which is based off a combination of substrate and subcellular localization [65, 66]. Type A HATs are localized in the nucleosome and act on histones in the chromatin, while type B HATs are seen in the nucleosome and the cytoplasm, but acetylate histones that are solubilized [13, 65, 66]. In humans and *Saccharomyces cerevisiae* histone N-acetyltransferase 1 (HAT1), a Type B HAT, is responsible for acetylation of K5 and/or K12 on H4 that is solubilized [67]. It has been suggested that HAT1 plays some role in DNA repair, and that there may be a correlation between expression levels of HAT1 and cancer [13, 65, 68]. As such, this makes HAT1 a potential therapeutic target for the treatment of cancer. Structures of HAT1 in complex with Acetyl-CoA and a peptide substrate similar to histone H4 showed that there were three domains for human HAT1 [69]. These were the N-terminal domain, the central domain, and a C-terminal domain [69]. Acetyl-CoA was bound in between the central, GNAT domain and the C-terminal domain, where a glycine rich region interacted with the pyrophosphate arm [69]. It should be noted that while this structure did have both acetyl-CoA and the arm of the H4 histone bound, the interactions between histone H4 and HAT1 were not captured in this structure. One question that arises from this work is whether or not it is possible to capture both. If the interactions between H4 and HAT1 are necessary for the reaction to occur due to a conformational change for example, then it may be that using acetyl-CoA would result in turnover for the enzyme, preventing the capture of the ternary complex and those necessary interactions. The use of acetyl-CoA analogs could help alleviate any problems that may arise as such.

The type A HAT Esa1 from *S. cerevisiae* is able to acetylate a few histones, including H4, H2A, and H2AZ [70-73]. It is the only pure HAT expressed in budding yeast, and much like HAT1 from humans, has a central GNAT domain surrounded by N- and C-terminal domains [74-76]. Interestingly, a study with a bisubstrate, H4K16CoA showed that K262 of ScEsa1 was autoacetylated and that it was necessary for ScEsa1 to autoacetylated for cell viability [77]. To some surprise, a study predicted a ping-pong mechanism for ScEsa1 due to an acetylated cysteine found in their crystal structure [76]. This was later disproven when mutagenesis of this cysteine to an alanine resulted in minimal changes to activity [78]. *S. cerevisiae* also contains GCN5 (scGCN5), another type A HAT, however it able to acetylate non-histone proteins in addition to histones H3 and H4 at K14 and K8/K16 respectively [79]. GCN5 is found in a variety of organisms, and is involved in apoptosis-related genes and the cell cycle [80], embryo development in mice [81], and the biosynthesis of amino acids in *S. cerevisiae* [82]. Structural studies with ScGCN5 showed that that there was a glutamate residue that was near the binding cleft and subsequent mutagenesis and kinetics confirmed that it was responsible for deprotonation of the amine from the lysine [83]. Homologs of ScGCN5 from human (hGCN5) in complex with acetyl-CoA [84] and *Tetrahymena thermophila* (TtGCN5) in complex with acetyl-CoA [85, 86] and in complex with CoA and an H3 peptide were also solved [19]. Both structures from human and *T. thermophila* has conserved glutamate residues which are predicted to be involved in deprotonation of the lysine from their substrate, however for TtGCN5, there is a well ordered water which may be directly responsible for deprotonation [84-86]. One of the more interesting discoveries from structure studies with TfGCN5 is a study with a bisubstrate, peptide-CoA inhibitor. This study suggested that H3 that has been acetylated is displaced from the binding site via a C-terminal domain rearrangement [87]. If taken into consideration with all of the other structures which either have one substrate or hydrolyzed substrate bound, it is possible that conformational changes may be occurring in other GCN5-like HATs, meaning that structural studies with analogs which are non-hydrolyzable may be necessary to fully understand all of the residues involved with catalysis. In addition, this suggests that having larger portions of the histone may show where some of these conformational changes are occurring; however, this may only be possible with non-hydrolyzable analogs of acetyl-CoA, rather than the natural substrate.

Lastly, Hpa2 from *S. cerevisiae* (ScHpa2) is responsible for acetylation of K4 and K14 from H3, and K5, K12, and K8 from H4 [88]. ScHpa2 has also been shown to acetylate a large variety

of non-histone primary amines including other chromosomal proteins and polyamines such as spermine, spermidine, and putrescine [88]. Interestingly, ScHpa2 turns from a dimer in solution to a tetramer in solution and crystallographically once it binds acetyl-CoA [89]. Within this tetramer, ScHpa2/Acetyl-CoA exists as a dimer of dimers [89]. One of the more fascinating features of the structure bound with acetyl-CoA is that the adenine ring from one dimer actually interacts with the adenine from the other dimer [89]. There is a tyrosine near the sulfur from acetyl-CoA which is believed to act as a general acid in the reaction [89] and is likely responsible since a tyrosine in spermidine/spermine N1-acetyltransferase, whose structure is very similar, was shown to be involved in catalysis [20]. One last interesting feature of ScHpa2 is the active site entrance, where there is a substantial positive charge which is believed to favor the deprotonated state of the amine which will become acetylated [89]. Despite the information gleaned from many of these HATs, there are still many questions left to answer, many of which will be discussed later on in this section.

Protein N-Myristoyltransferases (NMTs)

Myristate is a 14-carbon fatty acid which is saturated, and can be transferred onto glycine residues on the N-terminus of proteins in a variety of eukaryotes, protozoans, fungi, and viral proteins when attached to CoA [90-95]. Myristoylation is used to interact proteins and the cell membrane, enhance protein stability, and can cause reversible protein-protein interactions to form as well [90]. Many human diseases have been linked to abnormal levels of this modification, including genetic disorders, cancer, and infections from viruses [90]. Structures of NMTs have been solved in a variety of species including human [96], *Candida albicans* [97], *S. cerevisiae* [98], multiple *Plasmodium* [99-102], fungus [103], *Treponema brucei* [104], and multiple *Leishmania* [105-108]. CaNMT, for example, contains two GNAT domains and is a monomer with two-fold internal symmetry [97]. Interestingly, the two domains that are symmetrical actually have limited sequence identity despite the likelihood that the occurrence of the two domains resulted from a gene duplication event [97]. A homolog of CaNMT from *S. cerevisiae* in complex with Myristoyl-CoA and an inhibitor hypothesized that an approximately 30 residue portion on the N-terminus is involved in recognition of substrates [98, 109]. In ScNMT, the N-terminal GNAT domain is responsible for binding myristoyl-CoA, while the C-terminal GNAT domain is responsible for binding the protein that is being myristoylated [98]. When compared to other homologs, it was determined that the myristoyl-CoA binding site appeared to be in the same place, however the peptide binding site was variable [110].

This makes sense, as the binding partner of myristoyl-CoA varies from species to species. Despite this, NMTs follow an ordered sequential mechanism, similarly to other GNAT superfamily members [92]. While these structures have given some indication towards the residues responsible for catalysis, there is still information missing for some of these organisms. In addition, these proteins make good targets for future drug design since the substrates for infectious bacteria or virus proteins differs from the ones in humans.

Implications into the Future of Work for N-Acyltransferases

The last few decades have resulted in large amounts of structural information on N-acyltransferases, especially for the GNAT superfamily. Despite the low sequence similarity between the subfamilies, the overall fold appears to be similar for most of the superfamily members. The structural information, while invaluable as a starting point, still has some holes which need to be filled in. Interestingly, many N-acyltransferases, and most GNATs, are oligomeric, something which has been shown to be important towards their function. As a result, one place where there is a lack of information is the role that oligomerization has for catalysis. In addition, there is the question as to the role of oligomerization in substrate specificity as well. If oligomerization plays a role, it is possible that using final products or one substrate for structural determination may not result in a fully accurate picture. The use of non-hydrolyzable acyl-CoA analogs could help alleviate this as the reactions would not occur, allowing for trapping of the ternary complex. Another question which needs answering is whether present structural information can help determine whether enzymes in, for example, the GNAT superfamily follow an ordered or random sequential mechanism. Unfortunately, structures cannot solve this problem. Biochemical and biophysical methodologies such as isothermal calorimetry (ITC) may help alleviate this problem. For many of these enzymes, conformational changes are apparent, suggesting that the specific interactions necessary for catalysis may be more difficult to determine that previously thought. This may mean that larger peptide substrates or the entire protein target may be necessary for proper determination of residues involved in catalysis. While singular substrates or hydrolyzed substrates may help guide mutagenesis studies, non-hydrolyzable substrates would help clarify many specifics, and may allow for better drug design against the target enzyme/small molecule amine. This could be especially useful for determining the differences between enzymes using histidine to deprotonate versus enzymes using

aspartic/glutamic acid residues. Lastly, other questions arise when thinking about autoacylation. If autoacylation, as was seen for TtGCN5, is necessary for some acyltransferases, this could suggest one possible reason for oligomerization. It is also possible that oligomerization is a way of regulating the activity of these enzymes, especially the ones that are highly regulated. These questions may be possible to answer with the use of non-hydrolyzable analogs in conjunction with crystallography.

1.2.2 O-acyltransferases vary in overall structure more so than N-acyltransferases, making identification of their substrates from bioinformatics difficult

Acyltransferases that utilize oxygen as the nucleophile for attack are hard to categorize because they do not have the same level of conserved structural features that N-acyltransferases have, Figure 1.1B. In addition, O-acyltransferases utilize a variety of different substrates including serine/homoserine [111], sugars and anthocyanins [112, 113], fatty acids and small molecules like glycerol [10, 114], carnitine/choline [115, 116], and antibiotics, Figure 1.7 [5]. In order for acyl transfer to occur for O-acyltransferases, there are a few important factors that need to be taken into consideration. It should be noted that many of these factors are also important for acyl transfer in N-acyltransferases as well, however these are often much harder for an enzyme to do in O-acyltransferases compared to N-acyltransferases. The reason for this increased difficulty is the higher pK_a of a hydroxyl than an amine, thus making it more difficult to deprotonate.

The first factor to think about is desolvation. Computational studies have become increasingly useful for this, as it has become easier to calculate using a method called QM/MM. As such, one study was able to conclude that desolvation played a significant role by showing that there was a rate enhancement using DMSO, a protic solvent, over water [117]. It should be noted that there are also computational studies which state that it isn't desolvation that is used by enzymes, but in fact is 'specific solvation', which is specific for the transition state [118-120]. While both of these factors are different, they are both aimed at determining the factor that hydrogen bonding play on nucleophilic attack. 'Specific solvation', in a personal opinion, is looking more so at the next factor that is important, especially for O-acyltransferases. This factor is the ability of the acyltransferase to coordinate the alcohol for subsequent proton extraction. Coordination of the alcohol is, to some degree, the same idea as 'specific solvation' since the residues of the enzyme are going to be responsible for solvating the substrates in the proper orientation. They will also be

responsible for ionization of the alcohol, the next major factor that plays a role. Interestingly, the hydroxyl deprotonating rescues can vary, including histidine, lysine, aspartic acid, glutamic acid, and even sometimes metals [10, 118]. All of these factors may help split many of these direct transfer O-acyltransferases into families, however the best approach to do so is to look at structural similarities between the O-acyltransferases. In order to do this, the structural work already determined must be paired with future structural work to help tease apart the similarities and differences between all of the O-acyltransferases.
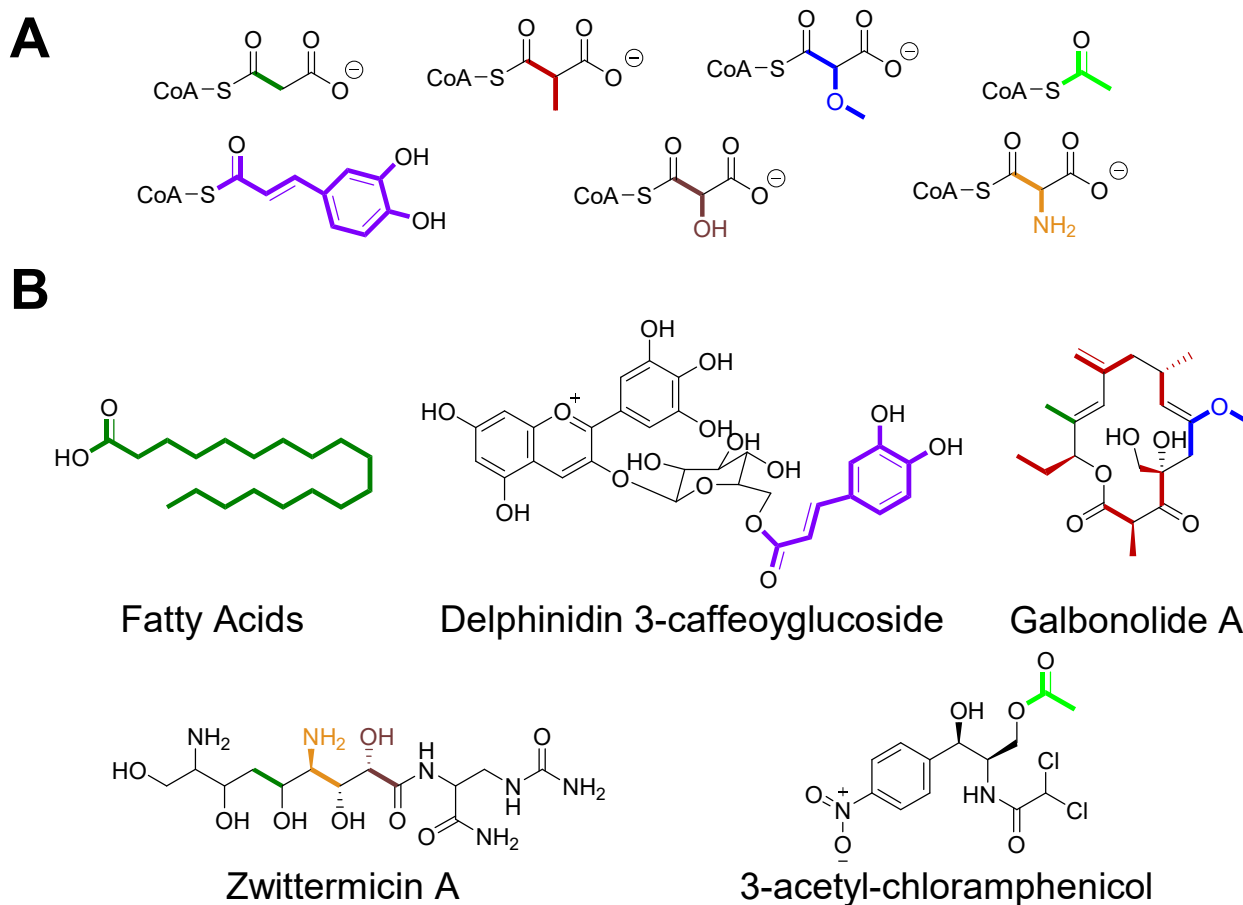
Figure 1.8 **A)** Varying acyl-CoAs that are used by acyltransferases. Dark green is malonyl-CoA, red is methylmalonyl-CoA, blue is methoxymalonyl-CoA, lime is acetyl-CoA, purple is caffeoyl-CoA, brown is hydroxymalonyl-CoA, and orange is aminomalonyl-CoA. **B)** Different molecules that are made from the varying acyl-CoAs. Colors represent the bonds from the different CoAs that are incorporated as parts of antibiotics, fatty acids, anthocyanins, or confer antibiotic resistance.

Glycerol and Glycerol-3-phosphate Acyltransferases (GPAT)

Glycerol and glycerol-3-phosphate are important molecules in the production of energy and cell membranes. As such, acyltransferases such as the glycerol-3-phosphate acyltransferases (GPAT) and 1-acylglycerol-3-phosphate or lysophosphatidic acid acyltransferases (LPAAT) are important enzymes to have knowledge about. Interestingly, homologs of these enzymes from humans, plants, bacteria, and yeast share a highly conserved active site motif, HxxxxD, where a histidine and an aspartic acid residue are separated by four other residues [121]. This motif is an important motif, as it is used in enzymes such as chloramphenicol acetyltransferase (CAT). Besides this motif in the active site, there is a large amount of variability between the remaining members of this family, other than certain short sequences, called blocks [121]. These blocks, ranging from blocks II to blocks IV, are seen conserved between some homologs such as animal, bacteria, and yeast, but not others such as plants [121]. The consistent motif of HxxxxD is considered block I [10]. In order to understand these enzymes better, chemical modifications and site-directed mutagenesis was performed on the *E. coli* homolog, PlsB [121, 122]. The mutagenesis of the conserved histidine to an alanine abolished activity of PlsB, although mutagenesis to a glycine maintained minimal levels of activity [121]. This result led to the prediction that the glycine mutant was more flexible, allowing another residue to take over as the base in deprotection [122]. Much of this work was corroborated when the structure of a GPAT from squash was solved, showing that the putative binding sites were in close proximity to the conserved HxxxxD [123]. Blocks II through IV of PlsB were determined to be important for binding, which was seen via mutagenesis and measurements of K_m values which showed decreased binding [122]. This class of enzymes is of interest as they are involved in the precursor steps to fatty acid biosynthesis, making them potential targets for drug design.

Membrane-Bound O-Acyltransferases (MBOAT)

Membrane-bound O-acyltransferases (MBOATs) are a family of enzymes that, much like the name states, are bound to the membrane. They have a histidine involved in catalysis similar to the GPAT family, although they have an asparagine in their active site. The histidine is surrounded by hydrophobic residues and the asparagine is in a hydrophilic region [114]. This family is able to act on cholesterol or diacylglycerols, amino acids within a protein or hormone, and lysophopholipids

[114]. MBOATs are involved in a variety of different functions for the cell including nutrient sensing, membrane lipid remodeling, embryogenesis, and neutral lipid biosynthesis [114]. The family has been known since the late 1950s, where it was first discovered from rat liver [124]. From there, it was shrouded somewhat in mystery until 1993, when the mouse acyl-coenzyme A;cholesterol acyltransferase (ACAT) member ACAT1 was sequenced [125]. It was not until the discovery of the unrelated enzyme porcupine and the determination of its' sequence in 2000, before this family was recognized based off of conserved regions that were shared by many proteins that had been previously identified [126]. From here, it was recognized that there were at least 11 members of this family in the human genome [114]. This family is split into 3 subgroups: MBOATs that act of neutral lipid biosynthesis, MBOATs involved in protein/peptide acylation, and MBOATs involved in remodeling of phospholipids.

The first subgroup consists of enzymes like ACAT1 which is responsible for the conversion of cholesterol into its' storable form, thus preventing excess cholesterol from building up in the membrane of the ER [127]. It was determined that ACAT1 was a homotetrameric protein that had 9 transmembrane domains [127]. It was also determined that there were two active sites; the first, His460, was in the 7th transmembrane domain and the second, Asn421, was within the 3rd cytosolic loop [128]. It is predicted that the histidine is responsible for catalysis and the asparagine may be involved with acyl-CoA binding and selectivity. In addition, studies showed that this subfamily may be targetable for diseases such as Alzheimer's [129] or atherosclerosis [130]. Within this same subgroup is ACAT2. ACAT2 is similar in function to ACAT1, however it is primary seen in the intestines [131]. Unfortunately, this subfamily has little information about its' membrane topography and requires further investigation. The other subfamily of this subgroup is diglyceride acyltransferase 1 (DGAT1). There are actually two DGAT members known to date, DGAT1 and DGAT2, however DGAT2 is part of a different subfamily of enzymes [132]. DGAT1 is able to catalyze a variety of different fatty acids esters including retinyl esters and triacylglycerol [132]. Unlike ACAT1, DGAT1 is found in the ER [133] and contains 3 transmembrane domains [134]. DGAT1 has been selected as a potential target for both type II diabetes as well as obesity [135, 136]. There is also some research that has shown that hepatitis C requires DGAT1 in order for infection to occur in cells [137]. Unfortunately, there is no crystal structure to this subgroup of MBOAT. The second subgroup consists of enzymes is able to acylated proteins and peptides. This subgroup has enzymes such as porcupine, which acylates serine or cysteine resides on the protein Wingless with either

palmitate or palmitoleate [138, 139]. Interestingly, there are multiple isoforms of Porcupine cDNA, however it is unknown whether or not all of the forms can be acylated. In addition to Porcupine, there is also Sonic hedgehog acyltransferase (HHAT). Much like Porcupine and its' pathway, the HHAT pathway is involved in development in many tissues from organisms such as humans or *Drosophila* [114]. Sonic hedgehog (SHH), the protein, is one of the better-studied ligands for HHAT. SSH undergoes auto-processing, where a C-terminal region is removed [140]. The N-terminal region of SHH is now modified by cholesterol near the new C-terminus [140]. Once SHH has undergone auto-processing, it is palmitoylated by HHAT using palmitoyl-CoA [141, 142]. Most palmitoylation is done by palmitoyl acyltransferases onto a cysteine, however this will be discussed in a later section. In this same subgroup is also the enzyme Ghrelin O-acyltransferase (GOAT) [114]. There is not a lot of information available about these enzymes, however it is known that the third serine of Ghrelin is octanoylated by GOAT and that GOAT does so with specificity towards octanoyl-CoA [143, 144]. The third and final subgroup of the MBOAT family is enzymes that are involved with phospholipid remodeling. Within this subgroup are the lysophospholipid acyltransferases (LPATs). LPATs have been shown to have 4 motifs which are novel to MBOATs through site-directed mutagenesis, 3 of which are involved in substrate binding [145].

For all of the MBOATs, there is minimal structural information available, likely due to the difficult nature of crystallizing membrane bound proteins. There is one structure of an MBOAT, however, DltB, an enzyme responsible for D-alanylation of the cell wall in Gram-positive bacteria [146]. The structure is at 3.15 Å, and shows two, well conserved, active site histidines at the bottom of a funnel in the enzyme [146]. Its' substrate, DltC(Ppant), is similar to an acyl carrier protein (ACP) seen in polyketide and fatty acid synthesis, however instead of a cysteine, there is a serine which the Ppant is attached to [146]. The structure is bound with the one of the phosphates attached to the serine of DltC and does not contain the alanine or rest of the pantetheine arm. Thus, the exact residues involved with the tetrahedral intermediate are only predicted. A few histidines in the active site seem likely to be involved in the tetrahedral intermediate as they are positioned in the tunnel of DltB where DltC binds. It should be noted that DltB is not a typical MBOAT, as most MBOATs utilize acyl-CoAs instead of ACPs [146]. As such, this structure may not provide us with many of the structural details needed for making proper mechanistic hypotheses. Non-hydrolyzable long-chain acyl-CoAs may allow for structures to be solved which can provide this

information. It is possible that non-hydrolyzable analogs may be able to trap MBOATs in one conformation, making it possible to see how this intriguing superfamily is able to act in the cell.

BEAT, AHCT, HCBT, and DAT (BAHD)

The BAHD superfamily is one of the more diverse superfamilies in the acyltransferase class. Enzymes from this superfamily are found in a variety of plants and have been shown to use acetyl, malonyl, benzoyl, hydroxy-cinnamoyl, and some medium to long acyl-CoAs and have all been identified as monomers to date [112]. Interestingly, the BAHD superfamily has sequence identities that range from 25% to 90 % where the family members with the same functionality has the highest similarity and the members with different functionality often having the lowest sequence identity [147, 148]. The enzymes in this superfamily can be split up into five different clades where each clade is differentiated by the substrates used and the conditions when the enzyme is present [149]. The motifs of each clade will be discussed in the next section, however briefly, the first clade consists predominantly of enzymes which modifies phenolic glucosides such as anthocyanins [150]. Clade II is smaller, consisting of two members, and is believed to be involved in extension of long-chain waxes, specifically epicuticular waxes [112]. Clade III mostly uses acetyl-CoA, and has subfamilies including one which modifies alkaloid compounds such as the precursor to morphine, thebaine [151, 152]. Clade IV consists of agmatine cumaroyltransferase (ACT), which interestingly is able to acylate a nitrogen similar to hydroxycinnamoyl/benzoyl-CoA:anthranilate N-hydroxycinnamoyl/benzoyltransferase (HCBT) and A*vena sativa* hydroxycinnamoyl-CoA:hydroxyanthranilate N-hydroxycinnamoyltransferase (AsHHT1) [112]. HCBT and AsHHT1 both belong to clade V, one of the largest clades in the superfamily [112]. Each clade has structural differences which allow for them to act on their differing substrates, however biochemical and structural data is not available for all of the members in each clade.

Despite the similarity differences of some of the superfamily members, there are conserved domains seen within the BAHD superfamily. One of the most interesting conserved domains is the HXXXDG domain found in acyl-CoA utilizing enzymes near the middle of the enzymes [112]. This motif is very similar to the CoA binding motifs of glycerol-acyltransferases and chloramphenicol acetyltransferases. A second motif is found near the C-terminus and has the sequence DFGWG [112]. Both of these motifs have been shown to be important for catalysis, as

mutagenesis studies have seen severely reduced enzyme activity when one or both of these motifs are deleted or modified [153, 154]. Within the clades there are a few structural motifs that are seen that may be unique to the clade. Clade I members, for example, have a relatively common YFGRC motif which has been predicted to likely be involved in substrate binding, however there is insufficient biochemical and structural data to support this yet [112, 155]. ACT from clade III has a slight modification to the DFGWG motif, where the tryptophan has been replaced by a glycine [156]. The first crystal structure of a BAHD member was published in 2005 of vinorine synthase [147]. Unfortunately, this structure did not have any ligands bound, however the active site was seen where the two halves of the enzyme surrounded a solvent channel [147]. The HXXXDG domain was seen directly in the active site and was predicted to deprotonate the nucleophile for attack of the carbonyl [147]. The structure, PDB: 2BGH, also showed that the DFGWG motif was unexpectantly away from the active site and was thusly predicted not to be involved in the catalytic mechanism [147]. Since this structure was solved, there have been a few more structures solved of other BAHD family members. Unfortunately, these structures have hydrolyzed substrates [157], only one substrate [113, 158], or are apo and have modeled in acyl-CoA using molecular modeling [159].

In one such structure, an anthocyanin acyltransferase that utilized malonyl-CoA was solved with malonyl-CoA bound [113]. Initially, this structure seemed promising, however upon closer review, it became apparent that the only hydrogen bond donor to the malonyl-CoA from the enzyme was a histidine, Figure 1.8. While it is possible for a singular residue to be involved in the tetrahedral intermediate, it is somewhat rare. In addition, in order for this to occur, the angle at which the residue involved in stabilization of the tetrahedral intermediate must be almost 180°. In the structure solved, the angle was about 90°, making it highly unlikely to be the sole contributor to stabilization, Figure 1.8. What makes this structure highly interesting is the fact that an aspartic acid residue can be seen four residues away from the histidine, suggesting that these two residues may be involved in deprotonation of the anthocyanin for attack, Figure 1.8. The authors of this paper mention the residue, but they do little other than mention that it is a part of the conserved motif seen in all BAHD family members [113]. After looking at the structure in detail, it is likely that the most likely residues to be involved in the stabilization of the tetrahedral intermediate would be Ser385, Gly386, and Thr387, Figure 1.8. This would likely result in a conformational change or flipping Asp174 so that it would interact with His170. This would allow for the pKa of the histidine to be correct for deprotonation and would make a proper proton shuttle. These conformational
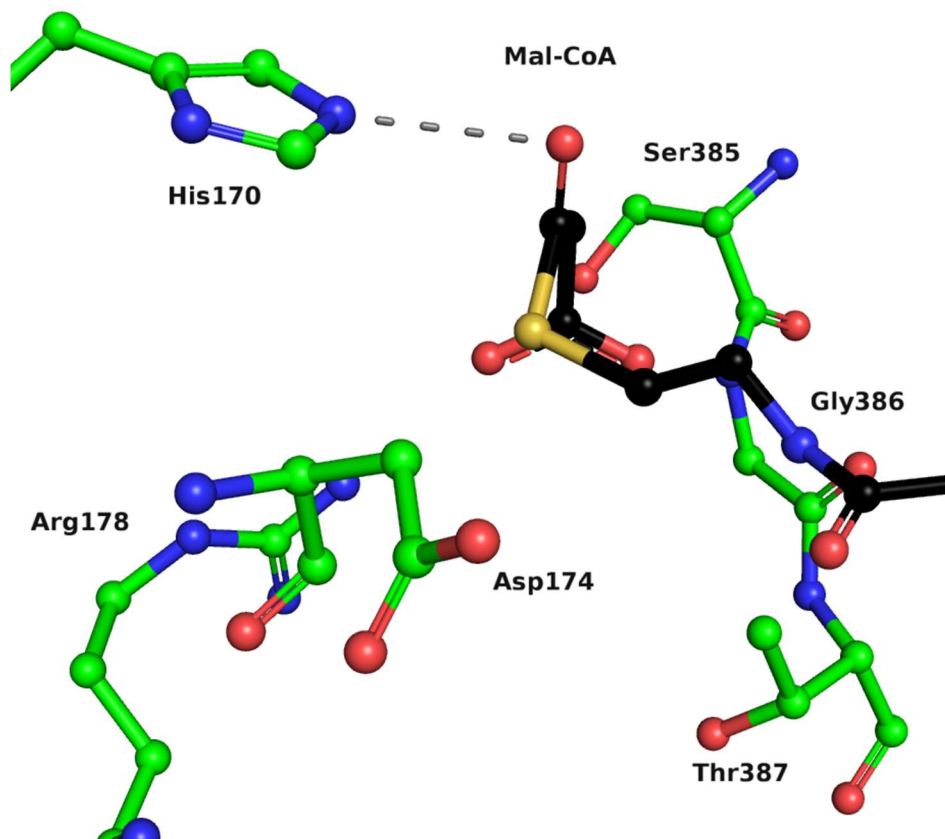
Figure 1.9 Structure of Dm3MaT3 in complex with malonyl-CoA (PDB: 2E1T). Dotted gray lines represent hydrogen bonds. There is a 90° degree between His170 and the thioester carbonyl of malonyl-CoA. Residues labeled are likely to be involved in the stabilization of the tetrahedral intermediate or in deprotonation of the anthocyanin substrate.

changes may also allow for water molecules to enter the active site, resulting in structures similar to the next category of enzymes, chloramphenicol acetyltransferase. This would mean that structurally, these two families of enzymes may be closer related than previously thought.

Chloramphenicol Acetyltransferase (CAT)

Chloramphenicol acetyltransferase (CAT) is an enzyme family that transfers an acetyl group from acetyl-CoA onto the C3 hydroxyl group. This chapter will discuss this family in brief as the third chapter of this thesis will go in much more depth. Interestingly, there have been approximately 16 subgroups which share over 80% sequence identity [160]. In addition, there is a conserved motif of HHxxxDG which is similar to that of the BAHD family and the glycerol

acyltransferase family [161-163]. For type III CAT, His195 is responsible for deprotonation of the C3 hydroxyl which can then attack the thioester carbonyl [163]. There are several structures of CAT, especially CATIII, however most of the structures are apo or have only chloramphenicol bound [164]. When looking at one of these structures, it is apparent that His195 is responsible for deprotonation of the C3 hydroxyl of chloramphenicol, Figure 1.9. Ser148 was predicted to be involved in the tetrahedral intermediate along with a water molecule which is hydrogen bonded to Thr174 [164]. The HHxxxDG motif found in CatIII is the same motif seen in the condensation domain of nonribosomal peptide synthases (NRPS) interestingly [165]. This motif is used in NRPS similarly to CAT, where the second histidine is involved in deprotonation of the nucleophile for attack of the carbonyl [166]. As such, structural information gained from any future structures with either type of enzyme may help provide more information for the other.
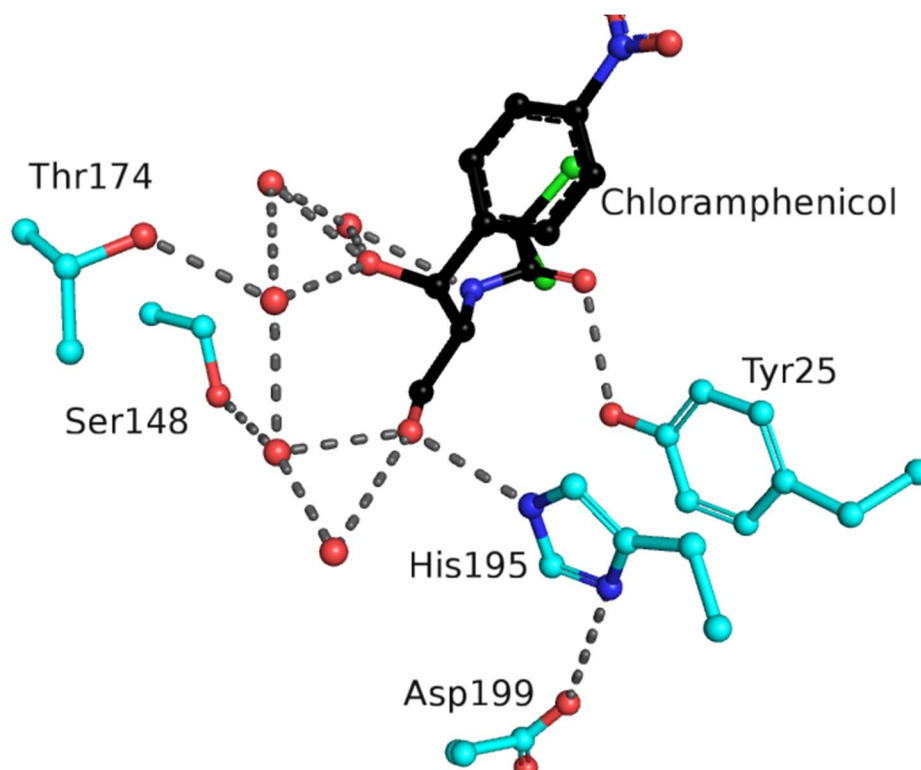
Figure 1.10 Structure of CatIII (PDB: 3CLA) in complex with chloramphenicol. Hydrogen bonds are represented by gray dotted lines. His195 is responsible for deprotonation of the C3 hydroxyl of chloramphenicol and is involved in a proton transfer with Asp199. Ser148 ad a water molecule hydrogen bonded to Thr174 are predicted to be involved in stabilization of the tetrahedral intermediate.

Implications into the Future of Work for Direct Transfer O-Acyltransferases

O-acyltransferases are a fascinating as most of the known enzymes in this family undergo direct transfer from acyl-CoAs to their secondary substrates. Many of the superfamilies/subfamilies within the O-acyltransferase family have limited structural information with substrates bound. While structures with one substrate bound help give some idea as to the residues involved in catalysis, often structures, such as the one in Figure 1.8, show mechanistically irrelevant positions to the substrates that are bound. It is important to remember that some of these acyltransferases use an ordered sequential mechanism, often having conformational changes. As such, one large question that arises is whether conformational changes upon binding of one substrate causes the proper orientation. If this is the case, which it likely is, then structures with one substrate bound will be insufficient to give structural information from which mechanistically relevant hypotheses can be made. While it is possible that soaking crystals with both substrates could help this, it is also more likely that this will not work as the reactivity of acyl-CoAs is high. The use of our analogs, which will be discussed later on in this chapter and chapter 2, will help alleviate these issues as they are similar enough to the natural acyl-CoA substrates, while being far less reactive. In addition, structural determination of MBOATs is traditionally challenging. As our methodologies for structure determination of membrane bound proteins has evolved, it is possible that our analogs may help with structure determination since they may trap MBOATs in a state that will allow for easier crystallization. Lastly, our analogs, as will be shown in chapter 3, will likely be useful for giving supporting or contradicting evidence to hypotheses that have been predicted previously using limited structural information. We will show that our Ac-O-CoA analog was able to do so for CATIII, an enzyme which has had its' structure known for over 20 years.

1.2.3 Ping-pong mechanism and sulfur utilizing acyltransferases are seen in a limited number of acyltransferases

While most acyltransferases utilize sequential mechanisms for acyl transfer, there are a few families within the acyltransferase family which use a ping-pong mechanism instead, Figure 1.1C. These enzymes involved in fatty acid synthase (FAS) and polyketide synthase (PKS) production. The domain which does this within PKS and FAS is the acyltransferase domain (AT). These ATs utilize an acyl-CoA and an ACP for eventual incorporation in the growing polyketide [167]. While

other families such as the cysteine S-palmitoylacyltransferases also have been shown to utilize a ping-pong mechanism, they are beyond the scope of this thesis and will not be discussed.

Acyltransferase Domain of PKS and FAS (AT)

Within PKS and FAS pathways is an enzyme or domain which is known as the acyltransferase (AT). This section will be brief, as it will be discussed more in a later section in this chapter and in chapter 2. Interestingly, many ATs involved in PKSs have been shown to be able incorporate a variety of different malonyl-CoA based substrates into the PKSs of which they are a part [167-169]. As such, structures of ATs may provide useful information for engineering of PKSs. Advances in high-throughput sequencing has allowed for hundreds of ATs to be sequenced, many of which have had their cluster characterized biochemically [170]. Luckily, many ATs share a high level of sequence similarity, upwards of 70 to 80% [171]. Interestingly, when substrate specificity is factored into phylogenetic analysis of ATs, two clades of AT appear based off of whether the AT utilizes malonyl- or methylmalonyl-CoA as a substrate [167, 170, 171]. There are several structures of ATs from PKS or FAS pathways, including two from the 6-deoxyerythronolide B (DEBS) pathway [172, 173], one from disorazole synthase [174], and three of FabD, one apo and one with malonyl-CoA bound from *E. coli* [175, 176] and one from *S. coelicolor* [177]. There is also a structure of an atypical AT from Pks13, a mycobacterial PKS, which utilizes long-chain acyl-CoAs instead of malonyl- or methylmalonyl-CoA [178]. Interestingly, the structure of FabD with malonyl-CoA captured the intermediate stage of the AT, after it had transferred the malonyl moiety to Ser92 [176]. In this structure, the sulfur of CoA is bending back onto itself, however there is a water molecule in the active site that likely is where the sulfur would be if the malonyl-CoA had not transferred onto the serine, Figure 1.10. In order to be able to engineer ATs for future work, which will be discussed in a later section, it is necessary to see the interactions that are made between the AT and substrate before transfer of the malonyl moiety has occurred. Thus, structures of ATs with non-hydrolyzable analogs bound in a mechanistically relevant manner will be invaluable for engineering in this class of enzymes.
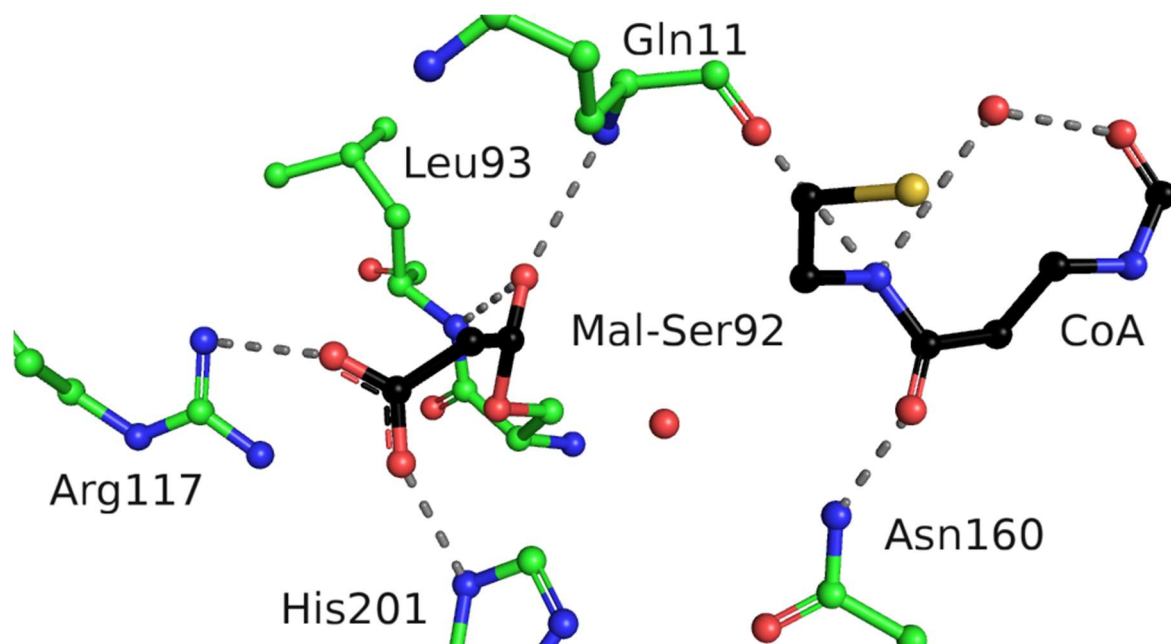
Figure 1.11 Structure of FabD co-crystallized with Mal-CoA (PDB: 2G2Z). Hydrogen bonds are represented by dashed gray lines. Serine 92 has had the malonyl moiety transferred onto it, resulting in the hydrolyzed CoA to be present in the active site. A water molecule resides in between the malonyl-Ser and CoA, likely where the thioester would normally be present if not hydrolyzed.

Ketoacyl Synthases (KS)

KSs are bifunctional, performing both an initial acyl transfer for loading, followed by decarboxylative Claisen-condensation to form the elongated polyketide [2, 179]. This section will be short because much like the AT section above, it will be discussed later on in Chapter 2. PKS and FAS pathways both utilize KS as the main module for forming carbon-carbon bonds. KS does this via a Claisen-condensation reaction where an acetylated cysteine in the active site is reacted with a malonyl/methylmalonyl-CoA molecule [3, 180]. In order to do this, however, the KS must first acylate the active site cysteine using acetyl-CoA. Unfortunately, there are mostly only structures of KSs in the apo form, although there are a couple of structures with long chain fatty acids or long chain-ACPs bound [181]. When looking closer, these experiments took advantage of crosslinking, something which does not accurately represent the reaction that occurs during acyl transfer. As such, it is more desirable to use non-hydrolyzable analogs which can give a better picture of enzyme:substrate complex.

Implications into the Future of Work for Ping-Pong Mechanism and S-acyltransferases

While this will be discussed a little bit more in a couple of sections and chapter 2, there are a few questions which have risen when looking at acyltransferases utilizing a ping-pong mechanism and/or sulfur as a nucleophile. One question for acyltransferases using a ping-pong mechanism is whether how they are able to select for their substrates. The acyltransferases in this family come from PKS and FAS pathways, which will be discussed in further detail in this chapter. Understanding the residues involved in selection of their substrates will be invaluable to the PKS and FAS fields, as this may help guide engineering attempts for the production of drugs. Another important question which arises is the nucleophile involved in the acyltransferases using ping-pong mechanisms. While the ATs in FAS and PKS both utilize a catalytic serine, the cysteine S-palmitoyltransferases utilize a sulfur as the nucleophile involved in attack. It is unknown how much the nucleophile plays a role in the mechanism. Understanding the energies associated with each of the nucleophiles may help give a better understanding to the fundamental differences between each family of acyltransferase. The use of our analogs may help with this endeavor, as energetics could be calculated through a variety of biophysical methodologies with enzymes of differing nucleophiles for comparison.

1.3 Antibiotic resistance has been an issue which has become more prevalent as the number of new drugs discovered has decreased

This section will discuss a group of enzymes which are involved in antibiotic resistance. The information about antibiotic resistance is limited. Thus, understanding our shortcoming will allow us to develop tools to study antibiotic resistance, as well as develop modifications to existing drugs to help synthesize more effective drugs. Antibiotic resistance is a problem which has grown increasingly worrying as the quantity of drugs discovered has decreased consistently for the past couple of decades [182, 183]. Antibiotics work in a number of ways, including inhibition of protein synthesis and disruption of membranes [182]. From around 1950 to 1970, novel classes of antibiotics were discovered in great abundance, giving many hope that infections would be treatable for an extended period of time [184]. Unfortunately, not only was this not true, it became apparent that antibiotic resistance in many bacteria could deplete all of the antibiotics discovered at that time. In addition, drugs discovered or synthesized as antibiotics began to decrease, causing more concern [182, 185]. This section will mainly focus on acyltransferases that play a role in antibiotic resistance.

In order to understand how antibiotic resistance and attempts to rectify resistance have evolved, it is necessary to look at the initial theory that humans were responsible for drug induced toxicity, and how that slowly evolved into the realization that the gut microbiota played a larger role in drug modification, including antibiotics, than we initially thought.

1.3.1 The human acyltransferase theory had flaws which could be explained by bacterial interaction with drugs

Initial studies looking into the effect of acetylation on drugs, especially arylamines, showed that acetylation played a role in the susceptibility of a patient to respond poorly to these drugs. The isoniazid class of arylamines was the first class to be studied as it showed toxicity because of acetylation [186]. It was initially predicted that dosage was responsible for this toxicity, however it was later shown that slower acetylation in patients was responsible for this toxicity [186]. Other drug classes, such as hydrazines, have been shown to induce diseases such as lupus [186]. Many of the studies done during this time led many to believe that human acetyltransferases were responsible for disease onset during therapy from various classes of drugs. Interestingly, a study done in 1972 showed that adding antibiotics such as rifampicin and streptomycin decreased the toxicity and the number of patients that were slow acetylators [187]. This was the one of the first indications that there were other factors that played a role in modification of drugs in humans.

1.3.2 Antibiotic resistance is caused by factors such as introduction into the environment through our waste and improper antibiotic treatment regiments

As the ability to culture cells and sequence genome increased, it became clear that bacteria in our gut had the ability to act on many drugs via acylation. These bacteria are constantly trying to get the edge on the surrounding bacteria so that they can utilize nutrients in their environment. This same principle is true for bacteria in the ground. It is known that many drugs and antibiotics that are taken by humans are found in human waste and that this waste, along with livestock waste, have been shown to introduce many of these drugs and antibiotics into the environment [188, 189]. When this happens, bacteria will uptake these drugs and antibiotics causing bacteria without resistance to antibiotics to be unable to survive. Those which can survive, will flourish, as they are now able to take up more nutrients that before. This same principle is seen in gut bacteria as well. While this is a factor that plays a role in antibiotic resistance, it is not the sole factor. It is important

to remember that bacteria are able to transfer genetic material between each other via plasmids and that selective pressure is induced by antibiotics [190, 191]. As such, bacteria often collect multiple resistance mechanisms, making it increasingly difficult to treat infection. This is made possible, and often worse when the full course of an antibiotic regiment is not taken properly. Studies from the United Kingdom showed that a little more than 11% of participants did not finish their last course of antibiotics, often because they felt better or because they forgot [192]. When a full course of antibiotics is not taken, there are often a few bacteria which slip through the cracks, which slowly accumulate resistance through mutations. Much of the resistance mechanisms and some uptake of drugs that use acyl transfer utilize N-acyltransferases to do so. As such, structural information of these N-acyltransferases may help provide valuable information to combat the increasing spread of antibiotic resistance. While structural information and subsequent design may be useful, there are other methodologies to overcome antibiotic resistance. One question that arises is how bacteria are able to compete for nutrients. Since many antibiotics and drugs are produced by bacteria, which will be discussed more in the following section, it is important to understand how these antibiotics are exported from the bacteria. In addition, it is unknown whether forced competition between bacteria would allow for discovery of new antibiotics. Another newer technology that has shown some promise as a potential fix for antibiotic resistance is the introduction of nanoparticles to the [183]. A few studies have found that the introduction of gold or silver nanoparticles along with vancomycin to vancomycin-resistant *Staphylococcus aureus* helped enhance the antibacterial effect of the vancomycin [193, 194]. Further investigation into how these nanoparticles are able to affect bacteria in conjunction with antibiotics may help alleviate some of the issues seen in antibiotic resistance. In combination with modifications to existing drugs that are guided by structural studies with acyltransferases involved in resistance, it may be possible to overcome antibiotic resistance while new drugs are being developed.

1.4 Polyketide synthase pathways contribute to one third of drugs and utilize the acyltransferase domain to select the substrates for incorporation into the growing polyketide

This section will discuss natural products and their synthesis from polyketide synthase pathways (PKS). These pathways are targets for engineering, as they may allow for the development of a variety of drugs. Previous attempts will be discussed, including the shortcomings

associated with many of these studies. Natural products are widely considered one of the major sources of drugs for the treatment of illnesses and diseases, making up nearly 35% of all drugs when taking into account for slight modifications to existing scaffolding [185]. Despite the increase in knowledge pertaining to PKS pathways, engineering of these pathways has shown little success. As discussed above, there are two domains in PKS pathways which utilize acyl transfer. For the sake of this thesis, the AT will be focused on, as the KS domain utilizes Claisen-condensation in addition to acyl transfer, making it more difficult to study. Structural studies, as mentioned above, are limited and most are in the apo form. As such, most of the work that has been done to understand how the ATs are able to select their substrates has been done through mutagenesis and some limited engineering. In order to understand what may be best for engineering these pathways, it is important to first understand how these pathways work. It is then important to look at what has been done so that the information gained from these studies can be applied to future investigations into engineering.

1.4.1 PKS use a combination of different substrates and domains to give diversity of polyketides formed

Polyketides made from the polyketide synthase pathways utilize a variety of domains to allow for variability in the elongating polyketide [3, 195, 196]. There are a few major domains seen in polyketide synthase pathways besides the KS and AT. It should be noted that these are not all or nothing. Some PKS pathways have all of these domains, while others only include one or two. The domains include: 1) ketoreductases (KR), which reduce the β-keto into a hydroxyl, 2) dehydratases (DH), which dehydrate the hydroxyl into a double bond, resulting in an α,β-unsaturated thioester, and 3) enoylreductases (ER), which saturate the double bond with hydrogens [180]. As a result, there are a diverse number of products which can be created by mixing and matching these domains. There are a variety of important factors to take into consideration when looking at ATs within PKS, including whether they act in cis- or trans-AT pathways. A simplified explanation of this would be that cis-ATs are localized in a specific domain of the module while for trans-ATs, these ATs are found externally from the module, despite the similarities between the two in architecture [167, 180]. In order to engineer these pathways effectively, it will be important to understand the similarities and differences in both types of PKS pathways.

Another way that diversity is seen in PKS pathways is in the substrates that each pathway uses. While most pathways utilize (methyl)malonyl-CoAs as extender units to grow the polyketide, some use unique substrates. There are a few different ATs which also utilize some unnatural extender units such as aminomalonyl-CoA in the production of zwittermycin A [168] or ethylmalonyl-CoA in the production of kirromycin [197], Figure 1.7. In order to better take advantage of these ATs for engineering of pathways, it will be necessary to have structures along with guided mutagenesis to tease apart the ability of these ATs to be used in customized pathways.

1.4.2 Previous AT engineering has resulted in the realization that ATs tend to have the ability to accept a variety of substrates

While the residues involved in catalysis and substrate specificity for ATs is largely understood, the most common approach to alter the specificity is to swap the entire AT domain for a homolog with a different preference in substrate [167]. While this has worked for some DEBS domains where the methylmalonyl-CoA utilizing AT was replaced by the malonyl-CoA utilizing AT domains from rapamycin [198-200], often replacements result in low yields of products [201]. Additionally, some domains appear to be more difficult than others to swap, potentially due to the interactions between the AT and its' flanking neighbors such as the KS [172, 173]. It is also possible that modules downstream of the replaced module are unable to accept the modified substrate, although this possibility seems slightly less likely than the previous [202]. As mentioned previously, there are some ATs which are able to incorporate unique extender units such as aminomalonyl-CoA. Studies published in 2018 showed that the ATs ZmaF and ZmaH from the zwittermycin A pathway were able to incorporate a variety of different substrates [168]. Substrates included the more unique ones such as aminomalonyl-CoA and hydroxymalonyl-CoA to simpler molecules such as malonyl-CoA [168]. As a result, it was argued that ZmaF may be one of the most promiscuous acyltransferases seen in PKS pathways. In terms of potential, this AT may be useful as a potential domain to swap with. All of the factors that led to failures for other ATs would have to be considered, however the ability of this AT to incorporate a variety of substrates may provide an idea into the importance of these factors. In addition to swapping out entire AT domains, some studies have utilized site-directed mutagenesis and hybridization of AT domains in an attempt to engineer these pathways. Interestingly, hybridization attempts with DEBS and rapamycin showed a region on the C-terminus called the 'hypervariable region' which was primarily responsible for

substrate specificity [203]. Unfortunately, there is not much known about the importance of this region for other ATs. Both attempts to domain swap and create hybrids have shown some success, however the difficulty of finding domains which will work as alternatives is often challenging. In addition to this, many of the interactions between the flanking proteins in the pathways and the original AT are unknown, complicating the ability to find proper substitutions.

Site-directed mutagenesis of ATs has the potential to be a less invasive methodology for engineering ATs in PKS pathways. Studies that have done so in the DEBS pathway have done so in a motif that is approximately 100 residues towards the C-terminus of the active site serine [204, 205]. These mutations allowed for promiscuity for both the natural substrate, methylmalonyl-CoA, and the new substrate, malonyl-CoA [204, 205]. One of the most important things to keep in mind when looking at most of the work for quantification of product formation is the fact that a majority of the work done has be done *in vivo*. This fact means that the substrates that may be wanted to incorporate may not be available naturally within the cells. As a result, it is important to test any results from *in vivo* studies, *in vitro* as well. The studies from the DEBS pathway also performed *in vitro* tests and showed decrease AT catalytic activity was likely the reason for incorporation on non-natural extender units, not increased specificity for the non-natural substrate [204, 205]. All of these studies have led to the realization that there is still a vast amount of knowledge needed to truly be able to engineer the ATs within PKS pathways.

1.4.3 In order to engineer ATs effectively, structures with substrates bound and knowledge of the protein-protein interactions needed for interactions between domains is necessary

Now that sequencing has increased rapidly, finding PKS pathways is less challenging than previously. As a result, the amount of ways that ATs that can be engineered via the methods mentioned briefly above are limitless. There are several areas, however, where information is lacking. Some of the more promiscuous ATs have not had their structures solved, resulting in a lack of information as to the specific residues that are involved in substrate interactions. In addition, even for the structures of ATs solved previously, there are no reports of any with substrates in the active site. Without this, it is difficult to determine the specific residues necessary for site-directed mutagenesis attempts. In addition to the lack of structural information for ATs, there is also a lack of knowledge pertaining to the protein-protein interactions between ATs and

both KSs and ACPs. These interactions likely play a large role in substrate specificity, as there are conformational changes that occur upon binding and complex formation. Without structural and biophysical information about the necessary interactions between these different domains, it will be difficult to engineer ATs effectively. This point is incredibly important to keep in mind, as structures alone may not be enough to determine the residues involved in specificity. If binding of the ACP causes large conformational changes, residues within the active site could change vastly, resulting in clashes which could hinder incorporation of the non-natural extender unit into the growing polyketide. This same principle would also apply to interactions between the ACP and KS, as that could also play a role in engineering these pathways properly. As mentioned previously, there are also smaller factors such as the C-terminal 'hypervariable region' which still have not been teased out yet. Mutagenesis and structural studies that focus on this region for a variety of different ATs would likely allow for a better understanding of substrate specificity for some ATs. Determining the residues for substrate specificity is often challenging in ATs, as there are not necessarily conserved residues involved in substrate specificity for each AT, especially in ATs that use a variety of different substrates. As such, computational methods to determine the residues involved in substrate specificity is often ineffective. Despite the lack of structures with substrates bound, there is much hope for the future of engineering of PKS pathways. The use of our non-hydrolyzable analogs may help pave the way for the discovery of residues involved in specificity when used to solve structures of ATs and KSs alike.

1.5 Acyl-CoA analogs used to mimic acetyl- and malonyl-CoA have shown some promise, albeit somewhat limited

This section will discuss the analogs which have been synthesized and how they have been used in initial studies. There have been many several analogs synthesized to help tease apart the mechanistic and structural components of acyl-CoA utilizing enzymes. These range from halo-acyl-CoAs to dethia-CoAs, from acetyl to
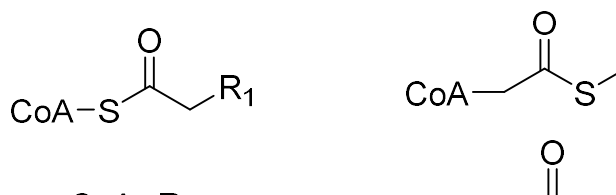
Figure 1.12 Previous analogs of acetyl- and malonyl-CoA utilized in varying studies from protein inhibition to structure-function. R_1 represents haloacyl-CoA analogs. R_2 represents dethia-CoA analogs. R_3 and R_4 represent thioester replacements and are called either an ester (oxygen), amide (nitrogen), or a carbonyl (carbon). Fluorinated versions of each of these analogs are referred to as fluoroacetyl-dethia-CoAs.

larger analogs such as malonyl-CoAs, Figure 1.11. Many of these analogs have been useful as inhibitors of the enzymes they were tested in or as probes for future enzyme studies. At the same time, the amount of information gained from these analogs in x-ray crystallography has been lacking.

1.5.1 Halo acetyl-Coenzyme A analogs have been useful for discovery of acyltransferases, but have been largely ineffective for structure-function studies

Bromine, chlorine, and fluorine are the three primary halogens used in studies with halo acyl-CoAs. The first, bromoacetyl-CoA was used in carnitine O-acetyltransferase as an inactivator of the enzyme [206, 207]. In addition to its' initial use in carnitine O-acetyltransferase, bromoacetyl-CoA was also used to inhibit activity in thiolase [208, 209]. In addition to bromoacetyl-CoA, chloroacetyl-CoA was also used on carnitine O-acetyltransferase initially [207]. It was found to inactivate carnitine O-acetyltransferase, however more interesting studies with chloroacetyl-CoA wouldn't be done till the late 1980s, when it was used in fatty acid synthases from lactating bovine mammary and chicken liver [210, 211]. In these studies, it was found that chloroacetyl-CoA inactivated the FAS rapidly and irreversibly [210, 211]. As a result of the studies of these halo acetyl-CoAs, researchers in the future would utilize their ability to fluorescently tag proteins, pulldown or immobilize substrates, and determine unknown proteins that utilized acetyl-CoA [14, 212].

While chloro- and bromoacetyl-CoA showed some promise for functions such as protein immobilization or fluorescent labeling, fluoroacetyl-CoA was not as successful for these same functions. It should be noted that chloro- and bromoacetyl-CoA were not useful in structure function studies, while fluoroacetyl-CoA showed more promise in this regard. Early studies of fluoroacetyl-CoA showed that the CoA was actually a substrate of enzymes such as acetyl-CoA carboxylase (ACC) [213]. Some studies also showed that the precursor, fluoroacetic acid, could be converted into fluoroacetyl-CoA by acetyl-CoA synthetase (ACS) [213]. Many of these studies also noted that fluoroacetyl-CoA was highly toxic due to a separate reaction where fluoroacetic acid would convert to fluorocitric acid and inhibit the citric acid cycle [213]. This was likely due to the smaller size and higher electronegativity of fluorine, which allowed the atom to be a substitute for hydrogen without reacting. One of the major reasons for the study of fluoroacetyl-CoA was due to the incorporation of fluorine in a variety of drugs such as fluoxetine (Prozac) [213]. While many animals found this analog to be toxic, there were some bacteria that had developed resistance

mechanisms against the analog. One such example was the enzyme fluoroacetyl-CoA thioesterase from *Streptomyces cattleya* [214]. In this study, the authors synthesized a variety of analogs which will be discussed in the next section, as it relates more to that section; however, suffice it to say that this study showed that there were resistance mechanisms in bacteria against analogs of acetyl-CoA like fluoroacetyl-CoA.

1.5.2 Replacements at the thioester have been valuable as inhibitors and may have use structurally in future studies

The thioester carbonyl in acyl-CoAs is a labile bond which makes acyl-CoAs incredibly useful for a variety of chemistries. As a result, many researchers have attempted to make slight alterations to the thioester in order to capture acyltransferases. The major changes seen to the thioester are the substitution of the thioester sulfur to an oxygen (oxygen), nitrogen (amide), or carbon (carbonyl), Figure 1.11 (R_3 and R_4). As mentioned from the previous section, the study with the fluoroacetyl-CoA thioesterase showed synthesis schemes for a few different analogs. This included the fluoro- and acetyl-CoA analogs where the sulfur was replaced as mentioned above. This study was used to look at the differences in binding between the fluoro- and acetyl-CoA analogs in the thioesterase, which showed a 5 to 20 fold difference in K_d [214]. The authors also used the carbon analog to look at dynamics via NMR spectroscopy, showing vital Phe residues that were involved in enzyme selectivity [214]. This study was not the first study to show the usefulness of the acetyl-carba(dethia)-CoA analog, or analogs similar to it. More about the synthesis of the ester and amide analogs of acetyl-CoA will be discussed in chapter 2.

The idea of replacing the thioester sulfur of acyl-CoAs with a carbon has been seen in the literature since the mid-1960s. The first studies used compounds such as Raney nickel to replace the sulfur of CoA with a methyl group [215]. This compound, called desulfoCoA, was then tested in a variety of enzymes, including carnitine acetyltransferase, phosphotransacetylase, citrate synthase, α-ketoglutarate dehydrogenase, β-ketothiolase, and acyl-CoA synthetase [215, 216]. These studies showed that desulfoCoA was a good inhibitor for some enzymes, although not for all of them. With the addition of the acetyl group, studies were able to show that acetyl-carba(dethia)-CoA was also a good inhibitor for enzymes such as citrate synthase [216, 217]. At the same time, there were enzymes where inhibition was poor such as in the case of chloramphenicol acetyltransferase (CAT) [218]. In some cases, such as ACC, acetyl-carba(dethia)-CoA was found to act as a substrate
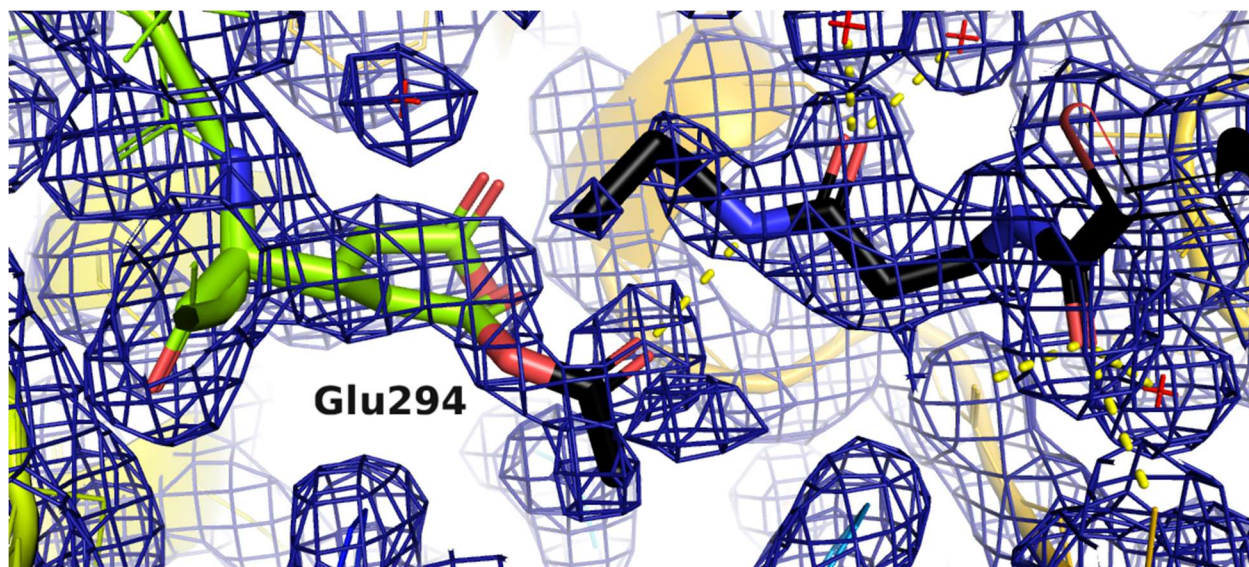
Figure 1.13 CoA-transferase succinyl-CoA:acetate CoA-transferase in complex with acetyl-carba(dethia)-CoA (PDB: 5E5H). Atoms in black come from acetyl-carba(dethia)-CoA while atoms in lime come from the protein. Authors modeled acetyl transfer onto Glu294, although they believe this is likely due to some form of contamination.

[219]. While limited, acetyl-carba(dethia)-CoA was also used in a structure-function study. The study looked at CoA-transferase succinyl-CoA:acetate CoA-transferase, where it found that the acetyl-carba(dethia)-CoA appeared to deacetylate onto Glu294, Figure 1.12 [220]. The authors noted, however, that this acetylation was likely due to contamination of some sort. This study is the only study that has been shown to use any of the acetyl-CoA analogs where the thioester sulfur is the sole atom to be changed to another atom. As a result, there is a lack of structure-function studies which show the usefulness of these analogs.

Lastly, it should be mentioned that a propionyl-phosphopantetheine analog with the sulfur replaced by an amide (nitrogen) and malonyl-CoA analogs where the thioester were replaced with an ester (oxygen), amide (nitrogen), or carbonyl (carbon) have also been reported. While the amount of information gained from these couple of studies is limited, these reports did show that synthesis of these analogs was indeed possible. The propionyl-amido(dethia)-phosphopantetheine analog was used in a study with a KS, DpsC [221]. Unfortunately, this structural study resulted in a structure with weak density. As a result, it is hard to make any hard conclusions about this analog, however it is believed that phosphopantetheine binds weaker than the CoA or the ACP. This could explain the results that were seen in this study. The first report of the malonyl-CoA analogs utilized

these analogs to try and trap PKS intermediates in stilbene synthase [222] while the second utilized carboxymethylproline synthase [223]. The first did not use malonyl-aza(dethia)-CoA, however both papers used the malonyl-oxa(dethia)-CoA and malonyl-carba(dethia)-CoA. In addition, both utilized the technique of MS/MS to determine if there were intermediates or products that had formed [222, 223]. The synthetic routes for both studies were somewhat complicated and expensive, however. In addition, the amount of information gleaned into the usefulness of these analogs was limited to MS/MS based studies. As a result, more information about both the acetyl- and malonyl-CoA analogs are needed in order to determine their usefulness in a variety of different studies. More about the synthesis of the ester and amide malonyl-CoA analogs will be discussed in chapter 2.

1.6   We are contributing more efficient syntheses analogs which will be mechanistically relevant and stable for structure-function studies

In the following chapters, I will demonstrate that the acetyl- and malonyl-CoA analogs where the thioester has been replaced by an ester or amide have been undervalued. I will show that we have successfully synthesized these analogs in higher yields and in a more efficient manner. In addition, I will show that these analogs are mostly stable in a couple of enzymes mentioned above. The usefulness of these analogs will be shown via a combination of enzymology and structure studies. The research provided in this thesis will be valuable for other labs looking to study acyltransferases that utilize acetyl- and malonyl-CoA as their natural substrate.

Synthesis of these analogs has been improved by replacing traditional methods of acylation of the protected pantetheine analog with acetic anhydride for the acetyl-CoA analogs and Meldrum's acid for the malonyl-CoA analogs. In addition, the synthesis of the CoA analogs from the pantetheine analogs have been improved to lessen the amount of ATP needed with the addition of an ATP regeneration system. This allows for simpler purification and allows for reagents to be saved that normally would be in excess. In addition, this helps provide higher yields as it is able to take advantage of Le Chatlier's principle to push the reaction close to completion.

The study of these analogs, along with acetyl-carba(dethia)-CoA, have also resulted in interesting results in enzymes such as 3-oxoacyl-[acyl-carrier-protein] synthase 3 (KasIII), malonyl CoA-acyl carrier protein transacylase (FabD), and chloramphenicol acetyltransferase type III (CATIII). These analogs, with the exception of acetyl-oxa(dethia)-CoA in KasIII have shown

to be stable within the enzymes listed previously. Interestingly, although acetyl-oxa(dethia)-CoA showed some ability to act as a substrate in KasIII, it was used to solve structures of CatIII with analog bound. This shows that this analog may be useful for enzymes that utilize oxygen as their nucleophile. Future structure-function studies are needed to determine the full effectiveness of these analogs, especially with the malonyl-CoA analogs. While these studies are currently underway, they have yet to provide structures to show their full potential. In addition, structures with acetyl-aza(dethia)-CoA and acetyl-carba(dethia)-CoA have resulted in weak density for both analogs, suggesting that optimization of these conditions is necessary.

1.7   References

[1] Witkowski, A., Joshi, A. K., and Smith, S. (2002) Mechanism of the beta-ketoacyl synthase reaction catalyzed by the animal fatty acid synthase, *Biochemistry 41*, 10877-10887.

[2] Staunton, J., and Weissman, K. J. (2001) Polyketide biosynthesis: a millennium review, *Nat Prod Rep 18*, 380-416.

[3] Lohman, J. R., Ma, M., Osipiuk, J., Nocek, B., Kim, Y., Chang, C., Cuff, M., Mack, J., Bigelow, L., Li, H., Endres, M., Babnigg, G., Joachimiak, A., Phillips, G. N., Jr., and Shen, B. (2015) Structural and evolutionary relationships of "AT-less" type I polyketide synthase ketosynthases, *Proc Natl Acad Sci U S A 112*, 12693-12698.

[4] Ramirez, M. S., and Tolmasky, M. E. (2010) Aminoglycoside modifying enzymes, *Drug Resist Updat 13*, 151-171.

[5] Shaw, W. V. (2008) Chloramphenicol Acetyltransferase: Enzymology and Molecular Biology, *Critical Reviews in Biochemistry 14*, 1-46.

[6] Yadav, M., Verma, M. K., and Chauhan, N. S. (2018) A review of metabolic potential of human gut microbiome in human nutrition, *Arch Microbiol 200*, 203-217.

[7] Rowland, I., Gibson, G., Heinken, A., Scott, K., Swann, J., Thiele, I., and Tuohy, K. (2018) Gut microbiota functions: metabolism of nutrients and other food components, *Eur J Nutr 57*, 1-24.

[8] Roth, S. Y., Denu, J. M., and Allis, C. D. (2001) Histone acetyltransferases, *Annu Rev Biochem 70*, 81-120.

[9] Favrot, L., Blanchard, J. S., and Vergnolle, O. (2016) Bacterial GCN5-Related N-Acetyltransferases: From Resistance to Regulation, *Biochemistry 55*, 989-1002.

[10] Rottig, A., and Steinbuchel, A. (2013) Acyltransferases in bacteria, *Microbiol Mol Biol Rev 77*, 277-321.

[11] Hupe, D. J., and Jencks, W. P. (1977) Nonlinear Structure-Reactivity Correlations - Acyl Transfer between Sulfur and Oxygen Nucleophiles, *Journal of the American Chemical Society 99*, 451-464.

[12] Magnet, S., and Blanchard, J. S. (2005) Molecular insights into aminoglycoside action and resistance, *Chem Rev 105*, 477-498.

[13] Salah Ud-Din, A. I., Tikhomirova, A., and Roujeinikova, A. (2016) Structure and Functional Diversity of GCN5-Related N-Acetyltransferases (GNAT), *Int J Mol Sci 17*.

[14] Yu, M., de Carvalho, L. P. S., Sun, G. X., and Blanchard, J. S. (2006) Activity-based substrate profiling for Gcn5-related N-acetyltransferases: The use of chloroacetyl-coenzyme A to identify protein substrates, *Journal of the American Chemical Society 128*, 15356-15357.

[15] Gu, L., Geders, T. W., Wang, B., Gerwick, W. H., Hakansson, K., Smith, J. L., and Sherman, D. H. (2007) GNAT-like strategy for polyketide chain initiation, *Science 318*, 970-974.

[16] Vetting, M. W., LP, S. d. C., Yu, M., Hegde, S. S., Magnet, S., Roderick, S. L., and Blanchard, J. S. (2005) Structure and functions of the GNAT superfamily of acetyltransferases, *Arch Biochem Biophys 433*, 212-226.

[17] Tanner, K. G., Trievel, R. C., Kuo, M. H., Howard, R. M., Berger, S. L., Allis, C. D., Marmorstein, R., and Denu, J. M. (1999) Catalytic mechanism and function of invariant glutamic acid 173 from the histone acetyltransferase GCN5 transcriptional coactivator, *J Biol Chem 274*, 18157-18160.

[18] De Angelis, J., Gastel, J., Klein, D. C., and Cole, P. A. (1998) Kinetic analysis of the catalytic mechanism of serotonin N-acetyltransferase (EC 2.3.1.87), *J Biol Chem 273*, 3045-3050.

[19] Rojas, J. R., Trievel, R. C., Zhou, J., Mo, Y., Li, X., Berger, S. L., Allis, C. D., and Marmorstein, R. (1999) Structure of Tetrahymena GCN5 bound to coenzyme A and a histone H3 peptide, *Nature 401*, 93-98.

[20] Hickman, A. B., Namboodiri, M. A. A., Klein, D. C., and Dyda, F. (1999) The structural basis of ordered substrate binding by serotonin N-acetyltransferase: Enzyme complex at 1.8 angstrom resolution with a bisubstrate analog, *Cell 97*, 361-369.

[21] Jana, S., and Deb, J. K. (2006) Molecular understanding of aminoglycoside action and resistance, *Appl Microbiol Biotechnol 70*, 140-150.

[22] Magalhaes, M. L., and Blanchard, J. S. (2005) The kinetic mechanism of AAC3-IV aminoglycoside acetyltransferase from Escherichia coli, *Biochemistry 44*, 16275-16283.

[23] Vetting, M. W., Hegde, S. S., Javid-Majd, F., Blanchard, J. S., and Roderick, S. L. (2002) Aminoglycoside 2'-N-acetyltransferase from Mycobacterium tuberculosis in complex with coenzyme A and aminoglycoside substrates, *Nat Struct Biol 9*, 653-658.

[24] Smith, C. A., Toth, M., Weiss, T. M., Frase, H., and Vakulenko, S. B. (2014) Structure of the bifunctional aminoglycoside-resistance enzyme AAC(6')-Ie-APH(2")-Ia revealed by crystallographic and small-angle X-ray scattering analysis, *Acta Crystallogr D Biol Crystallogr 70*, 2754-2764.

[25] Vetting, M. W., Park, C. H., Hegde, S. S., Jacoby, G. A., Hooper, D. C., and Blanchard, J. S. (2008) Mechanistic and structural analysis of aminoglycoside N-acetyltransferase AAC(6')-Ib and its bifunctional, fluoroquinolone-active AAC(6')-Ib-cr variant, *Biochemistry 47*, 9825-9835.

[26] Magalhaes, M. L., Vetting, M. W., Gao, F., Freiburger, L., Auclair, K., and Blanchard, J. S. (2008) Kinetic and structural analysis of bisubstrate inhibition of the Salmonella enterica aminoglycoside 6'-N-acetyltransferase, *Biochemistry 47*, 579-584.

[27] Burk, D. L., Xiong, B., Breitbach, C., and Berghuis, A. M. (2005) Structures of aminoglycoside acetyltransferase AAC(6')-Ii in a novel crystal form: structural and normal-mode analyses, *Acta Crystallogr D Biol Crystallogr 61*, 1273-1279.

[28] Draker, K. A., and Wright, G. D. (2004) Molecular mechanism of the enterococcal aminoglycoside 6'-N-acetyltransferase': role of GNAT-conserved residues in the chemistry of antibiotic inactivation, *Biochemistry 43*, 446-454.

[29] Draker, K. A., Northrop, D. B., and Wright, G. D. (2003) Kinetic mechanism of the GCN5-related chromosomal aminoglycoside acetyltransferase AAC(6')-Ii from Enterococcus faecium: evidence of dimer subunit cooperativity, *Biochemistry 42*, 6565-6574.

[30] Gao, F., Yan, X., Shakya, T., Baettig, O. M., Ait-Mohand-Brunet, S., Berghuis, A. M., Wright, G. D., and Auclair, K. (2006) Synthesis and structure-activity relationships of truncated bisubstrate inhibitors of aminoglycoside 6'-N-acetyltransferases, *J Med Chem 49*, 5273-5281.

[31] Wolf, E., Vassilev, A., Makino, Y., Sali, A., Nakatani, Y., and Burley, S. K. (1998) Crystal structure of a GCN5-related N-acetyltransferase: Serratia marcescens aminoglycoside 3-N-acetyltransferase, *Cell 94*, 439-449.

[32] Klein, D. C. (2007) Arylalkylamine N-acetyltransferase: "the Timezyme", *J Biol Chem 282*, 4233-4237.

[33] Obsil, T., Ghirlando, R., Klein, D. C., Ganguly, S., and Dyda, F. (2001) Crystal Structure of the 14-3-3ζ:Serotonin N-Acetyltransferase Complex, *Cell 105*, 257-267.

[34] Wolf, E., De Angelis, J., Khalil, E. M., Cole, P. A., and Burley, S. K. (2002) X-ray crystallographic studies of serotonin N-acetyltransferase catalysis and inhibition, *J Mol Biol 317*, 215-224.

[35] Iyer, L. M., Aravind, L., Coon, S. L., Klein, D. C., and Koonin, E. V. (2004) Evolution of cell-cell signaling in animals: did late horizontal gene transfer from bacteria have a role?, *Trends Genet 20*, 292-299.

[36] Cheng, K. C., Liao, J. N., and Lyu, P. C. (2012) Crystal structure of the dopamine N-acetyltransferase-acetyl-CoA complex provides insights into the catalytic mechanism, *Biochem J 446*, 395-404.

[37] Hickman, A. B., Klein, D. C., and Dyda, F. (1999) Melatonin biosynthesis: The structure of serotonin N-acetyltransferase at 2.5 angstrom resolution suggests a catalytic mechanism, *Mol Cell 3*, 23-32.

[38] Hintermann, E., Grieder, N. C., Amherd, R., Brodbeck, D., and Meyer, U. A. (1996) Cloning of an arylalkylamine N-acetyltransferase (aaNAT1) from Drosophila melanogaster expressed in the nervous system and the gut, *Proc Natl Acad Sci U S A 93*, 12315-12320.

[39] Coon, S. L., Begay, V., Deurloo, D., Falcon, J., and Klein, D. C. (1999) Two arylalkylamine N-acetyltransferase genes mediate melatonin synthesis in fish, *J Biol Chem 274*, 9076-9082.

[40] Khalil, E. M., and Cole, P. A. (1998) A potent inhibitor of the melatonin rhythm enzyme, *Journal of the American Chemical Society 120*, 6195-6196.

[41] Dempsey, D. R., Jeffries, K. A., Anderson, R. L., Carpenter, A. M., Rodriquez Opsina, S., and Merkler, D. J. (2014) Identification of an arylalkylamine N-acyltransferase from Drosophila melanogaster that catalyzes the formation of long-chain N-acylserotonins, *FEBS Lett 588*, 594-599.

[42] Voisin, P., Namboodiri, M. A., and Klein, D. C. (1984) Arylamine N-acetyltransferase and arylalkylamine N-acetyltransferase in the mammalian pineal gland, *J Biol Chem 259*, 10913-10918.

[43] Sim, E., Walters, K., and Boukouvala, S. (2008) Arylamine N-acetyltransferases: from structure to function, *Drug Metab Rev 40*, 479-510.

[44] Sim, E., Abuhammad, A., and Ryan, A. (2014) Arylamine N-acetyltransferases: from drug metabolism and pharmacogenetics to drug discovery, *Br J Pharmacol 171*, 2705-2725.

[45] Riddle, B., and Jencks, W. P. (1971) Acetyl-coenzyme A: arylamine N-acetyltransferase. Role of the acetyl-enzyme intermediate and the effects of substituents on the rate, *J Biol Chem 246*, 3250-3258.

[46] Watanabe, M., Sofuni, T., and Nohmi, T. (1992) Involvement of Cys69 residue in the catalytic mechanism of N-hydroxyarylamine O-acetyltransferase of Salmonella typhimurium. Sequence similarity at the amino acid level suggests a common catalytic mechanism of acetyltransferase for S. typhimurium and higher organisms, *J Biol Chem 267*, 8429-8436.

[47] Sinclair, J., and Sim, E. (1997) A fragment consisting of the first 204 amino-terminal amino acids of human arylamine N-acetyltransferase one (NAT1) and the first transacetylation step of catalysis, *Biochemical Pharmacology 53*, 11-16.

[48] Payton, M., Gifford, C., Schartau, P., Hagemeier, C., Mushtaq, A., Lucas, S., Pinter, K., and Sim, E. (2001) Evidence towards the role of arylamine N-acetyltransferase in Mycobacterium smegmatis and development of a specific antiserum against the homologous enzyme of Mycobacterium tuberculosis, *Microbiology 147*, 3295-3302.

[49] Bhakta, S., Besra, G. S., Upton, A. M., Parish, T., Sholto-Douglas-Vernon, C., Gibson, K. J., Knutton, S., Gordon, S., DaSilva, R. P., Anderton, M. C., and Sim, E. (2004) Arylamine N-acetyltransferase is required for synthesis of mycolic acids and complex lipids in Mycobacterium bovis BCG and represents a novel drug target, *J Exp Med 199*, 1191-1199.

[50] Ferguson, R. J., Doll, M. A., Rustan, T. D., and Hein, D. W. (1996) Cloning, expression, and functional characterization of rapid and slow acetylator polymorphic N-acetyl-transferase encoding genes of the Syrian hamster, *Pharmacogenetics 6*, 55-66.

[51] Wu, H., Dombrovsky, L., Tempel, W., Martin, F., Loppnau, P., Goodfellow, G. H., Grant, D. M., and Plotnikov, A. N. (2007) Structural basis of substrate-binding specificity of human arylamine N-acetyltransferases, *J Biol Chem 282*, 30189-30197.

[52] Lower, G. M., Jr., Nilsson, T., Nelson, C. E., Wolf, H., Gamsky, T. E., and Bryan, G. T. (1979) N-acetyltransferase phenotype and risk in urinary bladder cancer: approaches in molecular epidemiology. Preliminary results in Sweden and Denmark, *Environ Health Perspect 29*, 71-79.

[53] Sandy, J., Mushtaq, A., Holton, S. J., Schartau, P., Noble, M. E., and Sim, E. (2005) Investigation of the catalytic triad of arylamine N-acetyltransferases: essential residues required for acetyl transfer to arylamines, *Biochem J 390*, 115-123.

[54] Carper, S. W., Willis, D. G., Manning, K. A., and Gerner, E. W. (1991) Spermidine acetylation in response to a variety of stresses in Escherichia coli, *J Biol Chem 266*, 12439-12441.

[55] Limsuwun, K., and Jones, P. G. (2000) Spermidine acetyltransferase is required to prevent spermidine toxicity at low temperatures in Escherichia coli, *Journal of Bacteriology 182*, 5373-5380.

[56] Madeo, F., Eisenberg, T., Pietrocola, F., and Kroemer, G. (2018) Spermidine in health and disease, *Science 359*.

[57] Pegg, A. E. (2016) Functions of Polyamines in Mammals, *J Biol Chem 291*, 14904-14912.

[58] Matsui, I., Wiegand, L., and Pegg, A. E. (1981) Properties of Spermidine N-Acetyltransferase from Livers of Rats Treated with Carbon-Tetrachloride and Its Role in the Conversion of Spermidine into Putrescine, *Journal of Biological Chemistry 256*, 2454-2459.

[59] Forouhar, F., Lee, I. S., Vujcic, J., Vujcic, S., Shen, J., Vorobiev, S. M., Xiao, R., Acton, T. B., Montelione, G. T., Porter, C. W., and Tong, L. (2005) Structural and functional evidence for Bacillus subtilis PaiA as a novel N1-spermidine/spermine acetyltransferase, *J Biol Chem 280*, 40328-40336.

[60] Filippova, E. V., Kuhn, M. L., Osipiuk, J., Kiryukhina, O., Joachimiak, A., Ballicora, M. A., and Anderson, W. F. (2015) A novel polyamine allosteric site of SpeG from Vibrio cholerae is revealed by its dodecameric structure, *J Mol Biol 427*, 1316-1334.

[61] Burk, D. L., Ghuman, N., Wybenga-Groot, L. E., and Berghuis, A. M. (2003) X-ray structure of the AAC(6')-Ii antibiotic resistance enzyme at 1.8 A resolution; examination of oligomeric arrangements in GNAT superfamily members, *Protein Sci 12*, 426-437.

[62] Filippova, E. V., Weigand, S., Osipiuk, J., Kiryukhina, O., Joachimiak, A., and Anderson, W. F. (2015) Substrate-Induced Allosteric Change in the Quaternary Structure of the Spermidine N-Acetyltransferase SpeG, *J Mol Biol 427*, 3538-3553.

[63] Montemayor, E. J., and Hoffman, D. W. (2008) The crystal structure of spermidine/spermine N1-acetyltransferase in complex with spermine provides insights into substrate binding and catalysis, *Biochemistry 47*, 9145-9153.

[64] Hegde, S. S., Chandler, J., Vetting, M. W., Yu, M., and Blanchard, J. S. (2007) Mechanistic and structural analysis of human spermidine/spermine N1-acetyltransferase, *Biochemistry 46*, 7187-7195.

[65] Parthun, M. R. (2007) Hat1: the emerging cellular roles of a type B histone acetyltransferase, *Oncogene 26*, 5319-5328.

[66] Lee, K. K., and Workman, J. L. (2007) Histone acetyltransferase complexes: one size doesn't fit all, *Nat Rev Mol Cell Biol 8*, 284-295.

[67] Dutnall, R. N., Tafrov, S. T., Sternglanz, R., and Ramakrishnan, V. (1998) Structure of the histone acetyltransferase Hat1: a paradigm for the GCN5-related N-acetyltransferase superfamily, *Cell 94*, 427-438.

[68] Yang, X., Li, L., Liang, J., Shi, L., Yang, J., Yi, X., Zhang, D., Han, X., Yu, N., and Shang, Y. (2013) Histone acetyltransferase 1 promotes homologous recombination in DNA repair by facilitating histone turnover, *J Biol Chem 288*, 18271-18282.

[69] Wu, H., Moshkina, N., Min, J., Zeng, H., Joshua, J., Zhou, M. M., and Plotnikov, A. N. (2012) Structural basis for substrate specificity and catalysis of human histone acetyltransferase 1, *Proc Natl Acad Sci U S A 109*, 8925-8930.

[70] Smith, E. R., Eisen, A., Gu, W. G., Sattah, M., Pannuti, A., Zhou, J. X., Cook, R. G., Lucchesi, J. C., and Allis, C. D. (1998) ESA1 is a histone acetyltransferase that is essential for growth in yeast, *P Natl Acad Sci USA 95*, 3561-3565.

[71] Clarke, A. S., Lowell, J. E., Jacobson, S. J., and Pillus, L. (1999) Esa1p is an essential histone acetyltransferase required for cell cycle progression, *Mol Cell Biol 19*, 2515-2526.

[72] Babiarz, J. E., Halley, J. E., and Rine, J. (2006) Telomeric heterochromatin boundaries require NuA4-dependent acetylation of histone variant H2A.Z in Saccharomyces cerevisiae, *Genes Dev 20*, 700-710.

[73] Keogh, M. C., Mennella, T. A., Sawa, C., Berthelet, S., Krogan, N. J., Wolek, A., Podolny, V., Carpenter, L. R., Greenblatt, J. F., Baetz, K., and Buratowski, S. (2006) The Saccharomyces cerevisiae histone H2A variant Htz1 is acetylated by NuA4, *Genes Dev 20*, 660-665.

[74] Decker, P. V., Yu, D. Y., Iizuka, M., Qiu, Q., and Smith, M. M. (2008) Catalytic-site mutations in the MYST family histone Acetyltransferase Esa1, *Genetics 178*, 1209-1220.

[75] Yan, Y., Barlev, N. A., Haley, R. H., Berger, S. L., and Marmorstein, R. (2000) Crystal Structure of Yeast Esa1 Suggests a Unified Mechanism for Catalysis and Substrate Binding by Histone Acetyltransferases, *Mol Cell 6*, 1195-1205.

[76] Yan, Y., Harper, S., Speicher, D. W., and Marmorstein, R. (2002) The catalytic mechanism of the ESA1 histone acetyltransferase involves a self-acetylated intermediate, *Nat Struct Biol 9*, 862-869.

[77] Yuan, H., Rossetto, D., Mellert, H., Dang, W., Srinivasan, M., Johnson, J., Hodawadekar, S., Ding, E. C., Speicher, K., Abshiru, N., Perry, R., Wu, J., Yang, C., Zheng, Y. G., Speicher, D. W., Thibault, P., Verreault, A., Johnson, F. B., Berger, S. L., Sternglanz, R., McMahon, S. B., Cote, J., and Marmorstein, R. (2012) MYST protein acetyltransferase activity requires active site lysine autoacetylation, *EMBO J 31*, 58-70.

[78] Berndsen, C. E., Albaugh, B. N., Tan, S., and Denu, J. M. (2007) Catalytic mechanism of a MYST family histone acetyltransferase, *Biochemistry 46*, 623-629.

[79] Pollard, K. J., and Peterson, C. L. (1997) Role for ADA/GCN5 products in antagonizing chromatin-mediated transcriptional repression, *Mol Cell Biol 17*, 6212-6222.

[80] Kikuchi, H., Takami, Y., and Nakayama, T. (2005) GCN5: a supervisor in all-inclusive control of vertebrate cell cycle progression through transcription regulation of various cell cycle-related genes, *Gene 347*, 83-97.

[81] Xu, W., Edmondson, D. G., Evrard, Y. A., Wakamiya, M., Behringer, R. R., and Roth, S. Y. (2000) Loss of Gcn5l2 leads to increased apoptosis and mesodermal defects during mouse development, *Nat Genet 26*, 229-232.

[82] Hinnebusch, A. G., and Fink, G. R. (1983) Positive regulation in the general amino acid control of Saccharomyces cerevisiae, *Proc Natl Acad Sci U S A 80*, 5374-5378.

[83] Trievel, R. C., Rojas, J. R., Sterner, D. E., Venkataramani, R. N., Wang, L., Zhou, J., Allis, C. D., Berger, S. L., and Marmorstein, R. (1999) Crystal structure and mechanism of histone acetylation of the yeast GCN5 transcriptional coactivator, *Proc Natl Acad Sci U S A 96*, 8931-8936.

[84] Schuetz, A., Bernstein, G., Dong, A., Antoshenko, T., Wu, H., Loppnau, P., Bochkarev, A., and Plotnikov, A. N. (2007) Crystal structure of a binary complex between human GCN5 histone acetyltransferase domain and acetyl coenzyme A, *Proteins 68*, 403-407.

[85] Lin, Y., Fletcher, C. M., Zhou, J., Allis, C. D., and Wagner, G. (1999) Solution structure of the catalytic domain of GCN5 histone acetyltransferase bound to coenzyme A, *Nature 400*, 86-89.

[86] Clements, A., Poux, A. N., Lo, W.-S., Pillus, L., Berger, S. L., and Marmorstein, R. (2003) Structural Basis for Histone and Phosphohistone Binding by the GCN5 Histone Acetyltransferase, *Mol Cell 12*, 461-473.

[87] Poux, A. N., Cebrat, M., Kim, C. M., Cole, P. A., and Marmorstein, R. (2002) Structure of the GCN5 histone acetyltransferase bound to a bisubstrate inhibitor, *Proc Natl Acad Sci U S A 99*, 14065-14070.

[88] Sampath, V., Liu, B., Tafrov, S., Srinivasan, M., Rieger, R., Chen, E. I., and Sternglanz, R. (2013) Biochemical characterization of Hpa2 and Hpa3, two small closely related acetyltransferases from Saccharomyces cerevisiae, *J Biol Chem 288*, 21506-21513.

[89] Angus-Hill, M. L., Dutnall, R. N., Tafrov, S. T., Sternglanz, R., and Ramakrishnan, V. (1999) Crystal structure of the histone acetyltransferase Hpa2: A tetrameric member of the Gcn5-related N-acetyltransferase superfamily, *J Mol Biol 294*, 1311-1325.

[90] Wright, M. H., Heal, W. P., Mann, D. J., and Tate, E. W. (2010) Protein myristoylation in health and disease, *J Chem Biol 3*, 19-35.

[91] Towler, D. A., Adams, S. P., Eubanks, S. R., Towery, D. S., Jackson-Machelski, E., Glaser, L., and Gordon, J. I. (1988) Myristoyl CoA:protein N-myristoyltransferase activities from rat liver and yeast possess overlapping yet distinct peptide substrate specificities, *J Biol Chem 263*, 1784-1790.

[92] Rudnick, D. A., McWherter, C. A., Rocque, W. J., Lennon, P. J., Getman, D. P., and Gordon, J. I. (1991) Kinetic and structural evidence for a sequential ordered Bi Bi mechanism of catalysis by Saccharomyces cerevisiae myristoyl-CoA:protein N-myristoyltransferase, *J Biol Chem 266*, 9732-9739.

[93] Moriya, K., Nagatoshi, K., Noriyasu, Y., Okamura, T., Takamitsu, E., Suzuki, T., and Utsumi, T. (2013) Protein N-myristoylation plays a critical role in the endoplasmic reticulum morphological change induced by overexpression of protein Lunapark, an integral membrane protein of the endoplasmic reticulum, *PLoS One 8*, e78235.

[94] Maurer-Stroh, S., and Eisenhaber, F. (2004) Myristoylation of viral and bacterial proteins, *Trends Microbiol 12*, 178-185.

[95] Doerig, C., Rayner, J. C., Scherf, A., and Tobin, A. B. (2015) Post-translational protein modifications in malaria parasites, *Nat Rev Microbiol 13*, 160-172.

[96] Thinon, E., Serwa, R. A., Broncel, M., Brannigan, J. A., Brassat, U., Wright, M. H., Heal, W. P., Wilkinson, A. J., Mann, D. J., and Tate, E. W. (2014) Global profiling of co- and post-translationally N-myristoylated proteomes in human cells, *Nat Commun 5*, 4919.

[97] Weston, S. A., Camble, R., Colls, J., Rosenbrock, G., Taylor, I., Egerton, M., Tucker, A. D., Tunnicliffe, A., Mistry, A., Mancia, F., de la Fortelle, E., Irwin, J., Bricogne, G., and Pauptit, R. A. (1998) Crystal structure of the anti-fungal target N-myristoyl transferase, *Nat Struct Biol 5*, 213-221.

[98] Wu, J., Tao, Y., Zhang, M., Howard, M. H., Gutteridge, S., and Ding, J. (2007) Crystal structures of Saccharomyces cerevisiae N-myristoyltransferase with bound myristoyl-CoA and inhibitors reveal the functional roles of the N-terminal region, *J Biol Chem 282*, 22185-22194.

[99] Rackham, M. D., Brannigan, J. A., Rangachari, K., Meister, S., Wilkinson, A. J., Holder, A. A., Leatherbarrow, R. J., and Tate, E. W. (2014) Design and synthesis of high affinity inhibitors of Plasmodium falciparum and Plasmodium vivax N-myristoyltransferases directed by ligand efficiency dependent lipophilicity (LELP), *J Med Chem 57*, 2773-2788.

[100] Yu, Z., Brannigan, J. A., Moss, D. K., Brzozowski, A. M., Wilkinson, A. J., Holder, A. A., Tate, E. W., and Leatherbarrow, R. J. (2012) Design and synthesis of inhibitors of Plasmodium falciparum N-myristoyltransferase, a promising target for antimalarial drug discovery, *J Med Chem 55*, 8879-8890.

[101] Goncalves, V., Brannigan, J. A., Whalley, D., Ansell, K. H., Saxty, B., Holder, A. A., Wilkinson, A. J., Tate, E. W., and Leatherbarrow, R. J. (2012) Discovery of Plasmodium vivax N-myristoyltransferase inhibitors: screening, synthesis, and structural characterization of their binding mode, *J Med Chem 55*, 3578-3582.

[102] Wright, M. H., Clough, B., Rackham, M. D., Rangachari, K., Brannigan, J. A., Grainger, M., Moss, D. K., Bottrill, A. R., Heal, W. P., Broncel, M., Serwa, R. A., Brady, D., Mann, D. J., Leatherbarrow, R. J., Tewari, R., Wilkinson, A. J., Holder, A. A., and Tate, E. W. (2014) Validation of N-myristoyltransferase as an antimalarial drug target using an integrated chemical biology approach, *Nat Chem 6*, 112-121.

[103] Fang, W., Robinson, D. A., Raimi, O. G., Blair, D. E., Harrison, J. R., Lockhart, D. E., Torrie, L. S., Ruda, G. F., Wyatt, P. G., Gilbert, I. H., and van Aalten, D. M. (2015) N-myristoyltransferase is a cell wall target in Aspergillus fumigatus, *ACS Chem Biol 10*, 1425-1434.

[104] Frearson, J. A., Brand, S., McElroy, S. P., Cleghorn, L. A., Smid, O., Stojanovski, L., Price, H. P., Guther, M. L., Torrie, L. S., Robinson, D. A., Hallyburton, I., Mpamhanga, C. P., Brannigan, J. A., Wilkinson, A. J., Hodgkinson, M., Hui, R., Qiu, W., Raimi, O. G., van Aalten, D. M., Brenk, R., Gilbert, I. H., Read, K. D., Fairlamb, A. H., Ferguson, M. A., Smith, D. F., and Wyatt, P. G. (2010) N-myristoyltransferase inhibitors as new leads to treat sleeping sickness, *Nature 464*, 728-732.

[105] Brand, S., Cleghorn, L. A., McElroy, S. P., Robinson, D. A., Smith, V. C., Hallyburton, I., Harrison, J. R., Norcross, N. R., Spinks, D., Bayliss, T., Norval, S., Stojanovski, L., Torrie, L. S., Frearson, J. A., Brenk, R., Fairlamb, A. H., Ferguson, M. A., Read, K. D., Wyatt, P. G., and Gilbert, I. H. (2012) Discovery of a novel class of orally active trypanocidal N-myristoyltransferase inhibitors, *J Med Chem 55*, 140-152.

[106] Brannigan, J. A., Roberts, S. M., Bell, A. S., Hutton, J. A., Hodgkinson, M. R., Tate, E. W., Leatherbarrow, R. J., Smith, D. F., and Wilkinson, A. J. (2014) Diverse modes of binding in structures of Leishmania major N-myristoyltransferase with selective inhibitors, *IUCrJ 1*, 250-260.

[107] Olaleye, T. O., Brannigan, J. A., Roberts, S. M., Leatherbarrow, R. J., Wilkinson, A. J., and Tate, E. W. (2014) Peptidomimetic inhibitors of N-myristoyltransferase from human malaria and leishmaniasis parasites, *Org Biomol Chem 12*, 8132-8137.

[108] Hutton, J. A., Goncalves, V., Brannigan, J. A., Paape, D., Wright, M. H., Waugh, T. M., Roberts, S. M., Bell, A. S., Wilkinson, A. J., Smith, D. F., Leatherbarrow, R. J., and Tate, E. W. (2014) Structure-based design of potent and selective Leishmania N-myristoyltransferase inhibitors, *J Med Chem 57*, 8664-8670.

[109] Farazi, T. A., Waksman, G., and Gordon, J. I. (2001) Structures of Saccharomyces cerevisiae N-myristoyltransferase with bound myristoylCoA and peptide provide insights about substrate recognition and catalysis, *Biochemistry 40*, 6335-6343.

[110] Johnson, D. R., Bhatnagar, R. S., Knoll, L. J., and Gordon, J. I. (1994) Genetic and biochemical studies of protein N-myristoylation, *Annu Rev Biochem 63*, 869-914.

[111] Johnson, C. M., Roderick, S. L., and Cook, P. F. (2005) The serine acetyltransferase reaction: acetyl transfer from an acylpantothenyl donor to an alcohol, *Arch Biochem Biophys 433*, 85-95.

[112] D'Auria, J. C. (2006) Acyltransferases in plants: a good time to be BAHD, *Curr Opin Plant Biol 9*, 331-340.

[113] Unno, H., Ichimaida, F., Suzuki, H., Takahashi, S., Tanaka, Y., Saito, A., Nishino, T., Kusunoki, M., and Nakayama, T. (2007) Structural and mutational studies of anthocyanin malonyltransferases establish the features of BAHD enzyme catalysis, *J Biol Chem 282*, 15812-15822.

[114] Chang, C. C. Y., Sun, J., and Chang, T.-Y. (2011) Membrane-bound O-acyltransferases (MBOATs), *Frontiers in Biology 6*.

[115] Jogl, G., and Tong, L. (2003) Crystal structure of carnitine acetyltransferase and implications for the catalytic mechanism and fatty acid transport, *Cell 112*, 113-122.

[116] Ramsay, R. R., Gandour, R. D., and van der Leij, F. R. (2001) Molecular enzymology of carnitine transfer and transport, *Biochim Biophys Acta 1546*, 21-43.

[117] Acevedo, O., and Jorgensen, W. L. (2004) Solvent effects and mechanism for a nucleophilic aromatic substitution from QM/MM simulations, *Org Lett 6*, 2881-2884.

[118] Anderson, V. E., Ruszczycky, M. W., and Harris, M. E. (2006) Activation of oxygen nucleophiles in enzyme catalysis, *Chem Rev 106*, 3236-3251.

[119] Warshel, A., Aqvist, J., and Creighton, S. (1989) Enzymes work by solvation substitution rather than by desolvation, *Proc Natl Acad Sci U S A 86*, 5820-5824.

[120] Olsson, M. H., and Warshel, A. (2004) Solute solvent dynamics and energetics in enzyme catalysis: the S(N)2 reaction of dehalogenase as a general benchmark, *J Am Chem Soc 126*, 15167-15179.

[121] Heath, R. J., and Rock, C. O. (1998) A conserved histidine is essential for glycerolipid acyltransferase catalysis, *Journal of Bacteriology 180*, 1425-1430.

[122] Lewin, T. M., Wang, P., and Coleman, R. A. (1999) Analysis of amino acid motifs diagnostic for the sn-glycerol-3-phosphate acyltransferase reaction, *Biochemistry 38*, 5764-5771.

[123] Turnbull, A. P., Rafferty, J. B., Sedelnikova, S. E., Slabas, A. R., Schierer, T. P., Kroon, J. T. M., Simon, J. W., Fawcett, T., Nishida, I., Murata, N., and Rice, D. W. (2001) Analysis of the Structure, Substrate Specificity, and Mechanism of Squash Glycerol-3-Phosphate (1)-Acyltransferase, *Structure 9*, 347-353.

[124] Mukherjee, S., Kunitake, G., and Alfin-Slater, R. B. (1958) The esterification of cholesterol with palmitic acid by rat liver homogenate, *J Biol Chem 230*, 91-96.

[125] Chang, C. C., Huh, H. Y., Cadigan, K. M., and Chang, T. Y. (1993) Molecular cloning and functional expression of human acyl-coenzyme A:cholesterol acyltransferase cDNA in mutant Chinese hamster ovary cells, *J Biol Chem 268*, 20747-20755.

[126] Hofmann, K. (2000) A superfamily of membrane-bound O-acyltransferases with implications for wnt signaling, *Trends Biochem Sci 25*, 111-112.

[127] Chang, C. C., Lee, C. Y., Chang, E. T., Cruz, J. C., Levesque, M. C., and Chang, T. Y. (1998) Recombinant acyl-CoA:cholesterol acyltransferase-1 (ACAT-1) purified to essential homogeneity utilizes cholesterol in mixed micelles or in vesicles in a highly cooperative manner, *J Biol Chem 273*, 35132-35141.

[128] Guo, Z. Y., Chang, C. C., and Chang, T. Y. (2007) Functionality of the seventh and eighth transmembrane domains of acyl-coenzyme A:cholesterol acyltransferase 1, *Biochemistry 46*, 10063-10071.

[129] Bryleva, E. Y., Rogers, M. A., Chang, C. C., Buen, F., Harris, B. T., Rousselet, E., Seidah, N. G., Oddo, S., LaFerla, F. M., Spencer, T. A., Hickey, W. F., and Chang, T. Y. (2010) ACAT1 gene ablation increases 24(S)-hydroxycholesterol content in the brain and ameliorates amyloid pathology in mice with AD, *Proc Natl Acad Sci U S A 107*, 3081-3086.

[130] Chang, T. Y., Li, B. L., Chang, C. C., and Urano, Y. (2009) Acyl-coenzyme A:cholesterol acyltransferases, *Am J Physiol Endocrinol Metab 297*, E1-9.

[131] Buhman, K. K., Accad, M., Novak, S., Choi, R. S., Wong, J. S., Hamilton, R. L., Turley, S., and Farese, R. V., Jr. (2000) Resistance to diet-induced hypercholesterolemia and gallstone formation in ACAT2-deficient mice, *Nat Med 6*, 1341-1347.

[132] Yen, C. L., Stone, S. J., Koliwad, S., Harris, C., and Farese, R. V., Jr. (2008) Thematic review series: glycerolipids. DGAT enzymes and triacylglycerol biosynthesis, *J Lipid Res 49*, 2283-2301.

[133] Cheng, D., Meegalla, R. L., He, B. K., Cromley, D. A., Billheimer, J. T., and Young, P. R. (2001) Human acyl-CoA : diacylglycerol acyltransferase is a tetrameric protein, *Biochemical Journal 359*, 707-714.

[134] McFie, P. J., Stone, S. L., Banman, S. L., and Stone, S. J. (2010) Topological orientation of acyl-CoA:diacylglycerol acyltransferase-1 (DGAT1) and identification of a putative active site histidine and the role of the n terminus in dimer/tetramer formation, *J Biol Chem 285*, 37377-37387.

[135] Harris, C. A., Haas, J. T., Streeper, R. S., Stone, S. J., Kumari, M., Yang, K., Han, X., Brownell, N., Gross, R. W., Zechner, R., and Farese, R. V., Jr. (2011) DGAT enzymes are required for triacylglycerol synthesis and lipid droplets in adipocytes, *J Lipid Res 52*, 657-667.

[136] Lee, B., Fast, A. M., Zhu, J., Cheng, J. X., and Buhman, K. K. (2010) Intestine-specific expression of acyl CoA:diacylglycerol acyltransferase 1 reverses resistance to diet-induced hepatic steatosis and obesity in Dgat1-/- mice, *J Lipid Res 51*, 1770-1780.

[137] Herker, E., Harris, C., Hernandez, C., Carpentier, A., Kaehlcke, K., Rosenberg, A. R., Farese, R. V., Jr., and Ott, M. (2010) Efficient hepatitis C virus particle formation requires diacylglycerol acyltransferase-1, *Nat Med 16*, 1295-1298.

[138] Willert, K., Brown, J. D., Danenberg, E., Duncan, A. W., Weissman, I. L., Reya, T., Yates, J. R., and Nusse, R. (2003) Wnt proteins are lipid-modified and can act as stem cell growth factors, *Nature 423*, 448-452.

[139] Takada, R., Satomi, Y., Kurata, T., Ueno, N., Norioka, S., Kondoh, H., Takao, T., and Takada, S. (2006) Monounsaturated fatty acid modification of Wnt protein: its role in Wnt secretion, *Dev Cell 11*, 791-801.

[140] Porter, J. A., Young, K. E., and Beachy, P. A. (1996) Cholesterol modification of hedgehog signaling proteins in animal development, *Science 274*, 255-259.

[141] Chamoun, Z., Mann, R. K., Nellen, D., von Kessler, D. P., Bellotto, M., Beachy, P. A., and Basler, K. (2001) Skinny hedgehog, an acyltransferase required for palmitoylation and activity of the hedgehog signal, *Science 293*, 2080-2084.

[142] Buglino, J. A., and Resh, M. D. (2010) Identification of conserved regions and residues within Hedgehog acyltransferase critical for palmitoylation of Sonic Hedgehog, *PLoS One 5*, e11195.

[143] Gutierrez, J. A., Solenberg, P. J., Perkins, D. R., Willency, J. A., Knierman, M. D., Jin, Z., Witcher, D. R., Luo, S., Onyia, J. E., and Hale, J. E. (2008) Ghrelin octanoylation mediated by an orphan lipid transferase, *Proc Natl Acad Sci U S A 105*, 6320-6325.

[144] Yang, J., Brown, M. S., Liang, G., Grishin, N. V., and Goldstein, J. L. (2008) Identification of the acyltransferase that octanoylates ghrelin, an appetite-stimulating peptide hormone, *Cell 132*, 387-396.

[145] Shindou, H., Eto, M., Morimoto, R., and Shimizu, T. (2009) Identification of membrane O-acyltransferase family motifs, *Biochem Biophys Res Commun 383*, 320-325.

[146] Ma, D., Wang, Z., Merrikh, C. N., Lang, K. S., Lu, P., Li, X., Merrikh, H., Rao, Z., and Xu, W. (2018) Crystal structure of a membrane-bound O-acyltransferase, *Nature 562*, 286-290.

[147] Ma, X., Koepke, J., Panjikar, S., Fritzsch, G., and Stockigt, J. (2005) Crystal structure of vinorine synthase, the first representative of the BAHD superfamily, *J Biol Chem 280*, 13576-13583.

[148] Boatright, J., Negre, F., Chen, X., Kish, C. M., Wood, B., Peel, G., Orlova, I., Gang, D., Rhodes, D., and Dudareva, N. (2004) Understanding in vivo benzenoid metabolism in petunia petal tissue, *Plant Physiol 135*, 1993-2011.

[149] Stewart, C., Jr., Kang, B. C., Liu, K., Mazourek, M., Moore, S. L., Yoo, E. Y., Kim, B. D., Paran, I., and Jahn, M. M. (2005) The Pun1 gene for pungency in pepper encodes a putative acyltransferase, *Plant J 42*, 675-688.

[150] Nakayama, T., Suzuki, H., and Nishino, T. (2003) Anthocyanin acyltransferases: specificities, mechanism, phylogenetics, and applications, *Journal of Molecular Catalysis B: Enzymatic 23*, 117-132.

[151] St-Pierre, B., Laflamme, P., Alarco, A. M., and De Luca, V. (1998) The terminal O-acetyltransferase involved in vindoline biosynthesis defines a new class of proteins responsible for coenzyme A-dependent acyl transfer, *Plant J 14*, 703-713.

[152] Grothe, T., Lenz, R., and Kutchan, T. M. (2001) Molecular characterization of the salutaridinol 7-O-acetyltransferase involved in morphine biosynthesis in opium poppy Papaver somniferum, *J Biol Chem 276*, 30717-30723.

[153] Suzuki, H., Nakayama, T., and Nishino, T. (2003) Proposed mechanism and functional amino acid residues of malonyl-CoA : anthocyanin 5-O-glucoside-6 '''-O-malonyltransferase from flowers of Salvia splendens, a member of the versatile plant acyltransferase family, *Biochemistry 42*, 1764-1771.

[154] Bayer, A., Ma, X., and Stockigt, J. (2004) Acetyltransfer in natural product biosynthesis--functional cloning and molecular analysis of vinorine synthase, *Bioorg Med Chem 12*, 2787-2795.

[155] Suzuki, H., Sawada, S., Watanabe, K., Nagae, S., Yamaguchi, M. A., Nakayama, T., and Nishino, T. (2004) Identification and characterization of a novel anthocyanin malonyltransferase from scarlet sage (Salvia splendens) flowers: an enzyme that is phylogenetically separated from other anthocyanin acyltransferases, *Plant J 38*, 994-1003.

[156] Burhenne, K., Kristensen, B. K., and Rasmussen, S. K. (2003) A new class of N-hydroxycinnamoyltransferases. Purification, cloning, and expression of a barley agmatine coumaroyltransferase (EC 2.3.1.64), *J Biol Chem 278*, 13919-13927.

[157] Garvey, G. S., McCormick, S. P., and Rayment, I. (2008) Structural and functional characterization of the TRI101 trichothecene 3-O-acetyltransferase from Fusarium sporotrichioides and Fusarium graminearum: kinetic insights to combating Fusarium head blight, *J Biol Chem 283*, 1660-1669.

[158] Levsh, O., Chiang, Y. C., Tung, C. F., Noel, J. P., Wang, Y., and Weng, J. K. (2016) Dynamic Conformational States Dictate Selectivity toward the Native Substrate in a Substrate-Permissive Acyltransferase, *Biochemistry 55*, 6314-6326.

[159] Navarro-Retamal, C., Gaete-Eastman, C., Herrera, R., Caballero, J., and Alzate-Morales, J. H. (2016) Structural and Affinity Determinants in the Interaction between Alcohol Acyltransferase from F. x ananassa and Several Alcohol Substrates: A Computational Study, *PLoS One 11*, e0153057.

[160] Schwarz, S., Kehrenberg, C., Doublet, B., and Cloeckaert, A. (2004) Molecular basis of bacterial resistance to chloramphenicol and florfenicol, *FEMS Microbiol Rev 28*, 519-542.

[161] Kleanthous, C., Cullis, P. M., and Shaw, W. V. (1985) 3-(Bromoacetyl)chloramphenicol, an active site directed inhibitor for chloramphenicol acetyltransferase, *Biochemistry 24*, 5307-5313.

[162] Murray, I. A., Lewendon, A. N. N., Kleanthous, C., and Shaw, W. V. (1986) Catalytic mechanism of chloramphenicol acetyltransferase investigated by site-directed mutagenesis, *Biochemical Society Transactions 14*, 1227-1228.

[163] Lewendon, A., Murray, I. A., Shaw, W. V., Gibbs, M. R., and Leslie, A. G. (1994) Replacement of catalytic histidine-195 of chloramphenicol acetyltransferase: evidence for a general base role for glutamate, *Biochemistry 33*, 1944-1950.

[164] Lewendon, A., Murray, I. A., Shaw, W. V., Gibbs, M. R., and Leslie, A. G. (1990) Evidence for transition-state stabilization by serine-148 in the catalytic mechanism of chloramphenicol acetyltransferase, *Biochemistry 29*, 2075-2080.

[165] Bloudoff, K., and Schmeing, T. M. (2017) Structural and functional aspects of the nonribosomal peptide synthetase condensation domain superfamily: discovery, dissection and diversity, *Biochim Biophys Acta Proteins Proteom 1865*, 1587-1604.

[166] Stachelhaus, T., Mootz, H. D., Bergendahl, V., and Marahiel, M. A. (1998) Peptide bond formation in nonribosomal peptide biosynthesis. Catalytic role of the condensation domain, *J Biol Chem 273*, 22773-22781.

[167] Dunn, B. J., and Khosla, C. (2013) Engineering the acyltransferase substrate specificity of assembly line polyketide synthases, *J R Soc Interface 10*, 20130297.

[168] Carpenter, S. M., and Williams, G. J. (2018) Extender Unit Promiscuity and Orthogonal Protein Interactions of an Aminomalonyl-ACP Utilizing Trans-Acyltransferase from Zwittermicin Biosynthesis, *ACS Chem Biol 13*, 3361-3373.

[169] Ye, Z., Musiol, E. M., Weber, T., and Williams, G. J. (2014) Reprogramming acyl carrier protein interactions of an Acyl-CoA promiscuous trans-acyltransferase, *Chem Biol 21*, 636-646.

[170] Anand, S., Prasad, M. V., Yadav, G., Kumar, N., Shehara, J., Ansari, M. Z., and Mohanty, D. (2010) SBSPKS: structure based sequence analysis of polyketide synthases, *Nucleic Acids Res 38*, W487-496.

[171] Yadav, G., Gokhale, R. S., and Mohanty, D. (2003) Computational Approach for Prediction of Domain Organization and Substrate Specificity of Modular Polyketide Synthases, *Journal of Molecular Biology 328*, 335-363.

[172] Tang, Y., Chen, A. Y., Kim, C. Y., Cane, D. E., and Khosla, C. (2007) Structural and mechanistic analysis of protein interactions in module 3 of the 6-deoxyerythronolide B synthase, *Chem Biol 14*, 931-943.

[173] Tang, Y., Kim, C. Y., Mathews, II, Cane, D. E., and Khosla, C. (2006) The 2.7-Angstrom crystal structure of a 194-kDa homodimeric fragment of the 6-deoxyerythronolide B synthase, *Proc Natl Acad Sci U S A 103*, 11124-11129.

[174] Wong, F. T., Jin, X., Mathews, II, Cane, D. E., and Khosla, C. (2011) Structure and mechanism of the trans-acting acyltransferase from the disorazole synthase, *Biochemistry 50*, 6539-6548.

[175] Serre, L., Verbree, E. C., Dauter, Z., Stuitje, A. R., and Derewenda, Z. S. (1995) The Escherichia coli malonyl-CoA:acyl carrier protein transacylase at 1.5-A resolution. Crystal structure of a fatty acid synthase component, *J Biol Chem 270*, 12961-12964.

[176] Oefner, C., Schulz, H., D'Arcy, A., and Dale, G. E. (2006) Mapping the active site of Escherichia coli malonyl-CoA-acyl carrier protein transacylase (FabD) by protein crystallography, *Acta Crystallogr D Biol Crystallogr 62*, 613-618.

[177] Keatinge-Clay, A. T., Shelat, A. A., Savage, D. F., Tsai, S. C., Miercke, L. J., O'Connell, J. D., 3rd, Khosla, C., and Stroud, R. M. (2003) Catalysis, specificity, and ACP docking site of Streptomyces coelicolor malonyl-CoA:ACP transacylase, *Structure 11*, 147-154.

[178] Bergeret, F., Gavalda, S., Chalut, C., Malaga, W., Quemard, A., Pedelacq, J. D., Daffe, M., Guilhot, C., Mourey, L., and Bon, C. (2012) Biochemical and structural study of the atypical acyltransferase domain from the mycobacterial polyketide synthase Pks13, *J Biol Chem 287*, 33675-33690.

[179] White, S. W., Zheng, J., Zhang, Y. M., and Rock. (2005) The structural biology of type II fatty acid biosynthesis, *Annu Rev Biochem 74*, 791-831.

[180] Helfrich, E. J., and Piel, J. (2016) Biosynthesis of polyketides by trans-AT polyketide synthases, *Nat Prod Rep 33*, 231-316.

[181] Mindrebo, J. T., Patel, A., Kim, W. E., Davis, T. D., Chen, A., Bartholow, T. G., La Clair, J. J., McCammon, J. A., Noel, J. P., and Burkart, M. D. (2020) Gating mechanism of elongating beta-ketoacyl-ACP synthases, *Nat Commun 11*, 1727.

[182] Zaman, S. B., Hussain, M. A., Nye, R., Mehta, V., Mamun, K. T., and Hossain, N. (2017) A Review on Antibiotic Resistance: Alarm Bells are Ringing, *Cureus 9*, e1403.

[183] Sharma, V. K., Johnson, N., Cizmas, L., McDonald, T. J., and Kim, H. (2016) A review of the influence of treatment strategies on antibiotic resistant bacteria and antibiotic resistance genes, *Chemosphere 150*, 702-714.

[184] Davies, J., and Davies, D. (2010) Origins and evolution of antibiotic resistance, *Microbiol Mol Biol Rev 74*, 417-433.

[185] Newman, D. J., and Cragg, G. M. (2016) Natural Products as Sources of New Drugs from 1981 to 2014, *J Nat Prod 79*, 629-661.

[186] Weber, W. W., and Hein, D. W. (1985) N-acetylation pharmacogenetics, *Pharmacol Rev 37*, 25-79.

[187] Lal, S., Singhal, S. N., Burley, D. M., and Crossley, G. (1972) Effect of rifampicin and isoniazid on liver function, *Br Med J 1*, 148-150.

[188] Martinez, J. L. (2008) Antibiotics and antibiotic resistance genes in natural environments, *Science 321*, 365-367.

[189] Berendonk, T. U., Manaia, C. M., Merlin, C., Fatta-Kassinos, D., Cytryn, E., Walsh, F., Burgmann, H., Sorum, H., Norstrom, M., Pons, M. N., Kreuzinger, N., Huovinen, P., Stefani, S., Schwartz, T., Kisand, V., Baquero, F., and Martinez, J. L. (2015) Tackling antibiotic resistance: the environmental framework, *Nat Rev Microbiol 13*, 310-317.

[190] Galerunti, R. A. (1994) The Antibiotic Paradox - How Miracle Drugs Are Destroying the Miracle - Levy,Sb, *Health Val 18*, 60-61.

[191] Lowy, F. D. (2003) Antimicrobial resistance: the example of Staphylococcus aureus, *J Clin Invest 111*, 1265-1273.

[192] Woodhead, M., Finch, R., and Public Education Subgroup of, S. (2007) Public education - a progress report, *J Antimicrob Chemother 60 Suppl 1*, i53-55.

[193] Mohammed Fayaz, A., Girilal, M., Mahdy, S. A., Somsundar, S. S., Venkatesan, R., and Kalaichelvan, P. T. (2011) Vancomycin bound biogenic gold nanoparticles: A different perspective for development of anti VRSA agents, *Process Biochemistry 46*, 636-641.

[194] Mohammed Fayaz, A., Girilal, M., Rahman, M., Venkatesan, R., and Kalaichelvan, P. T. (2011) Biosynthesis of silver and gold nanoparticles using thermophilic bacterium Geobacillus stearothermophilus, *Process Biochemistry 46*, 1958-1962.

[195] Yu, D., Xu, F., Zeng, J., and Zhan, J. (2012) Type III polyketide synthases in natural product biosynthesis, *IUBMB Life 64*, 285-295.

[196] Ridley, C. P., Lee, H. Y., and Khosla, C. (2008) Evolution of polyketide synthases in bacteria, *Proc Natl Acad Sci U S A 105*, 4595-4600.

[197] Koryakina, I., McArthur, J., Randall, S., Draelos, M. M., Musiol, E. M., Muddiman, D. C., Weber, T., and Williams, G. J. (2013) Poly specific trans-acyltransferase machinery revealed via engineered acyl-CoA synthetases, *ACS Chem Biol 8*, 200-208.

[198] Oliynyk, M., Brown, M. J. B., Cortés, J., Staunton, J., and Leadlay, P. F. (1996) A hybrid modular polyketide synthase obtained by domain swapping, *Chemistry & Biology 3*, 833-839.

[199] Liu, L., Thamchaipenet, A., Fu, H., Betlach, M., and Ashley, G. (1997) Biosynthesis of 2-Nor-6-deoxyerythronolide B by Rationally Designed Domain Substitution, *Journal of the American Chemical Society 119*, 10553-10554.

[200] McDaniel, R., Thamchaipenet, A., Gustafsson, C., Fu, H., Betlach, M., and Ashley, G. (1999) Multiple genetic modifications of the erythromycin polyketide synthase to produce a library of novel "unnatural" natural products, *Proc Natl Acad Sci U S A 96*, 1846-1851.

[201] Liou, G. F., and Khosla, C. (2003) Building-block selectivity of polyketide synthases, *Curr Opin Chem Biol 7*, 279-284.

[202] Hans, M., Hornung, A., Dziarnowski, A., Cane, D. E., and Khosla, C. (2003) Mechanistic analysis of acyl transferase domain exchange in polyketide synthase modules, *J Am Chem Soc 125*, 5366-5374.

[203] Lau, J., Fu, H., Cane, D. E., and Khosla, C. (1999) Dissecting the role of acyltransferase domains of modular polyketide synthases in the choice and stereochemical fate of extender units, *Biochemistry 38*, 1643-1651.

[204] Reeves, C. D., Murli, S., Ashley, G. W., Piagentini, M., Hutchinson, C. R., and McDaniel, R. (2001) Alteration of the substrate specificity of a modular polyketide synthase acyltransferase domain through site-specific mutations, *Biochemistry 40*, 15464-15470.

[205] Sundermann, U., Bravo-Rodriguez, K., Klopries, S., Kushnir, S., Gomez, H., Sanchez-Garcia, E., and Schulz, F. (2013) Enzyme-directed mutasynthesis: a combined experimental and theoretical approach to substrate recognition of a polyketide synthase, *ACS Chem Biol 8*, 443-450.

[206] Clements, P. R., Wallace, J. C., and Keech, D. B. (1981) 2-Bromoacetyl-SCoA, In *Methods in Enzymology* (Press, A., Ed.), pp 578-579.

[207] Chase, J. F., and Tubbs, P. K. (1969) Conditions for the self-catalysed inactivation of carnitine acetyltransferase. A novel form of enzyme inhibition, *Biochem J 111*, 225-235.

[208] Bloxham, D. P. (1975) Selective inhibition of cholesterol synthesis by cell-free preparations of rat liver by using inhibitors of cytoplasmic acetoacetyl-coenzyme A thiolase, *Biochem J 147*, 531-539.

[209] Holland, P. C., Clark, M. G., and Bloxham, D. P. (1973) Inactivation of pig heart thiolase by 3-butynoyl coenzyme A, 3-pentynoyl coenzyme A, and 4-bromocrotonyl coenzyme A, *Biochemistry 12*, 3309-3315.

[210] Anderson, G. J., and Kumar, S. (1987) Transacylase activity of lactating bovine mammary fatty acid synthase, *FEBS Lett 220*, 323-326.

[211] Tian, W. X., Wang, Y. S., and Hsu, R. Y. (1989) Affinity labeling of chicken liver fatty acid synthase with chloroacetyl-CoA and bromopyruvate, *Biochim Biophys Acta 998*, 310-316.

[212] Blanchard, J. S. (2005) Assay for acetyltransferases and acetyltransferase substrates, (University, A. E. C. o. M. o. Y., Ed.) A61B ed., United States.

[213] Walt, D. R., Kao, J.-Y., and Ouyang, T. (1991) Enzyme-catalyzed synthesis of fluoromalonyl-CoA, *Bioorganic Chemistry 19*, 270-273.

[214] Weeks, A. M., Wang, N., Pelton, J. G., and Chang, M. C. Y. (2018) Entropy drives selective fluorine recognition in the fluoroacetyl-CoA thioesterase from Streptomyces cattleya, *Proc Natl Acad Sci U S A 115*, E2193-E2201.

[215] Chase, J. F., Middleton, B., and Tubbs, P. K. (1966) A coenzyme A analogue, desulpho-coA; preparation and effects on various enzymes, *Biochem Biophys Res Commun 23*, 208-213.

[216] Kurz, L. C., Roble, J. H., Nakra, T., Drysdale, G. R., Buzan, J. M., Schwartz, B., and Drueckhammer, D. G. (1997) Ability of single-site mutants of citrate synthase to catalyze proton transfer from the methyl group of dethiaacetyl-coenzyme A, a non-thioester substrate analog, *Biochemistry 36*, 3981-3990.

[217] Stewart, C. J., and Wieland, T. (1978) Synthesis of a Carba-analog of S-Acetyl CoA,Acetonyldethio CoA.Synthesis of a Carba-analog ofS-Acetyl Coenzyme A,Acetonyl-dethio Coenzyme A; an Effective Inhibitor of Citrate Synthase, *Justus Liebigs Annalen der Chemie 1978*, 57-65.

[218] Martin, D. P., Bibart, R. T., and Drueckhammer, D. G. (1994) Synthesis of Novel Analogs of Acetyl Coenzyme A: Mimics of Enzyme Reaction Intermediates, *Journal of the American Chemical Society 116*, 4660-4668.

[219] Nikawa, J., Numa, S., Shiba, T., Stewart, C. J., and Wieland, T. (1978) Carboxylation of acetonyldethio-coenzyme A by acetyl coenzyme A carboxylase, *FEBS Lett 91*, 144-148.

[220] Murphy, J. R., Mullins, E. A., and Kappock, T. J. (2016) Functional Dissection of the Bipartite Active Site of the Class I Coenzyme A (CoA)-Transferase Succinyl-CoA:Acetate CoA-Transferase, *Front Chem 4*, 23.

[221] Tosin, M., Spiteller, D., and Spencer, J. B. (2009) Malonyl carba(dethia)- and malonyl oxa(dethia)-coenzyme A as tools for trapping polyketide intermediates, *Chembiochem 10*, 1714-1723.

[222] Hamed, R. B., Henry, L., Gomez-Castellanos, J. R., Asghar, A., Brem, J., Claridge, T. D., and Schofield, C. J. (2013) Stereoselective preparation of lipidated carboxymethyl-proline/pipecolic acid derivatives via coupling of engineered crotonases with an alkylmalonyl-CoA synthetase, *Org Biomol Chem 11*, 8191-8196.

CHAPTER 2.   IMPROVED SYNTHESIS OF ACETYL/MALONYL-OXA/AZA(DETHIA)COAS AND REACTIVITY WITH FATTY ACID SYNTHASE ENZYMES

2.1   Abstract

Acetyl/malonyl-CoA are fatty acid biosynthesis substrates, while the oxy(dethia) and aza(dethia) analogs remain to be characterized as substrates or inhibitors. Here we report syntheses of oxy/aza analogs using improved routes and examine their stability and inhibitory activity of fatty acid biosynthetic enzymes. The malonyl-oxy/aza(dethia) analogs are stable towards decarboxylation and hydrolysis in the presence of enzymes, potentially making them ideal for enzymology and structure-function studies.

2.2   Acyltransferases and Ketosynthases have had some information teased out via substrate analogs, but information is limited

Analogs of acyl-CoAs have been used in a relatively small number of enzyme structure-function studies, where they are successfully used to determine or clarify the roles of residues involved in catalysis.[1] These stable analogs come in two flavors, replacement of the relatively labile thioester with esters/amides/ketones to examine enzymatic acyl transfer, or the generation of acyl-enolate isosteres to examine carbon-carbon bond forming enzymes. The thioester bond of malonyl-CoA is considered to be especially labile.[2] Thus, stable malonyl-thioester analogs are desired for use in structure-function studies,[3-5] where there are currently only 6 unique crystal structures with malonyl-CoA or malonyl-thioesters bound. Other uses for stable malonyl-CoA analogs include off-loading polyketide synthase metabolic intermediates, or as probes of enzymes like carboxymethylproline synthase, where the analogs participate as pseudo-substrates.[6-8]

The simplest changes to the thioester bond are replacement with an ester or amide. However, the ester bond may still be labile in certain enzymes and the amide has an extra hydrogen bond donor and partial double bond character not present in the thioester that can influence binding affinity and geometry. In order to gain further insight into the suitability of stable acyl-thioester analogs for use in fatty acid and polyketide synthase structure-function studies, we report improved or novel synthesis of acetyl-oxa(dethia)CoA/acetyl-aza(dethia)CoA (**1/2**), malonyl-oxa(dethia)CoA/malonyl-aza(dethia)CoA (**3/4**) and their stability with acyltransferase (AT) and ketosynthase (KS) enzymes, Figure 2.1.
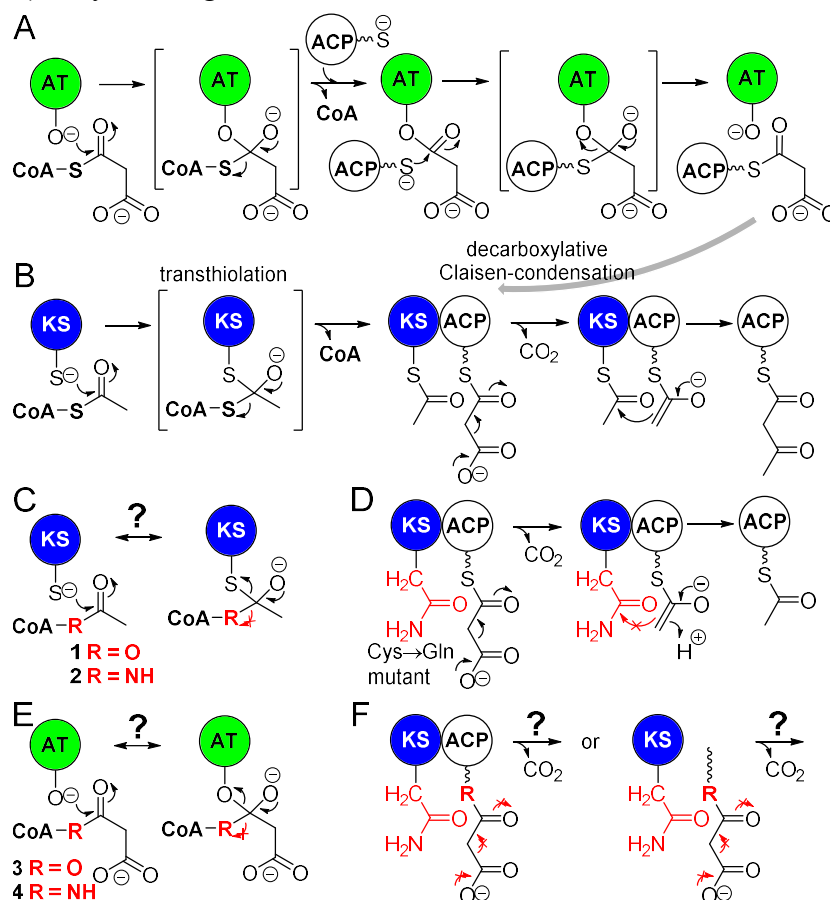
Figure 2.1 Initiation of fatty acid biosynthesis and potential substrate analogs. A) FabD activity. B) FabH activity. C) Possible inhibition of FabH by stable acetyl-CoA analogs. D) FabH C→Q mutant decarboxylation activity. E) Possible inhibition of FabD by stable malonyl-CoA analogs. F) Possible inhibition of FabH C→Q by stable malonyl-thioester analogs. Squiggly line represents phosphopantetheine. Question marks denote that it is unknown which state is more stable or if the analogs are reactants.

The carbon-carbon bonds in fatty acids are generated by condensation of acyl-thioesters and malonyl-thioesters, carried by either CoA or acyl carrier proteins (ACP), Figure 2.1.[9] In

Escherichia coli malonyl-*S*-ACP is generated by the transfer of malonate from CoA by ACP *S*-malonyltransferase (FabD), Figure 2.1A. The first fatty acid carbon-carbon bond formed is between acetyl-CoA and malonyl-*S*-ACP by β-ketoacyl-ACP synthase III (FabH), Figure 2.1B. FabH transfers the acetyl group of onto its active site cysteine followed by decarboxylation of malonyl-*S*-ACP forming an enolate intermediate that reacts with acetyl-*S*-FabH generating acetoacetyl-*S*-ACP. Mutation of the FabH active site cysteine to a glutamine is expected to generate a malonyl-S-ACP decarboxylase, similar to other β-ketoacyl-ACP synthases, Figure 2.1D.[10] Here we report the reactivity of FabD, FabH and FabH C→Q mutant with substrates and substrate analogs bearing thioester changes to esters or amides.

2.3   Synthesis of acetyl- and malonyl-CoA analogs

We synthesized acetyl-CoA and malonyl-CoA analogs using a strategy similar to our previous synthesis of methylmalonyl-CoA analogs, shown in scheme 2.1 with details in the supplemental information.[11] Acetonide protected oxy(dethia)pantetheine (**5**) and amino(dethia)pantetheine (**6**) were generated as previously published, with a couple modifications to improve purity. The acetonide pantetheine analogs **5** and **6** were treated with acetic anhydride with pyridine as a base to give acetyl-oxy(dethia)pantetheine acetonide (**7**) and acetyl-aza(dethia)pantetheine acetonide (**8**). Malonyl-oxy(dethia)-pantetheine acetonide (**9**) and malonyl-aza(dethia)pantetheine acetonide (**10**) were generated through reaction of **5** or **6** with Meldrum's acid at elevated temperature in acetonitrile, which in the case of **6** required the addition of triethylamine. The acetonides **7-10** were deprotected with formic acid in water and chemoenzymatically converted to the CoA analogs **1-4**. All of the analogs **1-4** are completely stable in buffer at pH 7 overnight, Supplemental Figure S1.

Our synthesis of the malonyl-CoA analogs used fewer steps than previous methods and gave essentially quantitative yields before purification as judged by analytical HPLC-MS.[6-8] No effort was made to improve purifications of **7-10** where the majority of loss occurred. Another improvement is the use of *E. coli* acetate kinase (AckA), an ATP regenerating enzyme that uses acetyl phosphate as the phosphoryl donor for conversion of the pantetheines to the CoAs. This allowed decreased use of ATP for the CoaA and CoaE reactions, which decreased cost, but also simplified preparative reverse phase chromatography, where unreacted ATP and the products ADP

tail into the peak of the desired CoA substrates and analogs on preparative scale, Supplemental Figure S2.
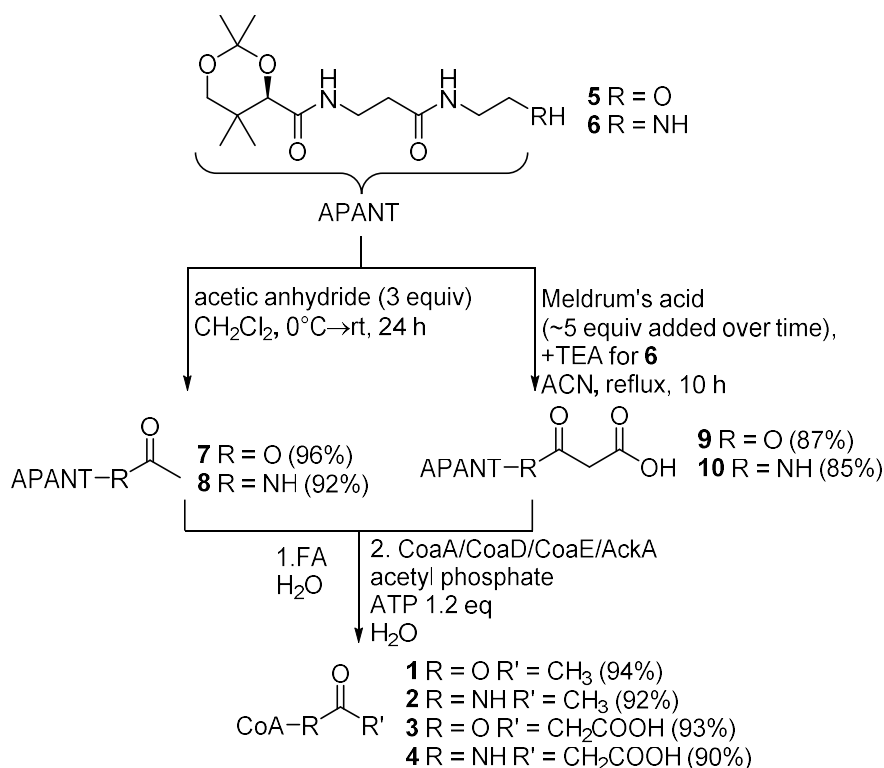

Scheme 2.1 Synthetic scheme for acetyl- and malonyl-CoA analogs.

2.4 Malonyl transfer in FabD is rapid and hydrolysis is rapid in the presence of a second substrate like dephospho-CoA

ACP *S*-malonyltransferase enzymes like FabD spontaneously hydrolyze the acyl-enzyme intermediate over time, which poses a problem for acquiring structures of the enzyme-substrate complex.[12] Here we monitored the stability of our malonyl-CoA analogs in the presence of FabD to determine their suitability for structural studies using an HPLC assay. We performed two types of reactions, one with just the malonyl-CoA or analog to examine the hydrolysis side reaction, Scheme 2.2. A second reaction contained 3'-dephospho-CoA as an acceptor to monitor for substrate or analog turnover. Using 600 µM malonyl-CoA, 20 µM FabD displayed hydrolysis with a k_{cat} of 0.0013 min^{-1}, Figure 2.2 panel I. Using FabD with 600 µM each of malonyl-CoA and 3'-dephospho-CoA, the enzyme (20 nM) was very active and the reaction went to completeness in
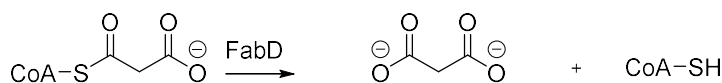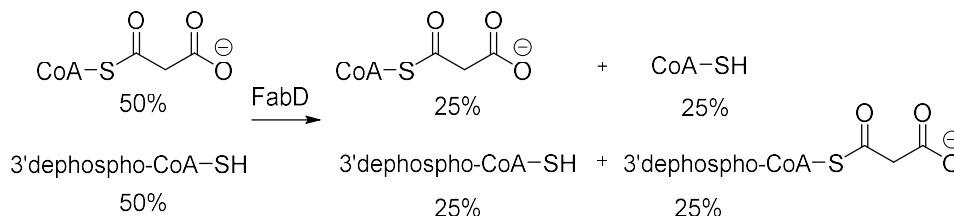
Scheme 2.2 FabD dephospho-CoA assay

less than 10 minutes, Figure 2.2 panel II. With active enzyme in hand, we tested the stability of our analogs. In the presence of 20 μM FabD, there was limited hydrolysis of **3** on relatively long timescales (about 5%), while **4** was completely stable over the course of a 24-hour, Figure 2.2 panels III and IV. Even in the presence of 3'-dephospho-CoA as an acceptor where the enzyme displays very high activity, there is no reaction with **3** or **4**. Thus, due to the stability against both hydrolysis and catalysis, we can conclude that either malonyl-CoA analog **3** or **4** is suitable for structure-function studies with the ACP *S*-malonyltransferase family of enzymes.

2.5   KasIII utilizes both acetyl- and malonyl-CoA making it ideal to test all of our analogs for stability and for inhibition

β-ketoacyl-ACP synthase enzymes also spontaneously hydrolyze acetyl-CoA via the acyl-enzyme intermediate over time, but also spontaneously decarboxylate the malonyl-thioester substrates presented. To establish our FabH enzyme is active we performed HPLC assays with acetyl-CoA and malonyl-CoA. We chose malonyl-CoA rather than malonyl-*S*-ACP for a couple reasons, one is the need for coupled enzyme assays to monitor product formation, second is the extra effort associated with production of the substrate, and finally it is easier to compare inhibition of our malonyl-CoA analogs with a substrate that appears similar. One complication of this HPLC assay is that the substrate acetyl-CoA peak overlaps with the product acetoacetyl-CoA, Figure 2.3. Nevertheless, the disappearance of malonyl-CoA and appearance of CoA can be easily monitored to provide kinetics. In typical assays, we used 20 μM FabH with 600 μM acetyl-CoA and malonyl-CoA, which went to completeness in about 30 minutes, giving a k_{cat} of 8.0±0.2 min^{-1}, Figure 2.3

73
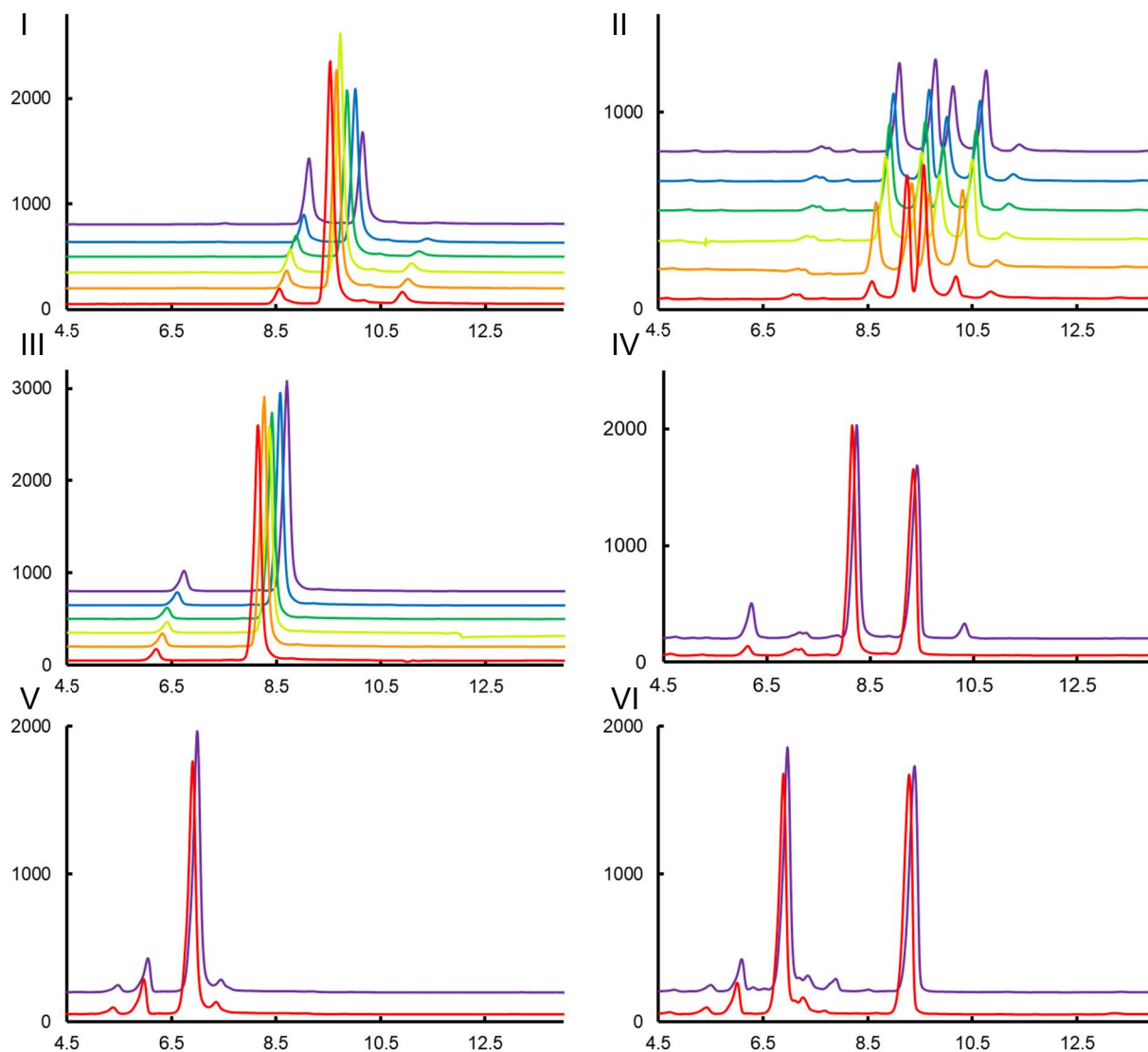
Figure 2.2 HPLC Traces of FabD with I) Mal-S-CoA, II) Mal-S-CoA + dephosphoCoA, III) Mal-O-CoA, IV) Mal-O-CoA + dephosphoCoA, V) Mal-N-CoA, and VI) Mal-N-CoA + dephosphoCoA. For I, III – VI, red = 0 hr, orange = 0.5 hr, yellow = 1 hr, green = 2 hr, blue = 4 hr, and purple = 24 hr. For II, red = 0 min, orange = 1 min, yellow = 5 min, green = 10 min, blue = 15 min, and purple = 30 min.

panel I. In previous reports with malonyl-S-ACP as an acceptor, the observed k_{cat}s are on the order of 2-3 s^{-1}, indicating malonyl-CoA is a reasonable but somewhat poor substrate. The hydrolysis of acetyl-CoA by FabH proceeds with a k_{cat} of 0.19 min^{-1}, Figure 2.3 panel II. In the presence of malonyl-CoA and absence of acetyl-CoA, the enzyme still generates acetoacetyl-CoA, by decarboxylating malonyl-CoA to acetyl-CoA, and gives an apparent k$_{cat}$ of 0.28 min^{-1} based on the disappearance of malonyl-CoA, Figure 2.3 panel III.

74
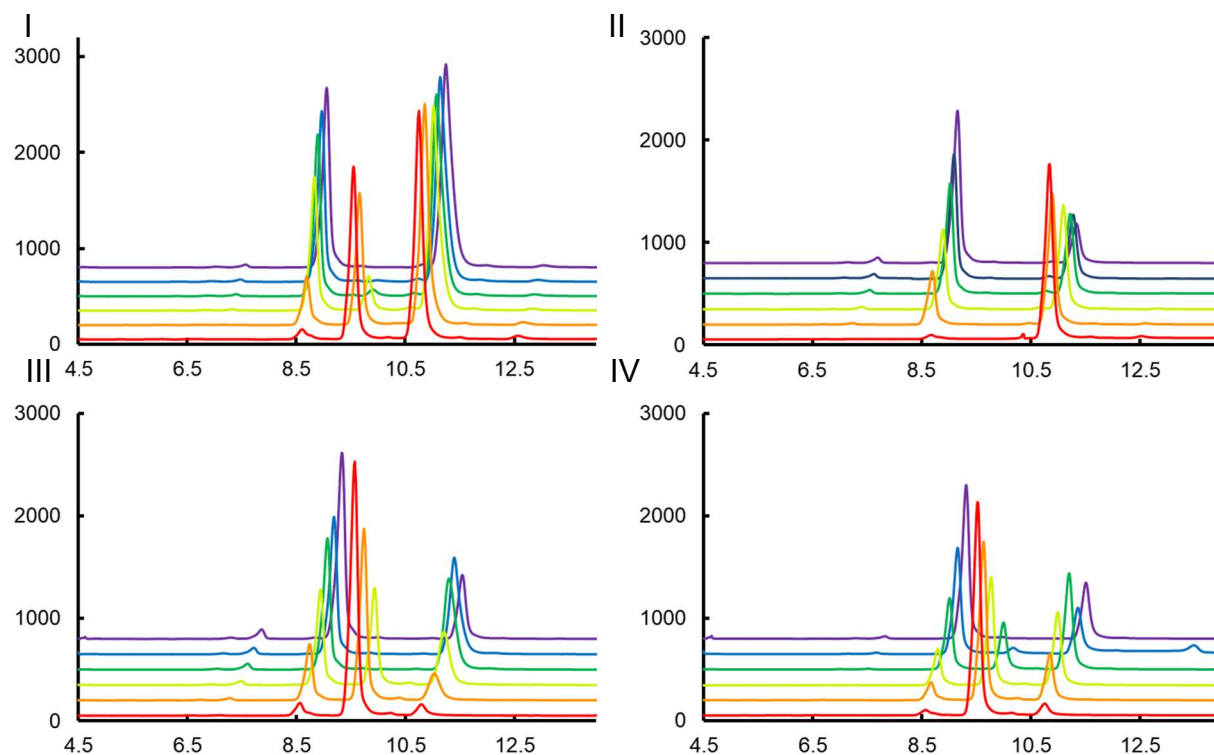
Figure 2.3 HPLC Traces of I) KasIII WT with Ac-S-CoA + Mal-S-CoA, II) KasIII WT with Ac-S-CoA, III) KasIII WT with Mal-S-CoA, and IV) KasIII C112Q with Mal-S-CoA. For I – IV, red = 0 min, orange = 1 min, yellow = 5 min, green = 10 min, blue = 15 min, and purple = 30 min.

With active enzyme in hand, we subjected the acetyl-CoA analogs to stability assays in the presence of FabH, Figure 2.4, and determined relative inhibition. The acetyl-oxy(dethia)CoA analog was hydrolyzed with a k_{cat} of 0.0075 min^{-1}, which is much slower than acetyl-CoA, but significant over a 24-hour period. The acetyl-aza(dethia)CoA analog was completely stable over the course of a day. Inhibition assays using 1 mM of the analogs gave ~30% inhibition for both 1 and 2 (Table 1), suggesting these analogs bind similar to the substrates.

We also tested the stability and inhibition of malonyl-CoA turnover by **3** and **4**. Both **3** and **4** were completely stable in the presence of FabH. In inhibition assays, at 1 mM 3 and 4 gave inhibition of 38% and 24%, respectively. The FabH active site C→Q mutation has not been previously characterized. In our assay, FabH C→Q had an interesting activity of almost 50% hydrolysis and decarboxylation, with a k_{cat} of 19±8 min^{-1}, Figure 2.3 panel IV. The rate of malonyl-CoA decarboxylation by FabH C→Q was similar to the rate of malonyl-CoA decarboxylative Claisen condensation by the wild-type enzyme. The hydrolysis of malonyl-CoA by FabH C→Q
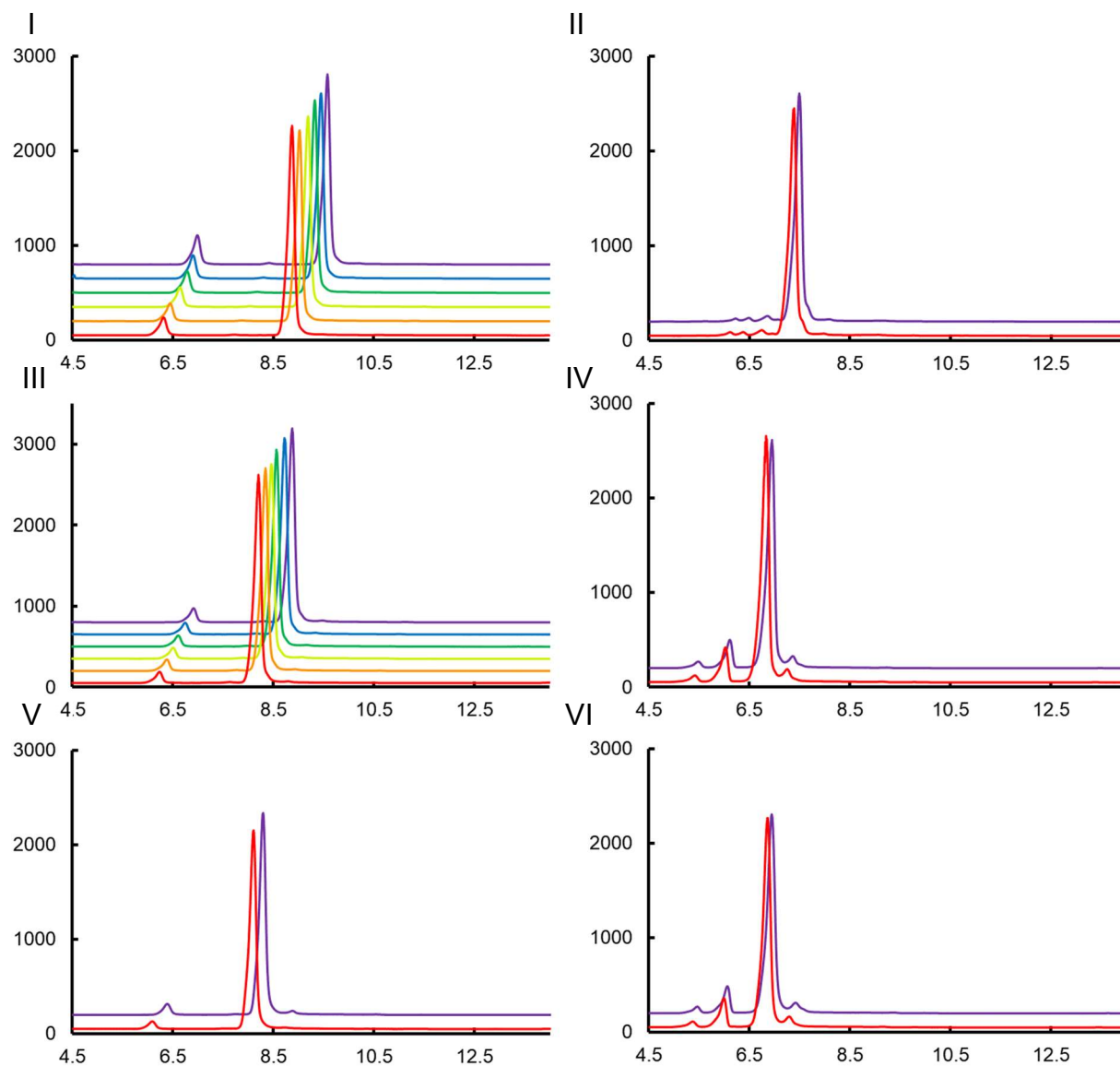
Figure 2.4 HPLC Traces of I) KasIII WT with Ac-O-CoA, II) KasIII WT with Ac-N-CoA, III) KasIII WT with Mal-O-CoA, IV) KasIII WT with Mal-N-CoA, V) KasIII C112Q with Mal-O-CoA, and VI) KasIII C112Q with Mal-N-CoA. For all, I – VI, red = 0 hr, orange = 0.5 hr, yellow = 1 hr, green = 2 hr, blue = 4 hr, and purple = 24 hr.

was unexpected especially since it was similar to the rate of decarboxylation. Nevertheless, our malonyl-CoA analogs **3** and **4** appeared to be completely stable over the course of 24 hours, similar to the wild-type enzyme. Thus, malonyl-oxa(dethia) and malonyl-aza(dethia)thioesters appear to be excellent candidates for enzyme structure-function studies by X-ray crystallography and cryo-EM.

We would like to note that in initial assays we attempted to follow the production of CoA from acetyl-CoA and malonyl-CoA via a 5,5-dithio-bis-(2-nitrobenzoic acid) (DTNB) assay. However, FabH activity is inhibited by DTNB similarly to other KS enzymes. Interestingly, the enzyme had activity in the initial portion, suggesting that it wasn't DTNB that inhibited activity, but rather it's likely the CoA-TNB mixed disulfide product from transthiolation, that generates a KS inactivating intermediate. This observation should serve as a warning against using a continuous assay with DTNB to monitor activity.

2.6   Conclusions

There are two previous reports of malonyl-aza(dethia)-CoA synthesis and use in enzyme assays. In both cases it was likely expected that the material would act as a pseudo substrate able to undergo decarboxylative Claisen condensation or decarboxylative Michael addition. We here demonstrate again that the malonyl-aza(dethia)-CoA is stable in the presence of an enzyme. We propose that this stability arises from the partial double bond character of the amide, which deactivates beta-keto acid decarboxylation. The decarboxylation would normally be enabled by the formation of an enolate intermediate, however the amide resonance competes with enolate formation, Scheme 5. The malonyl-oxa(dethia)CoA analog also likely behaves similar to the aza analog, since the pKa of the resulting enolates are far above that of the thioester. While malonyl-oxa(dethia) analogs have been demonstrated to be substrates elsewhere (polyketide synthase or crotonase type systems), those studies followed product formation by LCMS analysis, and didn't report rates. Our results here suggest that the rates are extremely slow supporting use in enzyme structure-function studies.
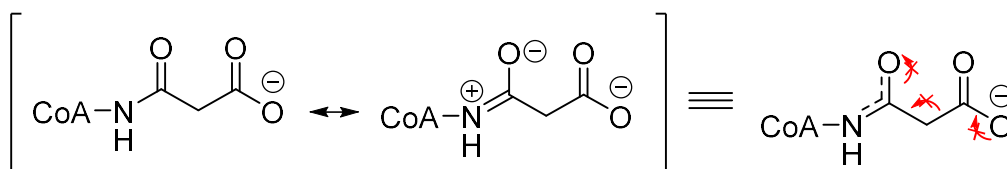
Scheme 2.3 Predicted reasoning behind the lack of decarboxylation or hydrolysis in both FabD and KasIII.

In conclusion, we have demonstrated here a simpler, more efficient way to synthesize acetyl- and malonyl-CoA analogs where the thioester has been replaced with an ester or amide. These analogs were found to be stable over a 24-hour time course in both an acyltransferase in

FabD and KasIII, an enzyme which performs acyl transfer, followed by a decarboxylative Claisen-condensation reaction. While these analogs only inhibited between 25 to 40%, the stability assays performed in this study gives us confidence that these analogs can be utilized for structure-function studies of both acyltransferases and decarboxylative Claisen-condensation enzymes. We hope that with these analogs, understanding substrate specificity and unraveling mechanistic information about both classes of enzyme will be possible, leading to bioengineering and drug discovery in the not so distant future.

2.7   Materials and Methods

Chemicals and solvents: All chemicals were purchased from Acros, Aldrich, Alfa Aesar, Fluka, Oakwood or TCI America and used without further purification. For reactions, technical grade solvents were used without further purification and dried over molecular sieves (size type here) when applicable. HPLC grade solvents were used for flash chromatography, analytical and preparative HPLC. Deuterated solvents were purchased from Acros or Sigma-Aldrich.

Reactions: All organic synthesis reactions were performed under normal atmosphere at room temperature unless otherwise noted. The reactions and purifications were not optimized. Reactions were magnetically stirred with Teflon coated stirbars. Flash chromatography was performed on a CombiFlash Rf200 (Teledyne ISCO) with 24 or 40 gram silica Flash Columns. Preparative HPLC chromatography was performed on an Agilent 1100 preparative HPLC with diode array UV/Vis detection over a Luna 5μ C18(2) 100 Å 250 x 21.2 mm column (Phenomenex). The reported yields are post purification and spectroscopically pure unless previously reported or otherwise indicated.

Analysis: Reactions and products were characterized by HPLC-MS on an Agilent 1100 HPLC with diode array UV/Vis detection over a Luna 5 μm C18(2) 100 Å 50 x 2 mm (Phenomenex) or Luna 5 μm C18(2) 100 Å 250 x 4.6 mm (Phenomenex) with low resolution mass spectrometry (LRMS) analysis in positive and negative modes by an Agilent 1100 G1946D quadrupole with electrospray ionization (ESI). NMR spectra were collected on a Bruker AV500HD equipped with a 5mm BBFO Z-gradient cryoprobe in the solvents indicated. 1H and 13C NMR spectra are referenced using the signals of the residual undeuterated solvent and where applicable tetramethylsilane. All spectra were collected at 298 K. Chemical shifts are reported in parts per million (ppm) and multiplicities are abbreviated as follows: s (singlet), d (doublet),

t (triplet), q (quartet), m (multiplet), br (broad), . Coupling constants (J) are reported in Hertz (Hz).

2.7.1 Experimental Procedures and Characterization Data

Below are the general procedures for all of the syntheses described in this chapter.

5 R = O
6 R = NH

7 R = O (96%)
8 R = NH (92%)
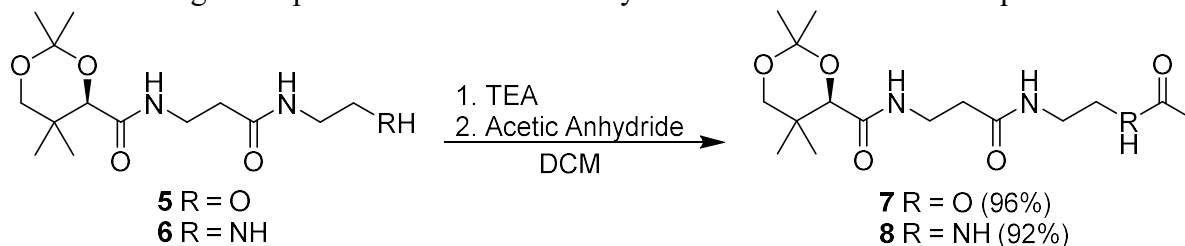
Preparation of 7-8 via 5-6:
General procedure
A solution of DCM containing **5-6** was mixed with TEA on ice. Acetic anhydride was added slowly, and the reaction was left stirring overnight at room temperature. The reaction was mixed with silica, the solvent removed, and subjected to flash chromatography (0 → 100% gradient of DCM → acetone or MeOH) affording **7-8**.

Acetyl-oxa(dethia)-pantetheine acetonide (7):
5 (1.0 g, 3.31 mmol) was reacted with TEA (4 mL, 22.96 mmol) and acetic anhydride (1 mL, 10.58 mmol) according to the general procedure above affording 7 (yellow oil, 1.1 g, 3.19 mmol 96%).
^{1}H NMR (500 MHz, CDCl$_3$) δ 6.97 (t, J = 6.3 Hz, 1H), 6.83 (t, J = 5.8 Hz, 1H), 3.97 (t, J = 5.6 Hz, 2H), 3.90 (s, 1H), 3.52 (d, J = 11.7 Hz, 1H), 3.41 (dt, J = 12.7, 6.4 Hz, 1H), 3.37 – 3.26 (m, 3H), 3.11 (d, J = 11.7 Hz, 1H), 2.31 (t, J = 6.3 Hz, 2H), 1.90 (s, 3H), 1.28 (d, J = 15.7 Hz, 6H), 0.86 (s, 3H), 0.80 (s, 3H).**^{13}C NMR** (126 MHz, CDCl3) δ 171.28, 170.83, 169.99, 98.93, 71.22, 62.97, 38.35, 35.62, 34.77, 32.80, 29.31, 22.01, 20.74, 18.76, 18.57. LRMS (ESI) *m/z* calculated for C16H28N2O6 ([M+H]$^+$) 345.41, found 345.0.

Acetyl-amido(dethia)-pantetheine acetonide (8):
6 (1.0 grams, 3.32 mmol) was reacted with TEA (4 mL, 28.68 mmol) and acetic anhydride (1 mL, 10.58 mmol) according to the general procedure above affording **8** (yellow oil, 1.05 g, 3.06 mmol 92%).
^{1}H NMR (500 MHz, CDCl$_3$) δ 7.38 – 7.33 (m, 3H), 3.43 (q, J = 7.0 Hz, 3H), 3.35 – 3.24 (m, 2H), 3.10 (q, J = 2.6 Hz, 2H), 2.91 (q, J = 7.3 Hz, 15H), 2.25 (t, J = 6.6 Hz, 1H), 1.77 (s, 12H), 1.25 – 1.22 (m, 2H), 1.20 (s, 2H), 1.10 (t, J = 7.4 Hz, 23H), 0.97 (t, J = 7.0 Hz, 4H), 0.78 (s, 2H), 0.74 (s, 2H). **^{13}C NMR** (126 MHz, CDCl$_3$) δ 175.86, 171.65, 169.95, 98.89, 76.92, 71.18, 58.07, 57.35, 45.49, 39.28, 35.38, 35.00, 32.73, 29.17, 22.67, 18.68, 18.52, 18.03. LRMS (ESI) *m/z* calculated for C16H29N3O5 ([M+H]$^+$) 344.42, found 344.0.

5 R = O
6 R = NH

1. TEA for **6**
2. Meldrum's Acid
ACN, △

9 R = O (87%)
10 R = NH (85%)
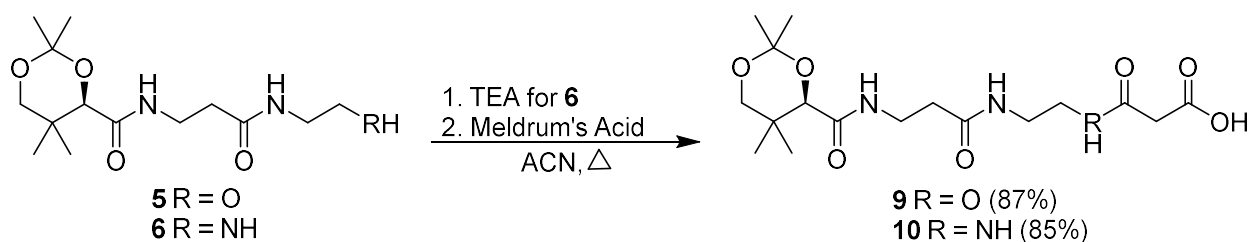
Preparation of 9-10 via 5-6:

General procedure

A solution of ACN containing **7-8** was mixed with TEA (for **6** only) and Meldrum's acid. The reaction was refluxed for about 10 hours. Every 2-3 hours, the reaction was monitored, and 1-2 equivalents of Meldrum's acid dissolved in ACN was added slowly if Meldrum's acid was used up. The reaction was mixed with silica, the solvent removed, and subjected to flash chromatography (0 → 50% gradient of DCM → acetone or MeOH) affording **9-10**.

Malonyl-oxa(dethia)-pantetheine acetonide (9):

5 (100 mg, 0.33 mmol) was reacted with Meldrum's acid (240 mg, 1.67 mmol) according to the general procedure above affording **9** (oil, 111.5 mg, 0.29 mmol 87%).

^{1}**H NMR** (500 MHz, CDCl$_3$) δ 7.90 (s, 5H), 7.19 (s, 0H), 4.36 (s, 1H), 4.22 (q, J = 7.1 Hz, 9H), 4.13 (s, 1H), 4.03 (d, J = 8.9 Hz, 1H), 3.98 – 3.92 (m, 1H), 3.78 – 3.70 (m, 1H), 3.63 (s, 1H), 3.44 (d, J = 7.5 Hz, 2H), 3.41 (s, 9H), 2.17 (s, 1H), 2.09 (s, 2H), 2.04 (s, 1H), 1.77 (s, 4H), 1.77 (s, 1H), 1.28 (t, J = 7.2 Hz, 13H), 1.24 (dd, J = 7.6, 4.6 Hz, 2H), 1.22 (s, 3H), 1.20 (s, 2H), 1.07 (s, 3H), 0.82 (s, 1H). ^{13}**C NMR** (126 MHz, CDCl3) δ 178.16, 177.15, 175.88, 171.00, 170.92, 167.09, 163.08, 106.37, 77.31, 77.05, 76.80, 76.62, 75.78, 61.97, 58.50, 52.76, 40.89, 40.23, 36.17, 30.93, 29.69, 27.58, 22.86, 22.52, 20.74, 18.82, 18.04, 14.00. MS (ESI) m/z calculated for C17H28N2O8 ([M-H]$^-$) 387.42, found 387.0.

Malonyl-amido(dethia)-pantetheine acetonide (10):

6 (100 mg, 0.33 mmol) was reacted with TEA (0.25 ml, 1.8 mmol) and Meldrum's acid (240 mg, 1.67 mmol) according to the general procedure above affording **10** (oil, 108.6 mg, 0.280 mmol 85%).

^{1}**H NMR** (500 MHz, CDCl$_3$ δ 8.67 (t, J = 5.8 Hz, 1H), 7.10 (dt, J = 21.3, 5.6 Hz, 1H), 3.66 (p, J = 6.7 Hz, 2H), 3.51 (ddq, J = 26.2, 13.6, 6.5 Hz, 1H), 3.43 – 3.31 (m, 6H), 3.28 – 3.19 (m, 3H), 3.15 – 3.08 (m, 1H), 3.06 (d, J = 7.4 Hz, 1H), 2.41 (t, J = 6.4 Hz, 1H), 1.95 (s, 3H), 1.45 (s, 1H), 1.39 (dd, J = 14.0, 7.0 Hz, 15H), 1.00 (s, 1H), 0.96 (s, 1H). ^{13}**C NMR** (126 MHz, CDCl3) δ 172.77, 172.65, 171.70, 171.06, 170.13, 170.07, 170.00, 99.08, 77.30, 77.04, 76.79, 71.46, 53.22, 43.04, 41.62, 40.47, 40.14, 38.98, 35.77, 35.04, 32.97, 29.46, 23.14, 22.16, 18.89, 18.72, 11.72. MS (ESI) m/z calculated for C17H28N2O8 ([M-H]$^-$) 386.43, found 386.0.

5 R = O
6 R = NH

PANT

7 R = O (96%)
8 R = NH (92%)

APANT−R

9 R = O (87%)
10 R = NH (85%)

APANT−R

1.FA
H₂O

11 R = O (98%)
12 R = NH (97%)

PANT−R

13 R = O (95.5%)
14 R = NH (97%)

PANT−R
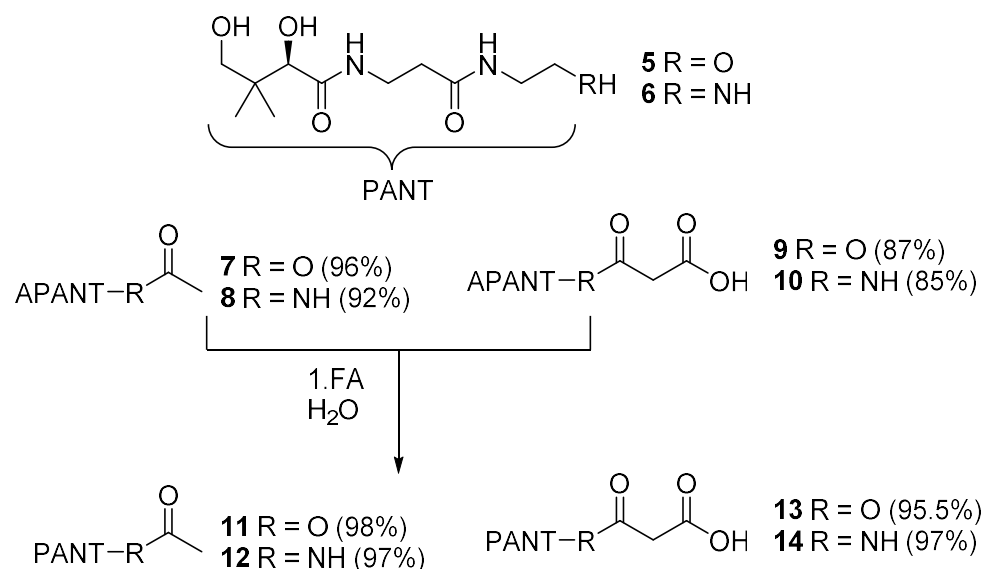
Preparation of 11-14 via 7-10:

General procedure

A solution of **7-10** was dissolved in water and was reacted with 5-10% FA overnight while stirring. The reaction was then air dried to remove FA and was subsequently frozen and lyophilized affording **11-14**.

Acetyl-oxa(dethia)-pantetheine (11):

7 (500 mg, 1.45 mmol) was used as starting material to afford **11** (oil, 435 mg, 1.43 mmol 98%).
¹H NMR (500 MHz, D₂O) δ 8.35 (s, 2H), 4.05 (t, J = 5.3 Hz, 2H), 3.87 (s, 1H), 3.47 – 3.36 (m, 4H), 3.35 (dd, J = 5.4, 2.1 Hz, 2H), 3.27 (d, J = 11.3 Hz, 1H), 2.39 (t, J = 6.5 Hz, 2H), 1.99 (s, 3H), 0.79 (d, J = 17.7 Hz, 6H). **¹³C NMR** (126 MHz, D₂O) δ 175.06, 174.26, 174.09, 170.94, 117.52, 115.20, 75.73, 68.36, 63.42, 38.58, 38.23, 35.40, 35.24, 20.49, 20.35, 19.07. LRMS (ESI) *m/z* calculated for C13H24N2O6 ([M+H]⁺) 305.34, found 305.0.

Acetyl-amido(dethia)-pantetheine (12):

8 (500 mg, 1.46 mmol) was used as starting material to afford **12** (oil, 428 mg, 1.41 mmol 97%).
¹H NMR (500 MHz, D₂O) δ 8.17 (s, 1H), 3.84 (s, 2H), 3.43 – 3.30 (m, 6H), 3.28 – 3.19 (m, 3H), 3.16 (s, 7H), 3.07 (q, J = 7.3 Hz, 7H), 2.35 (t, J = 6.6 Hz, 4H), 1.85 (s, 6H), 1.15 (t, J = 7.3 Hz, 11H), 0.85 (d, J = 12.7 Hz, 1H), 0.76 (d, J = 17.0 Hz, 11H). **¹³C NMR** (126 MHz, D₂O) δ 175.02, 174.52, 174.24, 174.10, 174.03, 166.69, 164.48, 164.04, 163.14, 162.87, 162.59, 162.30, 119.84, 117.52, 115.20, 75.73, 74.69, 69.87, 68.33, 52.19, 47.20, 46.62, 44.45, 44.32, 41.04, 38.63, 38.59, 37.56, 37.36, 37.21, 37.15, 35.40, 35.27, 31.94, 21.89, 21.85, 21.40, 20.47, 19.42, 19.09, 18.14, 12.73, 11.73, 8.21, 6.59. LRMS (ESI) *m/z* calculated for C13H25N3O5 ([M+H]⁺) 304.36, found 304.0.

Malonyl-oxa(dethia)-pantetheine (13):

9 (111.5 mg, 0.29 mmol) was used as starting material to afford **13** (oil, 95.5 mg, 0.27 mmol 95.5%).
¹H NMR (500 MHz, Deuterium Oxide) δ 3.86 (d, J = 3.5 Hz, 1H), 3.53 (ddd, J = 6.3, 5.5, 0.9 Hz, 2H), 3.46 – 3.33 (m, 3H), 3.32 – 3.12 (m, 3H), 3.09 (q, J = 7.3 Hz, 2H), 2.40 (t, J = 6.5 Hz, 2H),

1.16 (td, J = 7.4, 0.9 Hz, 3H), 0.79 (dd, J = 17.4, 2.6 Hz, 6H). ^{13}C NMR (126 MHz, D2O) δ 176.16, 175.12, 174.15, 172.35, 115.15, 75.73, 68.32, 59.85, 46.64, 41.43, 41.35, 38.54, 35.69, 35.42, 35.25, 34.73, 33.56, 31.93, 20.43, 19.02, 8.19. MS (ESI) *m/z* calculated for C14H24N2O8 ([M-H]$^-$) 347.35, found 347.0.

Malonyl-amido(dethia)-pantetheine (14):

10 (108.6 mg, 0.29 mmol) was used as starting material to afford **14** (oil, 94.5 mg, 0.27 mmol 97%).

^{1}H NMR (500 MHz, D2O) δ 8.36 (s, 14H), 3.89 (s, 2H), 3.46 – 3.35 (m, 5H), 3.29 (d, J = 11.2 Hz, 2H), 3.24 (d, J = 2.4 Hz, 7H), 3.10 (d, J = 9.7 Hz, 6H), 2.40 (t, J = 6.5 Hz, 3H), 1.89 (d, J = 0.8 Hz, 1H), 1.28 – 1.16 (m, 6H), 0.80 (d, J = 17.5 Hz, 10H). ^{13}C NMR (126 MHz, D2O) δ 175.18, 175.10, 174.43, 174.18, 171.57, 171.08, 75.77, 68.36, 54.37, 46.66, 45.24, 38.68, 38.64, 38.59, 35.46, 35.34, 21.96, 20.53, 19.11, 17.79, 16.87, 16.32, 12.19, 8.29. MS (ESI) *m/z* calculated for C16H28N2O6 ([M-H]$^-$) 346.37, found 346.0.
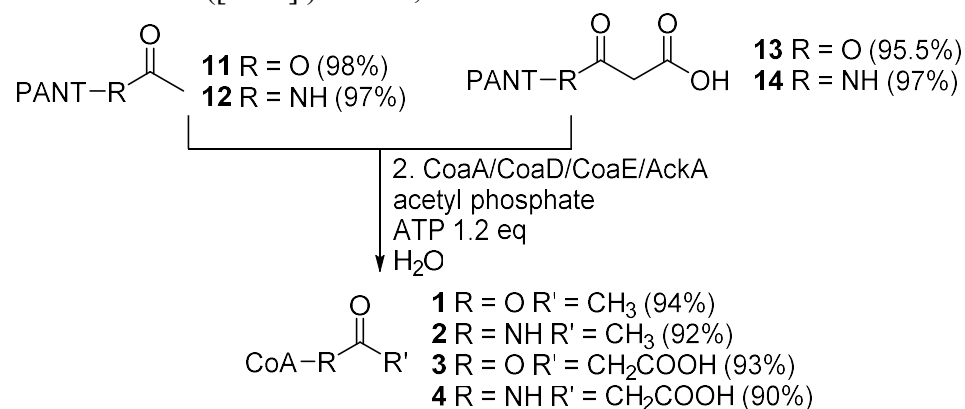
Chemoenzymatic preparation of 1-4:

General procedure

A solution containing 100 mM Tris (pH 8.0), 10 mM MgCl2, 50 mM NaCl, 10 mM TCEP (pH 8.0), 15 mM acetyl-phosphate, and 7.5 mM ATP was used to dissolve the **11-14** at a final concentration of 5.5 mM, ~20-100 mL total. Then CoaA and AckA were added to final concentrations of 2.7 μM and 7.5 μM respectively, and the reaction allowed to mix at room temperature for 1 hours. Then CoaD was added to a concentration of 5.6 μM and allowed to mix at room temperature for 1 hour. Then CoaE was added to a final concentration of 13.1 μM and allowed to mix at room temperature overnight. The reaction was quenched with 10% FA, precipitating the protein out of solution, which was removed by filtration. Reverse phase HPLC was used to purify the final products using a 0 → 20% gradient of 0.1% TFA in water → ACN over 30 minutes. Fractions were pooled, air dried overnight, and lyophilized.

Acetyl-oxa(dethia)-CoA (1):

11 (200 mg, mmol) was used as starting material to afford **1** (off white powder, 492 mg, 0.62 mmol 94%).

^{1}H NMR (500 MHz, D2O) δ 8.41 (s, 2H), 8.10 (s, 2H), 6.04 (d, J = 6.5 Hz, 2H), 4.70 (s, 14H), 4.46 (q, J = 2.7 Hz, 2H), 4.13 (dtdd, J = 14.3, 11.7, 7.4, 3.3 Hz, 4H), 3.99 (t, J = 5.2 Hz, 4H), 3.87 (s, 2H), 3.70 (dd, J = 9.8, 5.0 Hz, 2H), 3.61 (s, 14H), 3.43 (dd, J = 9.8, 4.9 Hz, 2H), 3.33 (td, J = 14.3, 13.9, 7.6 Hz, 5H), 3.28 (d, J = 5.3 Hz, 3H), 2.42 – 2.38 (m, 1H), 2.37 – 2.26 (m, 5H), 2.04 –

1.95 (m, 3H), 1.94 (s, 3H), 0.74 (s, 5H), 0.61 (s, 5H). **^{13}C NMR** (126 MHz, D$_2$O) δ 174.68, 174.23, 174.06, 155.53, 152.86, 149.25, 139.82, 118.48, 86.52, 83.90, 74.16, 74.05, 73.47, 71.85, 65.64, 63.34, 61.26, 59.41, 38.25, 38.17, 35.36, 35.26, 20.74, 20.30, 18.02. MS (ESI) m/z calculated for C23H38N7O18P3 ([M-H]$^-$) 792.51, found 792.0.

Acetyl-amido(dethia)-CoA (2):

12 (200 mg, 0.25 mmol) was used as starting material to afford **2** (off white powder, 484 mg, 0.61 mmol 92%).

^{1}H NMR (500 MHz, D$_2$O) δ 8.58 – 8.51 (m, 1H), 8.34 (s, 1H), 6.12 (dd, J = 5.7, 2.1 Hz, 1H), 4.84 – 4.77 (m, 2H), 4.53 – 4.49 (m, 1H), 4.18 (d, J = 7.9 Hz, 1H), 3.98 (d, J = 7.5 Hz, 1H), 3.92 (dd, J = 2.0, 1.0 Hz, 1H), 3.82 – 3.75 (m, 1H), 3.62 (dt, J = 2.1, 1.1 Hz, 5H), 3.58 – 3.52 (m, 1H), 3.41 – 3.35 (m, 2H), 3.32 (dt, J = 10.8, 3.2 Hz, 1H), 3.30 – 3.11 (m, 8H), 3.11 – 3.05 (m, 1H), 2.62 – 2.53 (m, 1H), 2.36 (td, J = 6.8, 6.4, 2.1 Hz, 2H), 2.16 – 2.07 (m, 1H), 1.99 (ddt, J = 14.9, 2.0, 1.0 Hz, 1H), 1.90 – 1.82 (m, 5H), 1.25 – 1.03 (m, 5H), 0.97 (dddd, J = 8.2, 7.2, 2.0, 1.0 Hz, 1H), 0.88 – 0.82 (m, 3H), 0.74 (d, J = 2.2 Hz, 3H). **^{13}C NMR** (126 MHz, D$_2$O) δ 174.72, 174.40, 174.17, 163.06, 162.78, 158.92, 149.86, 148.47, 144.69, 142.48, 118.54, 117.44, 115.12, 87.51, 83.37, 74.22, 73.84, 72.04, 65.12, 61.76, 61.42, 59.30, 46.65, 44.49, 44.37, 39.59, 39.14, 38.67, 38.59, 38.30, 37.15, 35.43, 35.36, 25.77, 22.08, 21.85, 21.81, 21.54, 20.75, 18.29, 13.79, 12.62, 11.63, 8.20. MS (ESI) m/z calculated for C23H39N8O17P3 ([M-H]$^-$) 791.53, found 791.0.

Malonyl-oxa(dethia)-CoA (3):

13 (50 mg, 0.14 mmol) was used as starting material to afford **3** (off white powder, 112 mg, 0.13 mmol 93%).

^{1}H NMR (500 MHz, D$_2$O) δ 8.58 (s, 3H), 8.34 (s, 3H), 6.12 (d, J = 5.5 Hz, 3H), 4.78 (s, 6H), 4.51 (s, 2H), 4.17 (s, 4H), 4.13 (t, J = 5.0 Hz, 2H), 3.93 (d, J = 2.0 Hz, 3H), 3.77 (dd, J = 10.1, 4.4 Hz, 3H), 3.62 (s, 10H), 3.56 – 3.48 (m, 9H), 3.38 (q, J = 4.7, 3.0 Hz, 8H), 3.19 (t, J = 5.5 Hz, 6H), 2.62 – 2.52 (m, 2H), 2.38 (q, J = 8.3, 7.5 Hz, 7H), 2.16 – 2.07 (m, 2H), 0.84 (s, 9H), 0.73 (s, 9H). **^{13}C NMR** (126 MHz, D$_2$O) δ 174.76, 174.18, 171.52, 144.72, 142.49, 87.44, 74.18, 73.97, 71.88, 61.41, 59.85, 59.28, 41.43, 38.28, 35.44, 35.35, 20.82, 18.18. MS (ESI) m/z calculated for C24H38N7O20P3 ([M-H]$^-$) 836.52, found 836.0.

Malonyl-amido(dethia)-CoA (4):

14 (50 mg, 0.14 mmol) was used as starting material to afford **4** (off white powder, 108.5 mg, 0.13 mmol 90%).

^{1}H NMR (500 MHz, D$_2$O) δ 8.39 (s, 1H), 8.10 (dd, J = 10.8, 0.7 Hz, 1H), 6.00 (dd, J = 20.1, 6.3 Hz, 1H), 4.46 – 4.41 (m, 1H), 4.11 – 4.05 (m, 2H), 3.85 (s, 1H), 3.69 – 3.60 (m, 2H), 3.59 (s, 6H), 3.58 – 3.52 (m, 1H), 3.39 (dd, J = 9.8, 5.0 Hz, 1H), 3.35 – 3.24 (m, 3H), 3.23 – 3.09 (m, 5H), 3.09 – 2.96 (m, 3H), 2.38 – 2.21 (m, 4H), 2.02 – 1.93 (m, 1H), 1.23 – 1.05 (m, 6H), 0.72 (d, J = 9.6 Hz, 3H), 0.61 (d, J = 29.7 Hz, 3H). **^{13}C NMR** (126 MHz, D$_2$O) δ 175.15, 174.63, 174.05, 171.49, 155.54, 152.84, 149.30, 139.83, 118.54, 86.47, 74.06, 73.70, 71.82, 65.60, 61.31, 59.31, 54.28, 46.52, 45.19, 42.48, 38.59, 38.51, 38.22, 38.16, 35.37, 35.30, 28.68, 20.74, 18.49, 17.96, 17.69, 16.23, 12.10, 8.18. MS (ESI) m/z calculated for C24H39N8O19P3 ([M-H]$^-$) 835.53, found 835.0.

2.7.2   Cloning of *fabD*, *fabH*, and *ackA* from *Escherichia coli*

A modified pRSF-Duet1 vector with a Gibson cloning site was used, which leads to the overexpression of proteins with an N-terminal sequence of MGSSHHHHHHSGSENLYFQ, which is cleaved by TEV protease and will be referred to as pRSF-TEV/GIB. Briefly, pRSF-TEV/GIB was digested with BseRI and purified by gel electrophoresis, mixed with with PCR fragments described below, and treated with Gibson Assembly Master Mix from New England Biolabs. The assembled vector were cloned into *E. coli* DH5α, and the resulting isolated plasmid sequences confirmed by sequencing. The *ackA*, *fabD*, and *fabH* genes were amplified by PCR from *E. coli* DH5α genomic DNA (or from plasmids containing the genes) using the following primers (overlapping regions with pRSF-TEV/GIB underlined, extra codons are in bold):

AckA-forward: 5′-<u>GAGAACCTCTACTTCCAA</u> **AGT**TCGAGTAAGTTAGTACTGG-3′

AckA-reverse: 5′-<u>CTCGAGGAGATTACGGATT</u>**A**TCAGGCAGTCAGGCGGCTC-3′

FabD-forward: 5′-<u>GAGAACCTCTACTTCCAA</u>**AGC**CAATTTGCATTTGTGTTCC-3′,

FabD+GG-forward: 5′-<u>GAGAACCTCTACTTCCAA</u>**AGTGGTGGT**CAATTTGCATTTGTGTTCC-3′,

FabD-reverse: 5′- <u>CTCGAGGAGATTACGGATT</u>**A**AAGCTCGAGCGCCGCTGCCATC-3′,

FabH-forward: 5′- <u>GAGAACCTCTACTTCCAA</u>**AGT**ATGTATACGAAGATTATTGGTAC-3′,

FabD+GG-forward: 5′-<u>GAGAACCTCTACTTCCAA</u>**AGTGGTGGT**CAATTTGCATTTGTGTTCC-3′,

FabH-reverse: 5′-<u>CTCGAGGAGATTACGGATT</u>**A**GAAACGAACCAGCGCGGAGCCC-3′,

Plasmids containing the appropriate genes were isolated and confirmed by DNA sequencing, yielding expression plasmids for AckA (pRSF-TEV/GIB-AckA), FabD (pRSF-TEV/GIB-FabD), FabD+GG (pRSF-TEV/GIB-FabD+GG), FabH (pRSF-TEV/GIB-FabH), and FabH+GG (pRSF-TEV/GIB-FabH+GG). The extra N-terminal glycines were added in order to yield protein that was cleavable by TEV protease.

2.7.3   Expression and Purification of ecFabD, KasIII(fabH), and AckA

Expression plasmids for fabD+GG, fabH+GG, and ackA were transformed into *E. coli* BL21 (DE3), and the resultant recombinant strains were grown overnight in 50 mL of LB and 50

μg/mL kanamycin. A 5 mL aliquot of the overnight culture was used to inoculate 1 L of LB containing 10 mM MgCl2, trace metals, and 50 μg/mL kanamycin, which was incubated at 37 ˚C while being shaken at 180 rpm. Once the OD_{600} reached ~0.5-0.6, the temperature was reduced to 18 ˚C. Once the cultures reached thermal equilibrium, gene expression was induced by the addition of isopropyl β-ᴅ-thiogalactopyranoside with a final concentration of 500 μg/mL, with incubation for an additional 16 hours. *E. coli* cells were harvested by centrifugation at 6300 rpm and 4 ˚C for 30 min.

E. coli cell pellets, carrying fabD+GG, fabH+GG, and ackA were re-suspended in lysis buffer 1 μg/mL DNase, 1 μg/mL lysozyme, 300 mM NaCl, 20 mM imidazole, 10% glycerol, and 20 mM Tris-HCl (pH 8.0)], sonicated (60 × 1 s on ice), and clarified by centrifugation at 11000 rpm and 4 ˚C for 30 min. The supernatant was filtered applied to a 5 mL HisTrap HP (GE Healthcare,) and washed with lysis buffer using an Äkta pure fast-performance liquid chromatography system (GE Healthcare,). Wash buffer [300 mM NaCl, 40 mM imidazole and 20 mM Tris-HCl (pH 8.0)] was used to remove additional contaminants, and proteins were eluted with wash buffer containing 500 mM imidazole. At this point the purity of fabD, fabH, and ackA from the fractions was analyzed by sodium dodecyl sulfate–polyacrylamide gel electrophoresis (SDS–PAGE). Pure fractions were pooled and cleaved using TEV protease to remove the 6His tag except for ackA. All three were then buffer-exchanged into 10 mM Tris-HCl (pH 8.0) and 200 mM NaCl, concentrated, and frozen in small aliquots with liquid nitrogen, and stored at −80 °C.

2.7.4 Stability and HPLC assay procedures for FabH and FabD

The stability reactions were performed in a 500 μL reaction mixture which contained 100 mM potassium phosphate buffer (KH2PO4/K2HPO4) at pH 7.0, 10 mM MgCl2, 20 μM enzyme (FabH wt, FabH C → Q, or FabD), and 600 μM acetyl- or malonyl-thioester analog. For FabD reactions were performed with or without 600 μM dephosphoCoA added. Reaction mixtures were incubated at 25 ˚C, 75 μL aliquots taken at times 0 hour, 30 minutes, 1 hour, 2 hours, 4 hours, and 24 hours were quenched with 25 μL of 50% TFA v/v, precipitating the protein. Centrifugation at 2000 rpm at 25 ˚C for 10 minutes was used to pellet the protein and the supernatant was analyzed via the procedure outlined below.

General procedure for determination of malonyl-thioester analog or hydrolyzed product. Malonyl-thioester analog and hydrolyzed product were determined using HPLC with detection at

A254 over the 250 x 4.6 mm C18(2) column. The analytes were separated with a 2 → 25% gradient of 0.1% TFA in water → ACN over 20 min. Peak areas of acetyl- and malonyl-thioester analogs and hydrolyzed product were determined and plotted over time.

The inhibition reactions were performed in a 500 µL reaction mixture which contained 100 mM potassium phosphate buffer (KH2PO4/K2HPO4) at pH 7.0, 10 mM MgCl2, 600 µM malonyl-CoA, 600 µM acetyl-CoA, 1 mM acetyl- or malonyl-thioester analog, and the reaction was initiated with the addition of 20 µM FabH. Reaction mixtures were incubated at 25 °C, 75 µL aliquots taken at times 0 hour, 1 minute, 5 min, 10 min, 15 min, and 30 min were quenched with 25 µL of 50% TFA v/v, precipitating the protein. Centrifugation at 2000 rpm at 25 °C for 10 minutes was used to pellet the protein and the supernatant was analyzed via the procedure outlined below.

General procedure for determination of malonyl-CoA, acetyl-CoA and CoA concentrations in FabH catalyzed assays. Substrate and product concentrations were determined using HPLC with detection at A254 over the 250 x 4.6 mm C18(2) column. The analytes were separated with a 2 → 25% gradient of 0.1% TFA in water → ACN over 20 min. Peak areas of substrate and products were converted to concentration by summing their areas and dividing each peak by this total to give relative percentages that were converted to concentration by adjusting to the starting concentration of acetyl- or malonyl-CoA. This data was then used to generate % inhibition based off initial rates for the three starting points.

2.7.5 NMRs from syntheses above (See below)

7

^{1}H in CDCl$_3$

7
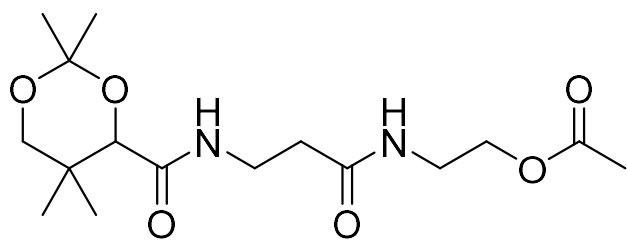
^{13}C in CDCl$_3$

7

COSY and HMQC in CDCl$_3$

8

^{1}H in CDCl$_3$

8
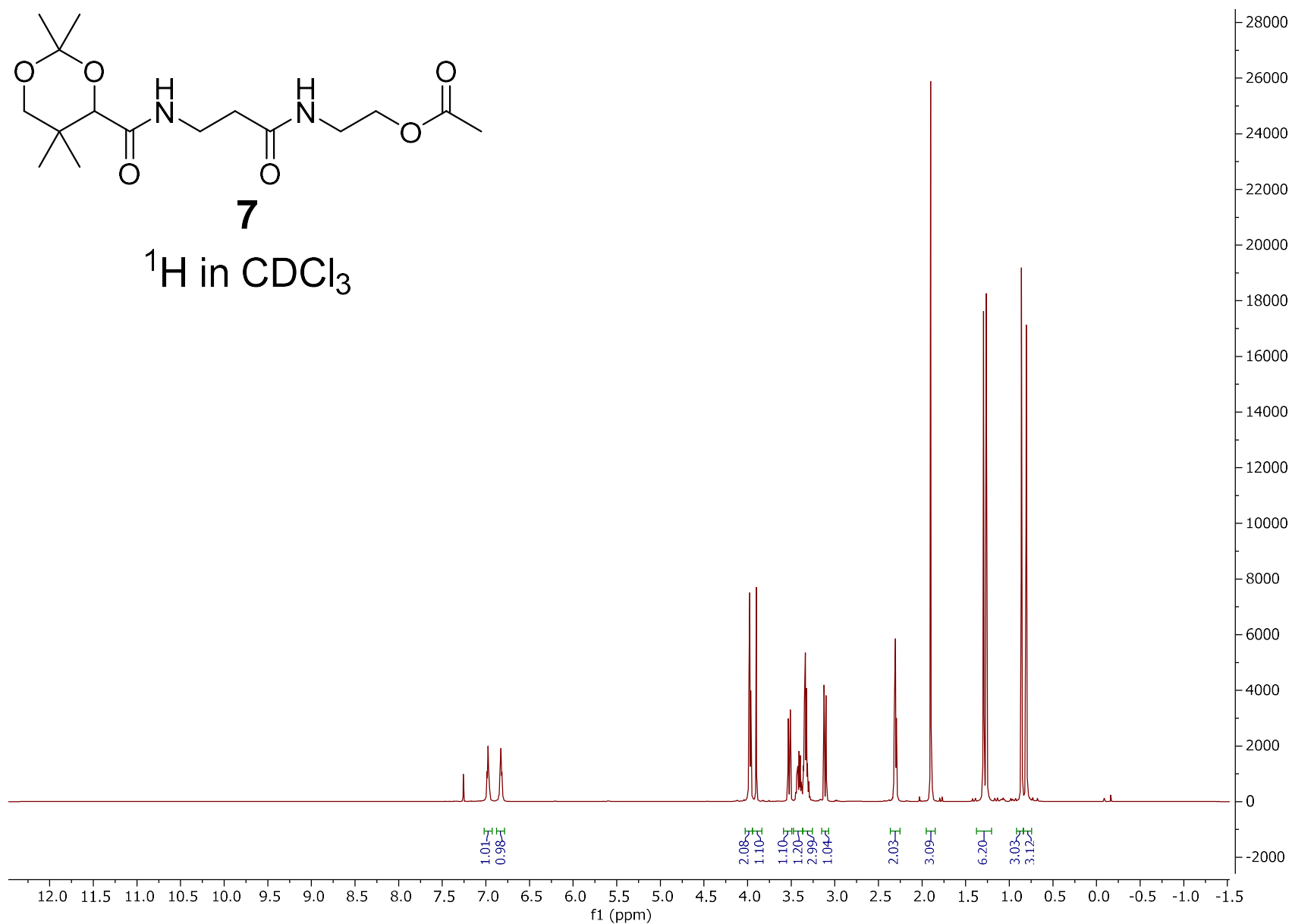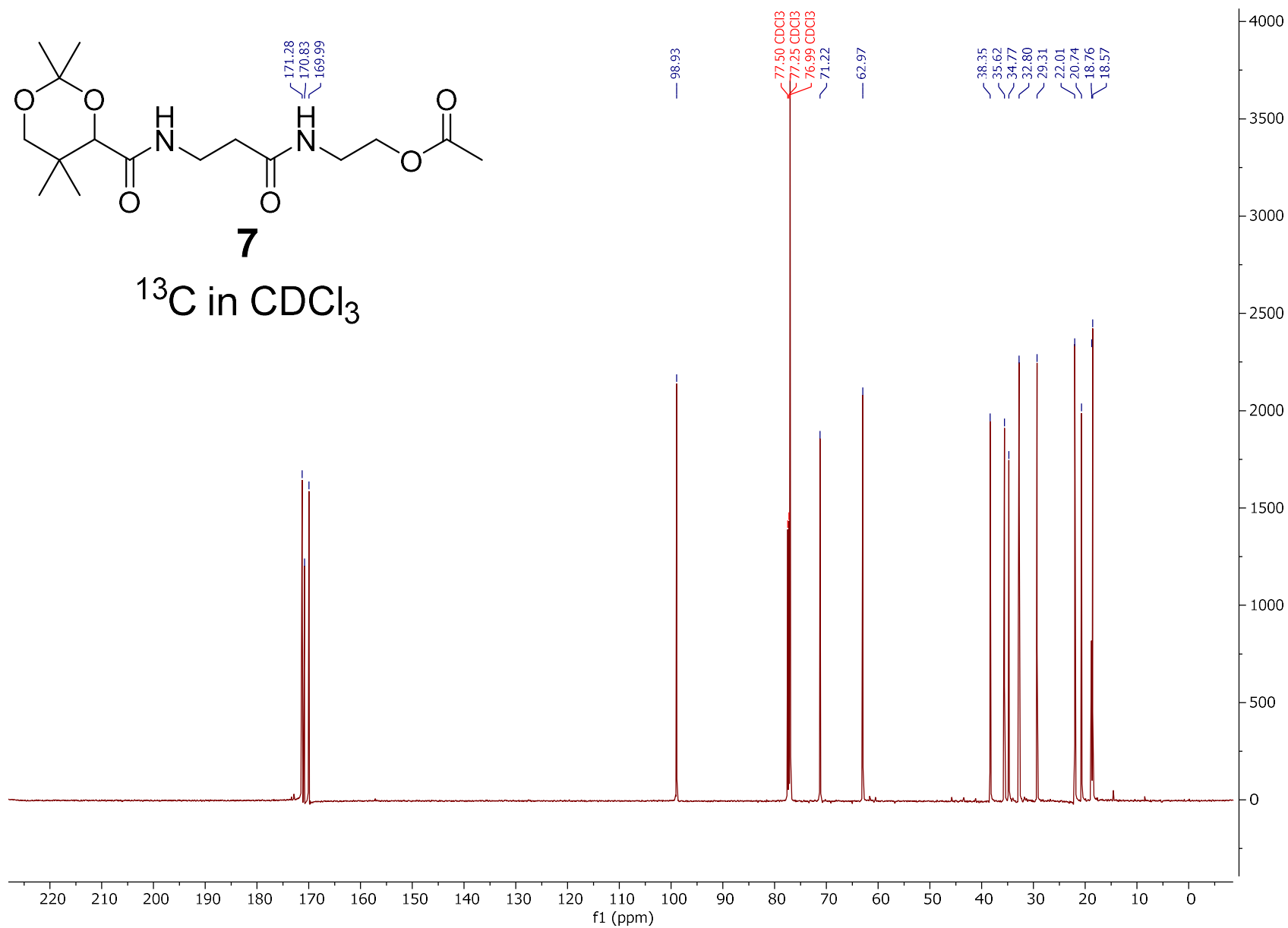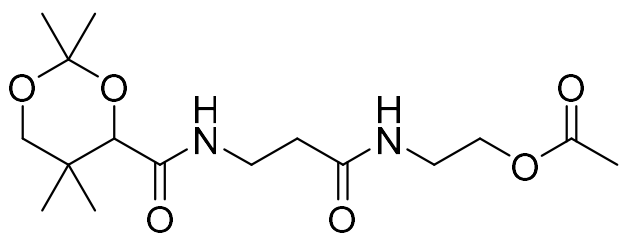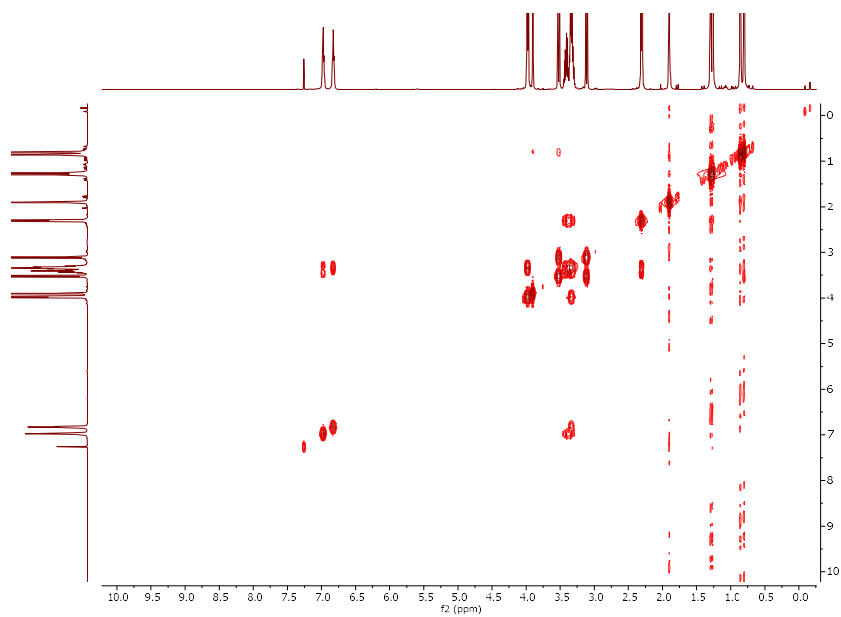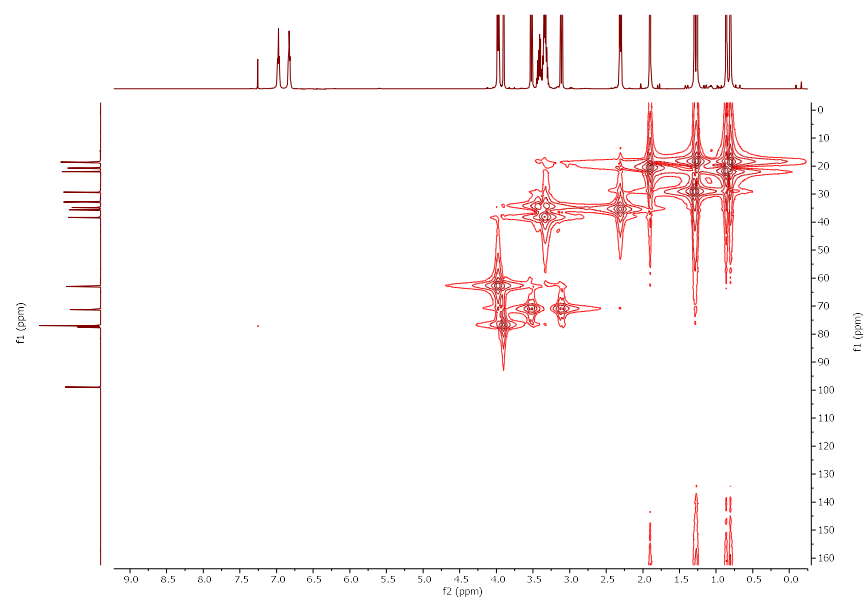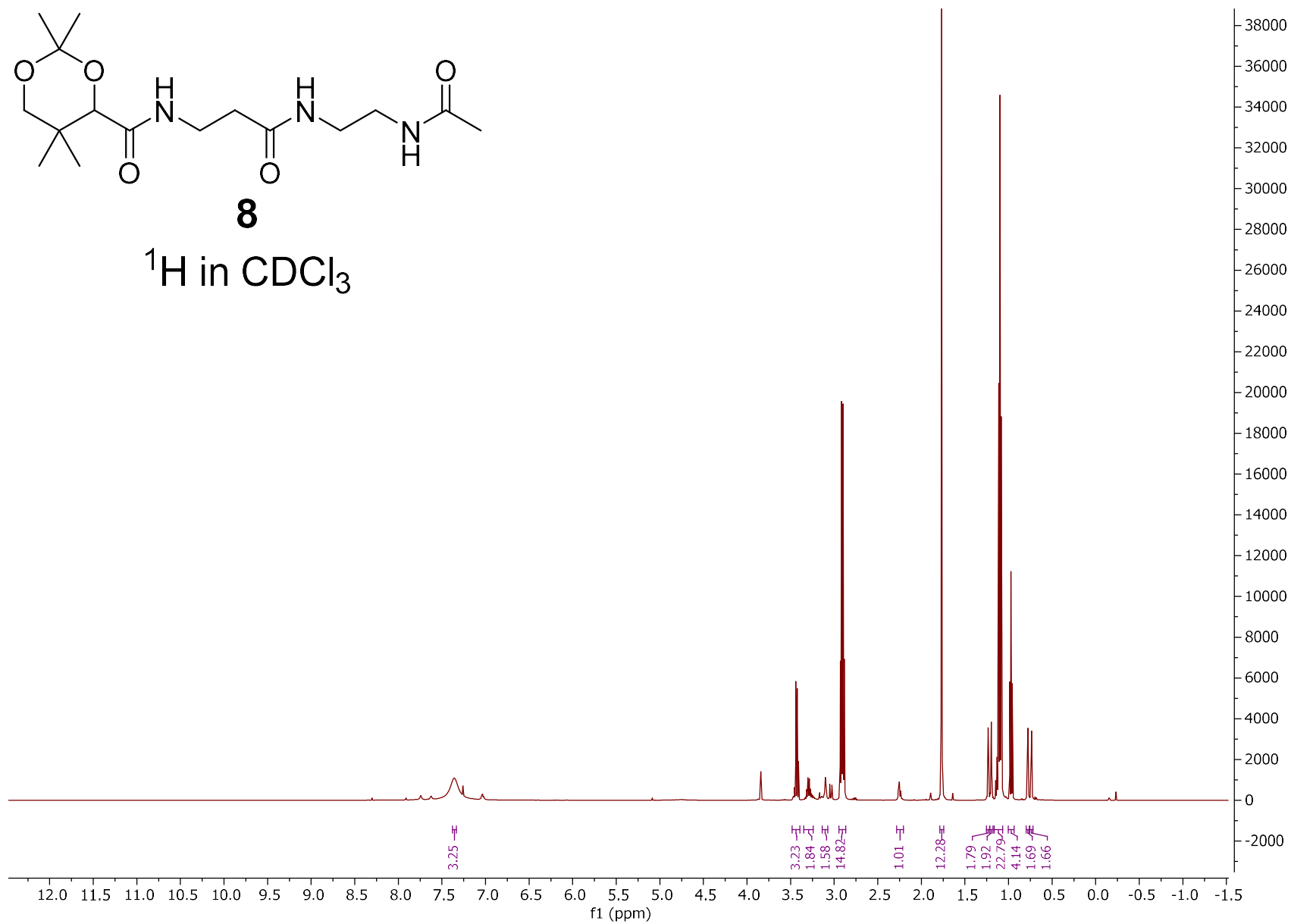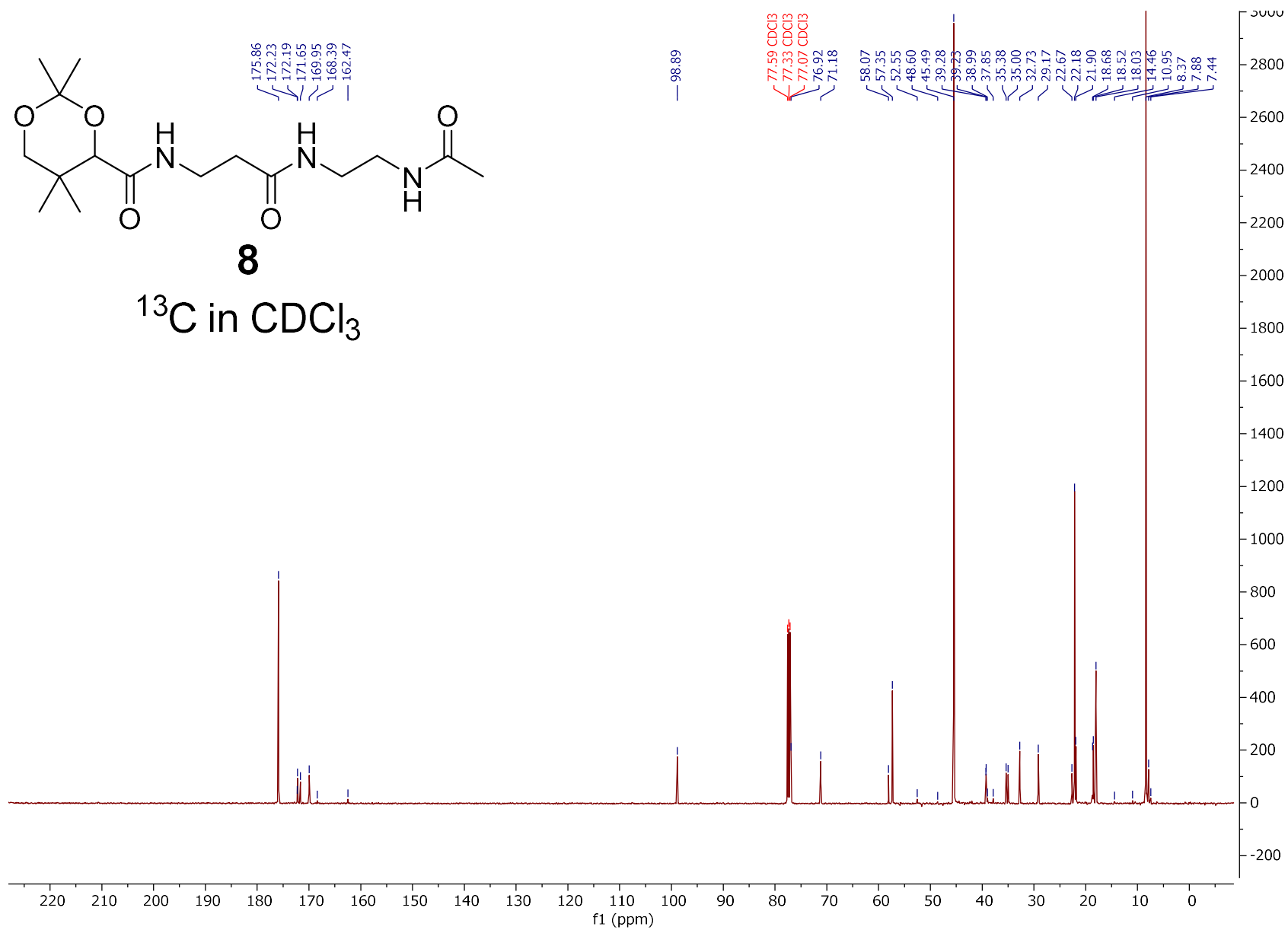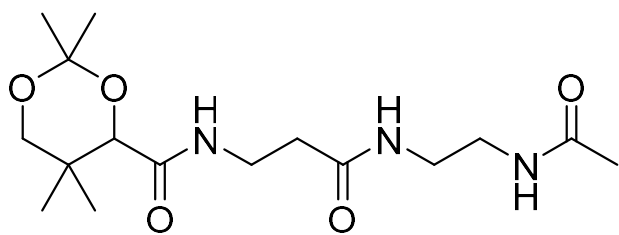
^{13}C in CDCl$_3$

COSY and HMQC in CDCl$_3$

9

^{1}H in CDCl$_3$

9
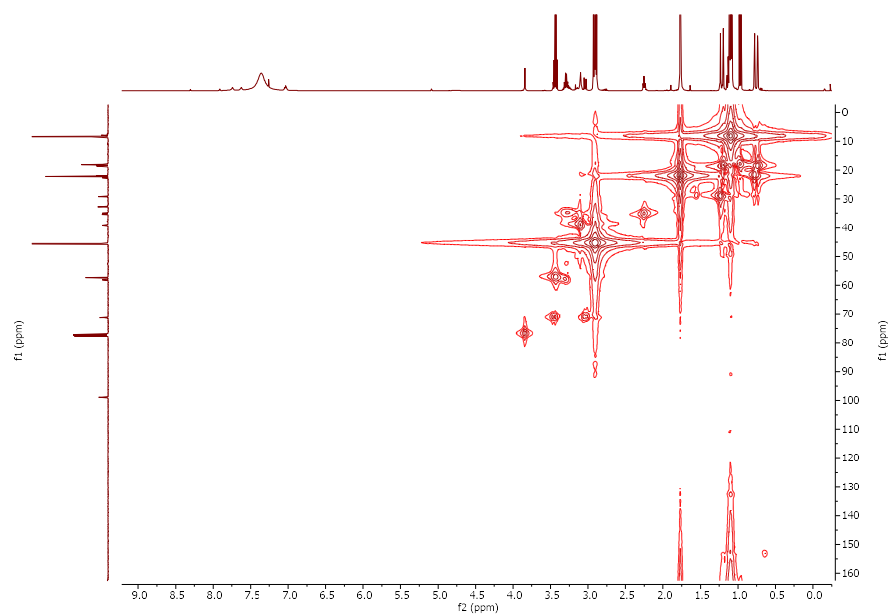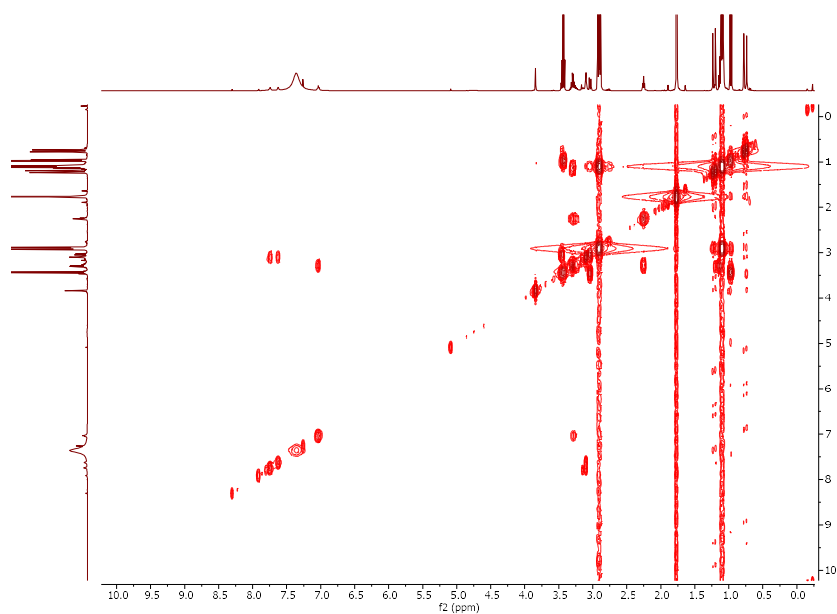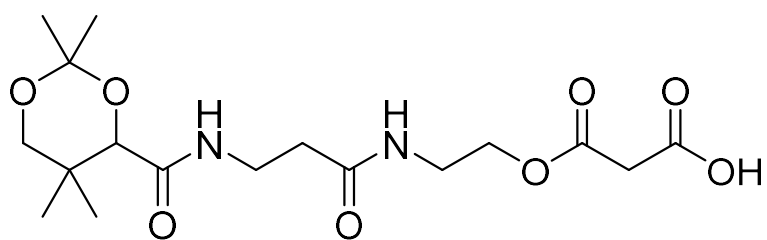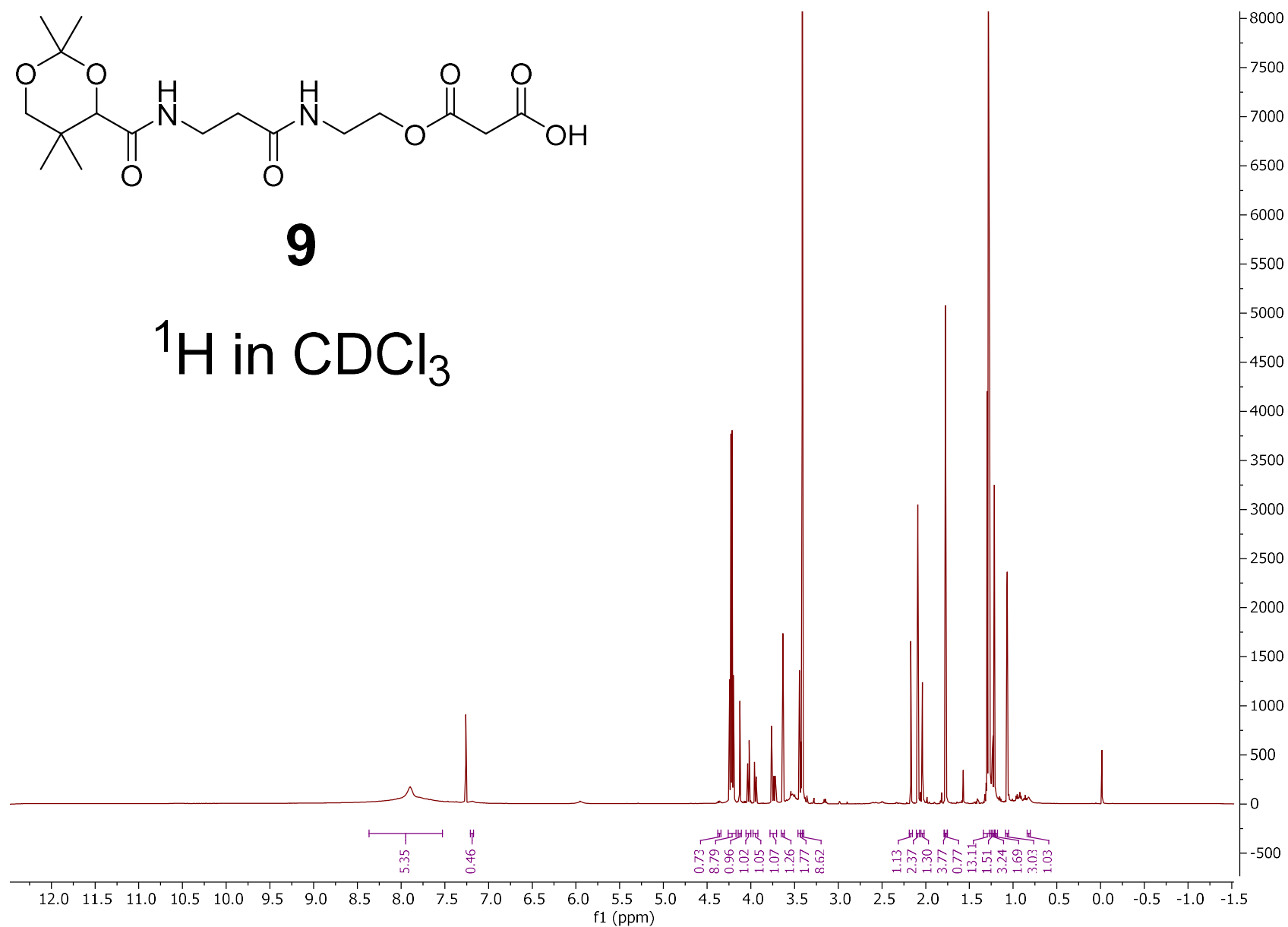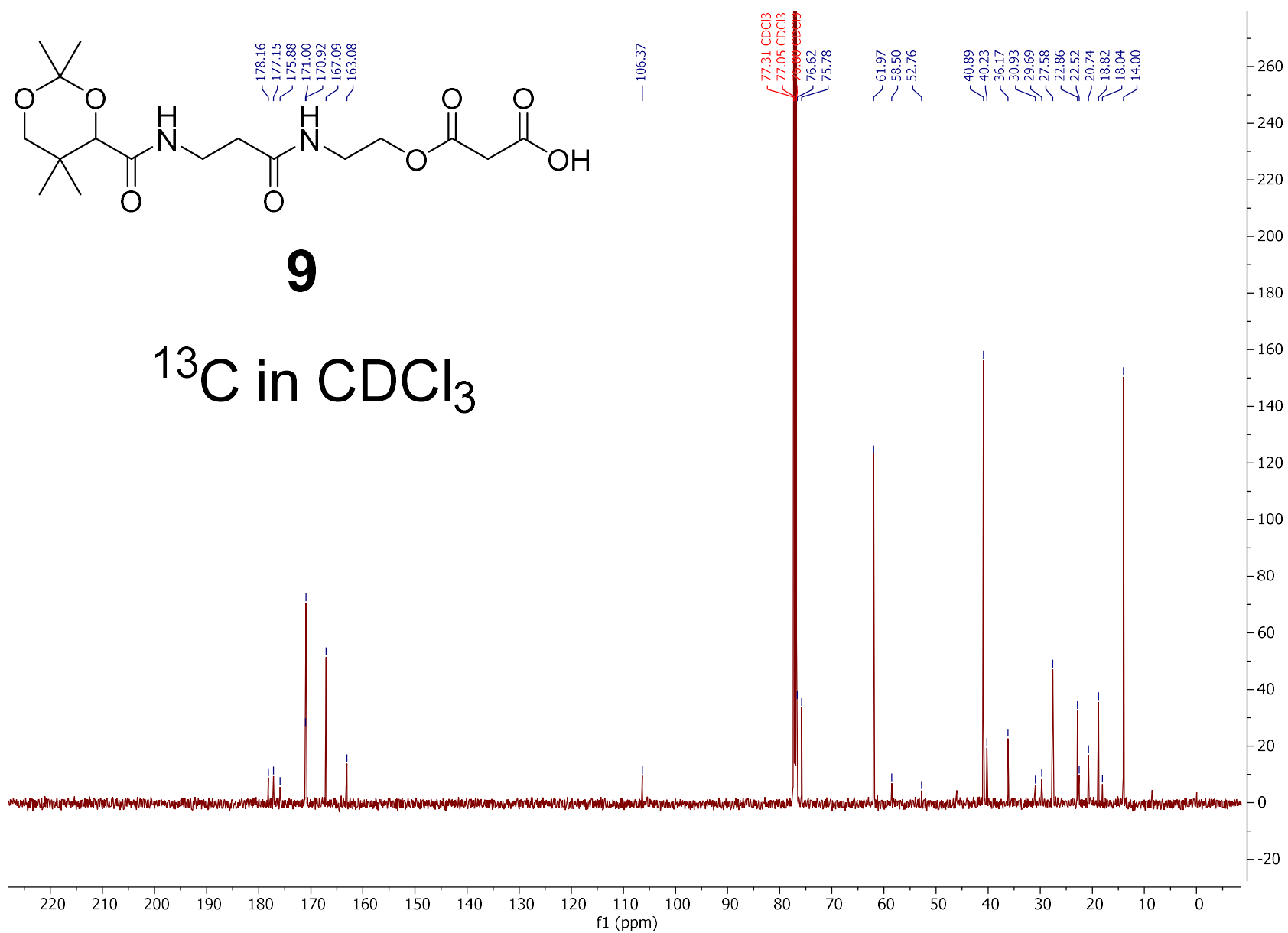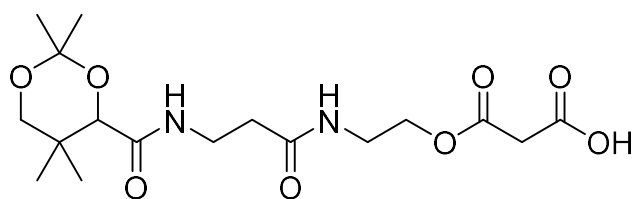
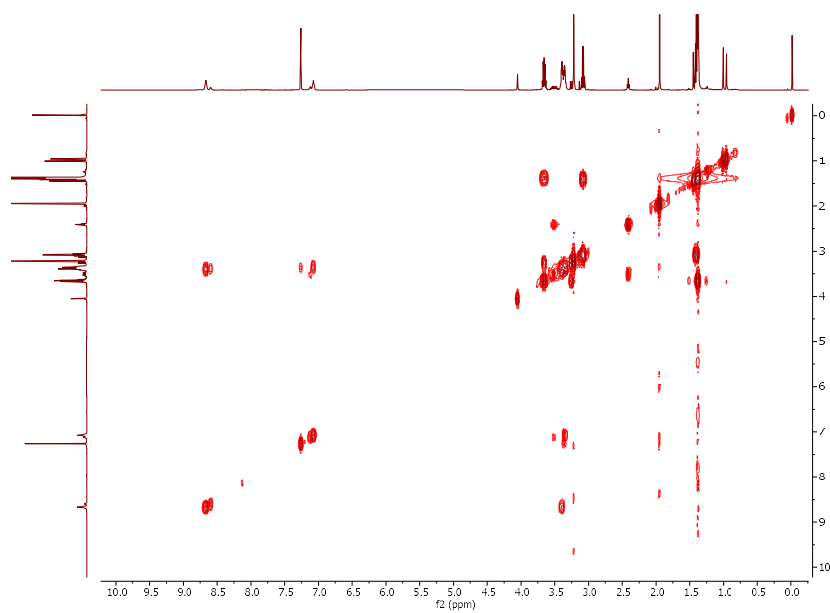^{13}C in CDCl$_3$

9

COSY and HMQC in CDCl$_3$

10

^{1}H in CDCl$_3$

10
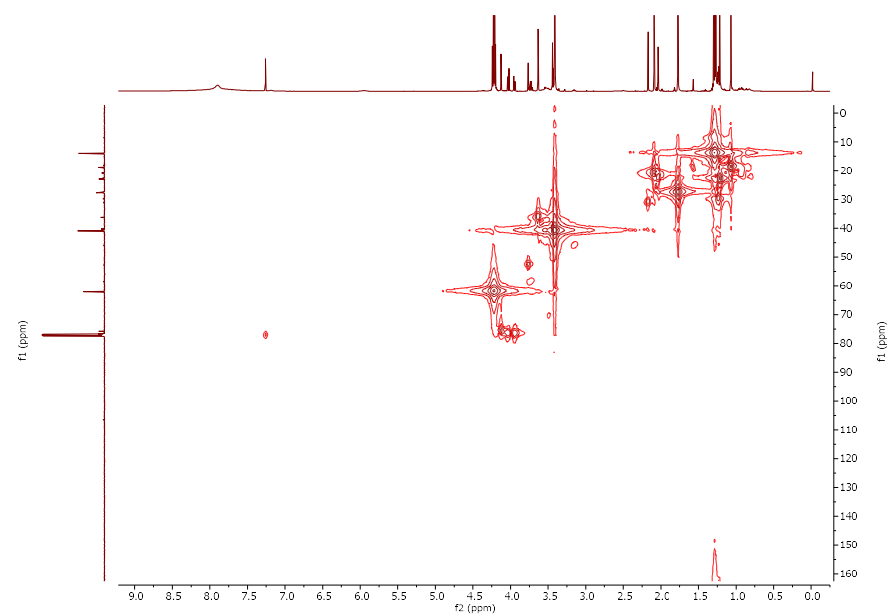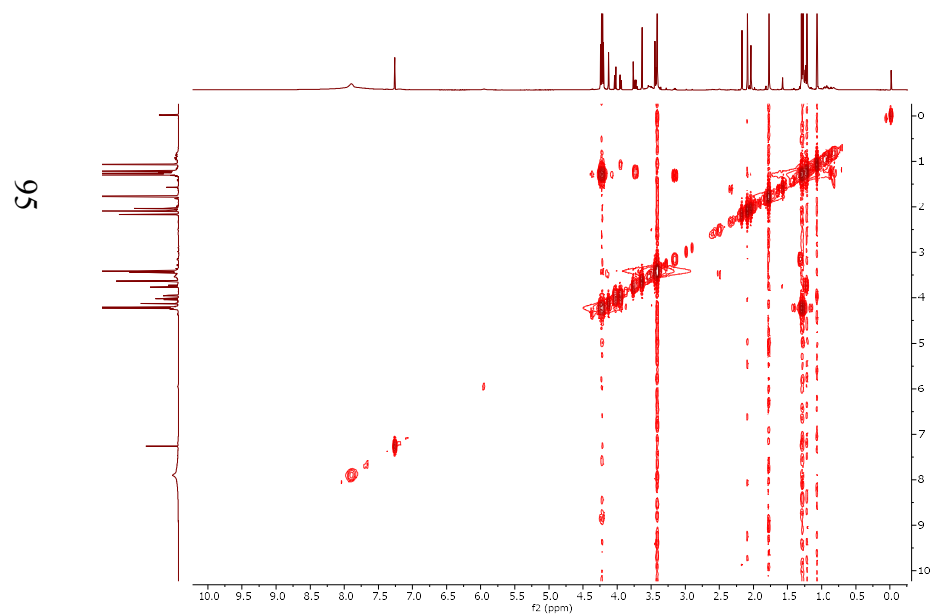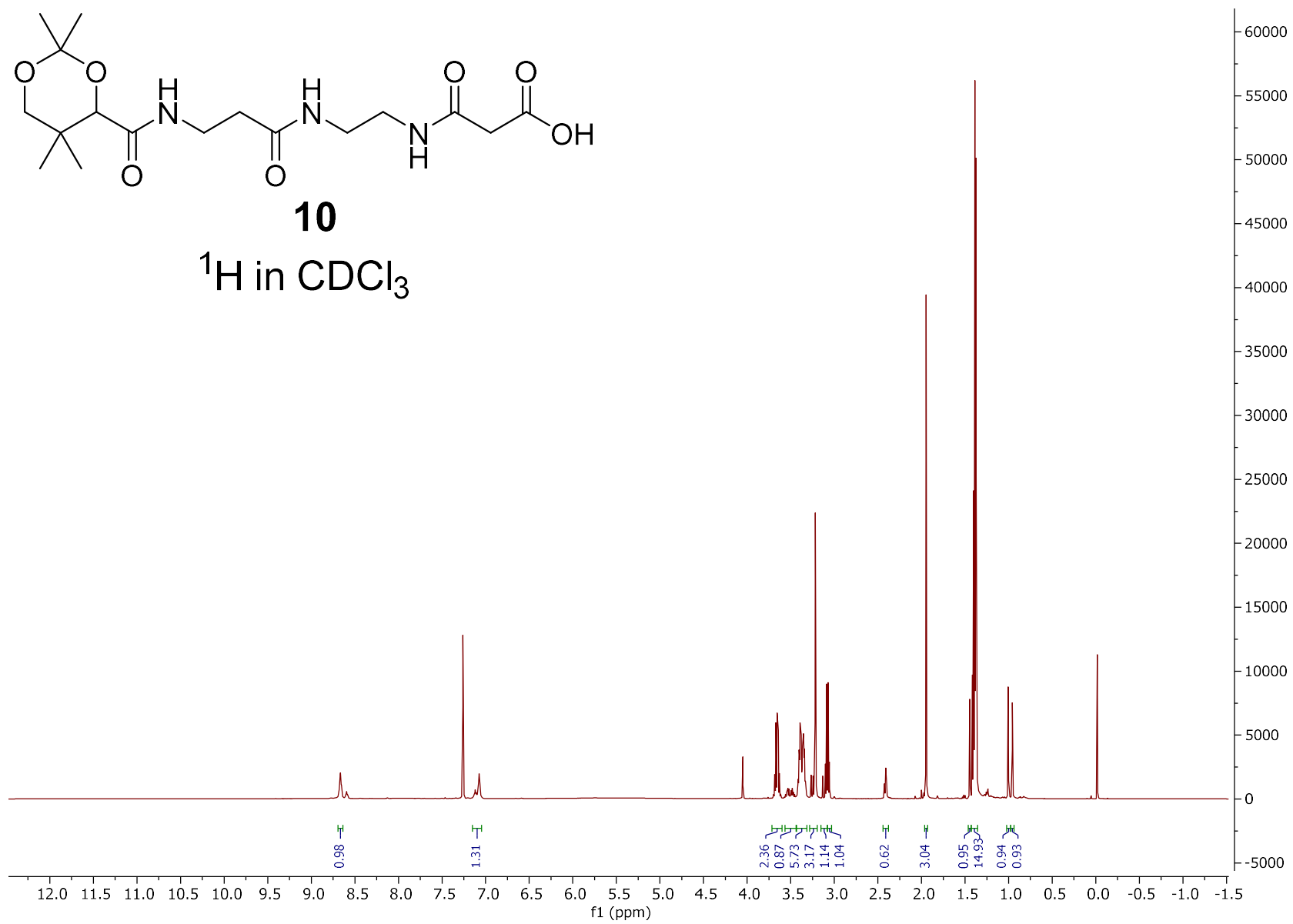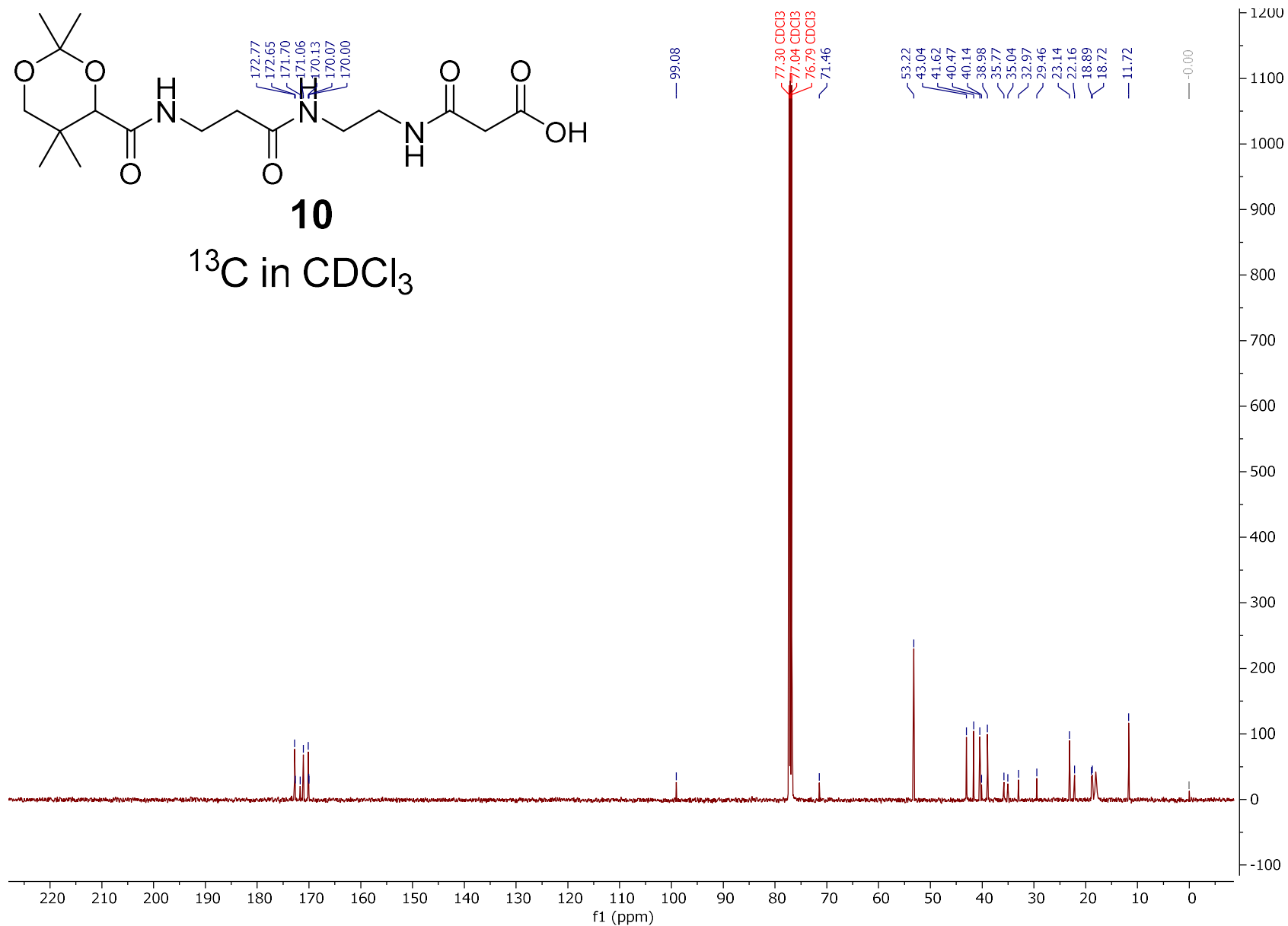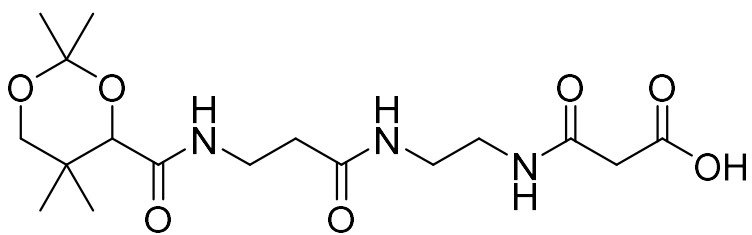
^{13}C in CDCl$_3$

10

COSY and HMQC in CDCl$_3$

11

^{1}H in D$_2$O

11
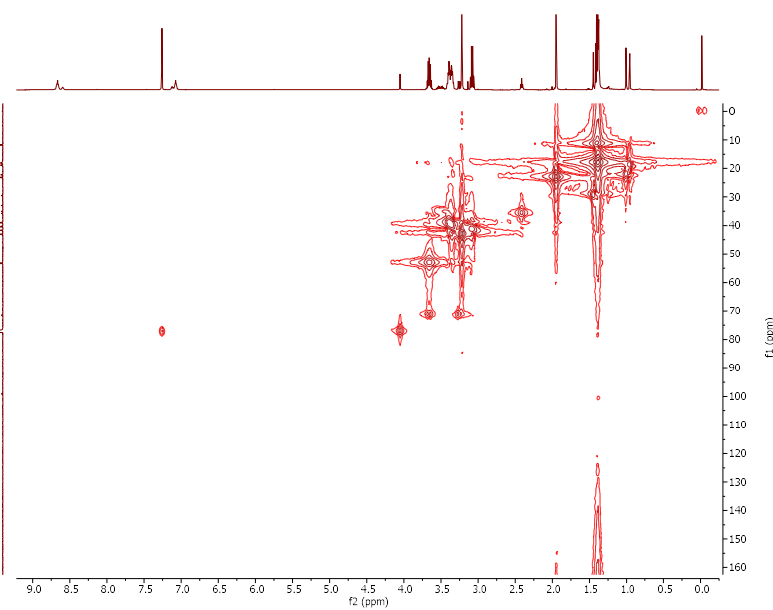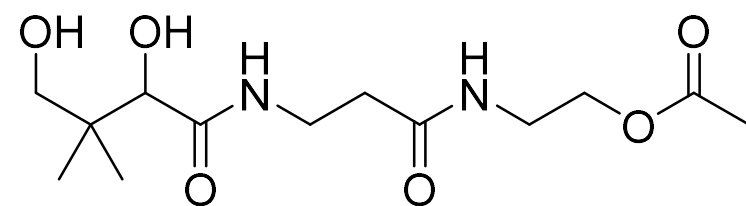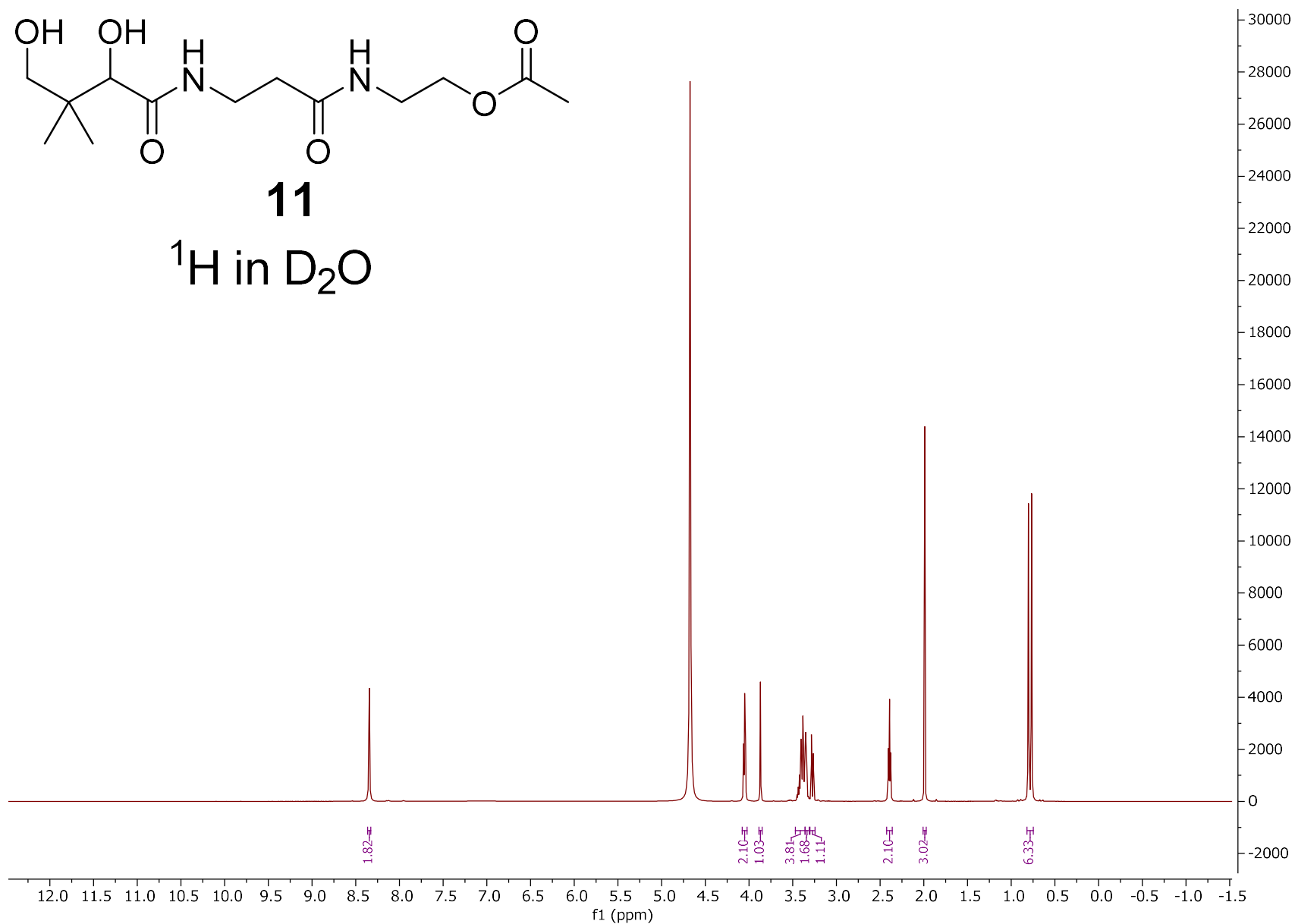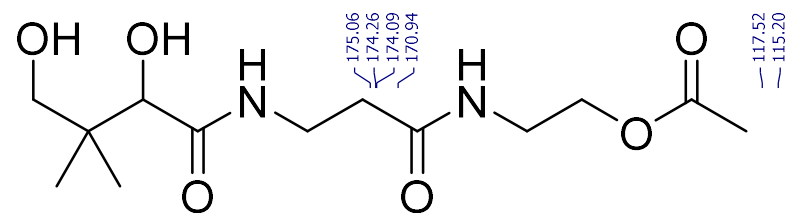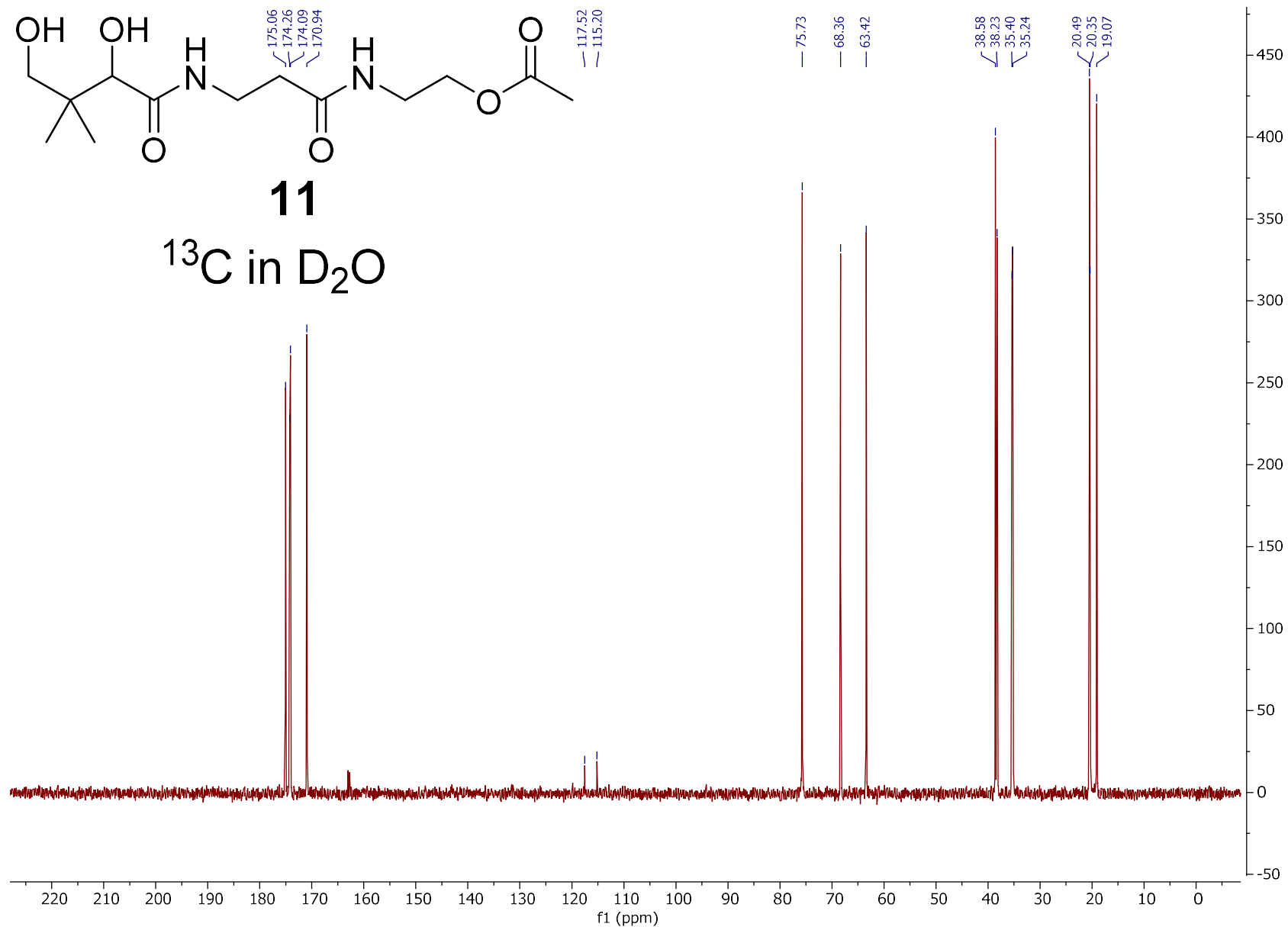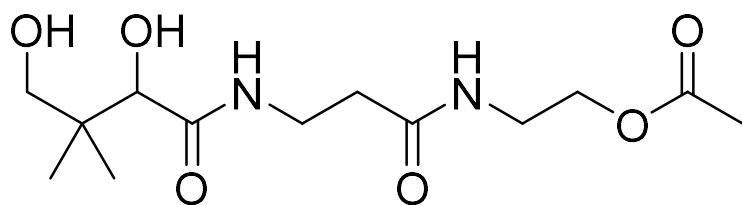
^{13}C in D$_2$O

11

COSY and HMQC in D$_2$O

12

^{1}H in D$_2$O

12
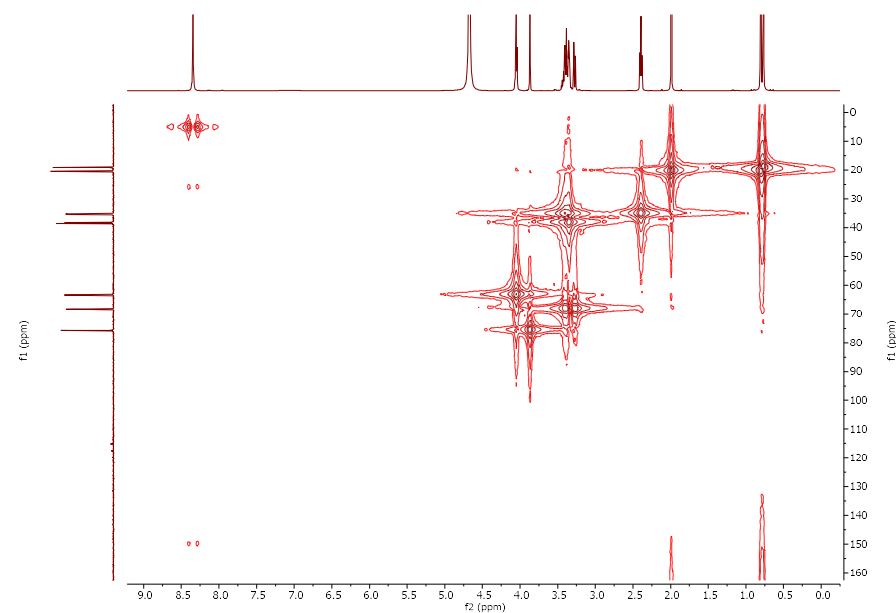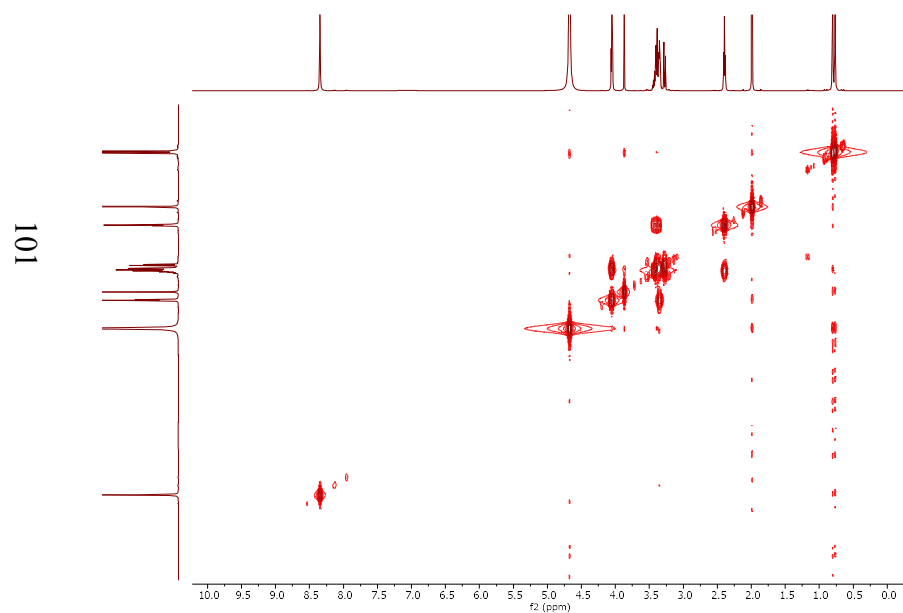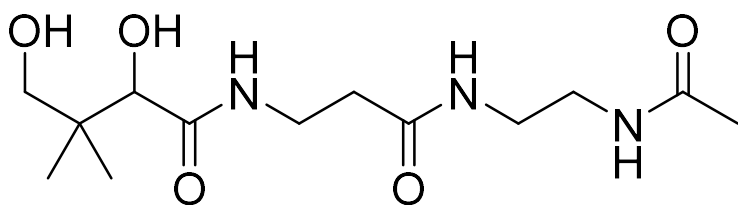
^{13}C in D$_2$O

12

COSY and HMQC in D$_2$O

13

^{1}H in D$_2$O

13
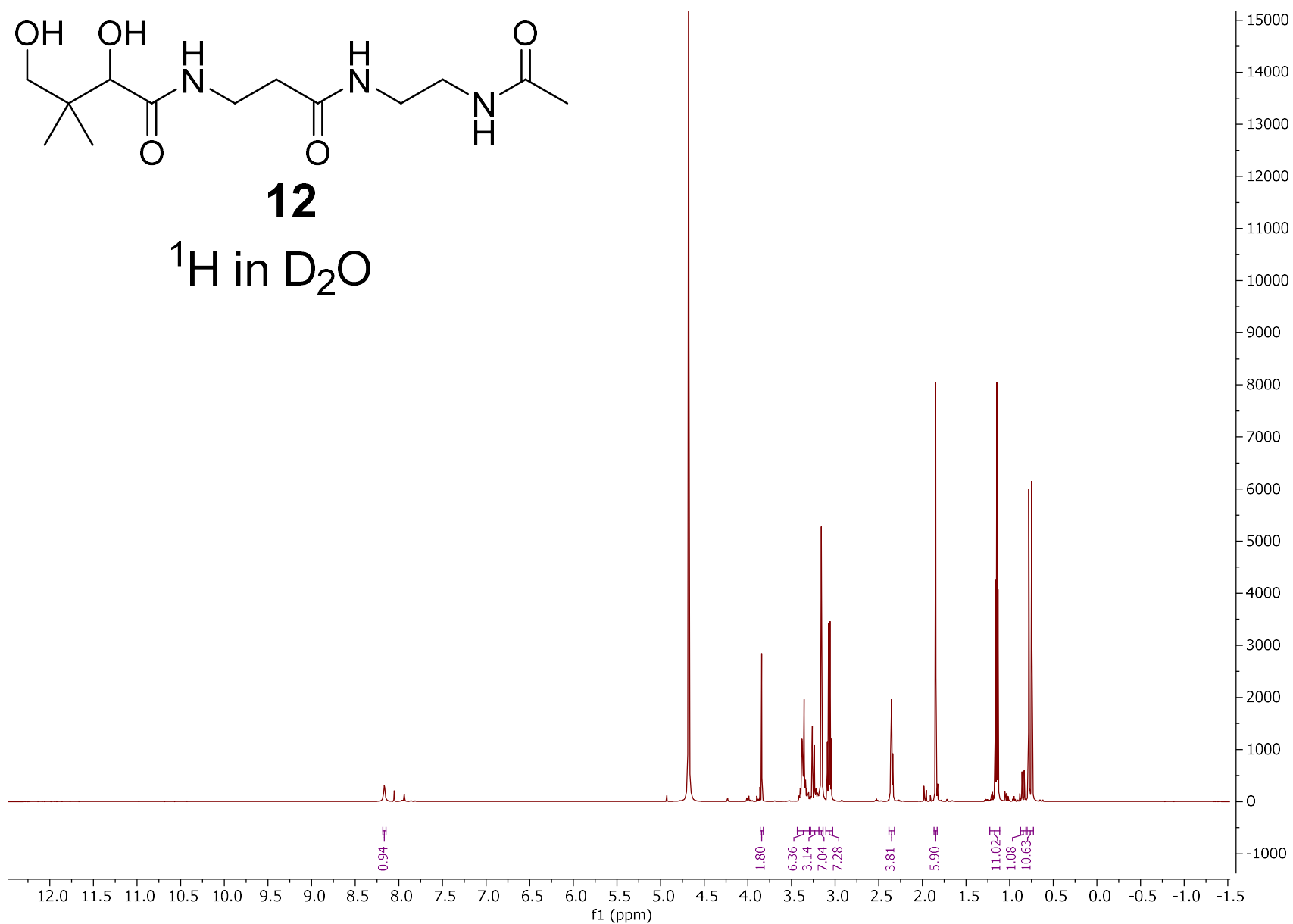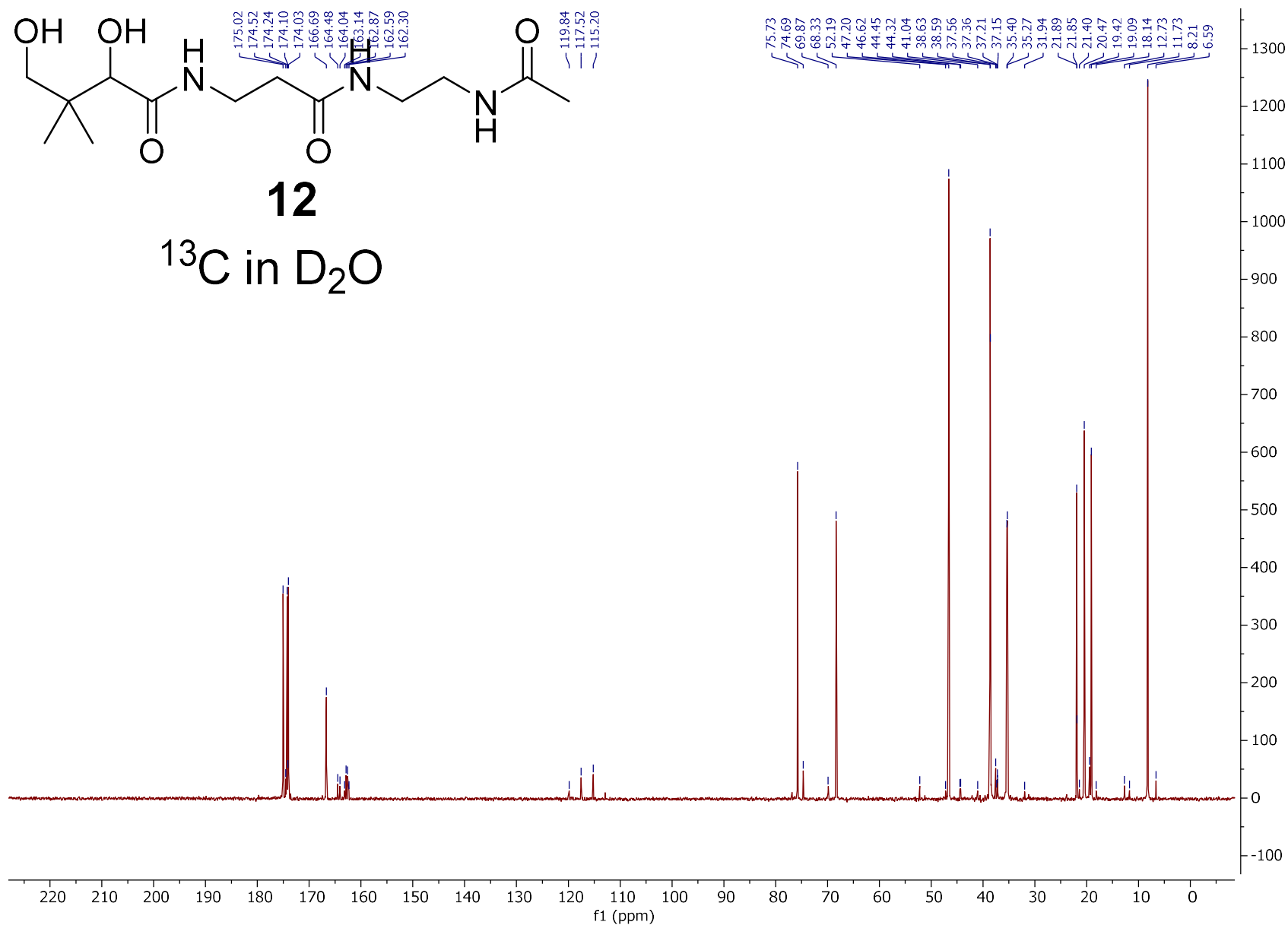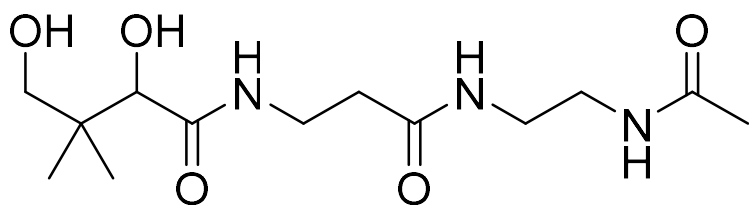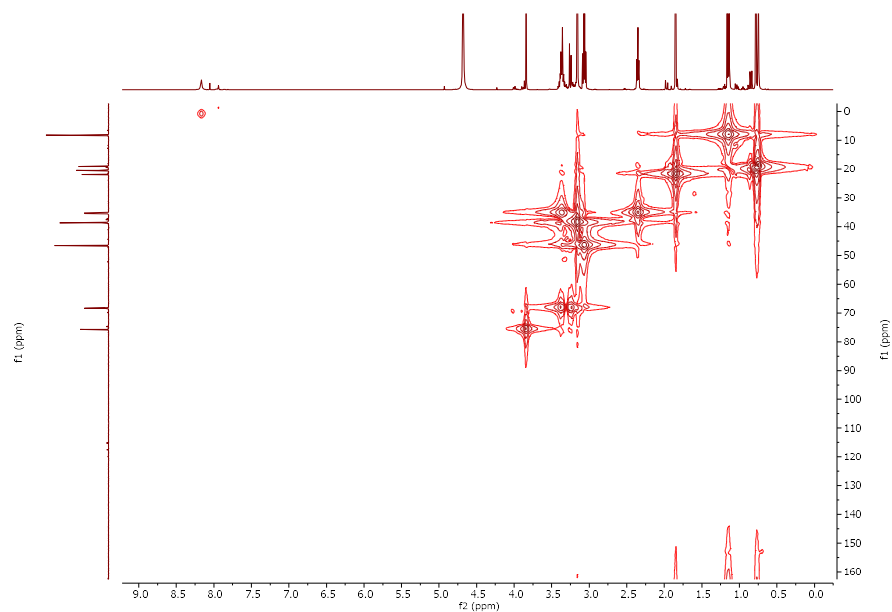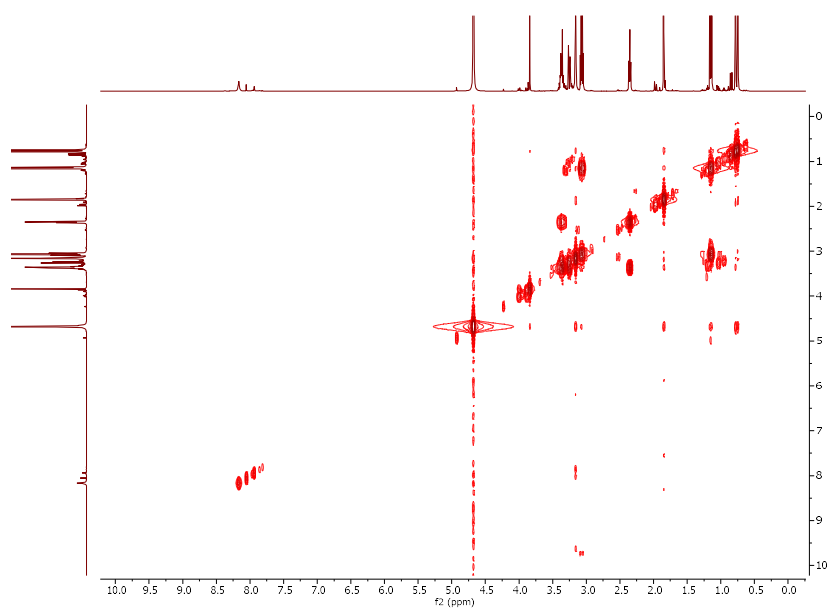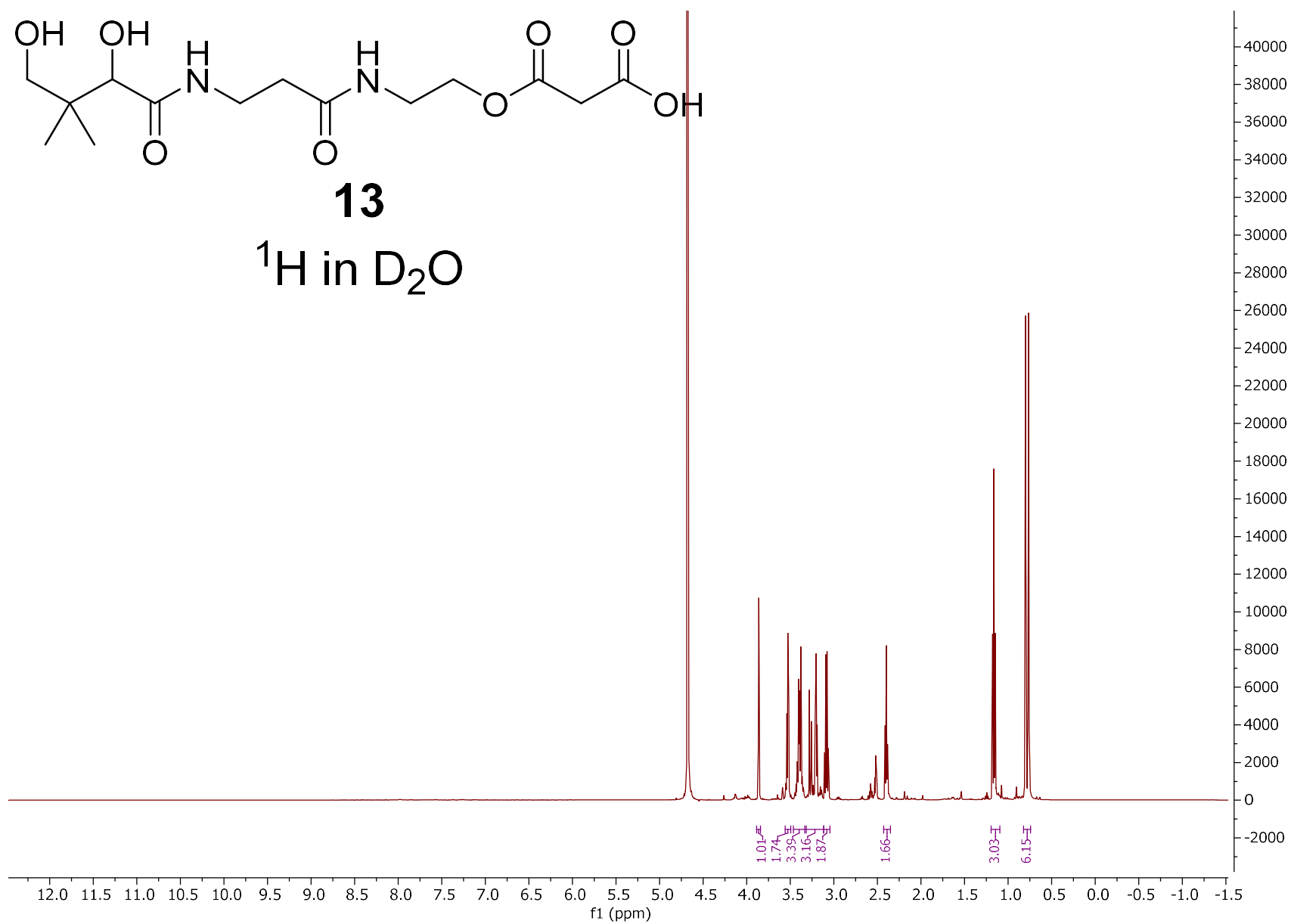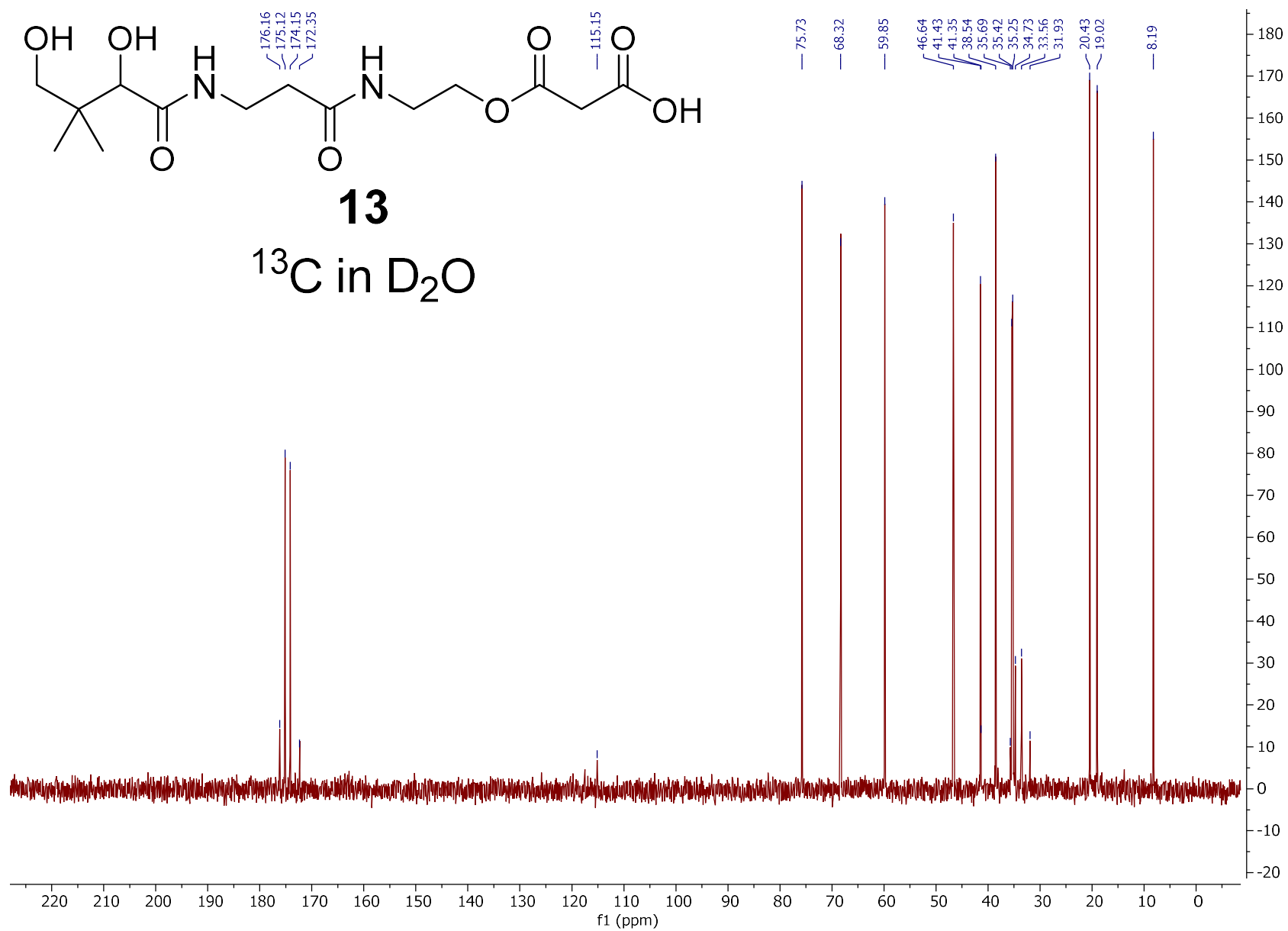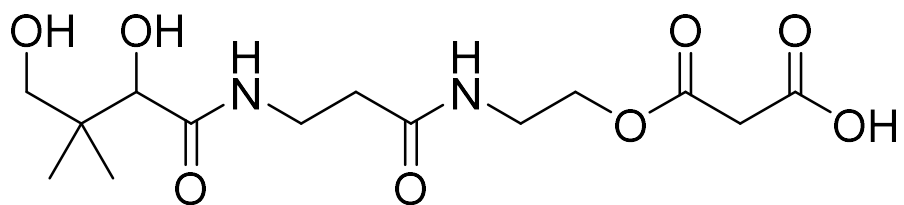
^{13}C in D$_2$O

13

COSY and HMQC in D$_2$O

14

^{1}H in D$_2$O

14
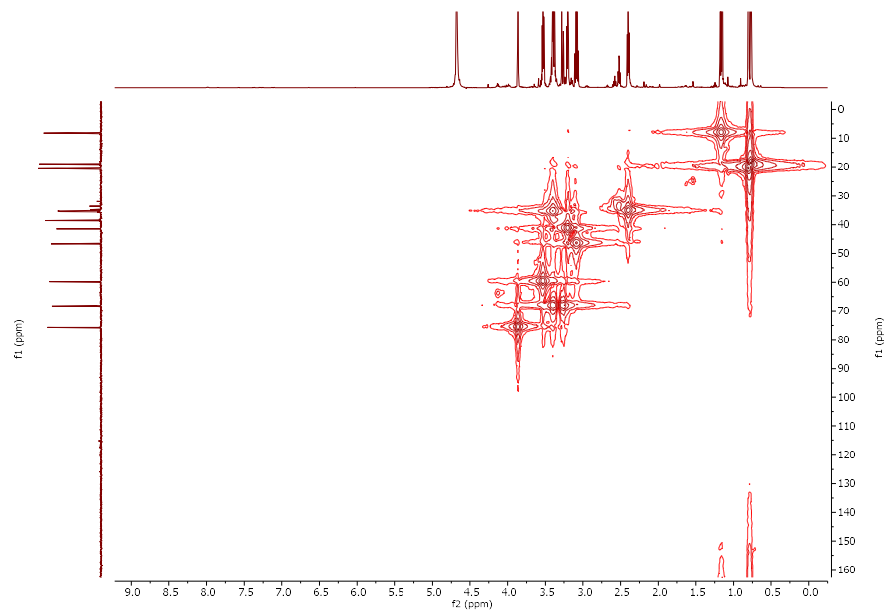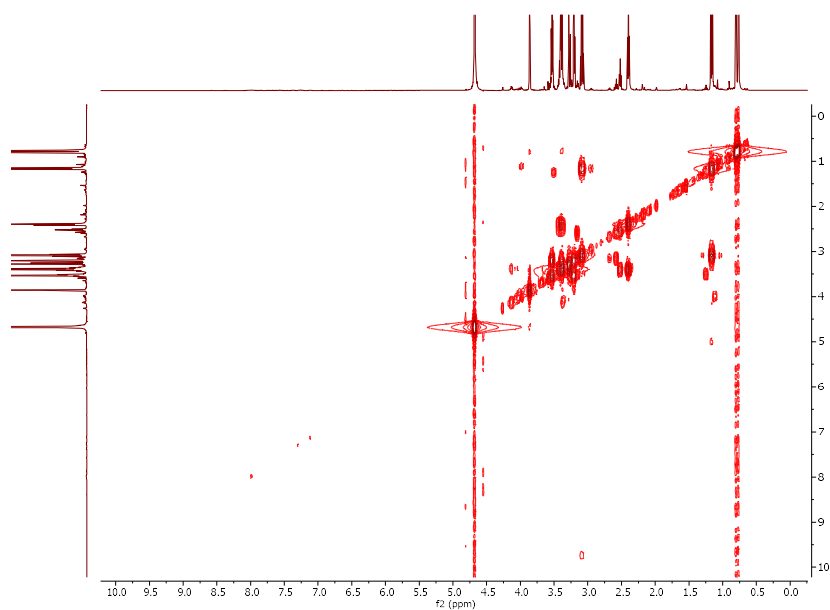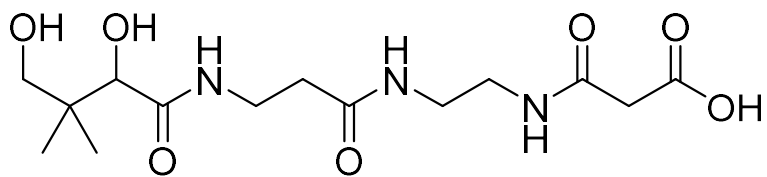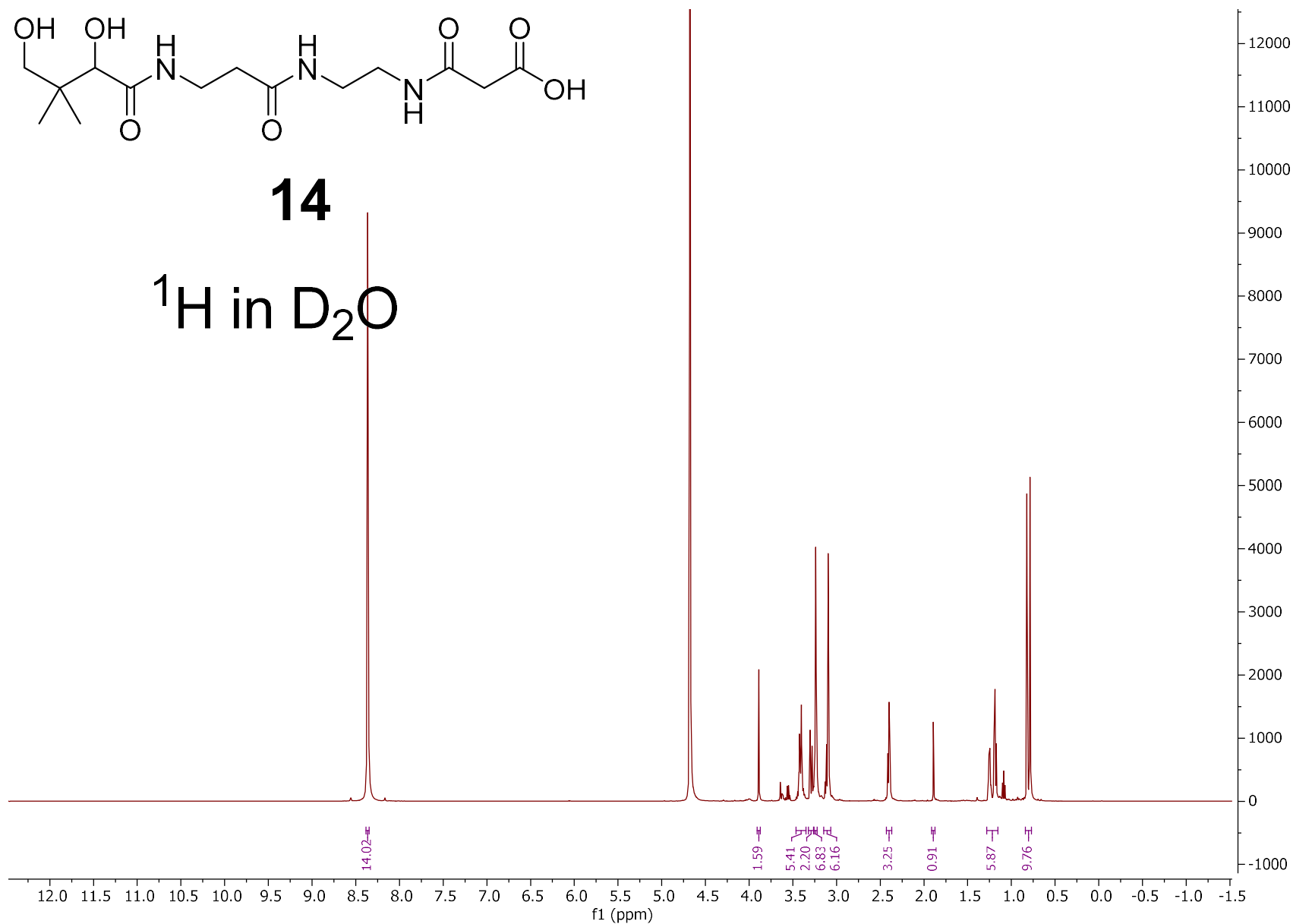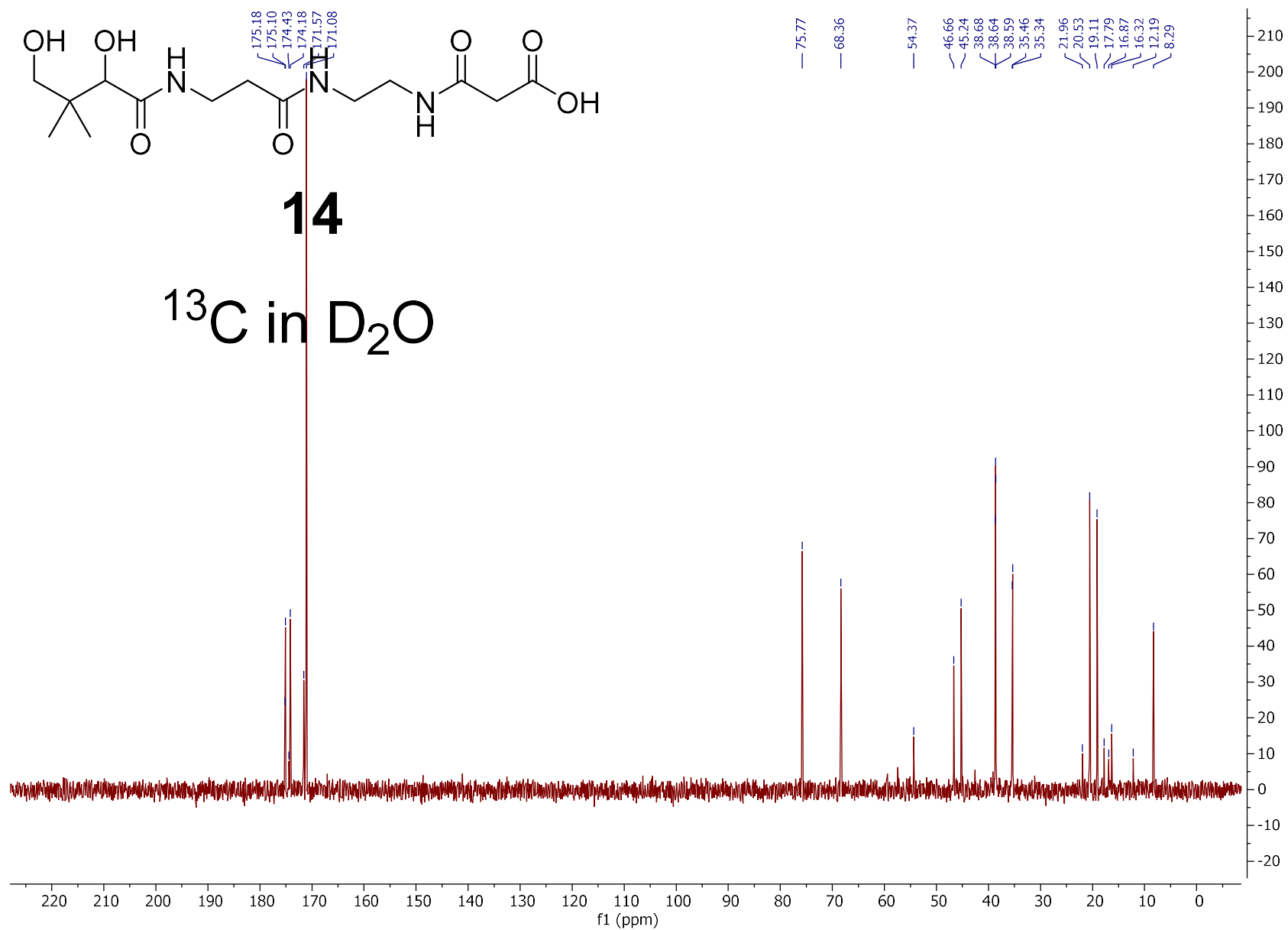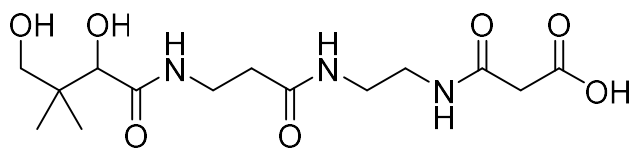
^{13}C in D$_2$O

14

COSY and HMQC in D$_2$O

1

^{1}H in D$_2$O

1

^{13}C in D$_2$O

1

COSY and HMQC in D$_2$O

2
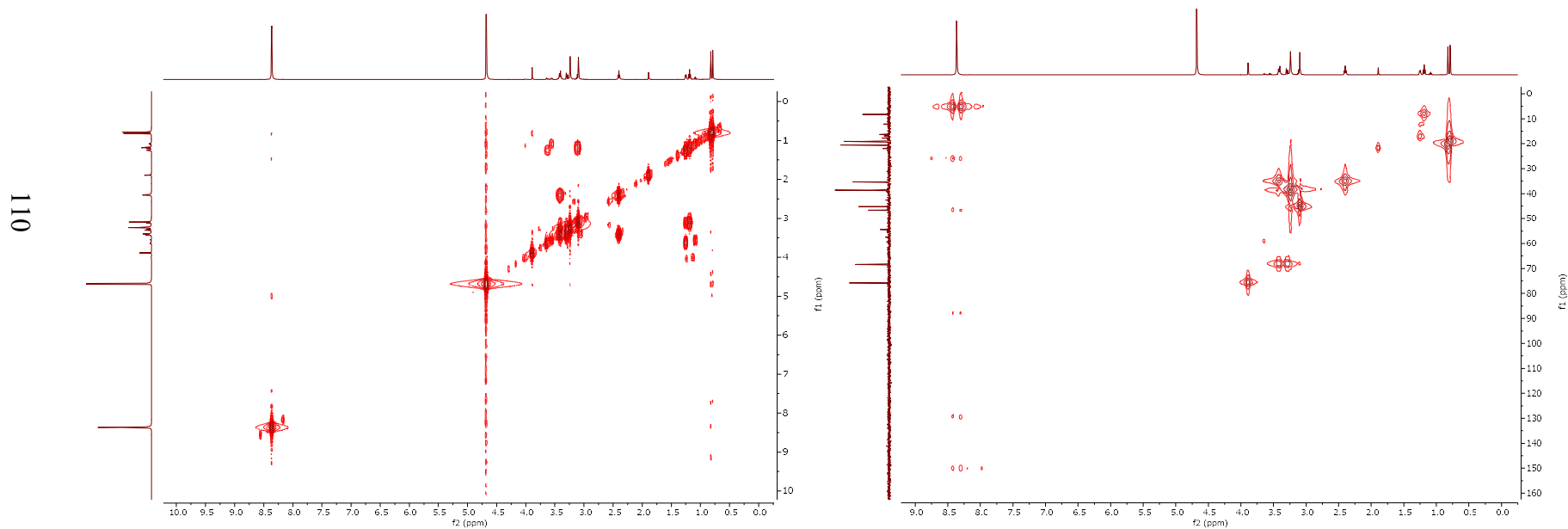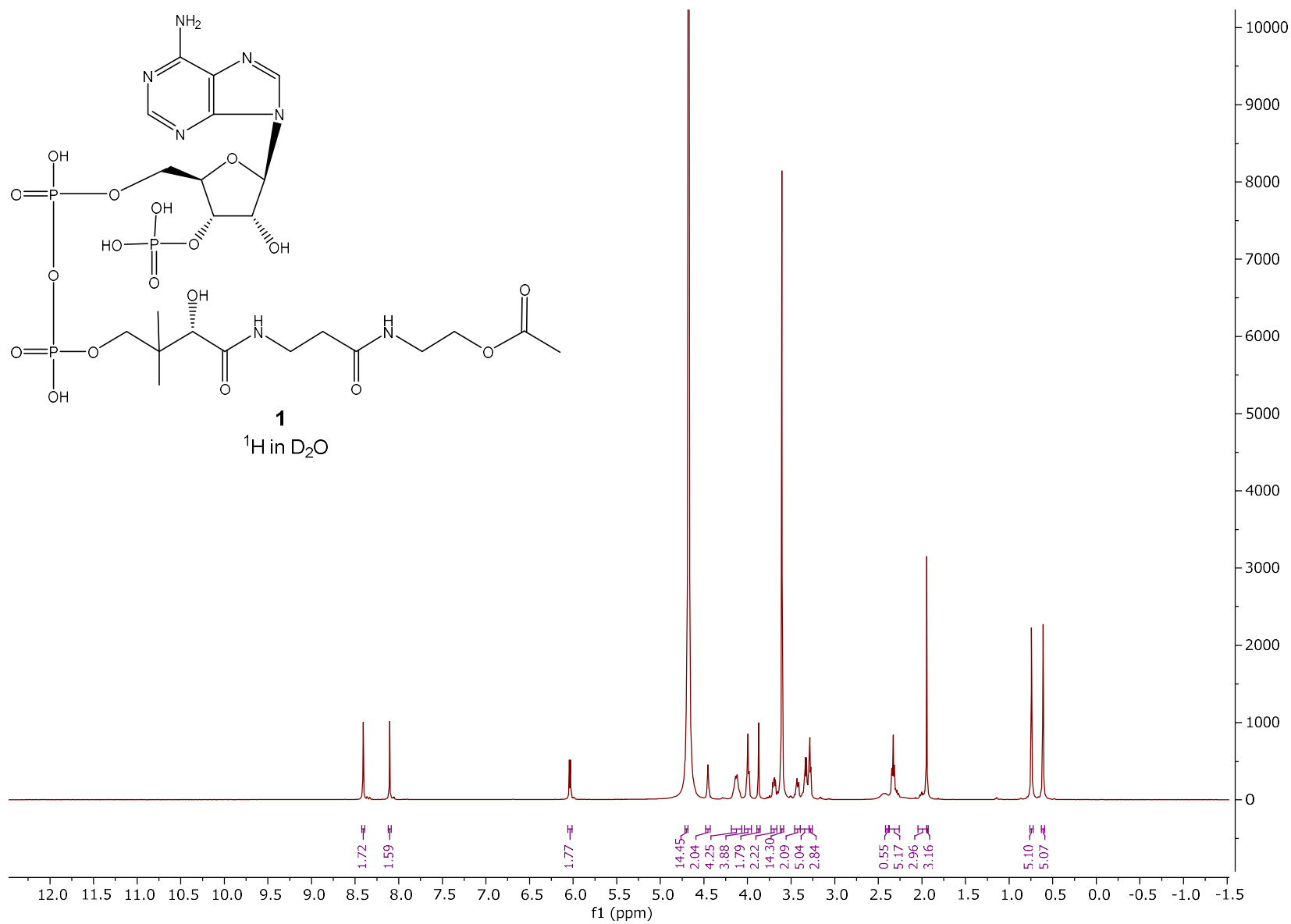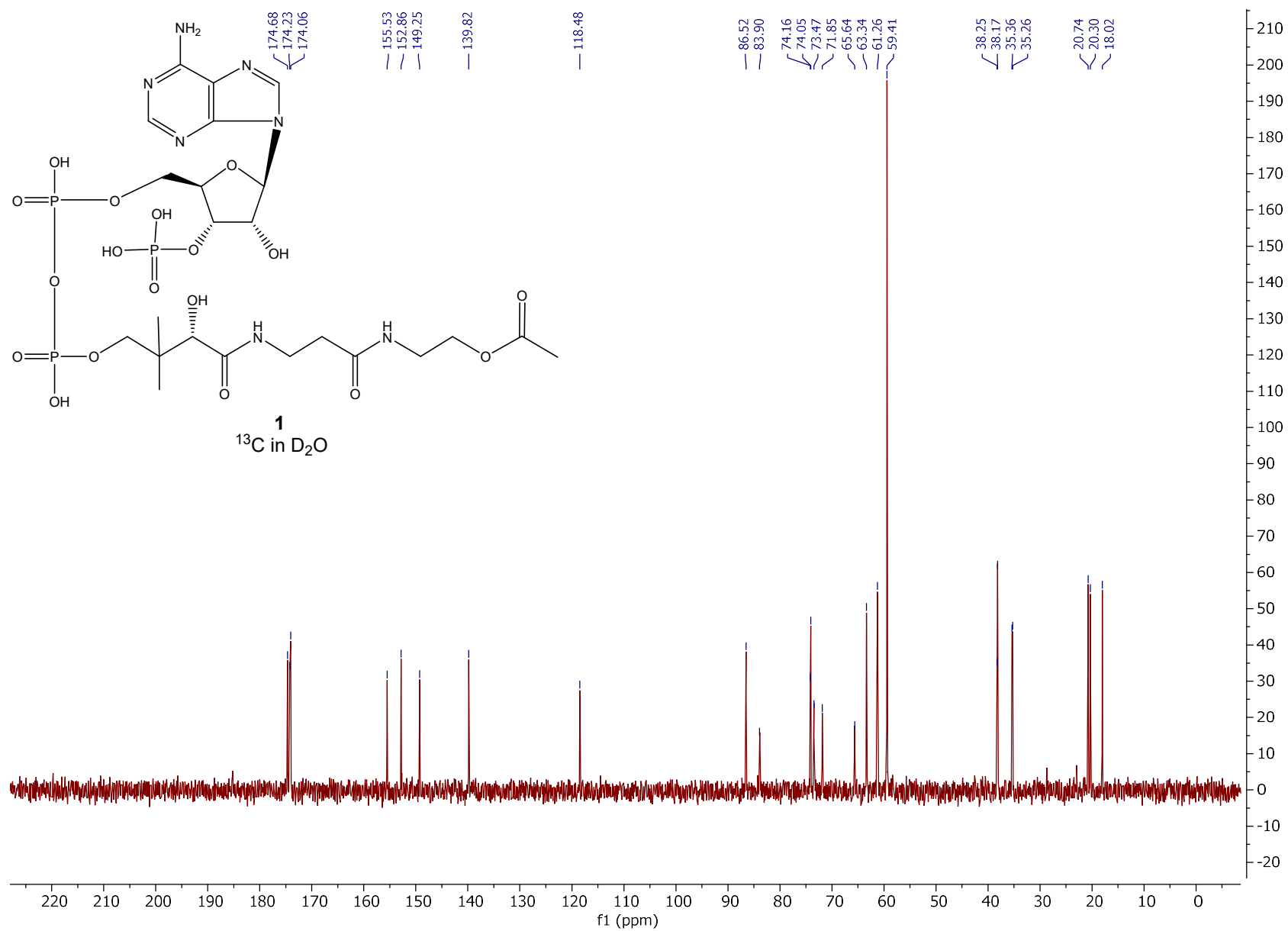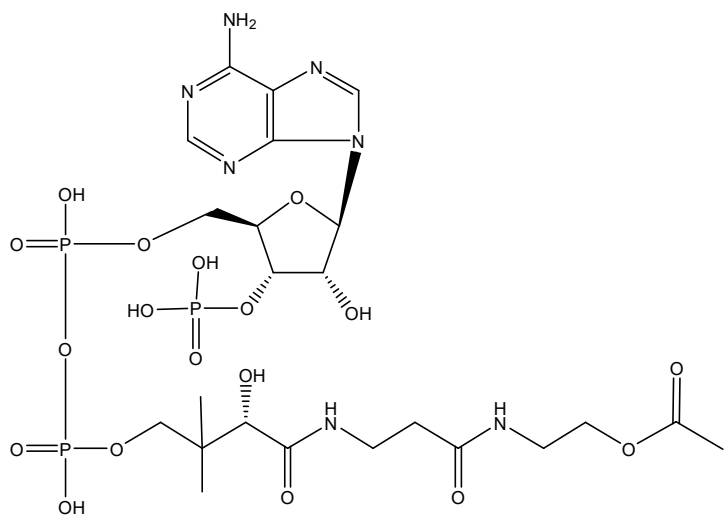
^{1}H in D$_2$O

2
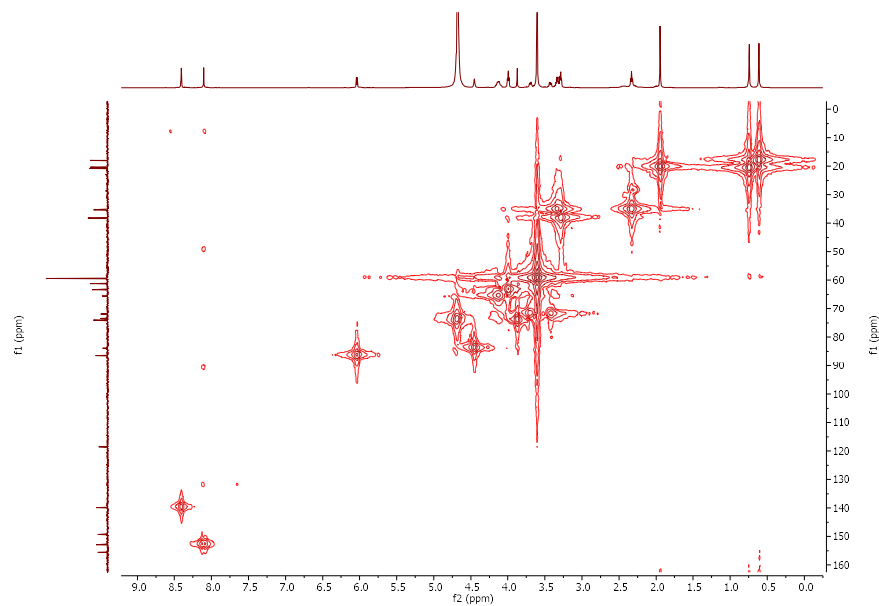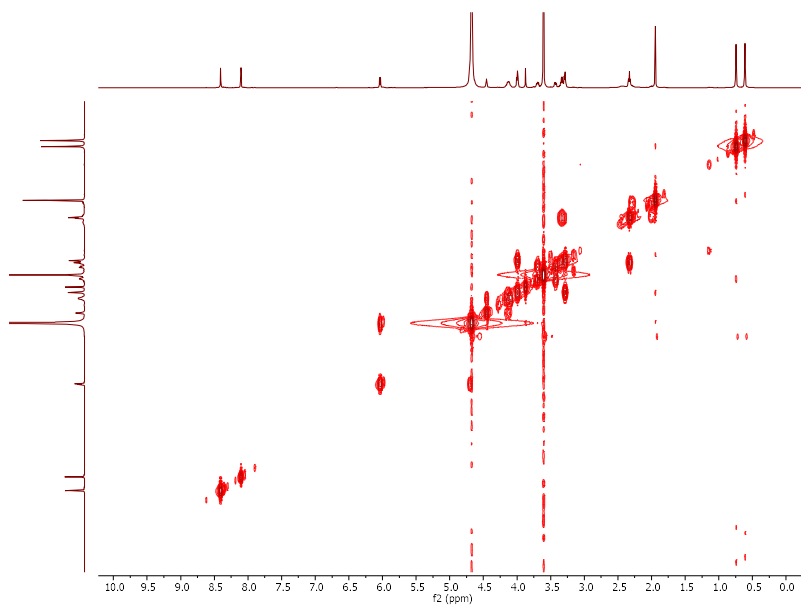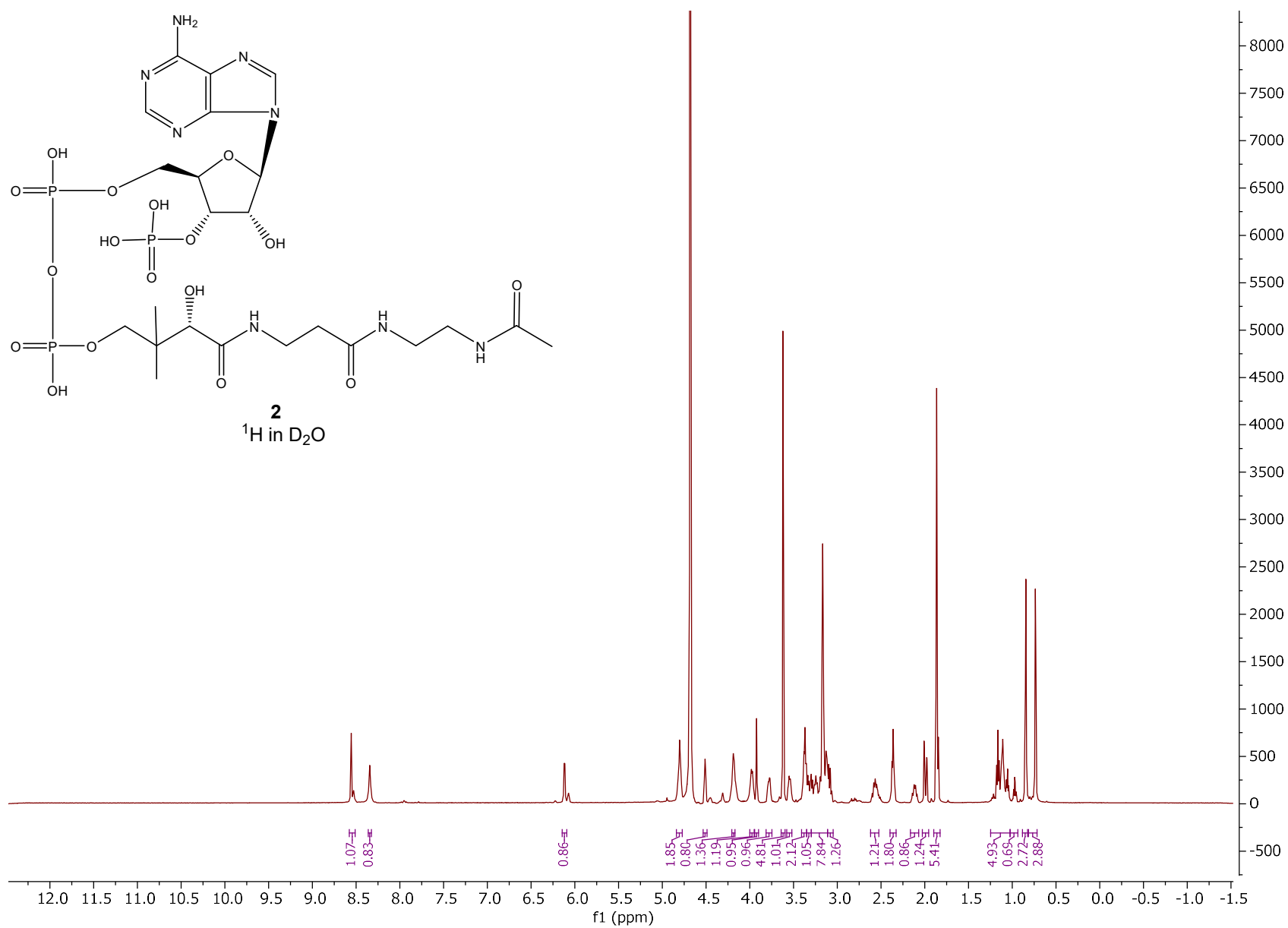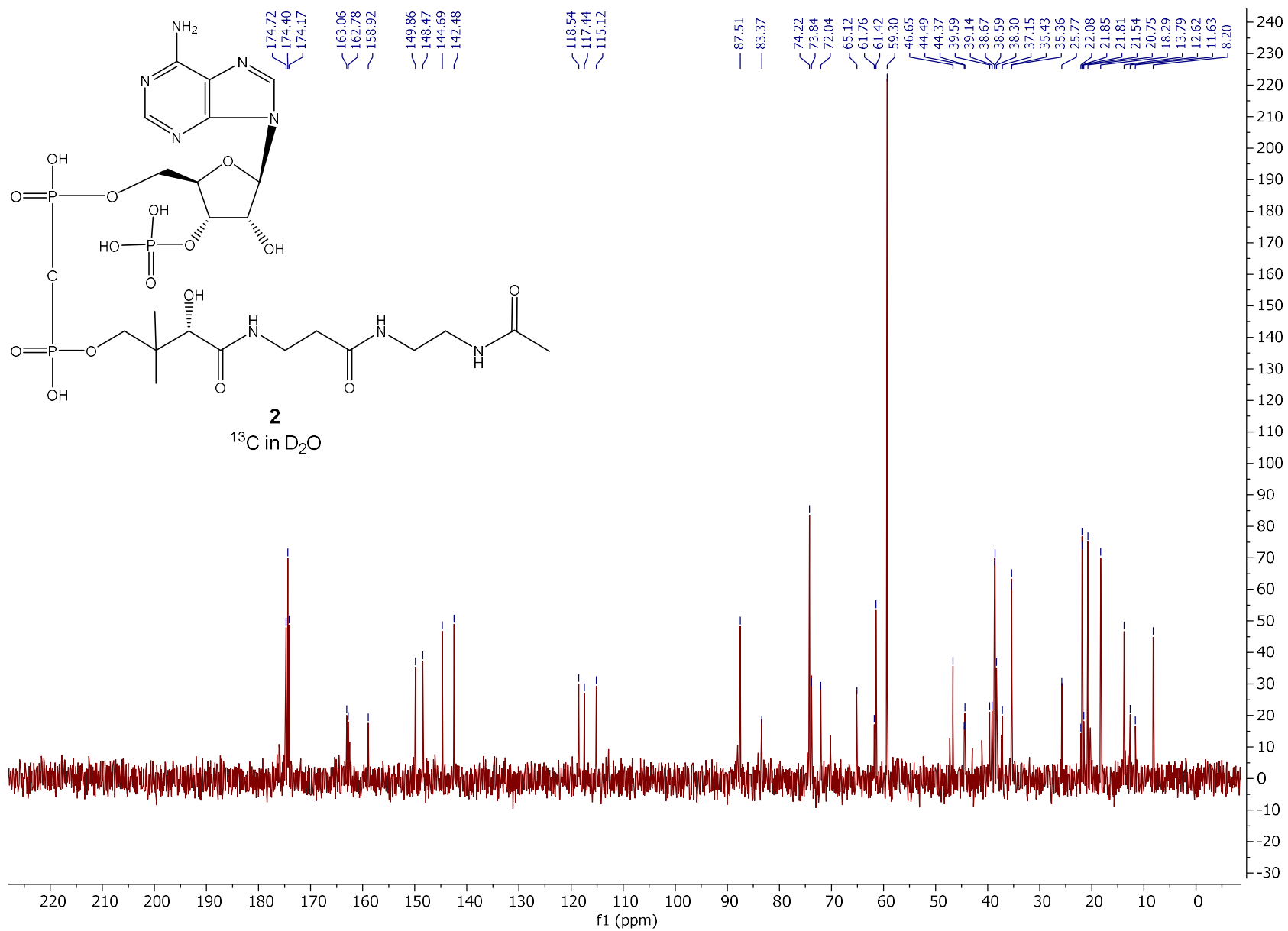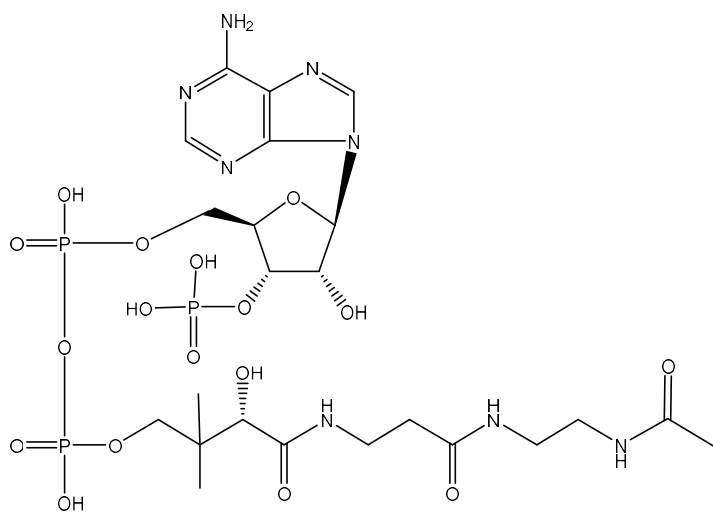
COSY and HMQC in D$_2$O

3

^{1}H in D$_2$O

3

^{13}C in D$_2$O

3

COSY and HMQC in D$_2$O

4

¹H in D₂O

4

^{13}C in D$_2$O

175.15
174.63
174.05
171.49
155.54
152.84
149.30
139.83
118.54
86.47
74.06
73.70
71.82
65.60
61.31
59.31
54.28
46.52
45.19
42.48
38.59
38.51
38.22
38.16
35.37
35.30
28.68
20.74
18.49
17.96
17.69
16.23
12.10
8.18

f1 (ppm)

4
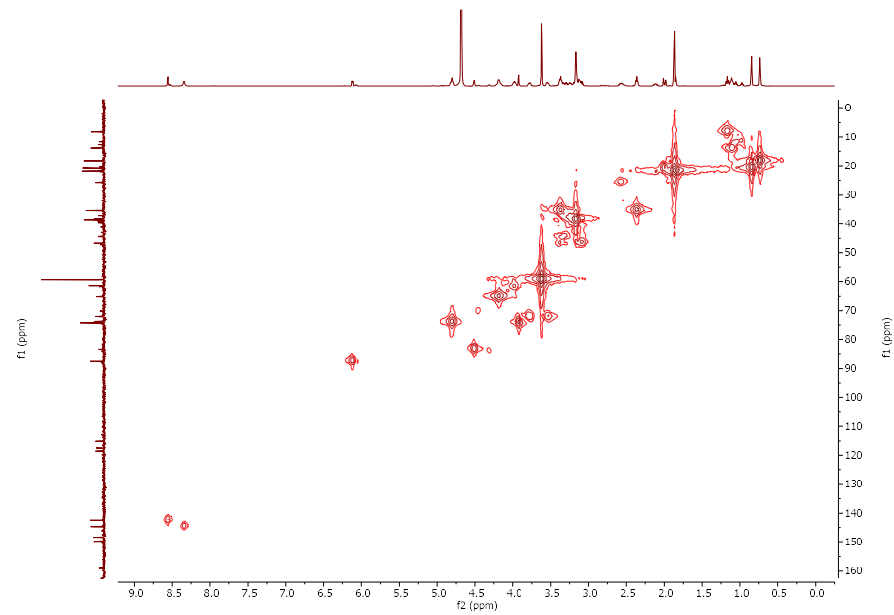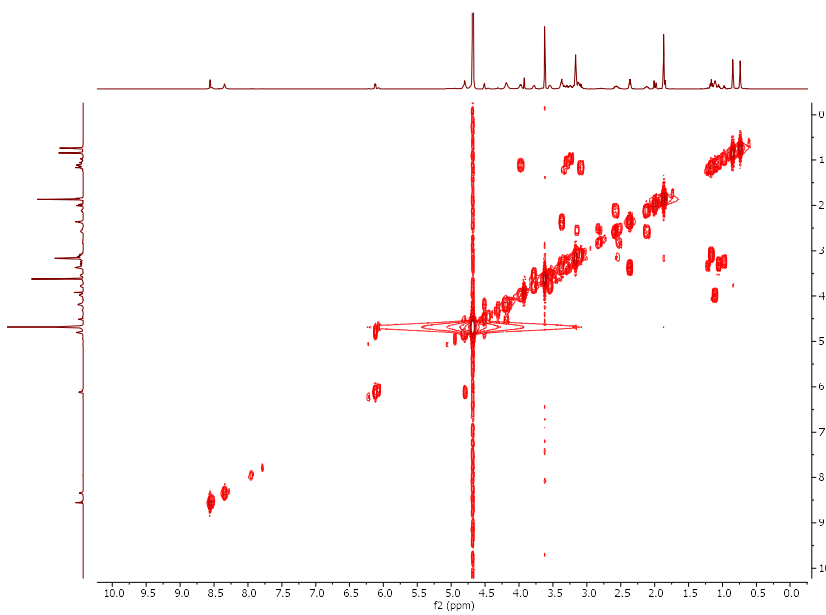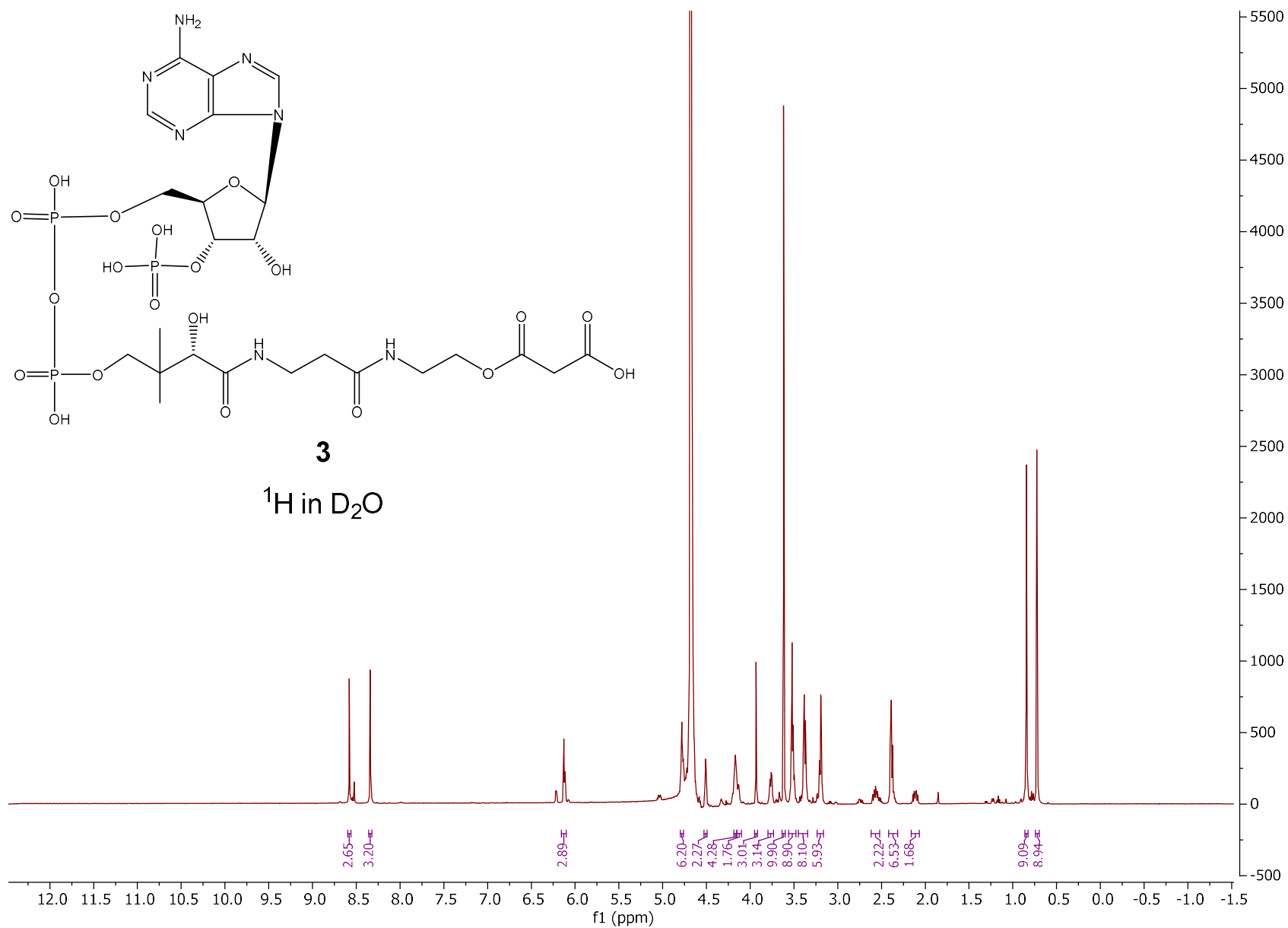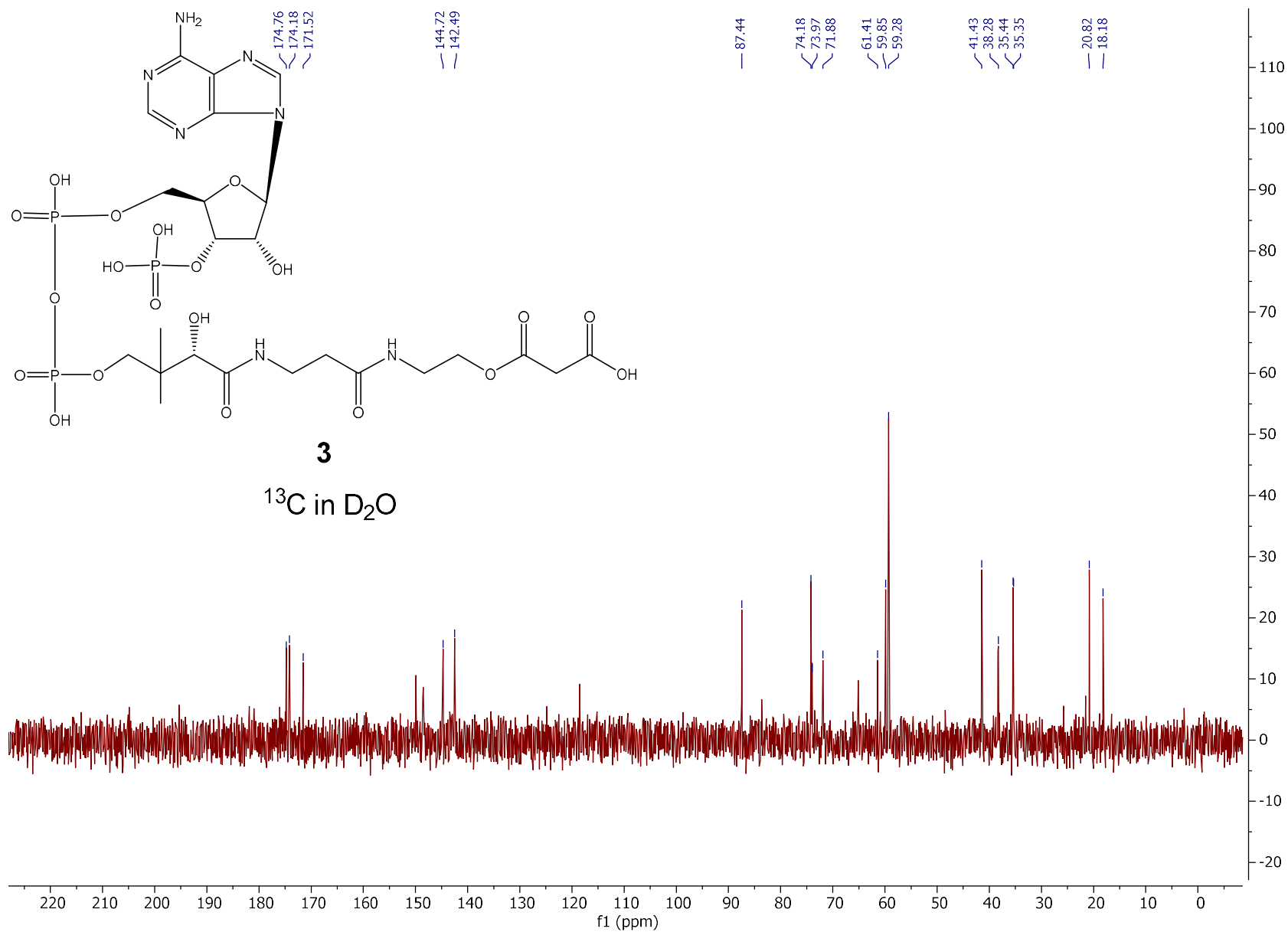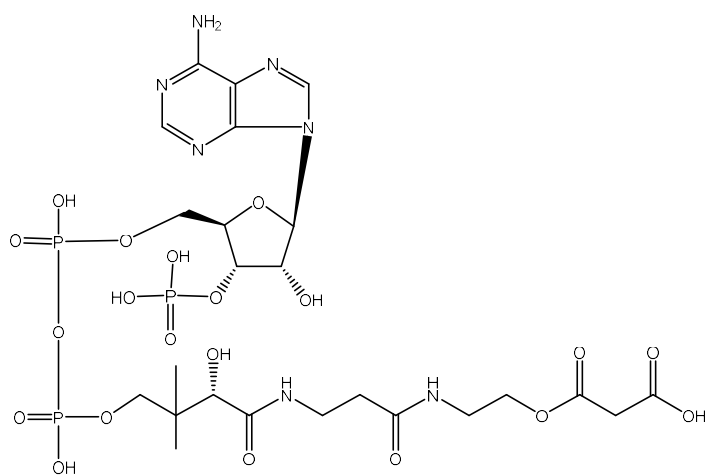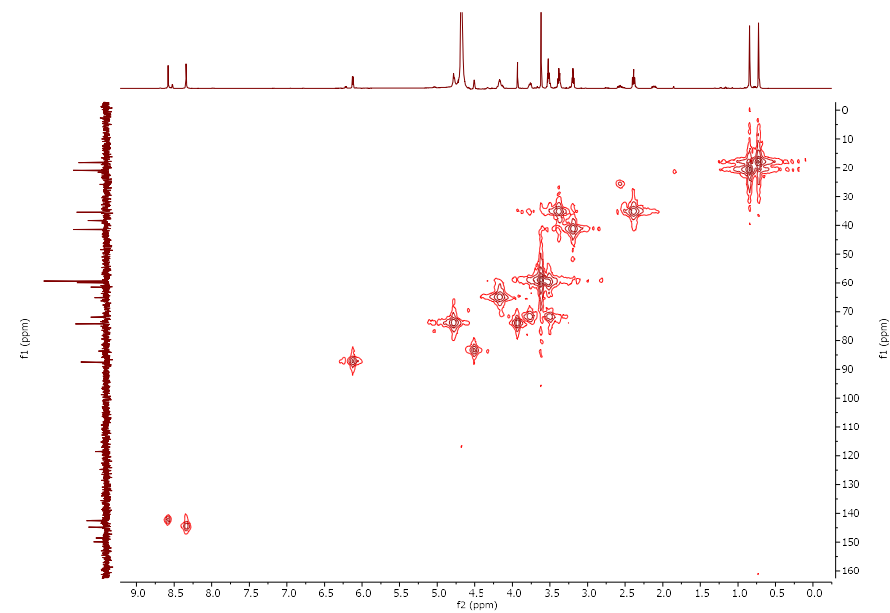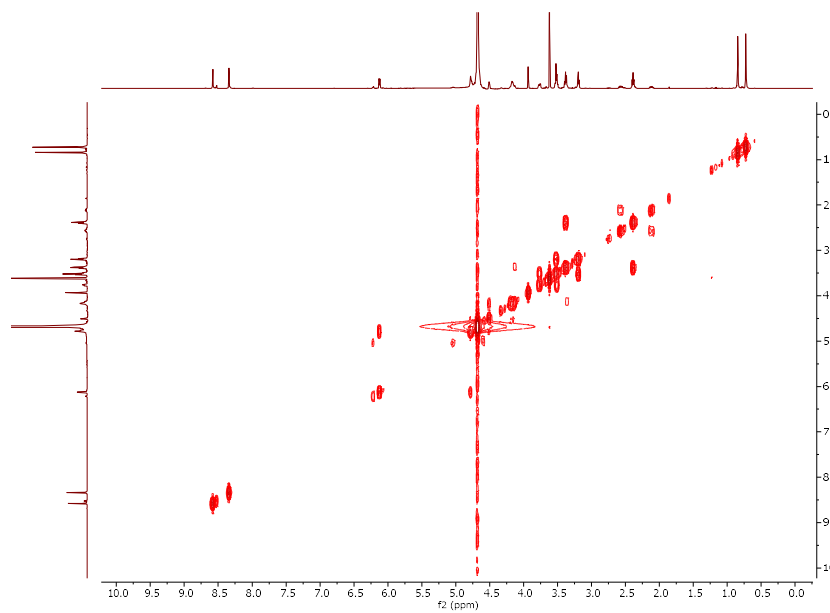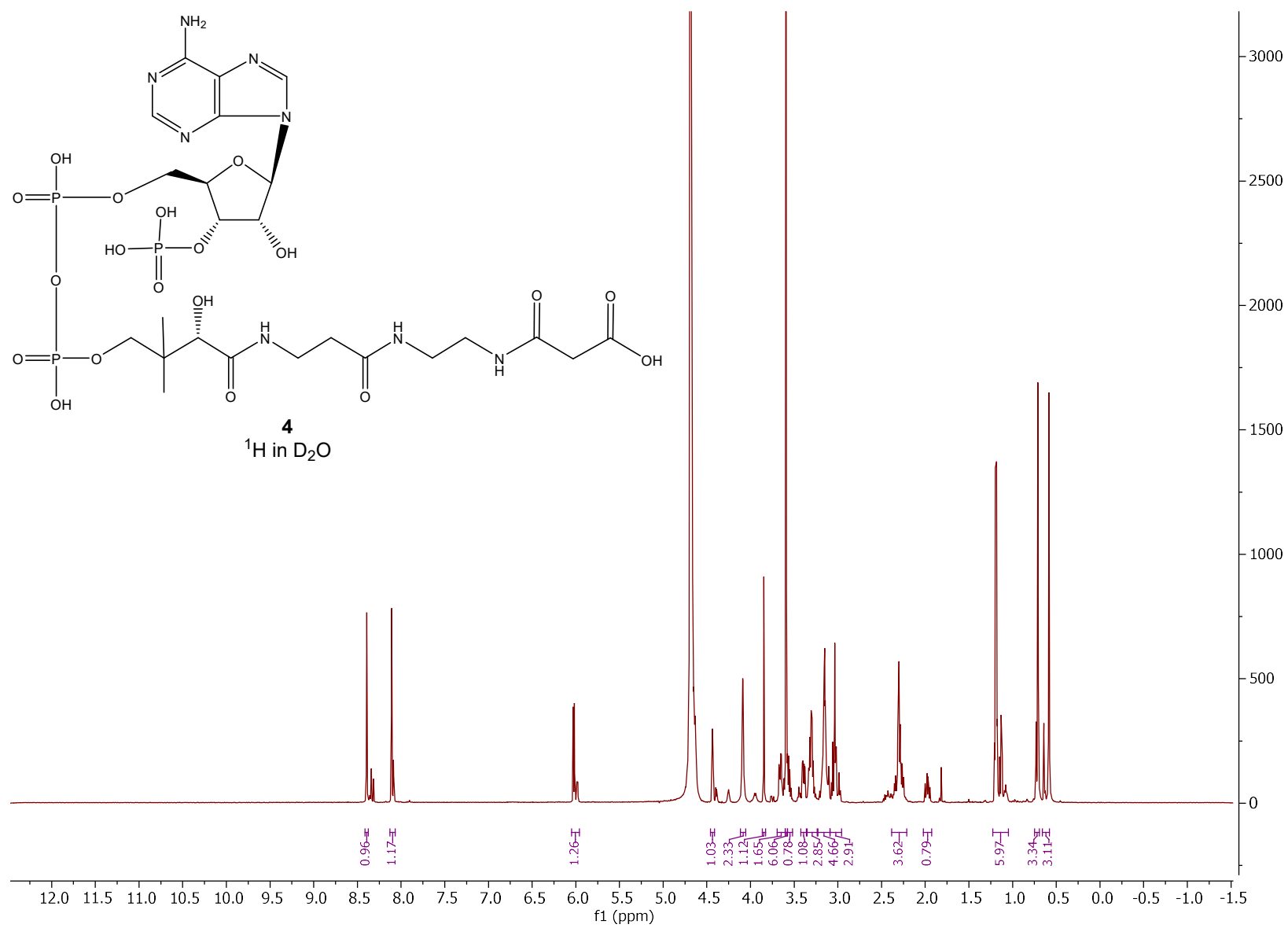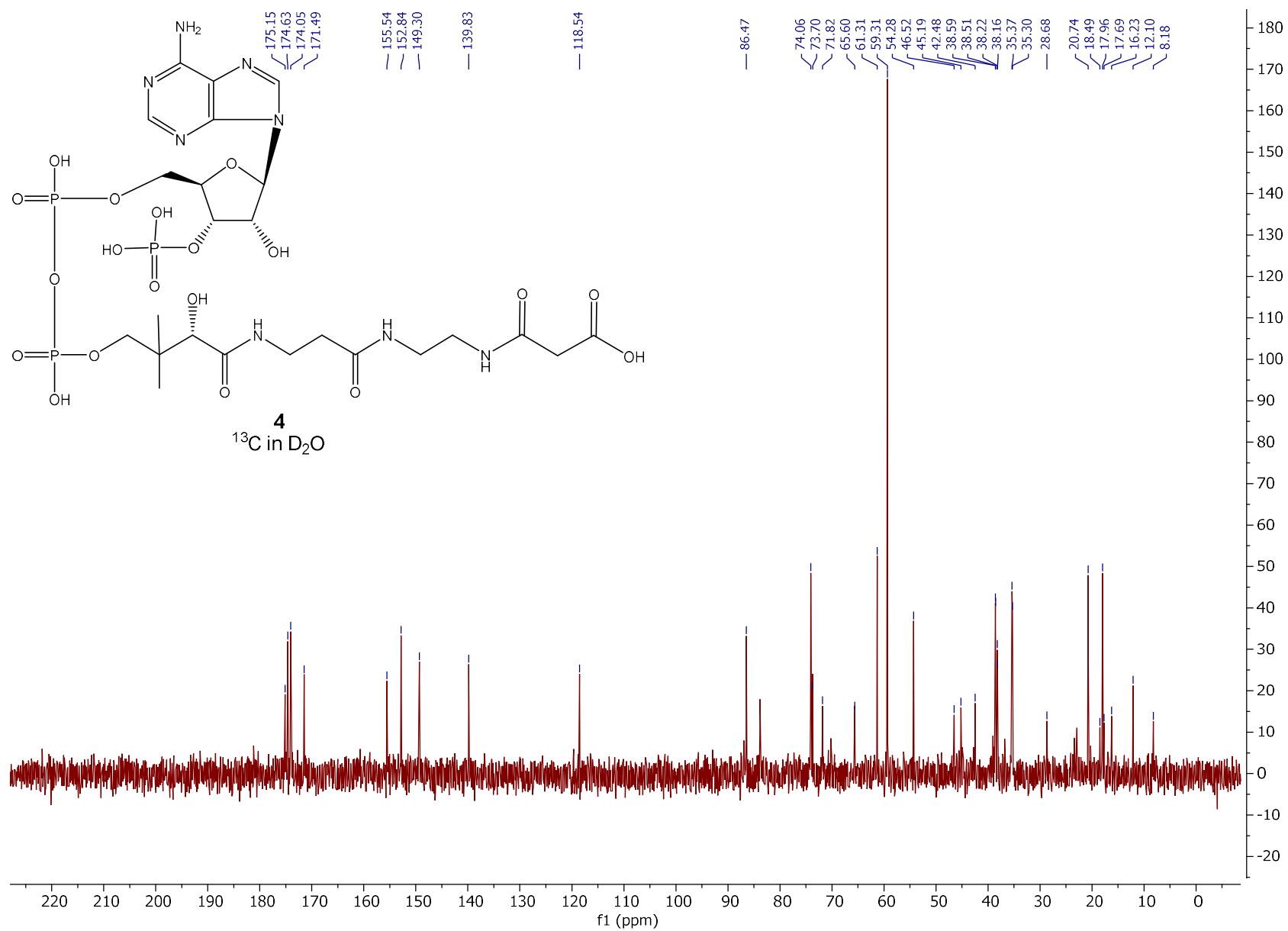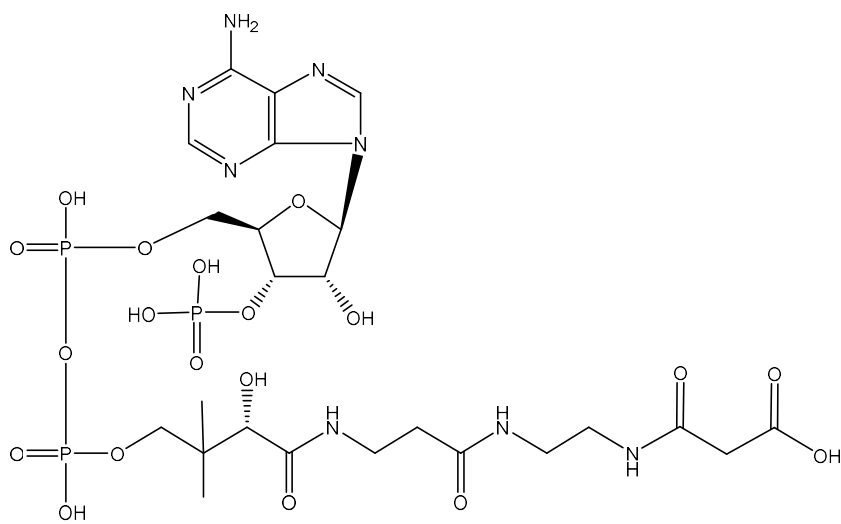
COSY and HMQC in D$_2$O
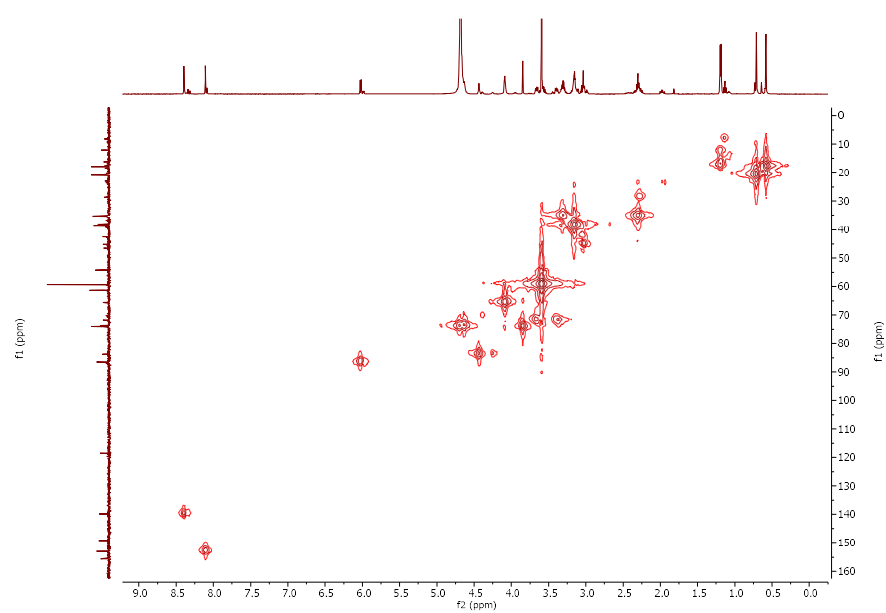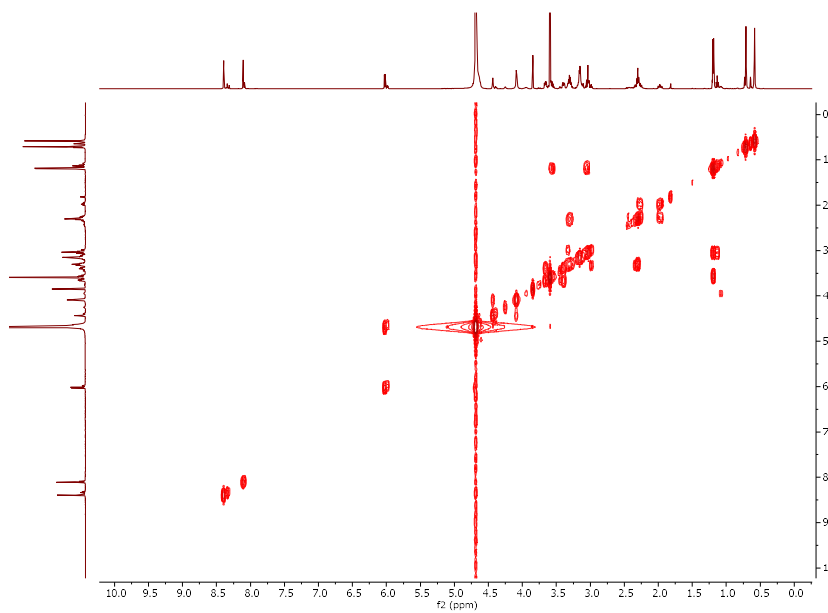
2.8 References

[1]   Mishra, P. K.; Drueckhammer, D. G., Coenzyme A Analogues and Derivatives: Synthesis and Applications as Mechanistic Probes of Coenzyme A Ester-Utilizing Enzymes. Chemical reviews 2000, 100 (9), 3283-3310.

[2]   Kulkarni, R. A.; Worth, A. J.; Zengeya, T. T.; Shrimp, J. H.; Garlick, J. M.; Roberts, A. M.; Montgomery, D. C.; Sourbier, C.; Gibbs, B. K.; Mesaros, C.; Tsai, Y. C.; Das, S.; Chan, K. C.; Zhou, M.; Andresson, T.; Weissman, A. M.; Linehan, W. M.; Blair, I. A.; Snyder, N. W.; Meier, J. L., Discovering Targets of Non-enzymatic Acylation by Thioester Reactivity Profiling. Cell Chem Biol 2017, 24 (2), 231-242.

[3]   Benning, M. M.; Haller, T.; Gerlt, J. A.; Holden, H. M., New reactions in the crotonase superfamily: structure of methylmalonyl CoA decarboxylase from Escherichia coli. Biochemistry 2000, 39 (16), 4630-9.

[4]   Ellis, B. D.; Milligan, J. C.; White, A. R.; Duong, V.; Altman, P. X.; Mohammed, L. Y.; Crump, M. P.; Crosby, J.; Luo, R.; Vanderwal, C. D.; Tsai, S. C., An Oxetane-Based Polyketide Surrogate To Probe Substrate Binding in a Polyketide Synthase. Journal of the American Chemical Society 2018, 140 (15), 4961-4964.

[5]   Mancia, F.; Smith, G. A.; Evans, P. R., Crystal structure of substrate complexes of methylmalonyl-CoA mutase. Biochemistry 1999, 38 (25), 7999-8005.

[6]   Tosin, M.; Spiteller, D.; Spencer, J. B., Malonyl carba(dethia)- and malonyl oxa(dethia)-coenzyme A as tools for trapping polyketide intermediates. Chembiochem : a European journal of chemical biology 2009, 10 (10), 1714-23.

[7]   Tosin, M.; Betancor, L.; Stephens, E.; Li, W. M.; Spencer, J. B.; Leadlay, P. F., Synthetic chain terminators off-load intermediates from a type I polyketide synthase. Chembiochem : a European journal of chemical biology 2010, 11 (4), 539-46.

[8]   Hamed, R. B.; Henry, L.; Gomez-Castellanos, J. R.; Asghar, A.; Brem, J.; Claridge, T. D.; Schofield, C. J., Stereoselective preparation of lipidated carboxymethyl-proline/pipecolic acid derivatives via coupling of engineered crotonases with an alkylmalonyl-CoA synthetase. Organic & biomolecular chemistry 2013, 11 (47), 8191-6.

[9]   White, S. W.; Zheng, J.; Zhang, Y. M.; Rock, The structural biology of type II fatty acid biosynthesis. Annual review of biochemistry 2005, 74, 791-831.

[10]   Witkowski, A.; Joshi, A. K.; Lindqvist, Y.; Smith, S., Conversion of a β-Ketoacyl Synthase to a Malonyl Decarboxylase by Replacement of the Active-Site Cysteine with Glutamine†. Biochemistry 1999, 38 (36), 11643-11650.

[11]   Stunkard, L. M.; Dixon, A. D.; Huth, T. J.; Lohman, J. R., Sulfonate/Nitro Bearing Methylmalonyl-Thioester Isosteres Applied to Methylmalonyl-CoA Decarboxylase Structure-Function Studies. Journal of the American Chemical Society 2019, 141 (13), 5121-5124.

[12]   Dunn, B. J.; Cane, D. E.; Khosla, C., Mechanism and specificity of an acyltransferase domain from a modular polyketide synthase. Biochemistry 2013, 52 (11), 1839-41.

CHAPTER 3.   CONTEXTUAL REACTIVITY ACETYL-OXA(DETHIA)COA IN CO-CRYSTAL STRUCTURES OF CHLORAMPHENICOL ACETYLTRANSFERASE I AND E. COLI B-KETOACYLSYNTHASE III

Contributions: Jeremy R. Lohman and Aaron B. Benjamin designed experiments, interpreted the resulting data, and wrote the manuscript. Aaron B. Benjamin carried out the vast majority of experiments. Lee Stunkard helped with data collection and processing. Jianheng Ling helped with some synthesis and protein purification.

Note: Literature references and chemical numbers within schemes are unique within this chapter.

3.1   Abstract

Acetyl-CoA is a reactive metabolite that non-productively hydrolyzes in a number of enzyme active sites on the crystallization time frame. In order to elucidate enzyme:acetyl-CoA interactions leading to catalysis, acetyl-CoA substrate analogs are needed. One possible analog for use in structural studies is acetyl-oxa(dethia)CoA (AcOCoA), where the sulfur of CoA is replaced by an oxygen. Here we present structures of chloramphenicol acetyltransferase III (CATIII) and E. coli ketoacylsynthase III (FabH) from crystals grown in the presence of partially hydrolyzed AcOCoA. The nucleophile of these two enzymes differs and our structures provide a close look at how the enzymes control the reactivity. The structure of CATIII reveals insight into the catalytic mechanism, with one active site of the trimer having relatively clear electron density for AcOCoA and chloramphenicol, and the other active sites having weaker density. The structure of FabH reveals a hydrolyzed AcOCoA product oxa(dethia)CoA (OCoA) and the acyl-enzyme intermediate. Together these structures provide preliminary insight into the use of AcOCoA for enzyme structure-function studies with very different nucleophiles.

3.2 Chloramphenicol acetyltransferase III and ketoacylsynthase III from *E. coli* both use acetyl-CoA to transfer an acetyl moiety

Chloramphenicol acetyltransferase III (CATIII) and *E. coli* ketoacylsynthase III (ecFabH) both transfer an acetyl group from acetyl-CoA to an acceptor, a hydroxyl and thiol/thiolate, respectively, Figure 3.1. These enzymes display negative cooperativity in acetyl-CoA substrate binding and catalysis.[1, 2] The function of negative cooperativity with respect to acetyl-CoA, is likely to decrease the amount of binding when no acceptor is present to prevent spontaneous hydrolysis. Thus, having structures of these enzymes in complex substrates would provide insights into the fundamental enzyme-substrate and protein-protein interactions leading to catalysis and cooperativity. The inherent equilibrium of the CATIII and EcFabH reactions with acetyl-CoA lie so far toward the products that substrate bound states are difficult to determine. In addition, the inherent reactivity of the acetyl-CoA thioester and non-productive activation by the enzyme often leads to hydrolysis during crystallization. While there are new methods that may be useful for overcoming the inherent side reactivity of acetyl-CoA during co-crystallization, such as using free-electron lasers and serial crystallography, not every system will be amenable as the crystals must survive conformational changes linked to substrate binding.[3] A tried-and-true method is the use of suitable stable substrate or transition state analogs.
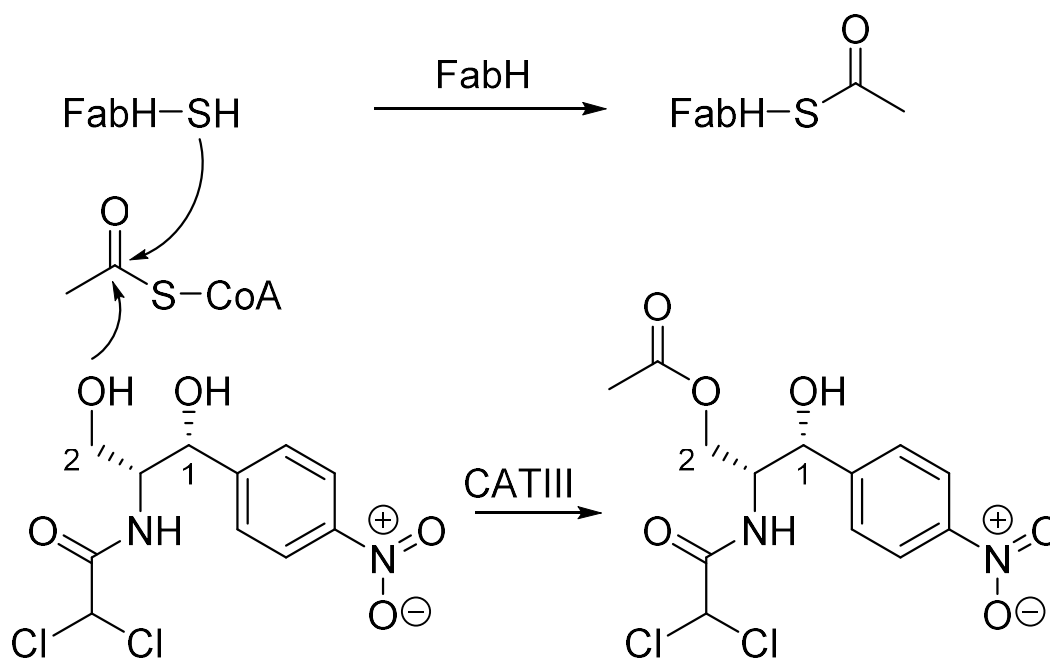
Figure 3.1 The transthiolation step of FabH and catalytic activity of CATIII.

3.3 Acetyl-oxa(dethia)-CoA is a suitable analog of acetyl-CoA to utilize in structure-function studies

Acetyl-oxa(dethia)CoA (AcOCoA) is expected to be more stable than acetyl-CoA in structure-function studies. However, there is only one report of the AcOCoA synthesis before ours.[4] In that study, a similar substrate analog, fluoroacetyl-oxa(dethia)CoA was hydrolyzed 500-fold slower by a thioesterase than the native fluoroacetyl-CoA substrate. A truncated AcOCoA substrate acetyl-oxa(dethia)pantetheine-pivoyl has been crystallized with a thiolase, where it did not participate in the transthiolation or carbon-carbon bond forming reactions.[5] Thus, we initially expected AcOCoA to be relatively stable in CATIII and ecFabH crystals, both of which crystallize overnight. However, during stability assays we found that ecFabH was able to hydrolyze AcOCoA to oxa(dethia)CoA (OCoA), likely through transthiolation and subsequent hydrolysis. We also found the hydrolysis of AcOCoA by ecFabH was much slower than acetyl-CoA. While improving on the synthesis of AcOCoA, we pursued crystal structures of the model enzymes CATIII and ecFabH with a sample of AcOCoA that contained some OCoA.

3.4 CatIII and KasIII have been studied to some extent, however some information is still needed to capture the full picture

CATIII has long been a model enzyme for structure-function studies with relevance to antibiotic drug development.[6] With the recent structure of the ribosome with chloramphenicol bound, there should be renewed interest in finding analogs that retain ribosome inhibition and overcome CATIII and other chloramphenicol acetyltransferase activities.[7] Based on the binding of CoA and chloramphenicol, Professor William Shaw and colleagues predicted that chloramphenicol 1-hydroxyl stabilized a water that acts as a member of the oxyanion hole.[8, 9] Thus, some of the catalytic activity and substrate specificity might come from the substrate itself. The chloramphenicol analog lacking the 1-hydroxyl is a much poorer substrate, supporting the hypothesis. A ternary structure of AcOCoA and chloramphenicol bound to CATIII could confirm the Shaw hypothesis. Furthermore, CATIII is a trimer that displays negative cooperativity with respect to acetyl-CoA. A structure with AcOCoA could reveal conformational differences between the monomers leading to the cooperative behavior. Our structures here reveal a mixture of AcOCoA and OCoA bound, but enough to support the Shaw hypothesis. In addition, each active

site of the biologically relevant trimer had varying levels of occupancy giving insight into cooperativity.

In *E. coli* and other similar bacteria, FabH, carries out the first acyl carrier protein (ACP) dependent carbon-carbon bond forming step, making it a target for antibiotic drug development. The two active sites in the ecFabH homodimer appear to have negative cooperativity in the binding of acetyl-CoA, based on time resolved fluorescence.[2] It's been proposed that one active site forms the acyl-enzyme intermediate, which decreases the affinity of the other for acetyl-CoA. Comparisons crystal structures in the presence and absence of CoA reveals positional variations in loops that interact between the monomers in the dimer, which may explain some of the negative cooperativity. However, the only structure with an acyl-enzyme intermediate bound has weak density. The ecFabH structures presented here with AcOCoA confirm that the acetyl group still gets transferred to generate the acyl-enzyme intermediate. These results reveal that other analogs such as acetyl-aza(dethia)CoA or acetyl-carba(dethia)CoA are needed to capture the substrate bound state of ecFabH.

The behaviors of CATIII and ecFabH with AcOCoA provides a comparison of how altering the electrophilic substrate from a thioester to an ester results in very different outcomes with respect to transition state stabilization. In one case, CATIII, the enzyme is unable to sufficiently stabilize the transition to the product, even on the crystallization time scale of days. Whereas with ecFabH, the enzyme is able to generate the thermodynamically unfavorable thioester, albeit with a large excess of substrate, within the same timeframe as CATIII. In order to fully comprehend how these enzymes carry out their reactions, it is likely neutron diffraction will be needed to confirm the positions of hydrogens, which are key for catalysis.

3.5   Structure of CATIII in complex with AcOCoA and chloramphenicol

We co-crystallized CATIII in the presence of our partially hydrolyzed AcOCoA and chloramphenicol. This produced crystals that grew overnight in various conditions. The vast majority of crystals gave diffraction patters that were difficult to index due to what appeared to be twinning problems. Serendipitously, we found a single large crystal that diffracted well, was easily indexed in the primitive tetragonal Bravais lattice, and solved in the $P4_22_12$ spacegroup with a trimer in the asymmetric unit, Table 1. The final structure had good refinement statistics and all residues for each monomer could be modeled. Although no transition metals were added to the

crystallization conditions, we found positions for three that we modeled as Ni^{2+}, which likely came from elution during the Ni-NTA purification. The metals are liganded by Glu18 and His22 in each chain, and the same residues in a symmetry mate trimer, with the pattern: chain A interacts with symmetry chain C, and chain B interacts with symmetry chain B. The previous deposited structures of CATIII were in spacegroup R32, with a single molecule per asymmetric unit. The R32 CATIII structures had two Co^{2+} metals bound (0.5 mM), one of which was in the same site as our structure, while the other occupied was on a special position situated between two backbone carbonyls of Asn68 and Asp87 with rather long interaction distances, ~4 Å. The shared metals generate a larger order hexamer in both crystal forms; however, all other crystal contacts are essentially unique. Differences in the N-termini of the CATIII from previous studies and ours likely lead to the crystal packing variations. The previous structures have an N-terminus starting at Met6 and the N-terminal amine has good packing with a hydrogen bond to the carbonyl of Lys217 that likely stabilizes the crystals. This R32 crystal packing was reported to deteriorate upon exposure to CoA, preventing elucidation of acetyl-CoA or analog binding via soaking. Our construct has an N-terminus with a Ser-Gly-Gly-Asn2 cloning artifact that would disrupt the packing seen in the R32 structures. Thus, our structure provides insight into engineering crystal contacts that allow production of trimers in the asymmetric unit in order to understand the subtle conformational changes associated with negative cooperativity.

Our structure has clear electron density for chloramphenicol in each monomer, which resides in exactly the same orientation as in previous structures. The electron density for the AcOCoA/OCoA is relatively clear in chain A, somewhat clear in chain B and difficult to model in chain C, Figure 3.2. We take the differences in electron density to correspond to negative cooperativity; however, it could be due to differences in crystal packing. The AcOCoA in chain A participates in crystal packing and is not free to leave, in chains B and C AcOCoA is open to solvent. Thus, the differences in electron density are likely to be part of the negative cooperativity. A comparison of the chains shows slight differences in the loops surrounding the CoA binding pocket in chain C, further supporting the idea of our electron density reflecting negative cooperativity.

In monomer A, we can clearly model the position of the acetyl group, even though the electron density supports about 20% OCoA, in which case a water molecule takes the place of the acetyl ketone oxygen, Figure 3.2. The binding of the acetyl-group is pretty much exactly what
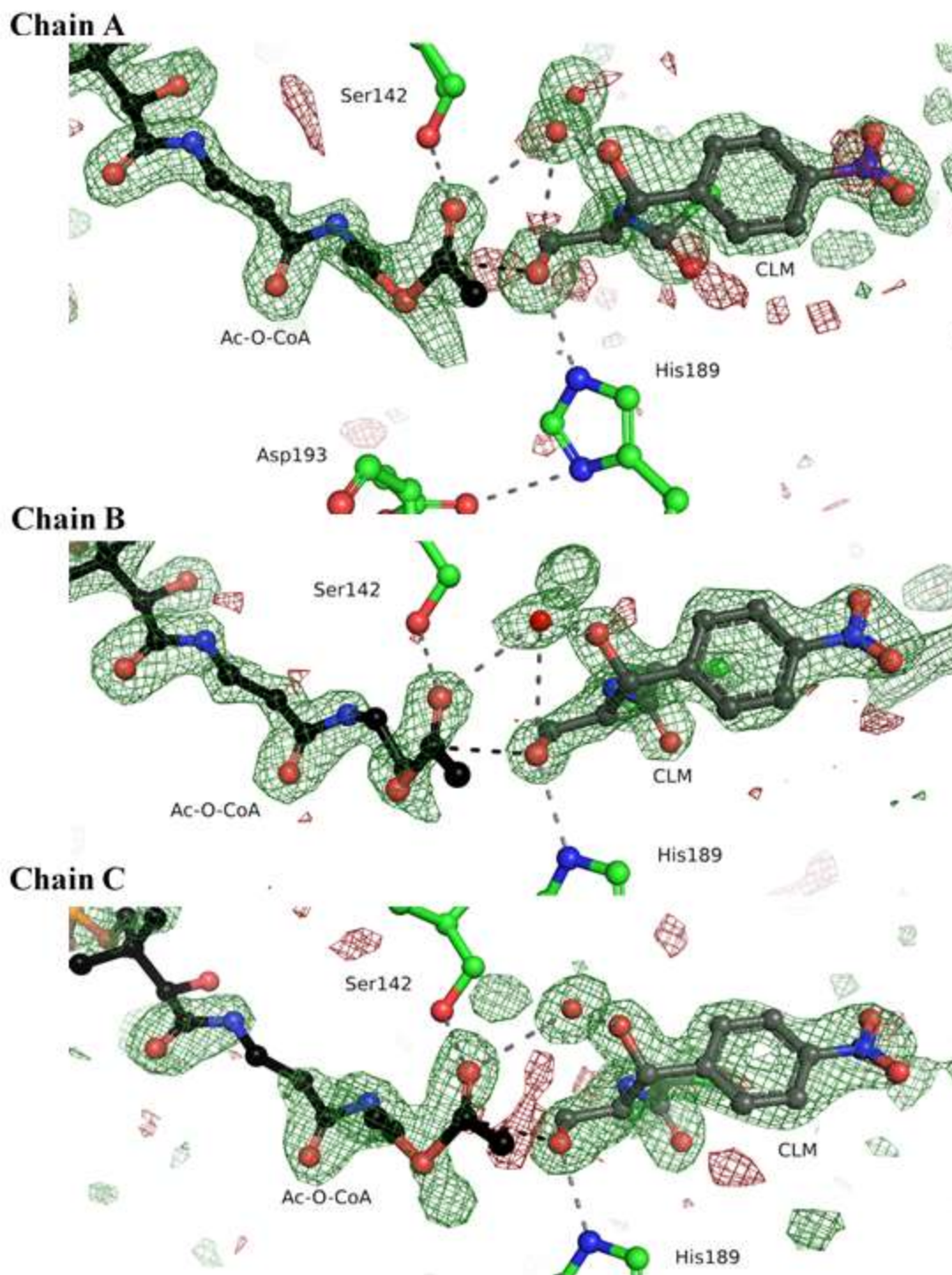
Figure 3.2 Three active sites for CATIII with acetyl-oxa(dethia)-CoA, in black, and chloramphenicol, seen in gray. Hydrogen bonds are seen in the dotted gray lines. The dotted black line represents the carbon which is attacked by the hydroxyl group of chloramphenicol.

Shaw predicted based on a structure with coenzyme A bound, Figure 3.3. The location of a water bound between the acetyl ketone and chloramphenicol 1-hydroxyl suggests that it stabilizes the transition states. While our structures finally provide evidence for the Shaw hypothesis, the positions of hydrogens remain to be determined. Our preliminary structures here provide a platform upon which to do neutron diffraction to obtain a clear idea of how the transition state is set up.
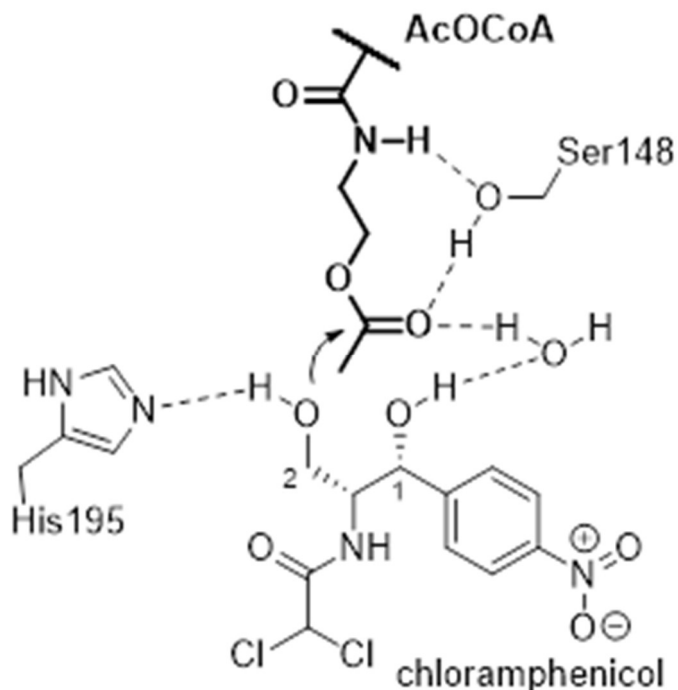
Figure 3.3 Active site interactions of AcOCoA with CATIII and chloramphenicol co-substrate. Notice a water bound to chloramphenicol helps create the oxyanion hole.

3.6 Structures of ecFabH crystallized in the presence of AcOCoA/OCoA

We co-crystallized ecFabH in the presence of our partially hydrolyzed AcOCoA. This produced crystals that grew overnight in various conditions. Crystals grown from 0.075M MgSO$_4$, 0.1M HEPES:NaOH pH 7.5, 23% PEG 3350, and 1.5% DMSO and 0.05 MgSO$_4$, 20% PEG 6K, and 3% PEG 400 diffracted well and were indexed in the primitive tetragonal Bravais lattice and solved in the P4$_1$2$_1$2 spacegroup (a = b = 73 Å) each with a monomer in the asymmetric unit, Table 1. The final structure had good refinement statistics and all residues for each monomer could be modeled. The previous structures of ecFabH fall into one of three crystal forms, crystal type I is identical to ours reported here, crystal type II is P2$_1$2$_1$2$_1$, a = 63 Å, b = 65 Å, c = 166 Å, with a

dimer in the asymmetric unit and crystal type III is $P2_12_12_1$, a = 64 Å, b = 81 Å, c = 122 Å with a dimer in the asymmetric unit. Solid density for the CoA (PDB 1HND) and acyl enzyme intermediate (PDB 1HNH) have only been seen in crystal type I, with weak CoA density in crystal type II (PDB 1EBL) and crystal type III (PDB 2EFT and 2GYO). Based on structural alignments between crystal type I and III, it appears that an N-terminal his tag may be responsible for favoring type III crystals, due to clashes that would be present in type I. In our crystals, we have some disorder in the Ser-Gly-Gly-Met1 tag artifact; however, there is enough room that the tag artifact still allows tight crystal packing. Elongating the tag may be a way to favor production of the type II/III crystals, which would be helpful for interpreting the negative cooperativity between the active sites.

Slight differences in the crystallization conditions resulted in differing amounts of density for the acyl-enzyme intermediate and OCoA product, Figure 3.4. Our structure with good electron
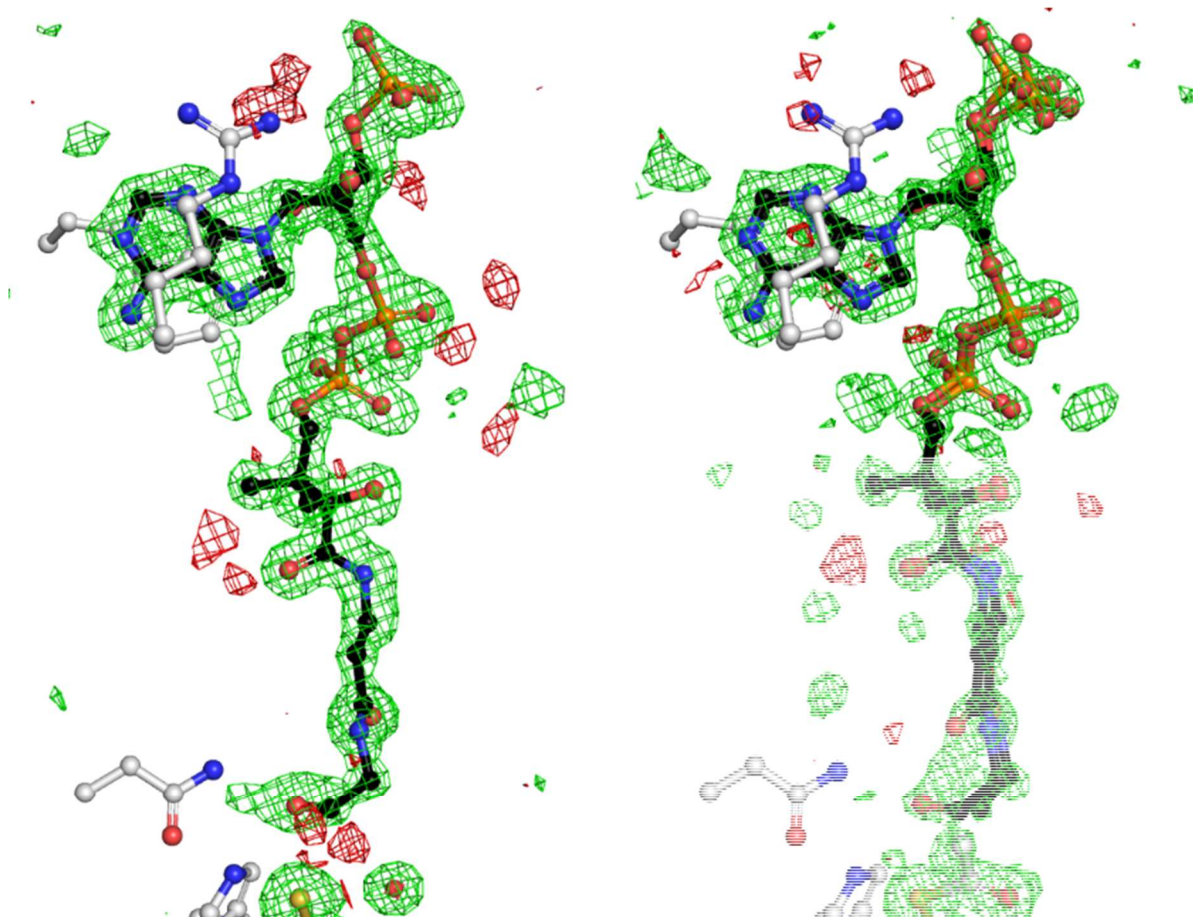
Figure 3.4 Electron density maps for our structure with clear density for OCoA on the left and for our structure with the acyl-enzyme intermediate on the right. Density is contoured at ±3 σ for sigmaA weighted omit maps.

density for the acyl-enzyme intermediate has somewhat poor electron density for the bound OCoA, while our structure with excellent density for OCoA has somewhat poor density for the acyl-enzyme intermediate. Taken together, we can get a clear view of how the enzyme interacts with the products of the pseudo substrate AcOCoA. The acyl-enzyme intermediate is very similar in structure to that previously determined with acetyl-CoA, albeit our structure has clearer electron density for the acyl-enzyme intermediate. Similarly, our structure with clear OCoA bound, is almost identical to having CoA bound.

Unfortunately, due to the presence of only a monomer in our asymmetric unit, it is difficult to gain insight into the negative cooperativity displayed by the enzyme. Nevertheless, careful inspection of the electron density maps, and comparisons with other structures reveals conformational heterogeneity that might help explain some of the cooperative behavior. The α-helix between Leu249-L258 has spurious density, suggesting the helix is in an alternate conformation part of the time. Alignment with structure 3CLA reveals the secondary conformation. In both of our structures, we modeled many waters in the active site in multiple conformations that likely correspond to changes in the protonation states of the active site residues, especially His244. One question remains concerning the transthiolation reaction, is the active site cysteine in the thiol or thiolate state, and how does the protonation state of His244 change before and after formation of the acyl-enzyme intermediate. The multiple water and nearby side chain conformations suggest we do not have the data to accurately interpret how the acyl-enzyme intermediate alters these protonation states. We expect that substrate analogs such as acetyl-aza(dethia)CoA or acetyl-carba(dethia)CoA are needed to capture a "substrate bound" state of ecFabH and to overcome the conformational heterogeneity found in these FabH structures.

3.7   Different behaviors for AcOCoA in CATIII/FabH active sites.

CATIII does not perform the forward reaction between AcOCoA and chloramphenicol during the crystallization time. The ΔG for the reaction is expected to be 0, which should give us an equal amount of substrate and product. In our case we used a large excess of chloramphenicol, which should have driven the reaction forward. We take this to mean that the $\Delta G^{\ddagger}$ is too large for transesterification to be overcome by the enzyme. In regard to the mechanism, the formation of the product may be limited by protonation of the leaving OCoA oxygen, whereas the respective thiolate of CoA is a reasonable leaving group. An alternative explanation is that due to geometric

considerations, the ester does not have strong enough interactions with the enzyme to form the tetrahedral intermediate. We expect follow up studies determining the binding affinities of acetyl-CoA and AcOCoA with non-reactive chloramphenicol analogs can shed light on which of these two hypotheses is correct.

On relatively short timeframes, FabH hydrolyzes AcOCoA. Our structural studies here confirm that the hydrolysis is through the acyl-enzyme intermediate. The formation of the acyl-enzyme intermediate is somewhat unexpected, as it is unfavorable with a positive ΔG. We used a large excess of substrate in our crystallization condition, which may have contributed to the spontaneous formation of the acyl-enzyme intermediate. The reverse reaction, while spontaneous, may be prevented by a large transition state energy for the deprotonation of the OCoA. We observe a 25-fold slower rate of hydrolysis for AcOCoA than acetyl-CoA, which likely reflects a slower rate of acyl-enzyme intermediate formation, as the rate of hydrolysis for the common acyl-enzyme intermediate should be the same. Similar to CATIII, it appears that either protonation of the OCoA leaving group or geometric considerations are what become rate limiting in the reaction of FabH with AcOCoA. The protonation state of the cysteine nucleophile in FabH may play a large role in the reactivity, which is reflected in the multiple conformations of active site waters in our structures. Future studies examining differences in the rate of hydrolysis of acetyl-CoA/AcOCoA as a function of pH are likely to shed light on the best pH to crystallize FabH to minimize the conformational heterogeneity seen in our structures.

Our structures demonstrate different behaviors for AcOCoA depending on the context, it is a substrate analog for CATIII but a pseudo substrate for FabH. It may be the case that hydroxyl acceptors in general will lead to substrate analog behavior and thiol acceptors will lead to product formation. In our synthesis study we also generated malonyl-oxy(dethia)CoA as a substrate analog with the malonyltransferase FabD, which has an active site serine. With FabD, malonyl-oxy(dethia)CoA was stable and did not undergo malonyl transfer or hydrolysis. With the aforementioned fluoroacetyl-CoA hydrolase, which generates a threonine based acyl-enzyme intermediate, fluoroacetyl-oxy(dethia)CoA was a substrate with a 500-fold slower rate.[4,10].Together it suggests that acyl-oxy(dethia)CoAs are likely to be useful tools for studying many enzymes with hydroxyl nucleophiles. The catalytic interactions for many Gcn5-related N-acetyltransferases (GNATs) still remains uncharacterized due to the spontaneous hydrolysis of acetyl-CoA and reactivity with the substrates. Our studies here with CATIII suggest that acyl-

oxy(dethia)CoAs will be effective for capturing the ternary complexes; however, the reactivity with amine nucleophiles remains to be examined.

3.8   Materials and Methods

Below is the materials and methods section of the work described in this chapter

3.8.1   Cloning, expression, and purification of FabH+GG and CatIII

Cloning and protein expression was done as previously reported [11] for both FabH+GG and CatIII+GG. For CatIII+GG, the primers used were:

CatIII+GG-forward: 5′-
GAGAACCTCTACTTCCAAAGTGGTGGTAACTATACAAAATTTGATG-3′,

CatIII+GG-reverse 5′-CTCGAGGAGATTACGGATTATTTTAATTTACTGTTACAC-3′,

3.8.2   Crystallization, X-ray Crystallographic Collection and Refinement of FabH+GG and CatIII

FabH+GG and CatIII were screened against 384 crystallization conditions in 500 nL sitting drops at 20˚C, set up with a Mosquito (TTPlabtech, Melbourne, Australia) to find initial conditions. FabH+GG [21 mg/mL in 10 mM Tris-HCl (pH 8.0) and 200 mM NaCl] and 10 mM **Ac-O-CoA** produced crystals by the hanging drop method over 1.0 mL wells containing 1.5% DMSO, 23% PEG 3350, 75 mM MgCl2, and 100 mM HEPES:NaOH (pH 7.5) and 20% PEG 6000, 3% PEG 400, and 100 mM MgCl2, and CatIII [24 mg/mL in 10 mM Tris-HCl (pH 8.0) and 200 mM NaCl], 10 mM **Ac-O-CoA**, and saturating concentrations of chloramphenicol were produced crystals by the hanging drop method over 1.0 mL wells containing 46% PEG 400, 100 mM MgCl2, 0.1 M Sodium Citrate:Citric Acid (pH 5.5), in 4 µL drops (1:3, protein:well). Crystals were looped and frozen directly out of the drops with liquid nitrogen. X-ray diffraction data for all datasets were collected at Advanced Photon Source LS-CAT beamline 21-ID-G (PDB: 6X7R, 6X7S, and 6X7Q) at a wavelength of 0.97856. Diffraction intensities were integrated, reduced, and scaled using HKL2000 [12], with data collection and refinement statistics listed in Table 3.3. Molecular replacement with the program Phaser was used to phase our structures of KasIII with degraded **Ac-O-CoA** (PDB: 6X7R) and Ac-KasIII (PDB: 6X7S) based off PDB 1HNJ coordinates.

Molecular replacement with the program Phaser was used to phase our structures of CatIII with **Ac-O-CoA** (PDB: 6X7Q) based off PDB 3CLA coordinates [13]. Refinement was conducted using Refmac [14] in the CCP4i package [15] with automated model building performed with ARP/wARP [16] and manual model building with Coot [13].

3.8.3   Supplemental Tables

Below are the two tables of statistics gathered from the chloramphenicol acetyltransferase structure discussed in this chapter. Each of these tables was used to determine occupancy of bound analog, Table 3.1, and compare the B factors for specific portions of the Ac-O-CoA bound in the active sites, Table 3.2.

Table 3.1 Ac-O-CoA, serine conformations, and waters near active site in chain C of CATIII: e⁻ and B factors

	Ester	**H2O Carbonyl**	**H2O Ester**	**H2O**	**Ser Conf 1**	**Ser Conf 2**
$e^-/Å^3$	0.7752	0.9962	0.6647	1.5977	0.5787	0.8365
fraction	0.49	0.62	0.42	1.00	0.36	0.52
B-Factors	32.57	27.59	39.04	13.91	15.45	20.23

The above table shows us the B-factor and where the electron density disappeared for the ester, carbonyl oxygen, water below the ester, water molecule near the Ac-O-CoA, and each of the serine conformations.

Table 3.2 Average B Factors per chain in CATIII: Adenine vs. Pantamide

	A	**B**	**C**
Adenine (average B)	17.895	21.581	27.639
Pantamide (average B)	22.311	25.277	36.889

The above table shows us the average B-factor for each of the chains in either the adenine ring or the pantamide portion of the pantetheine arm (up to the N2). As can be seen, there are lower B-factors in chain A which increase until the chain C. This suggests that the first active site has

the highest occupancy, while the third active site has the lowest occupancy. Using this information and the information in Table 3.1, we can determine relative occupancy to be approximately 50% for the chain C active site hydrolyzed Ac-O-CoA.

The table below provides the structure statistics for all three structures in this chapter.

Table 3.3 Structure Statistics

	KasIII 1-1-7	KasIII 1-2-2	Cat3 1-1-6
Data collection			
Wavelength	0.97856	0.97856	0.97856
Total reflections	224532	247744	311296
Unique reflections	60608	68034	84122
Space group	$P4_1\,2_1\,2$	$P4_1\,2_1\,2$	$P4_2\,2_1\,2$
Cell dimensions			
a, b, c (Å)	$a = b = 72.63$ $c = 102.87$	$a = b = 72.66$ $c = 102.85$	$a = b = 106.92$ $c = 126.60$
α, β, γ (°)	$\alpha = \beta = \gamma = 90$	$\alpha = \beta = \gamma = 90$	$\alpha = \beta = \gamma = 90$
Resolution (Å)	23.59-1.35 (1.40-1.35)	22.99-1.3 (1.35-1.3)	34.33-1.68 (1.74-1.68)
R_{merge}	0.085 (0.768)	0.068 (0.544)	0.147 (1.261)
R_{meas}	0.071 (0.797)	0.070 (0.454)	0.152 (1.308)
$I/\sigma(I)$	130.4(1.05)	34.45 (1.94)	23.5 (2.97)
$CC_{1/2}$	0.999 (0.936)	0.998 (0.948)	0.998 (0.813)
CC*	1.000 (0.983)	1.000 (0.986)	0.999 (0.947)
Completeness (%)	98.7 (100.0)	99.6 (96.5)	99.8 (100.0)
Redundancy	13.9 (13.7)	14.2 (12.0)	14.5 (14.3)
Wilson B-factor	19.0	12.7	18.3
Refinement			
Resolution (Å)	23.59-1.35	22.99-1.3	34.33-1.68
No. reflections	57495	64511	80050
R_{work}	0.1446	0.1472	0.1571
R_{free}	0.1757	0.1668	0.2010
No. atoms			
Protein	2423	2475	3873
Ligands	53	97	232
B-factors			
Protein	21.43	14.12	20.54
Ligands	26.42	22.98	33.14
Water	33.35	29.95	32.73
Ramachandran outliers	3	5	15

3.9 References

[1]   Ellis, J., Bagshaw, C. R., and Shaw, W. V. (2002) Substrate binding to chloramphenicol acetyltransferase: evidence for negative cooperativity from equilibrium and kinetic constants for binary and ternary complexes, Biochemistry 30, 10806-10813.

[2]   Alhamadsheh, M. M., Musayev, F., Komissarov, A. A., Sachdeva, S., Wright, H. T., Scarsdale, N., Florova, G., and Reynolds, K. A. (2007) Alkyl-CoA disulfides as inhibitors and mechanistic probes for FabH enzymes, Chemistry & biology 14, 513-524.

[3]   Chapman, H. N. (2019) X-Ray Free-Electron Lasers for the Structure and Dynamics of Macromolecules, Annual review of biochemistry 88, 35-58.

[4]   Weeks, A. M., Wang, N., Pelton, J. G., and Chang, M. C. Y. (2018) Entropy drives selective fluorine recognition in the fluoroacetyl-CoA thioesterase from Streptomyces cattleya, Proceedings of the National Academy of Sciences of the United States of America 115, E2193-E2201.

[5]   Merilainen, G., Schmitz, W., Wierenga, R. K., and Kursula, P. (2008) The sulfur atoms of the substrate CoA and the catalytic cysteine are required for a productive mode of substrate binding in bacterial biosynthetic thiolase, a thioester-dependent enzyme, The FEBS journal 275, 6136-6148.

[6]   Shaw, W. V., and Leslie, A. G. (1991) Chloramphenicol acetyltransferase, Annu Rev Biophys Biophys Chem 20, 363-386.

[7]   Svetlov, M. S., Plessa, E., Chen, C. W., Bougas, A., Krokidis, M. G., Dinos, G. P., and Polikanov, Y. S. (2019) High-resolution crystal structures of ribosome-bound chloramphenicol and erythromycin provide the ultimate basis for their competition, RNA 25, 600-606.

[8]   Lewendon, A., and Shaw, W. V. (1993) Transition state stabilization by chloramphenicol acetyltransferase. Role of a water molecule bound to threonine 174, The Journal of biological chemistry 268, 20997-21001.

[9]   Lewendon, A., Murray, I. A., Shaw, W. V., Gibbs, M. R., and Leslie, A. G. (1990) Evidence for transition-state stabilization by serine-148 in the catalytic mechanism of chloramphenicol acetyltransferase, Biochemistry 29, 2075-2080.

[10]   Dias, M. V., Huang, F., Chirgadze, D. Y., Tosin, M., Spiteller, D., Dry, E. F., Leadlay, P. F., Spencer, J. B., and Blundell, T. L. (2010) Structural basis for the activity and substrate specificity of fluoroacetyl-CoA thioesterase FlK, The Journal of biological chemistry 285, 22495-22504.

[11]   Benjamin A.B., Stunkard L.M., Boram T.J., Ling J., Bumbelburg C.M., Nice J.N., and Lohman J.R. Improved Synthesis Of Acetyl/Malonyl-Oxa/Aza(Dethia)Coas And Reactivity With Fatty Acid Synthase Enzymes. *In prep: Organic Letters*.

[12]   Otwinowski, Z.; Minor, W., Processing of X-ray diffraction data collected in oscillation mode. Meth. Enzymol. Macromolecular Crystallography, Pt A 1997, 276, 307-326.

[13]   Emsley, P.; Lohkamp, B.; Scott, W. G.; Cowtan, K., Features and development of Coot. Acta Crystallogr. D 2010, 66 (Pt 4), 486-501.

[14]   Murshudov, G. N.; Vagin, A. A.; Dodson, E. J., Refinement of macromolecular structures by the maximum-likelihood method. Acta Crystallogr. D 1997, 53 (Pt 3), 240-55.

[15]   Winn, M. D.; Ballard, C. C.; Cowtan, K. D.; Dodson, E. J.; Emsley, P.; Evans, P. R.; Keegan, R. M.; Krissinel, E. B.; Leslie, A. G.; McCoy, A.; McNicholas, S. J.; Murshudov, G. N.; Pannu, N. S.; Potterton, E. A.; Powell, H. R.; Read, R. J.; Vagin, A.; Wilson, K. S., Overview of the CCP4 suite and current developments. Acta Crystallogr. D 2011, 67 (Pt 4), 235-42.

[16]   Langer, G.; Cohen, S. X.; Lamzin, V. S.; Perrakis, A., Automated macromolecular model building for X-ray crystallography using ARP/wARP version 7. Nat. Protoc. 2008, 3 (7), 1171-9.

CHAPTER 4.   CONCLUDING REMARKS

Note: Literature references are unique within this chapter.

4.1   The labile thioester bond of acyl-CoAs make structure-function studies with acyl-CoAs challenging

The thioester bond of acyl-CoAs is highly reactive and is relatively easily broken, especially in the active site of many enzymes. As a result, studying how these enzymes select their substrates and how they are able to perform there chemistries mechanistically is incredibly challenging. While previously described analogs have shown some promise as inhibitors or in probing into mechanism with the addition of mutational analysis, the lack of structure-function studies with similar analogs is currently lacking. In this thesis, I have shown an improved synthesis acetyl- and malonyl-CoA analogs I have described above. In addition, I have shown that they are stable for use in most enzymes, with the exception of Ac-O-CoA in KasIII. I believe that these analogs will be invaluable to structure-function studies.

4.2   Additional analogs that have been synthesized may be useful in structure-function studies of acyltransferases, decarboxylases, and Claisen-condensing enzymes

While our acetyl- and malonyl-CoA analogs did not inhibit the malonyl acyltransferase, FabD or the bifunctional acyltransferase, decarboxylative Claisen-condensation utilizing, KasIII, with great affinity, they did show great stability over a 24-hour period within these enzymes. This leads us to believe that the ester and amide analogs may prove useful for future structure-function studies in the enzymes involved in PKS or FAS pathways. It is also possible that these analogs will be useful in other acyltransferases, however inhibition studies are still needed with several of these acyltransferases to truly show the usefulness of these analogs.

A collaboration with Dr. James Hougland at Syracuse University provided me with an opportunity to synthesize three medium chain acyl-CoA analogs where we replaced the thioester sulfur with an amide, Scheme 4.2. Dr. Hougland studies the enzyme GOAT, mentioned in the introduction, a member of the MBOAT superfamily. This family, as mentioned previously, has very little structural information known about it, thus analogs which may help stabilize the family

for crystallography may provide invaluable information towards the mechanism utilized by this superfamily. The ester versions were not synthesized; however, it is likely that these analogs may be valuable for crystallography experiments based off the fact that structures with CatIII with acetyl-oxa(dethia)-CoA have now been solved. Future studies with these analogs are necessary to determine whether or not they will have any ability to be used in structure-function studies.
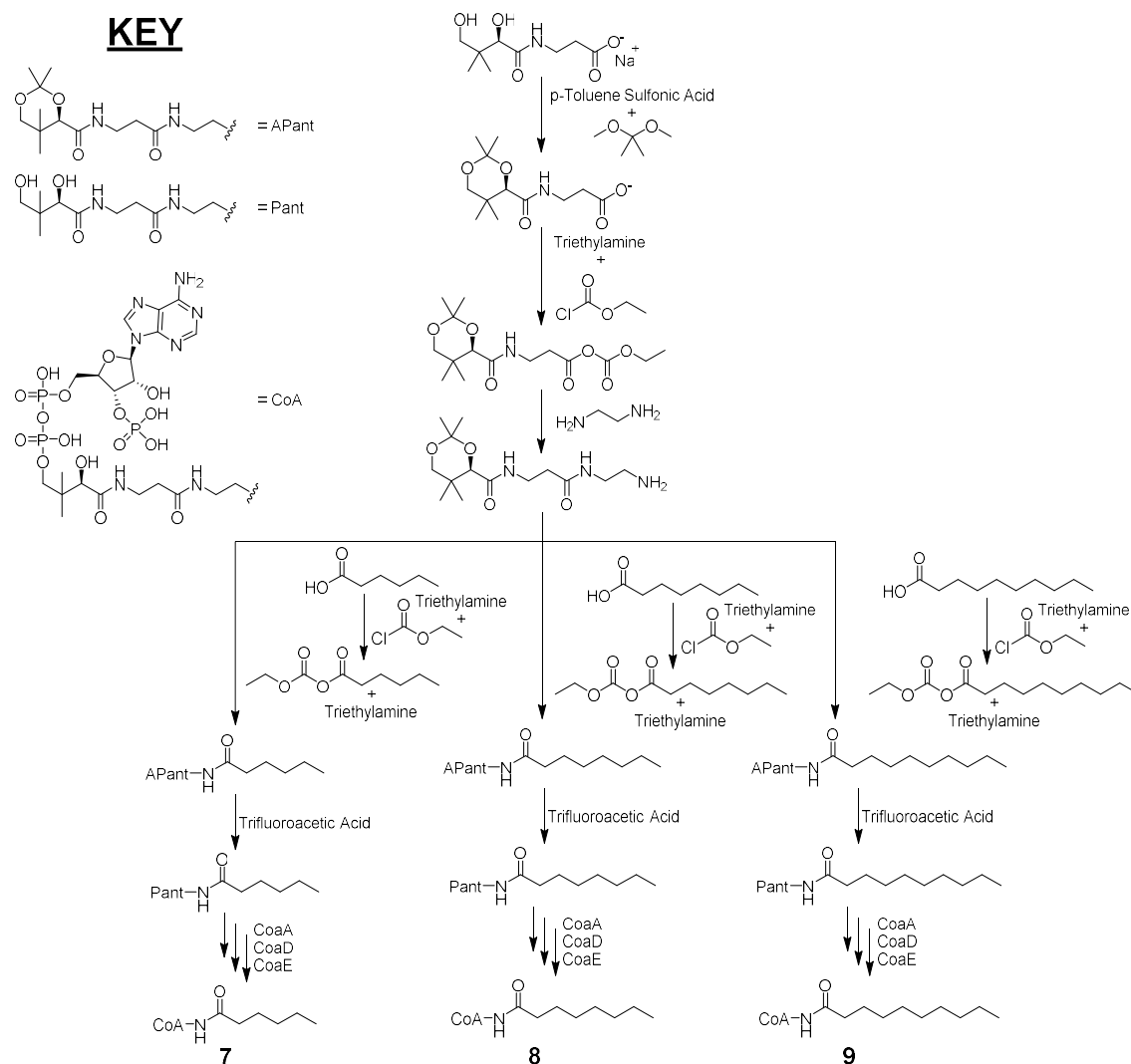
Scheme 4.1 Synthetic route for hexanoyl- (**7**), octanoyl- (**8**), and decanoyl-CoA (**9**).

4.3 Attempting to use our analogs to perform pulldowns were initially unsuccessful, however using slightly more complicated chemistry may help alleviate these problems

Initially, one of the projects I attempted to work on was the use of our analogs as probes for the discovery of novel acyltransferases in species which have not had their genomes explored thoroughly. In addition, we believed that we could use these analogs to potentially determine the substrates of acyltransferases which had not been biochemically characterized. Our initial strategy was to tag our acyl-CoA analogs at the γ-phosphate of the CoA, Figure 4.4, since it was exposed to the solvent in almost every structure that has CoA bound. Most pulldown assays we had researched into used the free amine of adenine to tag, however we also noticed that many of the structures with CoA bound had this amine hydrogen bonding with the enzyme in its' active site. Initial results showed that the chemistry we had used was resulting in a cyclic phosphate, so we attempted to resolve this issue by producing 2'-deoxyCoA, Figure 4.4. Unfortunately, purification attempts resulted in a loss of product which was likely due to acid hydrolysis. While time did not allow for the completion of this project, it is possible with alternative chemistry, it could be possible to protect the CoA analog so that future pull downs could be performed. If this chemistry works, it may be possible to use a combination of high-resolution LC-MS and proteomics to help elucidate novel acyltransferases and their substrates, opening the acyltransferase field up to a variety of new targets for drug development and general understanding of cellular function.
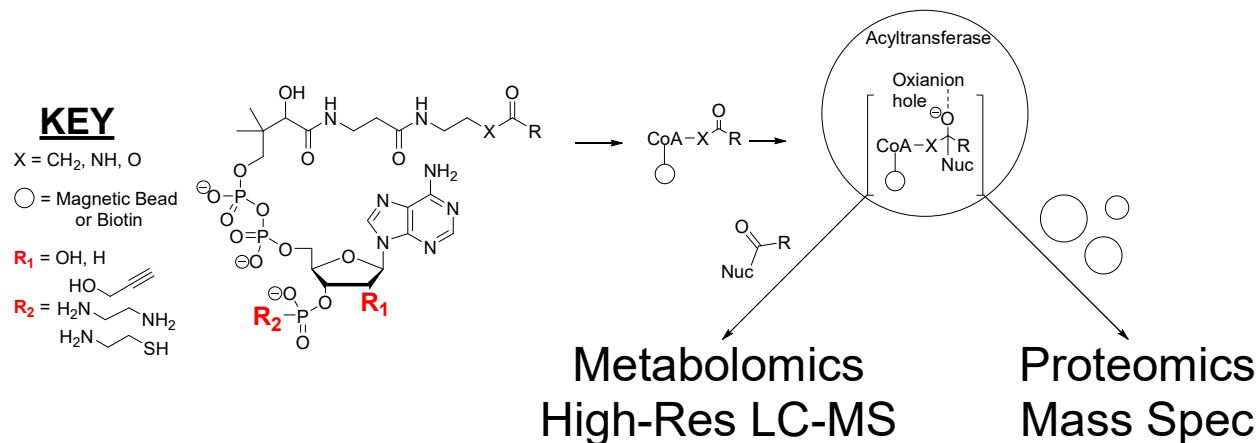

Figure 4.1 Overview of attempts to use acyl-CoA analogs to discover novel acyltransferases and their substrates through a combination of high-resolution LC-MS and proteomics.

4.4   Concluding remarks

Overall, I have been able to synthesize the ester and amide acetyl- and malonyl-CoA analogs more efficiently and in higher yields. I have also shown that these analogs are stable in enzymes that utilize acyl transfer and bifunctional acyl transfer and decarboxylative Claisen-condensation, with the exception of acetyl-oxa(dethia)-CoA in the ketosynthase enzyme family. We have also shown that the acetyl-oxa(dethia)-CoA analog may be useful for structure-function studies of O-acetyltransferases. There is potential for these analogs in a variety of enzyme classes, many of which lack sufficient structural information to generate mechanistic hypotheses for testing. While my work has focused on acyltransferases which utilize oxygen and sulfur as nucleophiles, it should be noted that acyltransferases utilizing nitrogen may also be able to capitalize on the usefulness of these analogs. Testing these analogs in both a biophysical and structural manner will help determine if these analogs are applicable to all acyltransferases. Another potential use for these analogs was attempted which was to utilize them as probes for determining natural substrates and discover new enzymes. While complications in this endeavor put this study on hold, new chemistries may be taken advantage of, allowing for potential to determine many acyltransferases not previously annotated or discovered in varying organisms. Continuing down this path would likely allow for a better understanding of the varying enzymes involved in metabolism, especially ones found in newly cultured bacteria.

4.5   References

[1] Apsimon, J., and Seguin, R. (1980) A Convenient Synthesis of 5-Bromo-2-Pentanone, *Synthetic Commun 10*, 897-898.

[2] Stewart, C. J., and Wieland, T. (1978) Synthesis of a Carba-analog of S-Acetyl CoA,Acetonyldethio CoA.Synthesis of a Carba-analog ofS-Acetyl Coenzyme A,Acetonyl-dethio Coenzyme A; an Effective Inhibitor of Citrate Synthase, *Justus Liebigs Annalen der Chemie 1978*, 57-65.

[3] Stunkard, L. M., Dixon, A. D., Huth, T. J., and Lohman, J. R. (2019) Sulfonate/Nitro Bearing Methylmalonyl-Thioester Isosteres Applied to Methylmalonyl-CoA Decarboxylase Structure-Function Studies, *J Am Chem Soc 141*, 5121-5124.

[4] Magalhaes, M. L., and Blanchard, J. S. (2005) The kinetic mechanism of AAC3-IV aminoglycoside acetyltransferase from Escherichia coli, *Biochemistry 44*, 16275-16283.

[5] Vetting, M. W., Park, C. H., Hegde, S. S., Jacoby, G. A., Hooper, D. C., and Blanchard, J. S. (2008) Mechanistic and structural analysis of aminoglycoside N-acetyltransferase AAC(6')-Ib and its bifunctional, fluoroquinolone-active AAC(6')-Ib-cr variant, *Biochemistry 47*, 9825-9835.